Los Alamos
NATIONAL LABORATORY
EST. 1943

Associate Director for ESH
Environment, Safety, and Health
P.O. Box 1663, MS K491
Los Alamos, New Mexico 87545
505-667-4218/Fax 505-665-3811

Environmental Management
Los Alamos Field Office, MS A316
3747 West Jemez Road
Los Alamos, New Mexico 87544
(505) 667-4255/FAX (505) 606-2132

Date:
Refer To: ADESH-15-068
LAUR: 15-22463
Locates Action No.: N/A

John Kieling, Bureau Chief
Hazardous Waste Bureau
New Mexico Environment Department
2905 Rodeo Park Drive East, Building 1
Santa Fe, NM 87505-6303

Subject: Submittal of the Sandia Wetland Performance Report, Performance Period April 2014–December 2014

Dear Mr. Kieling:

Enclosed please find two hard copies with electronic files of the Sandia Wetland Performance Report, Performance Period April 2014–December 2014. Los Alamos National Laboratory (the Laboratory) has prepared this report in response to requirements set forth in the document "Work Plan and Final Design for Stabilization of the Sandia Canyon Wetland." The requirement for design of a Sandia wetland monitoring program was previously set forth in New Mexico Environment Department's (NMED's) "Approval with Modification, Interim Measures Work Plan for Stabilization of the Sandia Canyon Wetland" in response to the Laboratory's "Interim Measures Work Plan for Stabilization of the Sandia Canyon Wetland."

If you have questions, please contact Steve Veenis at (505) 667-0013 (veenis@lanl.gov) or Ramoncita Massey at (505) 665-7771 (ramoncita.massey@em.doe.gov).

Sincerely,

Dave McInroy, Program Director
Environmental Remediation Program
Los Alamos National Laboratory

Sincerely,

Christine Gelles, Acting Manager
Environmental Management
Los Alamos Field Office

DM/CG/SV:sm

Enclosure: Two hard copies with electronic files – Sandia Wetland Performance Report, Performance Period April 2014–December 2014 (EP2015-0056)

Cy: (w/enc.)
Steve Veenis, ADEP ER Program, MS M992
Tadz Kostrubala, ADEP ER Program, MS M992
Public Reading Room (EPRR)
ADESH Records

Cy: (Letter and CD and/or DVD)
Laurie King, EPA Region 6, Dallas, TX
Steve Yanicak, NMED-DOE-OB, MS M894
Jeff Heikoop, EES-14, MS D462 (w/ MS Word files on CD)
Amanda White, ADEP ER Program, MS M997
PRS Database

Cy: (w/o enc./date-stamped letter emailed)
lasomailbox@nnsa.doe.gov
Annette Russell, DOE-EM-LA
Hai Shen, DOE-EM-LA
David Rhodes, DOE-EM-LA
Kimberly Davis Lebak, DOE-NA-LA
Dave McInroy, ADEP ER Program
Randy Erickson, ADEP
Tony Grieggs, ADESH-ENV-CP
Jocelyn Buckley, ADESH-ENV-CP
Alison Dorries, ADESH-ENV-DO
Michael Brandt, ADESH
Amy De Palma, PADOPS
Michael Lansing, PADOPS

LA-UR-15-22463
April 2015
EP2015-0056

Sandia Wetland Performance Report, Performance Period April 2014–December 2014

Los Alamos
NATIONAL LABORATORY
EST. 1943

Prepared by the Environmental Programs Directorate

EP2015-0056

Sandia Wetland Performance Report, Performance Period April 2014–December 2014

April 2015

Responsible project manager:

Steve Veenis	[signature] for	Project Manager	Environmental Programs	4.21.15
Printed Name	Signature	Title	Organization	Date

Responsible LANS representative:

Randall Erickson	[signature] for R. Erickson	Acting Associate Director	Environmental Programs	4/23/15
Printed Name	Signature	Title	Organization	Date

Responsible DOE representative:

Christine Gelles	[signature]	Acting Manager	DOE-EM-LA	4/29/15
Printed Name	Signature	Title	Organization	Date

EXECUTIVE SUMMARY

The Sandia wetland performance report for the period from April to December 2014 is the second annual report that will assess the overall condition of the wetland at the head of Sandia Canyon, including the chemical and physical stability of wetland sediments and the extent of wetland vegetation. The condition of the wetland is assessed in the context of the grade-control structure (GCS) completed in 2013 at the terminus of the wetland and changes to Los Alamos National Laboratory's operational practices that have affected outfall volumes discharging to the wetland. This report presents the results of monitoring conducted for surface water, alluvial groundwater, and geomorphology between April and December 2014. The data are assessed relative to baseline conditions presented in the Sandia Wetland Performance Report, Baseline Conditions 2012–2014, to identify any physical and geochemical changes during the monitoring period. In addition, quantitative baseline vegetation data are presented. Monitoring data include water levels and water chemistry from an array of 13 piezometers installed in the wetland; surface water and storm water data from 2 gaging stations located upstream of the wetland and 1 gaging station located downstream; vegetation monitoring; and geomorphic/topographic cross-sections.

The monitoring performed during the performance period indicates the Sandia wetland is stable following the installation of the GCS, even with declining effluent volumes entering the wetlands. The GCS has effectively arrested headcutting at the terminus of the wetland. Groundwater within the shallow alluvium remains reducing, and no obvious temporal trends in chemistry have been observed. Water levels have not dropped below the levels observed in 2013, even in light of reduced effluent volumes, and remain sufficiently high to sustain obligate wetland vegetation. Even the upper portion of Reach S-2 (the second reach down from the headwaters of Sandia Canyon and the reach that encompasses the Sandia wetland), which had been previously dewatered and is outside the current footprint of the wetland, retains reducing conditions at depth within alluvial groundwater. Storm water data indicate the GCS has had a positive impact in terms of contaminant mobility. Despite only slightly decreased storm flow discharge pre- and post-GCS, suspended sediment, polychlorinated biphenyls, and chromium concentrations have decreased significantly immediately downgradient of the wetland post-GCS, presumably from the elimination of headcutting at the terminus of the wetland.

Topographic surveys of cross-sections indicate erosion within the wetland proper is dominated by channel rearrangement (e.g., avulsion), and eroded areas are usually associated with nearby depositional pockets. In the upland/overbank zone, some areas of deposition are the result of sediment input (e.g., alluvial fans, slope wash) from side slopes and drainages, and some are localized scour within small side channels. Overall, erosion within the system seems to be associated with scouring in small side channels outside the wetland proper or channel rearrangement within the wetland proper.

In the upper (western) stretch of the reach, there appears to be some aggradation of the thalweg, but the overall thalweg gradient appears to be stable since the previous survey. There is some evidence for a lengthening of the thalweg in the lower portion of the reach (the thalweg is well-defined over a larger stretch of the reach than in the previous survey), possibly indicating a tendency towards more localized channelized versus distributed flow. However, in both the upper and lower stretches of the reach, where the thalweg is well defined, favorable thalweg sinuosity has changed little since the previous survey. There appears to be a new nick point in the lower (eastern) portion of the reach located within a stretch where the thalweg is otherwise characterized by a shallow slope. A new channel may be associated with the nick point, located upgradient of Sheet Pile 1, and local erosion below the new base level created by the GCS. Monitoring of these features in subsequent years will assess whether these features are transient adjustments to the new base level.

Quantitative vegetation results collected and presented in this report represent baseline conditions because vegetative surveys were initiated only in 2014. Baseline results indicate excellent ingrowth of newly planted wetland vegetation in the area of the GCS. Robust cattail-dominated vegetation was documented throughout the lower two-thirds of the wetland.

Overall, the wetland appears to have retained physical and chemical stability relative to baseline conditions during the monitoring period.

CONTENTS

Figures

Tables

Appendixes

1.0 INTRODUCTION

The Sandia Canyon wetland expanded from a relatively small footprint in the early 1950s in response to liquid effluent released by the Los Alamos National Laboratory (LANL or the Laboratory) at the head of Sandia Canyon. The wetland has been supported since then by continued effluent releases to the canyon. Contamination is present in wetland sediments because of historical releases from Laboratory operations (LANL 2009, 107453).

The Laboratory has prepared this “Sandia Wetland Performance Report, Performance Period April 2014–December 2014” in response to requirements set forth in the “Work Plan and Final Design for Stabilization of the Sandia Canyon Wetland” (LANL 2011, 207053). In that document, the Laboratory proposed reporting of Sandia wetland monitoring data to the New Mexico Environment Department (NMED) by April 30 of each year. The requirement for designing a Sandia wetland monitoring program was previously set forth in NMED’s “Approval with Modification, Interim Measures Work Plan for Stabilization of the Sandia Canyon Wetland” (NMED 2011, 203806) in response to the Laboratory’s “Interim Measures Work Plan for Stabilization of the Sandia Canyon Wetland” (LANL 2011, 203454). The monitoring plan was provided in the work plan (LANL 2011, 207053) and is summarized in section 1.5 of this report. The monitoring plan is designed to identify physical or chemical changes in the Sandia wetland related to (1) the installation of a grade-control structure (GCS) at the terminus of the wetland (LANL 2013, 251743) and (2) changes in outfall chemistry and discharge volumes related to the Sanitary Effluent Reclamation Facility (SERF) expansion (DOE 2010, 206433).

This report is the second annual report that will assess the overall condition and stability of the wetland in the context of the GCS at the terminus of the wetland and changes to the volume and chemistry of effluent released into Sandia Canyon resulting from changes in the Laboratory’s water-management practices associated with SERF and National Pollutant Discharge Elimination System (NPDES) Outfall 001. The results of monitoring conducted for surface water, alluvial groundwater, and geomorphology over the period from April 2014 to December 2014 are presented herein. Data are assessed relative to baseline conditions presented in the Sandia Wetland Performance Report, Baseline Conditions 2012–2014 (LANL 2014, 257590) to identify any physical and geochemical changes during the monitoring period. In addition, quantitative baseline vegetation data are presented. Monitoring data include water levels and water chemistry from an array of 13 piezometers installed in the wetland; surface water and storm water data from 2 gaging stations located upstream of the wetland and 1 gaging station located downstream; vegetation monitoring; and geomorphic/topographic cross-sections.

Hexavalent chromium [Cr(VI)] was historically released into liquid effluent from the Technical Area 03 (TA-03) power plant (TA-03-22) at the head of Sandia Canyon from 1956 to 1972. Some of the Cr(VI) made its way to the regional aquifer beneath Sandia and Mortandad Canyons, and Cr(VI) concentrations in the regional aquifer presently exceed NMED groundwater standards and U.S. Environmental Protection Agency (EPA) maximum contaminant levels. The Sandia Canyon wetland performance monitoring is related to the overall chromium remediation project because a large portion of the original chromium inventory and other contaminants (e.g., polychlorinated biphenyls [PCBs], see section 1.1) are currently sequestered in the wetland sediment, as described below. The results of characterization work conducted to date in Sandia Canyon are described in the “Investigation Report for Sandia Canyon” (hereafter, the Phase I IR) (LANL 2009, 107453), and in the “Phase II Investigation Report for Sandia Canyon” (hereafter, the Phase II IR) (LANL 2012, 228624).

Information on radioactive materials and radionuclides, including the results of sampling and analysis of radioactive constituents, is voluntarily provided to NMED in accordance with U.S. Department of Energy policy.

1.1 Project Goals

Geochemical reducing conditions within the Sandia wetland converted some of the Cr(VI) released from 1956 to 1972 to stable, relatively insoluble trivalent chromium [Cr(III)]. A significant inventory of chromium as Cr(III), possibly around 15,000 kg, remains in wetland sediment (LANL 2009, 107453). Although studies presented in the Phase I IR have shown the trivalent form of chromium is unlikely to oxidize and convert to mobile hexavalent chromium (LANL 2009, 107453), maintaining the reducing condition is a prudent measure to ensure stability of the chromium inventory within the wetland sediment. The wetland also contains constituents such as PCBs adsorbed to sediment that remain in situ as long as the wetland sediment remains physically stable because of the root-binding effects of vegetation. Abundant vegetation also enhances deposition of suspended solids from storm water. PCB loads in the wetland sediments are estimated to be 5.5 kg, 3.3 kg, 31.1 kg, and 24.4 kg for Aroclor-1242, Aroclor-1248, Aroclor-1254, and Aroclor-1260, respectively (LANL 2009, 107453).

The overall objective of this project is to monitor the physical and chemical stability of the Sandia wetland in the context of its contaminant inventory. Monitoring was initiated because of erosion at the terminus of the wetland, subsequent construction of the GCS, and anticipated decreases in discharge volume associated with the SERF expansion.

The monitoring presented in this report is intended, in part, to assess the stabilizing impacts of the GCS on the eastern terminus of the wetland. Before the GCS was constructed, the terminus of the wetland had an active headcut (up to 3 m high). Installation of the GCS has arrested the headcut, thereby stabilizing the grade, and monitoring indicates the GCS is promoting vegetative, hydrologic, and geochemical function at the easternmost end of the wetland by backing up groundwater because of its impervious subgrade face (section 1.3). Maintenance of physical and chemical stability will, in turn, help prevent potential physical mobilization of adsorbed contaminants associated with sediment and chemical mobilization of precipitated contaminants under changing geochemical conditions (LANL 2011, 203454; LANL 2011, 207053).

The Sandia wetland has concurrently experienced decreased liquid effluent volumes (both daily and annually) from NPDES-permitted Outfalls 001 and 03A027 as part of the SERF expansion project. As part of the SERF expansion, a portion of the effluent previously released to Sandia Canyon is now being rerouted to cooling towers at various facilities, including the Strategic Computing Complex (SCC). Effluent releases to Sandia Canyon may be reduced further, although at levels sufficient to maintain the ecologic, hydrologic, and geochemical functioning of the wetland. If changes to effluent volume or chemistry are shown to adversely impact the wetland, adaptive management will be used to ensure wetland stability (e.g., engineered controls to manage sediment and water distribution to increase the area of wetland saturation).

More detailed background on the SERF-related outfall chemistry and discharge volume changes is provided in section 1.4. The monitoring plan and associated rationale designed to identify physical and chemical changes in the wetland are presented in section 1.5. A conceptual model for wetland performance is presented in section 1.6. Sampling and analysis during the performance period April 2014 to December 2014 is presented in section 2, with results of monitoring presented in section 3. Section 4 details monitoring results in the context of wetlands performance metrics and suggests proposed changes to the monitoring plan.

1.2 Timeline

A graphical timeline showing changes related to outfall discharge and chemistry, the construction of the GCS, the addition of piezometer monitoring locations, and associated sampling events is shown in Figure 1.2-1. The following sections refer to this timeline.

1.3 Design and Function of the Grade-Control Structure

The location of the GCS is shown in Figure 1.3-1. The overall objectives of the GCS were to arrest the headcut in the lower portion of the wetland and to maintain hydrologic and geochemical conditions to minimize contaminant migration. The GCS was designed to meet the following objectives:

- Provide an even grade to allow wetland expansion and further stabilization
- Be sufficiently impervious to prevent the draining of alluvial soils and promote a high water table
- Facilitate nonchannelized flow
- Minimize erosion during large flow events
- Support wetland function under potentially reduced effluent conditions

The GCS transitions the grade approximately 11 vertical feet from the elevation of the wetland just upgradient of the former headcut location to the natural stream bed just upstream of gage E123. To maintain grade and to reduce the overall fill and size of a single structure, a set of three steel-sheet-pile walls was installed with smaller elevation drops. Downstream of the third sheet-pile wall, a cascade pool was constructed of boulders and cobbles to transition to the final grade. The transition from the wetland above the GCS to the stream channel below is gradual, smooth, and stepped to prevent erosive flows that could scour and destabilize the stream reach below the structure (LANL 2013, 251743). Design features should also allow reduction of outfall effluent in the canyon without compromising the physical and geochemical function of the wetland, particularly of the eastern terminus where the GCS controls wetland water levels. The area behind the GCS was backfilled and wetland vegetation was planted to allow expansion of the wetland area. These measures physically stabilize the wetland by reducing sediment and associated contaminant transport into the lower sections of the canyon and should also maintain reducing conditions within the sediment near the terminus of the wetland, thus contributing to the goal of reducing potential contaminant transport (LANL 2013, 251743). A set of as-built diagrams for the GCS can be found in Appendix C of the completion report for the construction of the GCS (LANL 2013, 251743).

Previous stabilization efforts involved the planting of cottonwood and willow stems in March and April 2007 to help stabilize contaminated sediment deposits, slow floodwaters, enhance the deposition of sediment and associated contaminants, and improve habitat (LANL 2009, 107453).

1.4 Sandia Canyon Outfalls and SERF

Outfalls have released liquid effluent to Sandia Canyon since the development of TA-03 in the early 1950s. Currently, three NPDES-permitted outfalls release to upper Sandia Canyon upstream of the wetland: Outfalls 001, 03A027, and 03A199 (EPA 2007, 099009) (Figure 1.3-1). Effluent releases at these outfall discharge points are monitored in compliance with the Laboratory's industrial NPDES permit (Permit No. NM0028355, EPA 2014, 600257). Since the Laboratory's investigation of chromium contamination in groundwater began in 2006 and until mid-2012, releases to the canyon were generally as follows. NPDES Outfall 001 discharged liquid effluent, predominantly from the Laboratory's TA-46 Sanitary Waste Water System (SWWS) plant, the TA-03 steam plant boilers, and TA-03 power plant cooling towers. Figure 1.4-1 shows daily, monthly, and yearly average effluent volumes since 2006 for Outfall 001, which releases the greatest volume of effluent to Sandia Canyon. From 2006 to 2011, average discharge ranged from approximately 230,000 to 300,000 gallons per day (gpd). NPDES Outfalls 03A027 and 03A199 (Figure 1.3-1) associated with facility cooling of the SCC and the Laboratory Data Communications Center (LDCC), respectively, also discharge to upper Sandia Canyon. Figure 1.4-1 shows daily releases from August 2007 to January 2010 and from November 2012 to December 2014 for these two outfalls. These two outfalls contributed approximately 50,000 to 100,000 gpd of cooling water effluent to the canyon between 2007 and 2010. The water source for both the SCC and LDCC cooling towers was potable water during that time period. Together, these three outfalls (001, 03A027, and 03A199) have provided sufficient water to maintain wetland vegetation growth, which promotes stability of the wetland. The more current discharge histories of these outfalls are described below.

In August 2012, the SERF expansion project enabled tertiary treatment of SWWS effluent so the water can be reused/recycled in Laboratory cooling towers and the effluent meets new stricter EPA limits on PCB discharge concentrations. The treatment methods employed at SERF are chemical precipitation, flocculation, microfiltration, reverse osmosis (RO), and pH adjustment. Figure 1.4-2 shows a process schematic for water flow through SWWS to SERF, the power plant, and to cooling towers, and the subsequent connections to Outfalls 001 and 03A027. The schematic shows treated sanitary effluent can go either to TA-03 (reuse tank/SERF) or to Outfall 13S in Cañada del Buey. It should be noted that treated sanitary effluent has never been discharged to Cañada del Buey. That pathway (Outfall 13S) remains in the NPDES permit as an option. The SERF RO product water is extremely pure; the process removes metals, silica, organic compounds, and inorganic salts. The SERF product water is blended at an approximate 4:1 ratio with SWWS effluent (i.e., 4 parts SERF RO product to 1 part SWWS effluent) for reuse in the SCC cooling towers or to be released at Outfall 001. The use of the SERF-blended water has been phased in according to the following schedule and has resulted in the following changes to effluent volume and water quality released to the wetland, as shown in Figure 1.2-1.

August 2012: The SERF expansion began operation, treating SWWS effluent to meet PCB effluent standards. SERF RO to SWWS waters were blended at approximately a 4:1 ratio and released at Outfall 001. The resulting blended water chemistry has increased water quality over previous effluent chemistry because constituent concentrations in the SERF-blended water are approximately 20% of concentrations present in the SWWS effluent. Direct effluent from the power/steam plant is also released at Outfall 001. The August 2012 operational change had little, if any, effect on effluent volumes because no reuse in cooling towers occurred during this time period. Figures D-1.0-1 through D-1.0-3 in Appendix D demonstrate the SERF expansion has lowered the chloride, nitrate plus nitrite, and silicon dioxide concentrations at Outfall 001. Effluent concentrations in the winter months are thought to be elevated compared with the summer months because a greater volume of power/steam plant effluent is released to the outfall during the winter months, and that water is not treated through the SERF.

April 2013: The SCC cooling towers switched their water source from potable water to SERF-blended water. Figure 1.4-3 shows effluent volumes released at Outfall 001 and from the SCC cooling towers, which release to Outfall 03A027, from November 2012 to December 2014. The figure also shows the water sources used at the SCC cooling towers, which include potable water and SERF-blended water. Between November 2012 and April 8, 2013, the SCC cooling towers underwent a trial period in which they transitioned from using potable water to using SERF-blended water, which had been previously released at Outfall 001. That trial period is evident in the early-time information shown in Figure 1.4-3, where the quantities of potable makeup water (blue line) and SERF makeup water (red dotted line) are highly variable. On April 9, 2013, the transition was completed, and since then the cooling towers have almost exclusively used SERF-blended water as their cooling water source, resulting in lower effluent releases at both Outfalls 001 and 03A027. Overall, the transition has substantially decreased effluent volumes at Outfall 001. For example, the long-term average discharge at Outfall 001 between 2006 and 2012 was 279,000 gpd and for 2014 it was 156,000 gpd. This represents a long-term decrease of 123,000 gpd (44%) at this outfall. Daily variations in effluent flow have also decreased. Outfall volumes at Outfall 001 vary seasonally with higher releases during the winter months than in the summer months. The steam plant releases more water to the outfall during the winter because it is used for steam heating of several large buildings. In addition, the cooling towers require less cooling water during the winter months, and more SERF-blended water is released directly Outfall 001. The spike in effluent volume on September 13 and 14, 2013, corresponds to the large rain event (Figure 1.2-1) because the evaporation basins at SWWS took on many inches of rainwater that were routed up through the treatment system. The use of SERF-blended water in the SCC cooling towers has allowed for additional cycling of cooling water in the towers without buildup of precipitates from lower levels of silica in SERF-blended water as compared with potable water. With the additional cycles, effluent volumes at Outfall 03A027 have dropped from approximately 50,000 gpd to 26,000 gpd. The LDCC cooling towers continue to use potable water at rates that have not changed with the SERF expansion.

Future: Future plans allow for the SERF to run at full capacity so Laboratory computing facilities have access to larger amounts of SERF-blended water for cooling. The variability in effluent volumes and water chemistry that may be released to the wetland will depend on return flow from facilities to outfalls that release to the wetland.

1.5 Monitoring Performed during the Performance Period

The detailed monitoring plan for the Sandia wetland is found in section 6.0 of the "Work Plan and Final Design for Stabilization of the Sandia Canyon Wetland" (LANL 2011, 207053). Proposed revisions to the monitoring plan were presented in the Sandia Wetland Performance Report, Baseline Conditions 2012–2014 (LANL 2014, 257590).

The initial work plan (LANL 2011, 207053) called for a multiphased approach to monitoring to evaluate hydrologic and geochemical changes associated with the GCS and/or with the SERF expansion and subsequent effluent reduction:

- Evaluate changes in hydrology and key geochemical indicators to monitor the health of the wetland at 12 alluvial wells
- Evaluate transport of metals and organic chemicals through the wetland by monitoring surface-water base flows and storm flows at three gaging stations
- Monitor vegetation every 2 yr via photo surveys
- Conduct periodic geomorphic surveys to evaluate erosion and aggradation of sediments within the wetland.

Monitoring of alluvial chemistry has been accomplished through a series of 13 drive-point piezometers arranged in 4 transects in the wetland (Figure 1.3-1) that were scheduled to be sampled quarterly. Figure 1.5-1 is a schematic of piezometer transects and depths with recent water levels.

The piezometer transects are as follows.

- Piezometers SCPZ-1 to SCPZ-3 are located on a sand-and-gravel terrace near the active channel (c1 geomorphic unit) towards the western end of the wetland, which has experienced channel incision and dewatering relative to historical conditions. These piezometers are located on the c3 geomorphic unit away from the active channel and associated inset terrace (c2a geomorphic unit), which are locations of recent cattail expansion. Piezometer SCPZ-1 is screened towards the base of alluvial fill, while the top of the screens in piezometers SCPZ-2 and SCPZ-3 are approximately 6 ft and 3 ft below ground surface (bgs), respectively (see Table 1.5-1 and Figure 1.5-1). The ground surface is predominantly dry at this transect.

- Piezometers SCPZ-4 to SCPZ-6 form a transect in the widest portion of the wetland, and the tops of their screens are approximately 3 ft bgs. The wetland water level is at or very near the ground surface at this transect. It is at these shallowest depths that changes in water level and sediment oxidation state are expected to manifest as a result of reduced effluent discharge. Similarly, the lateral margins of the wetland may dewater before the longitudinal axis of the wetland as a result of reduced effluent volumes. This effect could be most pronounced where the wetland is widest and water flux is most spread out. It is also at such locations that preferential flow paths within the alluvium might be expected to form.
- Piezometer transect SPCZ-7 to SCPZ-9 is located in a narrow part of the wetland closer to its distal (eastern) end. This set of piezometers includes two shallow piezometers and one piezometer screened slightly deeper (see Table 1.5-1 and Figure 1.5-1). The wetland water level is at or just below the ground surface at this transect. These piezometers provide indications of changes near the surface of the wetland and at depth in a narrow portion of the wetland where preferential flow paths are less likely to develop.
- The final transect of piezometers SCPZ-10 to SCPZ-12 is located next to alluvial well SCA-1-DP (and the previous location of SCA-1) and will monitor the effect of the GCS. The wetland water level is at or near the surface at this transect. Water was routed around this area during the period of construction of the GCS. Data from these piezometers have not been reported previously because of difficulties in sampling. Representative samples were obtained during the current performance period and are reported herein.

The sampling and analysis plan for the July and November rounds of 2014 at these piezometers is provided in Table 1.5-2. Most of the analyses were designed as indicators of redox changes and/or indicators of organic matter degradation associated with potential dewatering of the wetland. Piezometers were also instrumented with sondes for continuous monitoring of water levels, specific conductance, and temperature. The same analytical suite was monitored at surface water gaging stations E121, E122, and E123 (see Figure 1.3-1). Analyses of storm water samples collected in 2014 were planned as presented in Table 1.5-3. Analytical results are discussed in section 3 with data plots provided in Appendix D and analytical data available on CD (Appendix E).

Input and output water volumes are measured at gaging stations E121, E122, and E123 (Figure 1.3-1), and water levels are monitored in the piezometers.

Baseline and repeat topographic cross-sections were surveyed throughout the wetland to assess possible geomorphic change in the wetland. Details of the monitoring scheme and results are presented in Appendix B. The Laboratory also established baseline vegetation cross-sections to quantitatively define the extent of obligate wetland species that depend upon saturated wetland conditions. Details of the monitoring scheme and the results from these baseline surveys and associated photographs are shown in Appendix C. This monitoring effort replaces and supersedes that originally proposed.

The GCS is inspected quarterly and following rain events with discharges greater than 50 cubic feet per second (cfs) (LANL 2014, 600083). If erosion or any indications of instability are observed, appropriate actions will be taken to ensure continued stability and functionality of the GCS. Inspections also assess sediment inputs from the County landfill such as those that occurred during September 2013 flooding (LANL 2014, 600083).

1.6 Conceptual Model for Assessing Wetland Performance

1.6.1 Hydrologic and Geochemical Status

The Sandia wetland is predominantly an effluent-supported cattail wetland. Mapping of the generally organic-rich wetland sediment shows thicknesses ranging from approximately 13 ft at the western end of the wetland to approximately 8 ft at the eastern end (LANL 2009, 107453, Figure 7.1-1). Based on the presence of anthropogenically derived materials throughout the sediment deposits, much of the sediment has accumulated since 1942 as Laboratory development and operations in upper Sandia Canyon have occurred. Shallow alluvial groundwater, perched on Bandelier Tuff, is present throughout the wetland and expresses as surface water in the middle and lower portions. Surface waters generally pass over the wetland with a short residence time (LANL 2009, 107453; LANL 2014, 257590). Surface water flow within the wetlands occurs both as unchannelized flow in locations where no channel exists (the central portion of the wetlands) and as channelized flow (the western and eastern extent of the wetlands). Water present within the alluvial/wetland sediment has much longer residence times. Minor infiltration and mixing of alluvial water by base flow surface water appears to occur (LANL 2014, 257590). The sediment is generally fully saturated at the eastern end of the wetland; these conditions extend westward, but near-surface sediment is unsaturated at the margins and at the western end of the wetland, which was largely dewatered more than a decade ago when the outfall was relocated and the associated channel incised. The history of effluent discharges is discussed in section 1.4. Substantial decreases in effluent volumes have occurred recently from the recycling of SERF water in the cooling towers and could potentially lead to dewatering of portions of the wetland. The upper portion of the wetland is the most vulnerable because the GCS is designed to maintain saturated conditions in the lower portions of the wetland.

A water-balance analysis conducted during 2007 and 2008 is summarized in the Phase I Sandia Canyon IR (LANL 2009, 107453). That study showed little surface water loss (approximately 2% of both effluent and runoff) occurs through the wetland area. A direct-current (DC) electrical-resistivity–based geophysical survey was conducted as part of the Phase II Sandia Canyon investigation to provide a model of electrical properties of subsurface materials of the region beneath and adjacent to the wetland in upper Sandia Canyon (LANL 2012, 228624). The DC resistivity survey found that large continuous areas of the wetland are underlain by highly resistive welded tuffs (Qbt2 of the Tshirege Member of the Bandelier Tuff) that probably represent a significant barrier to the infiltration of surface and alluvial water into the subsurface. A very conductive layer extending from the surface to 20 ft to 25 ft bgs (6.1 m to 7.6 m bgs) correlates well with an alluvial aquifer perched on a welded tuff unit. In several areas, the survey also identified subvertical conductive zones that penetrate the upper bedrock units and in some cases appear to correlate with mapped fault and/or fracture zones. These subvertical conductive zones are noted because they may represent present-day or historical infiltration pathways. However, the DC resistivity data do not differentiate between conductive zones that contain higher water content (possibly representing active infiltration) and wetted clay-rich fracture fill that may hinder infiltration.

Storm water–induced flooding can cause erosion and, most importantly, headcutting at the terminus of the wetland. As such, sediment stability is key to wetland performance and was one of the major objectives for construction of the GCS. The wetland vegetation community is important in mitigating storm water–related mobilization of contaminants through root binding and physical trapping of suspended sediments in storm flow. Wetland vegetation may also directly uptake certain contaminants (LANL 2009, 107453). In many ways, the vegetation community can be seen as a surrogate for the depth of the water table in the wetland. For example, if the water table rises and persistently saturates soils around ponderosa pines located along the margin of the wetland, they will likely die. Conversely, when the water table lowers, wetland vegetation is replaced by upland species. Healthy cattail wetlands require a high water table because cattails are obligate wetland species.

The chemistry of effluent water entering the wetland has recently changed as a result of changes in blended ratios of SERF to SWWS water and in cooling tower recycling (see section 1.4). Depending upon the amount of exchange between surface water and groundwater, “cleaner” input waters could potentially affect contaminant stability, although blending of SERF and SWWS water should effectively preclude this possibility. Surface water measured under base flow conditions at gage E121 is affected by the water chemistry of the effluent released at Outfalls 001 and 03A027. Water chemistry measured under base flow conditions at gaging station E122 is affected by effluent chemistry from Outfall 03A199 (Figure 1.3-1). Outfall 001 discharges a much greater volume of water than the other two outfalls, and SERF-related chemistry and discharge volume changes are limited to outfalls flowing to gaging station E121.

Alluvial saturation, along with significant amounts of solid organic matter (SOM) produced from wetland vegetation, results in reducing alluvial aquifer conditions as indicated by detectable concentrations of ammonia and sulfide, high dissolved iron and manganese concentrations, and low nitrate and sulfate in alluvial water (LANL, 2014, 257590). Nitrogen isotope studies of cattails also verify the strong reducing conditions in the wetland sediments by demonstrating that the wetland is an actively denitrifying environment (Heikoop et al. 2002, 107001; Fair and Heikoop 2006, 098045).

1.6.2 Contamination in Wetland Sediment

Detailed sediment mapping was performed during the Phase I investigation of Sandia Canyon (LANL 2009, 107453). Sediment Reach S-2, which contains the Sandia wetland, is the most important reach in Sandia Canyon in the context of sediment contamination. It contains the highest concentrations and proportion of the contaminant inventory because of its proximity to contaminant sources, the large volume of sediment deposited during the period of active contaminant releases, the presence of high concentrations of organic matter in the wetland, and the presence of large amounts of silt and clay. Contaminants commonly adsorb to, or are precipitated in association with, sediment particles or organic matter. The fine-grained sediment in the wetland reach has a higher silt and clay content than the other reaches, contributing to higher contaminant concentrations (average of 60% silt and clay in Reach S-2 fine-grained sediments, compared with averages of 30% to 43% in other investigation reaches in the western part of Sandia Canyon).

Chromium is the major inorganic contaminant in the wetland that could be affected by both redox changes in the wetland and physical destabilization. Sections 1.0 and 1.1 present background on chromium contamination in wetland sediments. Arsenic may also be released from wetland sediments upon dewatering (LANL 2009, 107453). Two important organic contaminants, PCBs and polycyclic aromatic hydrocarbons (PAHs), are primarily subject to physical transport in floods because of low solubilities and a strong affinity for organic material and sediment particles. Important source areas for these contaminants are the former outfall for the power plant cooling towers in upper Sandia Canyon (chromium), a former transformer storage area along the south fork of Sandia Canyon (PCBs), and the former asphalt batch along the north fork of Sandia Canyon (PAHs) (LANL 2009, 107453).

1.6.3 Cr(III) Stability in the Sandia Wetland

Dewatering could reduce the physical stability of alluvial sediments and could lead to physical contaminant mobilization. It is possible, although unlikely, that the existing chromium inventory within the wetland could be oxidized to its mobile Cr(VI) state though oxidation of Cr(III) to Cr(VI). Oxidation by atmospheric oxygen at environmental temperatures is not a known mechanism based on review of the relevant literature. Direct oxidation of Cr(III) to Cr(VI) by atmospheric oxygen has only been associated with high-temperature forest fires and burning of organic matter to produce alkaline vegetation ash (Panichev et al. 2008, 256734). Oxidation by manganese oxides under aqueous conditions is the primary mechanism responsible for oxidation of Cr(III) to Cr(VI) (Rai et al. 1989, 249300).

A critical topic to address regarding Cr(III) stability in the Sandia wetland is the presence and reactivity of chemical reductants, including Fe(II) and SOM, to prevent or limit oxidation of Cr(III) to Cr(VI) (discussed in more detail in Appendix J of the Phase I IR [LANL 2009, 107453]). Mass balance calculations were performed to quantify the reducing capacity of the Sandia wetland by measuring sediment concentrations of one of the reductants, Fe(II), and an important oxidant, Mn(IV), to determine if there are excess concentrations of Fe(II) to keep Cr(III) stable within the wetland. Complete oxidation of Cr(III) to Cr(VI) is likely to take place if the molar concentrations of Mn(IV) exceed those of Fe(II), Cr(III), and organic carbon. This situation, however, is rare within the active Sandia wetland because concentrations of total iron, consisting mainly of Fe(II), and SOM are present at much higher weight-percent concentrations than Mn(IV), which is usually present in the ppm range. During wetland drying and oxidation, however, Fe(II) can oxidize to Fe(III) and Mn(II) can oxidize to Mn(IV), making Mn(IV) available to oxidize Cr(III) to Cr(VI).

Experiments were conducted on several Sandia wetland samples to quantify the potential release of chromium during dewatering and drying of the wetland material (LANL 2009, 107453). Dried samples were leached both with deionized and SWWS water. Total chromium concentrations in the SWWS effluent ranged from 1.4 ppb to 5 ppb in samples collected from February 2001 to June 2009. Most of the dissolved chromium in the wetland leachates occurred as Cr(III). Cr(VI) ranged from 0.06 ppb to 14.49 ppb in the leachates. With the exception of one sample from the SOM-poor gravel and sand bank of the already dewatered upper portion of the wetland, Cr(VI) concentrations in leachates were less than 1 ppb. During drying, Cr(III) in most samples appears to remain stable, suggesting insufficient Mn(IV) is produced to oxidize appreciable amounts of Cr(VI).

Total “dissolved” chromium in leachates was primarily in the form of Cr(III), indicating most chromium measured in a filtered sample occurs as colloids. This explanation is supported by analytical results for surface water collected downstream of the wetland at gage E123 that was filtered through 0.45-, 0.22-, and 0.02-µm membranes before acidification and analyses for chromium. Concentrations of total chromium decreased dramatically in the 0.02-µm aliquot relative to typical filtration at 0.45 µm, suggesting the presence of colloidal chromium, possibly stable as amorphous $Cr(OH)_3$ or $Fe_xCr_{1-x}(OH)_3$ and/or as chromium species adsorbed onto clay minerals and iron oxides and hydroxides.

Some evidence from the leaching experiments indicates that atmospheric oxygen may be an important component for enhancing the leaching of chromium from the wetland samples. In some cases, higher leached concentrations of Cr(VI) were seen in samples that were oven or air dried versus samples that were vacuum dried. This likely does not represent direct oxidation of Cr(III) to Cr(VI) but rather oxidation of Mn(II) to Mn(IV), which was then available to oxidize Cr(III) in the leaching experiments.

1.6.4 Current State of the Sandia Wetland

Data from geochemical studies presented in the Phase I IR (LANL 2009, 107453) indicate chromium in wetland sediments is predominantly geochemically stable as Cr(III) and the proportionally high chromium inventory in the wetland is not likely to become a future source of chromium contamination in groundwater, especially if saturated conditions can be maintained within the wetland.

With installation of the GCS, the downgradient portion of the wetland should remain both physically and geochemically stable. Ongoing monitoring will determine the ultimate efficacy of the GCS in maintaining wetland stability. Monitoring will also help determine wetland response to changing outfall discharge volumes. Results from baseline monitoring of the wetland (LANL 2014, 257590) also suggest the system is remaining chemically and physically stable.

2.0 SAMPLING AND ANALYSIS

The original work plan (LANL 2011, 207053) stipulated quarterly monitoring. However because of issues with freezing temperatures in the wetland during the winter and the need to coordinate sampling with quarterly sampling of the Chromium Monitoring Group, sampling was conducted only three times in 2014 (March, July, and November). March sampling was reported in the baseline monitoring report (LANL 2014, 257590). The quarterly sampling is now coordinated with Chromium Monitoring Group sampling that is part of the Interim Facility-wide Groundwater Monitoring Plan. Sampling is conducted at 14 locations within the wetland, including 13 piezometers and 1 drive-point alluvial well (SCA-1DP) as well as at surface water gaging stations E121 and E122 (above the wetland) and E123 (below the wetland) (Figure 1.3-1). Microfiltration was added to samples for metals analysis from the piezometers to reduce colloidal effects. Samples for metals analysis were microfiltered at 0.2 µm during the March 2014 sampling event and at 0.02 µm during the July and November 2014 events. Plots of microfiltered metal concentrations are compared with 0.45-µm filtered data in Appendix D.

Sondes located at SCPZ-5 and SCPZ-9 were lost in the flood event that occurred in September 2013, and the remaining sondes were removed in November 2013 to prevent them from freezing. Sondes were reinstalled in all of the piezometer locations, except at SCPZ-7, in June 2014. It was determined that the sondes at locations within the channel would likely not freeze and thus these sondes were left in place for the 2014–2015 winter season (locations SCPZ-1, SCPZ-5, SCPZ-8, and SCPZ-12).

Full suites were collected at SCPZ-1 through SCPZ-6, SCPZ-11B, SCPZ-12, and all three gaging stations. Prioritized suites were collected at SCPZ-7, SCPZ-9, SCPZ-10, and SCPZ-11A for at least one of the two sampling events. A summary of analytical samples collected is provided in Table 2.0-1. The piezometers yielded insufficient nitrate for isotopic analysis. Some sulfide and ammonium samples exceeded holding times and are therefore assessed in terms of their presence or absence rather than absolute values to determine if reducing conditions were present. Cr(VI) was not measured during the July 2014 and November 2014 rounds but was collected during the February 2015 round and will be reported in the next in this series of wetlands performance reports. Field parameter data were collected for both sampling rounds and are provided in Table 2.0-2. Water level, specific conductance, and temperature data collected by the sondes are discussed in section 3.3.

Surface water gaging stations E121 and E122 are located on the western boundary of the Sandia Canyon watershed. Surface water gaging station E123 is located at the eastern boundary below the terminus of the wetland. Figure 1.3-1 shows the location of the gaging stations, outfalls, and the extent of the Sandia wetland. Station E121 measures discharge from Outfalls 001 and 03A027 and storm water runoff from approximately 50 acres from TA-03. Station E122 measures discharge from Outfall 03A199 and storm water runoff from approximately 50 acres from TA-03. Station E123 measures surface water flow below the wetland, including discharge from all three outfalls and storm water runoff from approximately 185 acres, 100 acres of which are from E121 and E122.

In 2014, ISCO 3700 automated samplers attempted to collect storm water samples when discharge at the gaging station was greater than 10 cfs at E121 and E123, and greater than 5 cfs at E122. Storm water analyses in 2014 were conducted according to the analyses listed in Table 1.5-3. The sampler at E121 was turned on for the monsoon season June 5, 2014, and turned off for the winter on November 24, 2014. The sampler at E122 was turned on June 5, 2014, and turned off for the winter on November 11, 2014. The sampler at E123 was turned on May 21, 2014, and turned off for the winter on November 24, 2014. Stations E121 and E123 are equipped with a Sutron 9210 data logger, an MDS 4710 radio transceiver, and a Sutron Accubar bubbler. Station E122 is equipped with a Sutron 9210 data logger, an MDS 4710 radio transceiver, and a Siemens Milltronics ultrasonic probe. Stage is recorded every 5 min and transmitted to a base station where it is archived in a database. All three stations are equipped with two automated ISCO samplers: one with a 24-bottle base for SSC analyses, and one with a 12-bottle base for collection of chemistry samples.

For each sample-triggering storm event in 2014, Table 2.0-3 shows precipitation at rain gage RG121.9 and storm water peak discharge and whether a sample was collected at E121, E122, and E123. Storm water discharge at E121 equaled or exceeded 10 cfs eight times during 2014; samples were collected from five of these discharge events and on one event when discharge was less than 10 cfs. Discharge at E122 equaled or exceeded 5 cfs on seven occasions; samples were collected on four of these events. Discharge at E123 exceeded 10 cfs nine times during 2014; samples were collected from seven of these events.

The “Work Plan and Final Design for Stabilization of the Sandia Canyon Wetland” (LANL 2011, 207053) specified semiannual vegetation photo monitoring be performed every 2 yr beginning in 2012. Initially photo surveys provided by the Laboratory’s Environmental Protection Division seemed to be adequate to fulfill this requirement. However, upon review of these photos, it was determined they did not sufficiently capture wetland margins essential for detecting early changes in vegetation. In May 2014, a set of 10 new photo locations was surveyed and was presented in Appendix B of the 2014 report (LANL 2014, 257590). In November, 2014, a more detailed approach to vegetation monitoring was adopted. Vegetation transect surveys were added to the photo documentation to further improve detection of changes in the wetland margins. A full description of the approach and results is presented in Appendix C.

Discussion of efforts to use new methods to collect wetland waters is presented in section 4.6.

3.0 MONITORING RESULTS

3.1 Analytical Results from Surface Water Gaging Stations E121, E122, and E123

As noted in the baseline performance report (LANL 2014, 257590), similar base flow chemistry for many constituents between upgradient and downgradient locations indicates a relatively short residence time for surface water and little interaction (exchange) with alluvial groundwater. This is shown for chloride, nitrate plus nitrite, and silica, which are indicators of water quality in outfall discharge, in the context of chemistry from Outfall 001 (Figures D-1.0-1 to D-1.0-3). Improvements in water chemistry discharged from Outfall 001 are obvious for chloride and silica and also for total dissolved solids (TDS), a general indicator of water quality in outfall discharge (Figures D-1.0-1 and D-1.0-3). In addition, two sensitive redox indicators, manganese and sulfate, are discussed because these base flow constituents show some evidence for temporal trends. Base flow data for two key contaminants that can be eroded from wetland sediments and entrained in surface flow, PCBs and chromium, are discussed below along with storm flow data.

In terms of indicators of improved water quality associated with SERF expansion, no strong base flow temporal concentration trends exist for filtered chloride or nitrate plus nitrite (Figures D-1.0-1 and D-1.0-2, respectively). While chloride does not show an overall concentration trend, variation post-SERF expansion is somewhat similar at gaging locations to that observed in outfall discharge (Figure D-1.0-1). Interestingly, chloride and nitrate have consistently lower concentrations at gaging station E123 relative to E121 (Figures D-1.0-1 and D-1.0-2). In the case of nitrate, this is expected because nitrate is not only a water-quality indicator, it is also a plant nutrient and a redox-sensitive species that may be reduced and assimilated during surface water transport through the wetland. Chloride, however, is a conservative species, so lower concentrations at gage E123 may be related to dilution by surface water inputs from side drainages to the wetland. Surface water base flow silicon dioxide concentrations are plotted in Figure D-1.0-3. TDS is also plotted as a general indicator of water quality associated with outfall discharge. The effect of the SERF upgrade on both parameters is clear (Figure D-1.0-3).

Among redox sensitive species, dissolved manganese in base flow also appears to be showing water quality improvements through time, including before the GCS was installed (Figure D-1.0-4). The cause of periodic spikes in manganese concentrations is not clear, but the large spike before the GCS was completed is likely associated with construction activities. Following completion of the GCS, manganese concentrations reached their lowest levels, presumably because head cutting at the terminus of the wetland ceased. Because the vast majority of the wetland is still saturated (section 3.3), it is unlikely that trends in manganese concentrations at downstream gage E123 reflect changes in redox conditions within the wetland. Further monitoring should help clarify the cause of the apparent decrease through time. Dissolved concentrations of manganese are consistently higher at gaging station E123 because alluvial waters in the wetland have high manganese levels, probably as Mn(II) (see section 3.2). The manganese detected at E123 may be present partially as Mn(II) because of relatively slow oxidation kinetics, although speciation would need to be done to confirm this hypothesis. Mn(IV) colloids are also a distinct possibility. Sulfate in surface water base flow at gaging stations E121 and E123 increases post-SERF expansion (Figure D-1.0-5). This may reflect increased use of sodium bisulfite for dechlorination of SCC cooling water. Sulfate concentrations also appear to be dropping at E123 since construction of the GCS (Figure D-1.0-5), perhaps indicating that sulfate is reducing to sulfide as waters move across the wetland.

Surface water at gaging stations E121, E122, and E123 is perennial; thus, the results for primary contaminants PCBs and chromium are separated into base flow and storm flow components. Figure D-1.0-6 shows the discharge measured at E121, E122, and E123 from 2010 to 2014 and the varying base flow at each station during this period. This figure also shows the total discharge from the three outfalls and how each gaging station is influenced by this discharge, particularly E123. For both base flow and storm flow, box and whisker plots of discharge, SSC/total suspended sediments (TSS), PCBs, and chromium are presented in Figure D-1.0-7.

The wetland contains an inventory of contaminants, including PCBs and chromium; therefore, these analytes, along with measurements of SSC and discharge, were identified as key parameters to track the performance of the GCS. Results from stations E121 and E122, which monitor most of the surface water flow into the wetland, and station E123, which monitors surface water flow out of the wetland, are plotted together to show changes in surface water discharge and chemistry from upgradient to downgradient of the wetland (Figure D-1.0-7). These plots show the range of concentrations and represent a historical baseline before GCS construction (pre-GCS) and the first year of performance monitoring after GCS construction (post-GCS). Multiple years of data are needed to fully delineate the metrics of performance for the GCS.

In Figure D-1.0-7, storm flow discharge is expectedly greater than base flow discharge for all the gaging stations. The post-GCS base flow and storm flow discharges are slightly less than the pre-GCS discharges at gaging station E123. At E121, the slight decrease from pre- to post-GCS base flow and storm flow discharges are most likely because of the outfall effluent reduction. At E122, there is little difference in base flow and storm flow discharges from pre- to post-GCS conditions. Hydrographs for the nine sample-triggering storm events recorded at E121, E122, and E123 from May 23 to July 31, 2014, are presented in Figure D-1.0-8. From the hydrographs it is apparent flow at E123 is greater than the combined flow from E121 and E122, indicating additional flow into the wetlands from tributaries downstream of E121 and E122 occurs during storm events. Table 3.1-1 shows the timing of the transmission of flood bore, or peak, from E121 and E122 downstream to E123. The average time of transmission from E121 to E123 is approximately 40 min, and the average transmission time from E122 to E123 is approximately 38 min. This indicates storm water from both upgradient stations flows through the wetland in approximately the same amount of time and quite rapidly.

Returning to Figure D-1.0-7, while base flow was not sampled for TSS after the GCS was constructed, the pre-GCS base flow TSS is significantly less than the storm flow SSC, which is typical for storm water because of the greater erosive energy of the increased discharge. Note that base flow is sampled for TSS, and storm flow is sampled for TSS pre-GCS and SSC post-GCS. The SSC in base flow is low compared with storm flow; thus, inaccuracies associated with measuring TSS in sediment-laden storm water tend not to apply. As expected, storm flow SSC at E121 and E122 are not significantly different pre- to post-GCS; however, at E123 storm flow SSC is significantly reduced after construction of the GCS, possibly because of cessation of headcutting at the terminus of the wetland. This is noteworthy because contaminants in the wetland tend to attach to sediments, and a reduction in SSC signals a potential reduction in contaminants downgradient of the wetland.

The box and whisker plots in Figure D-1.0-7 indicate that PCB and chromium concentrations in storm flow at E123 are significantly reduced after the GCS was constructed. While PCB concentrations in storm flow were significantly higher downgradient of the wetland (relative to upgradient locations E121 and E122) before the GCS was built, the concentrations are now similar upgradient and downgradient of the wetland after the GCS was constructed. In general, chromium concentrations are higher downgradient of the wetland, indicating that surface water tends to entrain colloidal Cr(III) in the wetland.

Figure D-1.0-9 shows time series plots of SSC, PCBs, and chromium concentrations for each sample-triggering storm event and their variation with the hydrograph. A fairly consistent linear correlation exists between SSC, PCBs, chromium, and discharge and is further illuminated in Figure D-1.0-10. There are exceptions to these strong linear correlations (E121 for SSC and PCBs, and E122 for chromium), yet in general these relationships are strong. The linear relationships shown in Figure D-1.0-10 were obtained after removing four SSC data points from when the ISCO sampler malfunctioned or the intake was clogged (E121 on July 7, 2014, at 16:40; E122 on July 27, 2014, at 21:24 and 21:34; and E122 on July 31, 2014, at 18:04), and then removing outliers using the standardized residual outlier method.

In addition to using the linear relationships, the sediment flux was computed for the storm water using only the samples collected (Table 3.1-2). The relationship between sediment volume and peak discharge for storm water tends to be a stronger relationship than SSC and discharge, and for all of Sandia Canyon this relationship is (R^2=0.66):

$$\text{sediment volume} = 0.08 * \text{peak discharge} - 0.81$$ **Equation 3.1-1**

3.2 Analytical Results from Piezometers

Selected analytical results for water chemistry time-series (filtered) from the piezometer array are presented in Figures D-2.0-1 to D-2.0-9. In Figures D-2.0-10 and D-2.0-11, microfiltered data for arsenic, chromium, iron, and manganese are shown for comparison. Select cross-plots for arsenic, iron, and manganese are shown in Figures D-2.0-12 to D-2.0-14. Samples were additionally microfiltered at 0.2 µm during the March 2014 round and at 0.02 µm during the July and November 2014 rounds in an attempt to eliminate colloidal particles. Time-series plots are presented in the relative spatial distribution of the piezometers in the wetland (i.e., upper plots are from the most northerly piezometer in each transect, ordered from west to east, the middle set of plots are from piezometers in the center of each transect, again ordered from west to east, and bottom plots are from the southernmost piezometer in each transect, in the same orientation) with four transects running north to south. Additionally surface water entering the wetland, E121, and exiting the wetland, E123, are plotted at the western and easternmost parts of the wetland, respectively, serving as a comparison of input and output base flow chemistry. Data from the easternmost array of piezometers was not collected for all sampling rounds because of insufficient water. Missing data are indicated by points that are not connected by a line. Because of the relatively short period of record, less emphasis is placed on temporal trends, although historical ranges in data from alluvial wells

SCA-1 and SCA-1-DP from 2006 to 2011 are included as gray-shaded areas on the SCPZ-10 (the closest piezometer to SCA-1-DP) plot to provide a longer baseline context. It is recognized that with little data from the easternmost transect, all of which is post-SERF upgrade in age, comparison with historical SCA-1 and current SCA-1-DP data must be made with caution. More emphasis is placed on spatial relationships that might indicate preferential flow paths within the wetland sediment, redox domains, and/or areas subject to dewatering. Differences between base flow data and alluvial water may indicate subsurface processes (e.g., reduction) and provide information about residence times in the alluvial system. Key analytes plotted include a major cation (magnesium); a major conservative anion (chloride); a species that reflects changes in outfall chemistry (silicon dioxide); key contaminants (dissolved arsenic and chromium); and redox-sensitive species (sulfate, iron, manganese, and ammonium).

Magnesium concentrations show no consistent temporal trends and only minor spatial variation between sites (Figure D-2.0-1). Concentrations are highest at locations SCPZ-10 and SCPZ-11(A), locations disturbed during GCS construction. Magnesium concentrations measured at SCA-1 are within the range of historical data from alluvial wells SCA-1 and SCA-1-DP. Concentrations at E121 and E123 are similar, and slightly lower than concentrations in piezometers, consistent with shorter residence times for surface water compared with the alluvial system.

Chloride concentrations show no significant temporal trends or spatial variability (Figure D-2.0-2). Surface water and alluvial chloride concentrations are relatively similar. The pattern of temporal variation seen at SCPZ-1, SCPZ-2, SCPZ-3, and SCPZ-4 is somewhat similar to that seen at surface water location E121, and recent concentrations at SCA-1 are lower than historical concentrations, possibly because of improved water quality at Outfall 001 associated with the SERF expansion (Figure D-1.0-1). These lines of evidence may suggest some exchange between surface water and alluvial water.

Silicon dioxide concentrations show no significant temporal trends (Figure D-2.0-3) but are slightly higher at SCPZ-2, SCPZ-3, and SCPZ-4 compared with other locations in the alluvial systems. Higher silica at these locations may reflect greater degrees of water-mineral sediment interaction. These locations have greater amounts of mineral sediment versus organic matter than most other locations. Locations SCPZ-2 and SCPZ-3 are in coarse shallow alluvium near the head of the wetland, and location SCPZ-4 is nearby an alluvial fan prograding into the wetland from the south (Figure 1.3-1). Concentrations in the alluvial system are largely similar to those at E121 and E123. Recent dissolved silicon dioxide concentrations at well SCA-1 (and easternmost transect piezometers) may be slightly lower than historical values at SCA-1 and SCA-1DP, perhaps as a function of improvements in outfall water quality following the SERF upgrade. This would indicate some degree of infiltration and mixing of surface water with alluvial water.

A general decrease in arsenic concentrations has been observed at many of the piezometers over the last 2 yr (Figure D-2.0-4), but longer time series will be required for verification of the significance of these trends. Whether this decrease is related to the minor decrease in wetland surface water input concentrations, as suggested at surface water location E121, remains to be seen. Arsenic concentrations are highest at SPCZ-5, SPCZ-6, and SPCZ-1 (higher than concentrations in surface water), suggesting these locations may be the most reducing. Arsenic can exist as As(III), which is relatively mobile under reducing conditions. The ratio of As(III) to As(V) (possibly present as colloids <0.45 µm) in these samples is not known. There is weak evidence that arsenic concentrations at SCA-1 (and in the easternmost transect piezometers) may be lower than the historical range at SCA-1 and SCA-1DP.

Dissolved chromium concentrations in the wetland alluvial system are quite high (Figure D-2.0-5) but predominantly reflect colloidal Cr(III). Cr(VI) concentrations measured in the March 2013 round were all nondetects (LANL 2014, 257590), reflecting the strong reducing conditions in the wetland. No significant temporal trends are noted. Given the colloidal nature of chromium, it is difficult to make meaningful spatial comparisons, but locations SCPZ-2, SCPZ-3, SCPZ-10, SCPZ-11(A), and SCPZ-11(B) and alluvial well

SCA-1 have higher concentrations on average. This may reflect disturbance associated with GCS construction for locations in the easternmost transect. The reason for higher colloidal Cr(III) in the westernmost transect is unclear, but no Cr(VI) was detected in these piezometers in March 2013. Alluvial concentrations are higher than surface water concentrations, presumably because of the abundance of Cr(III) colloids in the subsurface.

No temporal trends are apparent in sulfate concentrations (Figure D-2.0-6). With the exception of locations SCPZ-2 (head of wetland; shallow coarse-grained sediments), SCPZ-7, SCPZ-10, and alluvial well SCA-1, all alluvial locations have lower sulfate concentrations than surface water input to the wetland, reflecting the strong reducing conditions in wetland sediments. The latter two locations are in an area disturbed by construction of the GCS. Locations SCPZ-5, SCPZ-6, SCPZ-8 and, in the most recent two events, SCPZ-9 appear to be particularly reducing based on lower sulfate concentrations relative to other locations. Location SCPZ-6 is sited in a very stagnant area based on observations of limited standing water with no apparent flow. Piezometers SCPZ-5 and SCPZ-8 are in or next to the central surface water flow path in the wetland but may be completed in tighter, more reducing sediments. Sulfide was detected at all piezometer locations in the November 2014 round and at all locations but SCPZ-5 and SCPZ-6 in the July 2014 round, further emphasizing the reducing nature of the system.

Piezometer iron concentrations are higher than in surface water, presumably reflecting dissolved Fe(II) present under reducing conditions (Figure D-2.0-7). No temporal trends are observed and the iron concentrations are higher than in the historical record from SCA-1 and SCA-1-DP. Location SCPZ-5 and piezometers in the easternmost transect have the highest concentrations of iron.

Similarly, alluvial manganese concentrations are typically higher than concentrations in surface water at E121 and no temporal trends are observed (Figure D-2.0-8), again reflecting reducing conditions. All the locations appear to be strongly reducing with respect to manganese at the depth of screen completion. Locations SCPZ-2 and SCPZ-3 have somewhat lower manganese concentrations, consistent with their shallow completion depths in sands and gravels. Interestingly, location SCPZ-4 also has somewhat lower manganese. In May 2014, no surface water was present at this location.

Ammonium concentrations are generally nondetect in surface waters but show frequent detects in the alluvial system, confirming the reducing nature of wetland sediments (Figure D-2.0-9). Ammonium is stable under reducing conditions in the wetland and likely derives from mineralization of organic matter (e.g., dead cattail fronds). High concentrations of ammonium are not necessarily expected in the subsurface, however, because of potential nutritive uptake by wetland plants. Ammonium nitrogen isotope values varied between approximately 6% and 17 % in July and November 2014 (see Appendix E) and are similar to values seen previously (LANL 2014, 257590). The relatively high $\delta^{15}N$ values for ammonium likely result from decay of plants with high $\delta^{15}N$, related, in turn, to inputs of sewage-related nitrate with historically high $\delta^{15}N$ into the wetland and subsequent denitrification (see section 1.6.1).

Nitrate was not detected in any alluvial wells at concentrations amenable to nitrate isotopic analysis in the July 2014 and November 2014 rounds. Nitrate isotopes are no longer routinely analyzed in these wells (Table 1.5-2). One point of interest, however, is that $\delta^{15}N$ of nitrate at E121 was 4‰ in July and 12.6‰ in November 2014. These values are much lower than previous values, which were greater than 30‰. It appears that the high $\delta^{15}N$ signature associated with sewage is being eliminated as the proportion of background nitrate to nitrate discharged from Outfall 001 increases as a result of effluent treatment at SERF. This change in signal could be a valuable tracer in the downgradient alluvial, intermediate, and regional aquifer systems.

As a result of baseline monitoring in the Sandia wetland, an apparent decreasing trend in $\delta^{18}O$ of water in the alluvial system was noted (LANL 2014, 257590). This trend is no longer apparent based on inclusion of data from the last two rounds (Appendix E).

In addition to the 0.45-μm filtration, 0.02-μm filtration (in July 2014 and November 2014) and 0.2-μm filtration (in March 2014), filtration was used during the last three rounds of water collection in hopes of eliminating <0.45-μm colloids (Figures D-2.0-10 and D-2.0-11). Microfiltered arsenic concentrations are similar to those found when samples are filtered at 0.45 μm, suggesting most of the arsenic is present as dissolved As(III), whereas microfiltered chromium concentrations are typically lower (Figure D-2.0-10). Microfiltered chromium concentrations, however, are still higher than direct Cr(VI) measurements (all nondetects in March 2013), suggesting colloidal Cr(III) can even pass through 0.02-μm filters. Filtering at 0.02 μm is difficult and can sometimes result in filter rupture and breakthrough, which may partially explain results compared with Cr(VI) measurements. Colloidal effects are obvious for iron but much less so for manganese (Figure D-2.0-11), suggesting iron is present as a mix of dissolved Fe(II) and Fe(III) colloids while manganese is likely present as dissolved Mn(II).

Figures D-2.0-12, D-2.0-13, and D-2.0-14 show cross-plots for arsenic versus iron, arsenic versus manganese, and manganese versus iron, respectively. Based on the lower iron, manganese, and arsenic concentrations in surface waters compared with alluvial waters, the reducing nature of wetland sediments is evident. Lower iron, manganese, and arsenic concentrations at more oxidizing locations SCPZ-2, SCPZ-3, and SCPZ-4 are also clear.

3.3 Water-Level Results from Piezometers

Water-level data were continuously recorded in several piezometers throughout the wetland (Figure 1.3-1) using Aqua TROLL Sondes between April 2013 and November 2013 and again between June 2014 and November 2014. The sondes were removed during the winter months to avoid damage to the instruments from freezing temperatures. Water-level data collected at the piezometers are presented in Figure D-3.0-1 and D-3.0-2. The plots are arranged within the figure to represent the spatial distribution of the piezometers throughout the wetland. Daily flows at gaging station E121 and precipitation data from precipitation gaging stations E 121.9 are plotted along with the piezometer water-level data. The E121 data reflect inputs from Outfalls 001 and 03A027 as well as surface water flow from precipitation and runoff. The results are discussed below:

- *SCPZ-1 to SCPZ-3*: The 2014 data for this transect (SCPZ-1, SCPZ-2, and SCPZ-3; Figure D-3.0-1) showed the water levels responded almost immediately to precipitation events (tenths of feet to 1.5 ft depending on the size of the event). In addition, water levels responded quickly but to a lesser extent (about 0.1 ft) to changes in base flow (driven by effluent releases at Outfalls 001 and 03A027), as evidenced by the correlated fluctuations in flow at gage E121 when precipitation is light to absent. This suggests the aquifer material in this narrow transect is relatively transmissive and storage is minimal. The water level rose close to 1.5 ft following the July 2014 rain events, which were the most significant of the year, and it appears they remained elevated throughout the rest of the season.
- *SCPZ-4 to SCPZ-6*: In 2014, water levels at the second transect (SCPZ-4, SCPZ-5, and SCPZ-6; Figure D-3.0-1) also responded almost immediately both to precipitation and to flow at gage E121. The variations are generally only a few tenths of a foot, except during the rainy July 2014 month, when they temporarily rose up to about 0.5 ft, but did not remain elevated. The smaller water-level fluctuations are attributed to the following factors at this transect. First, the wetland is much broader and is well vegetated. Surface flow has spread across the wetland because of the low topographic gradient, and interaction with cattails and other wetland vegetation. Second, the water table is very near or at the surface in this area, so the piezometers are measuring filling of a small depth of nearly saturated wetland sediment, probably accompanied by changes in the water level of ponded surface water. The alluvial material in this area is finer grained and has a lower hydraulic conductivity so it probably neither drains nor fills rapidly, causing a small subsurface response.

- *SCPZ-8 and SCPZ-9*: In 2014, water levels at the third transect (SCPZ-8 and SCPZ-9; Figure D-3.0-1) responded quickly to both precipitation events and to outfall-driven changes in base flow. Water levels temporarily rose close to 2 ft during the July 2014 storms but were not sustained. There appears to be no time lag, although this transect is located farther downstream within the wetland, illustrating that the response is driven by surface flow. Water levels at these locations may be influenced by storm runoff entering the wetland from side tributaries as well. The water table is very near the surface in this area, and this rapid response implies the water level is likely responding to ponded or flowing surface water rather than to filling of pore space within the alluvial/wetland material.
- *SCPZ-10 to SCPZ-12*: In 2014, water levels at the fourth transect (SCPZ-10, SCPZ-11A, SCPZ-11B and SCPZ-12; Figure D-3.0-1) responded much like those in the first and third transects, with rapid and significant responses to both precipitation events and to variations in outfall flows (as measured by gage E121). Variations of close to 1 ft occurred following the July 2014 storm events and remained elevated for a few weeks, indicating some storage within the wetland/alluvial fill at this location, which is close to the GCS.

3.4 Geomorphic Survey Results

Detailed geomorphic survey results are presented in Appendix B, including calculations of net erosion that has occurred in sections of the Sandia wetland since baseline surveys. Overall, erosion within the system seems to be associated with scouring in small side channels outside the wetland proper or to channel rearrangement within the wetland proper. There is evidence of increased channelization in the lower part of the wetland and a new nick point, located upgradient of Sheet Pile 1.

3.5 Vegetation Monitoring

Baseline quantitative vegetation survey results are presented in Appendix C. While these are baseline data, healthy growth and development of planted wetland vegetation in and around the GCS has been noted. Robust wetland vegetation, largely dominated by cattails, is found throughout the lower two-thirds of the wetland.

4.0 RESULTS FROM WETLANDS PERFORMANCE METRICS

4.1 Spatial and Temporal Geochemical Patterns

Stiff diagrams demonstrate that major element chemistry is relatively consistent throughout the wetland, with the exception of chemistry at location SCPZ-10, which was disturbed during construction of the GCS (Figure D-4.0-1). Stiff diagrams for gaging stations E121 and E123 show the similarity of these waters and their major ion difference compared with the piezometers. Base flow water quality indicators show the impact of recent improvements in water quality because of the SERF upgrade. Redox indicators potentially show evidence of chemical reduction as surface water flows through the wetland (e.g., lower nitrate at gaging station E123 relative to E121). Manganese discharge from the wetland has decreased significantly following construction of the GCS, although presumably as a result of termination of headcutting at the terminus of the wetland rather than from redox-related changes.

No obvious temporal trends have developed in any of the piezometers that monitor alluvial saturation. Several analytes clearly reflect reducing conditions in all piezometers throughout the wetland (sulfate, arsenic, iron, manganese, nitrate, ammonium, and sulfide). For example, sulfide and ammonium are present at all locations and bound most of the redox ladder (Figures D-4.0-2 and D-4.0-3). Piezometer locations SPCZ-5, SCPZ-6, and SCPZ-8 seem to be the most reducing locations (based on alluvial arsenic, iron, manganese, and sulfate concentrations), while locations SCPZ-2, SCPZ-3, and perhaps

SCPZ-4 are somewhat more oxidizing (based on alluvial manganese concentrations). While no preferential flow paths were identified in the alluvium, there do appear to be distinct geochemical domains in terms of redox conditions. A trilinear plot of major ion chemistry of the piezometers and gaging stations illustrates changes to outfall chemistry from SERF (Figure D-4.0-4). The similarity of major ion chemistry between surface water and piezometers in the November 2014 plot is of particular interest and will continue to be monitored in conjunction with chemistry changes in SERF. Location SCPZ-10 has somewhat different major element chemistry when plotted on a trilinear plot than the rest of the piezometers, likely reflecting disturbance from construction of the GCS (Figure D-4.0-4). Further monitoring of this location will help to evaluate this hypothesis.

Storm water data indicate suspended sediment, PCBs, and chromium concentrations have decreased at gaging station E123 post-GCS, presumably by eliminating headcutting at the terminus of the wetland.

4.2 Temporal and Spatial Trends in Water Levels

Monitoring of water levels will continue as a means to determine how operational effluent releases affect the overall wetland hydrology. Comparisons between the 2013 and 2014 water levels, shown in Figure D-3.0-2, do not indicate that water levels have dropped, although outfall volumes have dropped, as described in section 1.4. Because the wetland sediment is very wet and close to saturated at most of the piezometers, the lower outfall releases may impact the surface water balance more so than manifest in decreased water levels within the wetland. A longer period of record and additional observations related to the wetland margins will be helpful for determining overall impact to the wetland.

4.3 Geomorphic Trends in the Wetland

Topographic surveys of cross-sections indicate erosion within the wetland proper is dominated by channel rearrangement (e.g., avulsion), and eroded areas are usually associated with nearby depositional pockets. In the upland/overbank zone, some areas of deposition occur as a result of sediment input (e.g., alluvial fans, slope wash) from side slopes and drainages, and some localized scour within small side channels. Overall, erosion within the system seems to be associated with scouring in small side channels outside the wetland proper or channel rearrangement within the wetland proper. In the upper (western) stretch of the reach, there appears to be some aggradation of the thalweg, but the overall thalweg gradient appears to be stable since the previous survey. There is some evidence for a lengthening of the thalweg in the lower portion of the reach (the thalweg is well-defined over a larger stretch of the reach than in the previous survey), possibly indicating a tendency towards more channelized versus distributed flow. However, in both the upper and lower stretches of the reach, where the thalweg is well defined, thalweg sinuosity has changed very little since the previous survey. There appears to be a new nick point in the lower (eastern) stretch of the reach. The nick point is located within a stretch where the thalweg is otherwise characterized by a shallow slope. There appears to be a new channel associated with the nick point, located upgradient of Sheet Pile 1, and local erosion below the new base level created by the GCS. Monitoring of these features in subsequent years will assess whether these features are transient adjustments to the new base level.

4.4 Vegetation Baseline Observations

During baseline vegetation monitoring, healthy growth and development of planted wetland vegetation in and around the GCS were noted. Robust wetland vegetation, largely dominated by cattails, was found throughout the lower two-thirds of the wetland. Future monitoring will determine if any changes in wetland vegetation cover and abundance are occurring in the system.

4.5 Performance of Grade-Control Structure

The GCS was completed in August 2013, before the September 13, 2013, flood that occurred across the Laboratory, including in Sandia Canyon. The GCS prevented significant erosion within the wetland associated with that flood event. The GCS also prevented significant erosion associated with flood events in 2014. Alluvial sediments just above the GCS remain reducing and saturated. Storm water data indicate the GCS has had a positive impact in terms of contaminant mobility. Despite only slightly lower storm flow discharge pre- and post-GCS, suspended sediment, PCBs and chromium concentrations have decreased at E123 post-GCS, presumably as a result of the elimination of headcutting at the terminus of the wetland.

4.6 Total Wetland System Performance

Thus far, no evidence of significant dewatering of the wetland related to the SERF expansion was found. Water-level data suggest the alluvial system remains saturated, and chemical data indicate reducing conditions in the alluvial system are stable. Given the recent installation of the GCS and the amount of sediment moved around during its construction, decreases in storm water and base flow contaminant fluxes from the wetland may not be observed immediately. However, storm water data post-GCS show decreases in suspended sediment, PCB, and chromium concentrations at surface water gaging station E123. These improvements are related to cessation of headcutting at the terminus of the wetland. Minor erosion and deposition have occurred within the wetland, consistent with a dynamic wetland system. No significant overall degradation of the physical stability of the wetland has been noted. Planted wetland vegetation is rapidly establishing around the GCS. Healthy wetland vegetation should minimize erosion and lead to stable or aggrading sediments.

4.7 Key Monitoring Locations and Performance Metrics

The monitoring locations and metrics proposed in the Sandia wetland baseline conditions report (LANL 2014, 257590) remain applicable and appropriate.

Gaging station E121 is a good location to monitor the integrated impacts of changing input chemistry and decreasing effluent volumes from Outfalls 001 and 03A027 in base flow.

Gaging station E123 is the key integrating location of total wetland performance. Monitoring of storm water at E123 will reveal if anomalously high levels of sediment and contaminants are mobilized during floods because of reduction in chemical and/or physical stability in the wetland. Monitoring during base flow conditions will indicate changes in outfall chemistry and changes associated with wetland biogeochemistry and function. The metric for identifying deleterious impacts monitored at this location would be increases in base flow or storm water contaminant concentrations that occur year after year following installation of the GCS.

The piezometer array provides valuable water-level and alluvial water chemistry data. These locations monitor potential changes associated with outfall volumes, evolving hydrogeomorphology, redistribution of reducing zones, and changes in chemistry of the outfall (in the case of more conservative constituents). Locations SCPZ-1, SCPZ-2, and SCPZ-3 are particularly interesting as they are located in an area of the wetland that had dewatered resulting from channel incision during the early 2000s. It is encouraging that these locations remain reducing, though locations SCPZ-2 and SCPZ-3 look slightly more oxidizing than other piezometer locations. The chemistry of these locations may provide a preview of what signals of dewatering may be expected in the rest of the wetland. The easternmost piezometer transect will be key to monitoring GCS function in terms of maintaining reducing conditions near the terminus of the wetland. The metrics for identifying deleterious impacts as monitored in the alluvial wells would be (1) persistent increases in contaminant concentrations and/or increases in oxidizing conditions as indicated by redox-sensitive species and (2) decreases in water levels that have deleterious effects on obligate wetland vegetation.

The existing geomorphic transect locations are ideal for assessing hydrogeomorphic changes and the physical stability in the system (see Appendix B). Evidence for deleterious impacts would include widespread, persistent erosion over large portions of the wetland that cannot be attributed to the wetland readjusting its grade in response to installation of the GCS or to previous incisions that occurred in the upper part of the wetland. Persistent erosion below the new base level established by the upper wall of the GCS would be of particular concern. Particular attention will be paid to ensure the area of the plunge pool remains geomorphically stable and no significant headcutting is occurring at the terminus of the wetland near the GCS.

The new quantitative vegetation cross-section locations (see Appendix C) will help monitor both the physical stability and the saturation state of the wetland, as indicated by changes in obligate and facultative wetland vegetation. Increases in upland vegetation within the current extent of the wetland would indicate deleterious impacts on wetland function.

Different metrics will be important to monitor at each of the monitoring locations identified earlier in this section. Significant metrics function as early warning indicators of detrimental changes in physical or chemical stability occurring in the wetland. For example, at gaging station E123, key metrics will be concentrations of contaminant chromium and PCBs. Hydrographs from this location will continue to be important to understand the hydrology of the wetland and the effects of the GCS in terms of flood attenuation. Hydrographs and chemical data from gage E121 will be important to understand wetland inputs. In the wetland proper, measurements of water levels and significant contaminant and redox parameters will be of paramount importance for signs of dewatering and changing geochemistry with respect to contaminants in the sediment. Key chemical species include chromium and arsenic (as primary contaminants) and iron, manganese, sulfate, sulfide, nitrate, and ammonia as important redox-sensitive indicator species. In the regional aquifer, iron and manganese are used as indicators of adverse conditions in wells for obtaining representative chemistry. In the Sandia wetland, however, these species are key indicators of favorable reducing conditions.

It is important to note that changes in any one metric do not necessarily represent a detriment to the overall function of the wetland and to contaminant release. The wetland should be evaluated in terms of total system performance.

It is proposed that an end date for annual reporting of the Sandia wetland performance monitoring effort be defined. The Laboratory proposes that monitoring continue through calendar year 2018, by which time a robust conceptual model for overall system performance that captures interannual variability can be proposed in the 2019 final performance report (due April 30, 2019). This will provide a full 5 yr of record following the construction of the CGS and will capture the potential range of variability in outfall volume and chemistry. During the 2015 to 2018 annual monitoring periods, the Laboratory will continue to refine and improve the monitoring plan in an effort to fully identify, and monitor for, key criteria that are reliable proxies for wetland stability (e.g., vegetation, spatial contaminant trends, geomorphic stability, and key redox indicators). By the 2019 final performance report, the Laboratory will identify threshold values and conditions for these key criteria based on the conceptual model that, if exceeded, would trigger a summary report to NMED for that year. Monitoring of the key criteria would continue after the 2019 final performance report is submitted, but reporting would only occur if threshold values are triggered.

4.8 Proposed Changes to Monitoring Plan

To ensure data representativeness for the alluvial system, the Laboratory is currently piloting the use of more robust permanent alluvial wells and suction lysimeters for sampling within the wetland. Tests with alluvial wells will include sampling with passive diffusion cells. These wells and lysimeters were installed at the end of calendar year 2014 and were first sampled in February 2015 at the same time as sampling of the piezometers. Completion information for these wells and comparisons of analytical data from piezometers, alluvial wells, and lysimeters will be presented in next year's performance report, due April 30, 2016. Any changes to sampling methodology proposed as a result of pilot testing will be made with the concurrence of NMED.

While pilot testing is carried out, surface water and piezometers will be sampled, as proposed in Table 4.6-1. The main changes relative to sampling in 2014 are as follows: (1) ammonium ^{15}N, deuterium, and oxygen isotopes have been removed because they were providing only marginal information on wetland stability; (2) microfiltration of metals has been removed and replaced by quarterly sampling and analysis for speciated Cr(VI); and (3) quarterly unfiltered metals and PCB congener analysis has been added at gaging stations E121, E122, and E123. Nitrate isotopes will be measured whenever sufficient nitrate is detected in samples collected. It is anticipated that this will primarily occur in surface water samples from gaging stations E121, E122, and E123. Storm water sampling will continue, as presented in Table 1.5-3. Topographic surveys will be repeated as in 2014 and vegetation cross-sections will be resurveyed, with the possible addition of extra cross-sections as mentioned in Appendix C.

Base flow and piezometer sampling will continue to occur quarterly in conjunction with monitoring of the rest of the chromium monitoring group as proposed in the Interim Facility-Wide Groundwater Monitoring Plan.

5.0 CONCLUSIONS

The monitoring performed during the performance period indicates that the Sandia wetland is stable following the installation of the GCS, even with declining effluent volumes entering the wetlands. This performance period is the first year following baseline monitoring and is the baseline year for wetland vegetative monitoring. Therefore, the conceptual model for the Sandia wetland is evolving and improving as data are obtained. Threshold exceedance values for key criteria are being developed through the iterative monitoring and evaluation cycle that occurs each annual monitoring period. Within the alluvial system, wetland sediments remain reducing and no obvious temporal trends in chemistry have been noted. Even the upper portion of Reach S-2 (the second reach down from the headwaters of Sandia Canyon and the reach that encompasses the Sandia wetland), which had been previously dewatered and is outside the current footprint of the wetland, retains reducing conditions in alluvial groundwater at depth.

Water levels have not dropped below the levels observed in 2013, despite reduced effluent volumes and remain sufficiently high to sustain obligate wetland vegetation. Continuing vegetation monitoring in future years will be valuable in assessing wetland performance, with abundant wetland vegetation promoting sediment stability. Overall, erosion within the system seems to be associated with scouring in small side channels outside the wetland proper, or channel rearrangement within the wetland proper. There is evidence of increased localized channelization in the lower part of the wetland and a new nick point, located upgradient of Sheet Pile 1. Monitoring of these geomorphic changes in subsequent years will assess whether these features are transient adjustments to the new base level established by the GCS. The GCS has arrested headcutting at the terminus of the wetland. Storm water data indicate that the GCS has had a positive impact in terms of contaminant mobility. Despite only slightly lower storm flow discharge pre- and post-GCS, suspended sediment, PCBs and chromium concentrations have decreased at E123 post-GCS, presumably because headcutting at the terminus of the wetland.

Ongoing monitoring will continue to allow the Laboratory to assess changes within the Sandia wetland related to the GCS, changes in effluent chemistry, and decreases in effluent volumes and discharge rates. The Laboratory will respond with an adaptive management strategy should adverse changes be noted.

6.0 REFERENCES

The following list includes all documents cited in this report. Parenthetical information following each reference provides the author(s), publication date, and ER ID or ESH ID. This information is also included in text citations. ER IDs were assigned by the Environmental Programs Directorate's Records Processing Facility (IDs through 599999), and ESH IDs are assigned by the Environment, Safety, and Health (ESH) Directorate (IDs 600000 and above). IDs are used to locate documents in the Laboratory's Electronic Document Management System and, where applicable, in the master reference set.

Copies of the master reference set are maintained at the NMED Hazardous Waste Bureau and the ESH Directorate. The set was developed to ensure that the administrative authority has all material needed to review this document, and it is updated with every document submitted to the administrative authority. Documents previously submitted to the administrative authority are not included.

DOE (U.S. Department of Energy), August 24, 2010. "Final Environmental Assessment for the Expansion of the Sanitary Effluent Reclamation Facility and Environmental Restoration of Reach S-2 of Sandia Canyon at Los Alamos National Laboratory, Los Alamos, New Mexico," U.S. Department of Energy document DOE/EA-1736, Los Alamos Site Office, Los Alamos, New Mexico. (DOE 2010, 206433)

EPA (U.S. Environmental Protection Agency), June 8, 2007. "Authorization to Discharge under the National Pollutant Discharge Elimination System, NPDES Permit No. NM 0028355," Region 6, Dallas, Texas. (EPA 2007, 099009)

EPA (U.S. Environmental Protection Agency), September 25, 2014. "NPDES Permit No. NM0028355 Final Permit Decision," U.S. Environmental Protection Agency Region 6, Dallas, Texas. (EPA 2014, 600257)

Fair, J.M., and J.M. Heikoop, 2006. "Stable Isotope Dynamics of Nitrogen Sewage Effluent Uptake in a Semi-Arid Wetland," *Environmental Pollution,* Vol. 140, pp. 500-505. (Fair and Heikoop 2006, 098045)

Heikoop, J.M., D.D. Hickmott, D. Katzman, P. Longmire, and R.S. Beers, 2002. "N-15 Signals of Nitrogen Source and Fate in a Semiarid Wetland," Wetlands and Remediation II, Proceedings of the Second International Conference on Wetlands and Remediation, September 5–6, 2001, Burlington, Vermont, pp. 355–362. (Heikoop et al. 2002, 107001)

LANL (Los Alamos National Laboratory), October 2009. "Investigation Report for Sandia Canyon," Los Alamos National Laboratory document LA-UR-09-6450, Los Alamos, New Mexico. (LANL 2009, 107453)

LANL (Los Alamos National Laboratory), May 2011. "Interim Measures Work Plan for Stabilization of the Sandia Canyon Wetland," Los Alamos National Laboratory document LA-UR-11-2186, Los Alamos, New Mexico. (LANL 2011, 203454)

LANL (Los Alamos National Laboratory), September 2011. "Work Plan and Final Design for Stabilization of the Sandia Canyon Wetland," Los Alamos National Laboratory document LA-UR-11-5337, Los Alamos, New Mexico. (LANL 2011, 207053)

LANL (Los Alamos National Laboratory), September 2012. "Phase II Investigation Report for Sandia Canyon," Los Alamos National Laboratory document LA-UR-12-24593, Los Alamos, New Mexico. (LANL 2012, 228624)

LANL (Los Alamos National Laboratory), December 2013. "Completion Report for Sandia Canyon Grade-Control Structure," Los Alamos National Laboratory document LA-UR-13-29285, Los Alamos, New Mexico. (LANL 2013, 251743)

LANL (Los Alamos National Laboratory), June 2014. "Sandia Wetland Performance Report, Baseline Conditions 2012–2014," Los Alamos National Laboratory document LA-UR-14-24271, Los Alamos, New Mexico. (LANL 2014, 257590)

NMED (New Mexico Environment Department), June 9, 2011. "Approval with Modification, Interim Measures Work Plan for Stabilization of the Sandia Canyon Wetland," New Mexico Environment Department letter to G.J. Rael (DOE-LASO) and M.J. Graham (LANL) from J.E. Kieling (NMED-HWB), Santa Fe, New Mexico. (NMED 2011, 203806)

Panichev, N., W. Mabasa, P. Ngobeni, K. Mandiwana, and S. Panicheva, May 2008. "The Oxidation of Cr(III) to Cr(VI) in the Environment by Atmospheric Oxygen during the Bush Fires," *Journal of Hazardous Materials,* Vol. 153, No. 3, pp. 937–941. (Panichev et al. 2008, 256734)

Rai, D., L.E. Eary, and J.M. Zachara, October 1989. "Environmental Chemistry of Chromium," *Science of the Total Environment,* Vol. 86, No. 1–2, pp. 15–23. (Rai et al. 1989, 249300)

Sandia Canyon Wetland Timeline

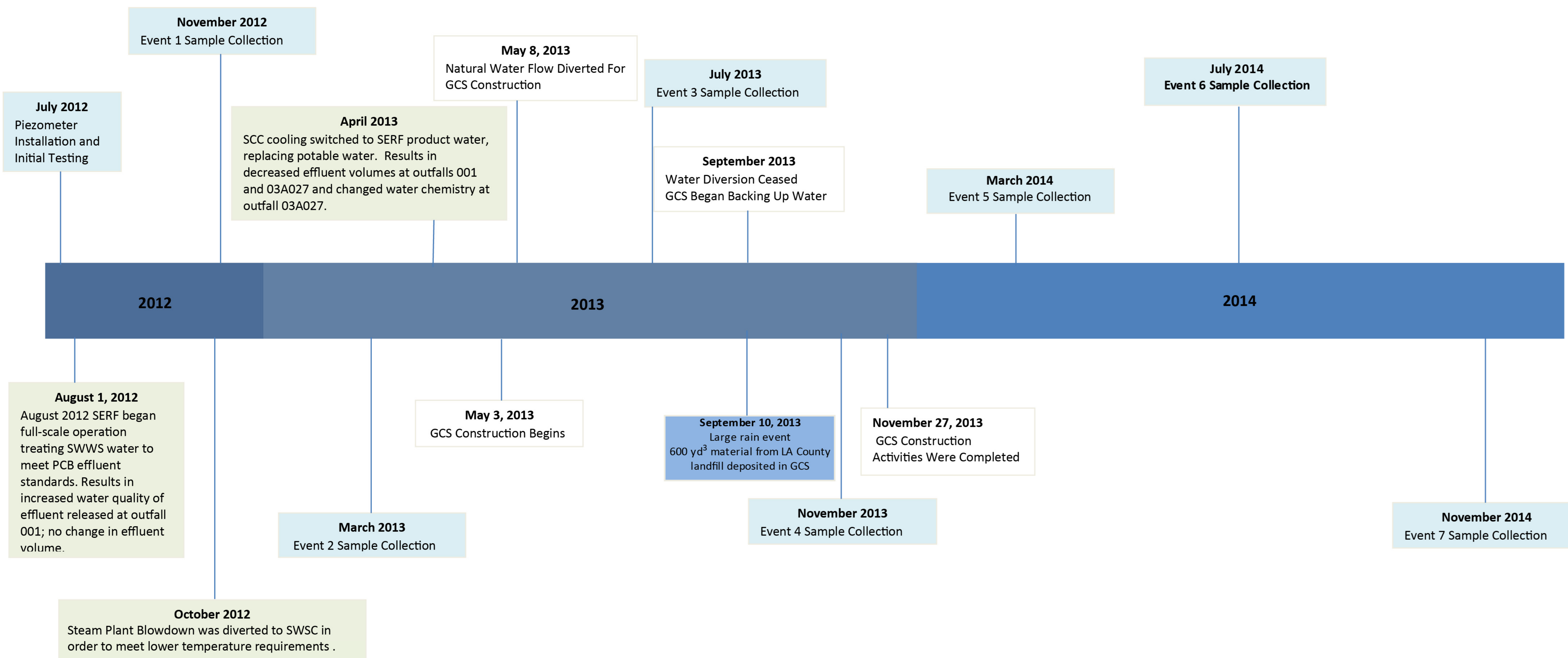

Figure 1.2-1 Sandia Canyon wetland timeline

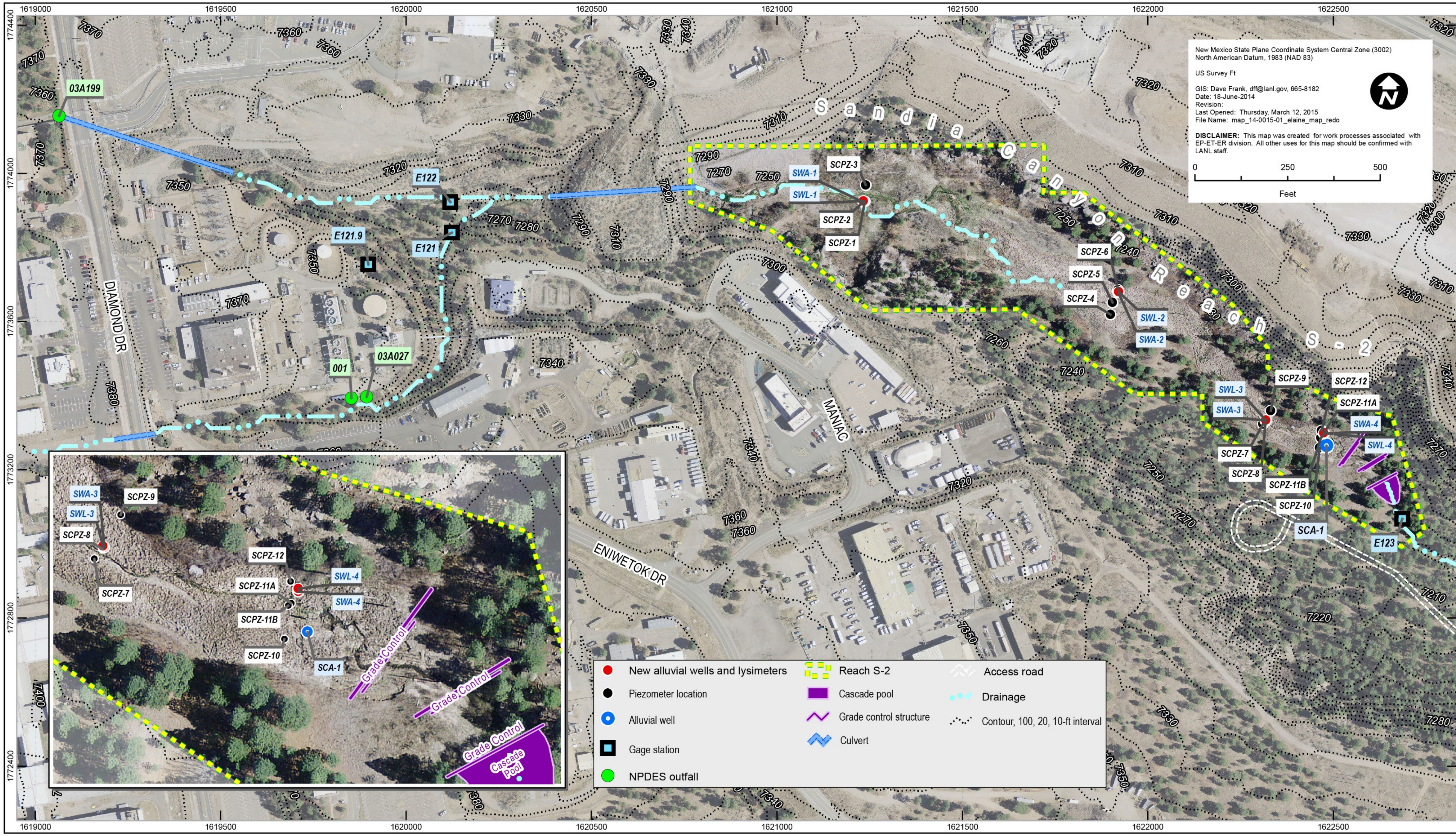

Figure 1.3-1 Locations of the Sandia GCS, NPDES outfalls, piezometers, alluvial wells, surface and storm water gaging stations, and Reach S-2

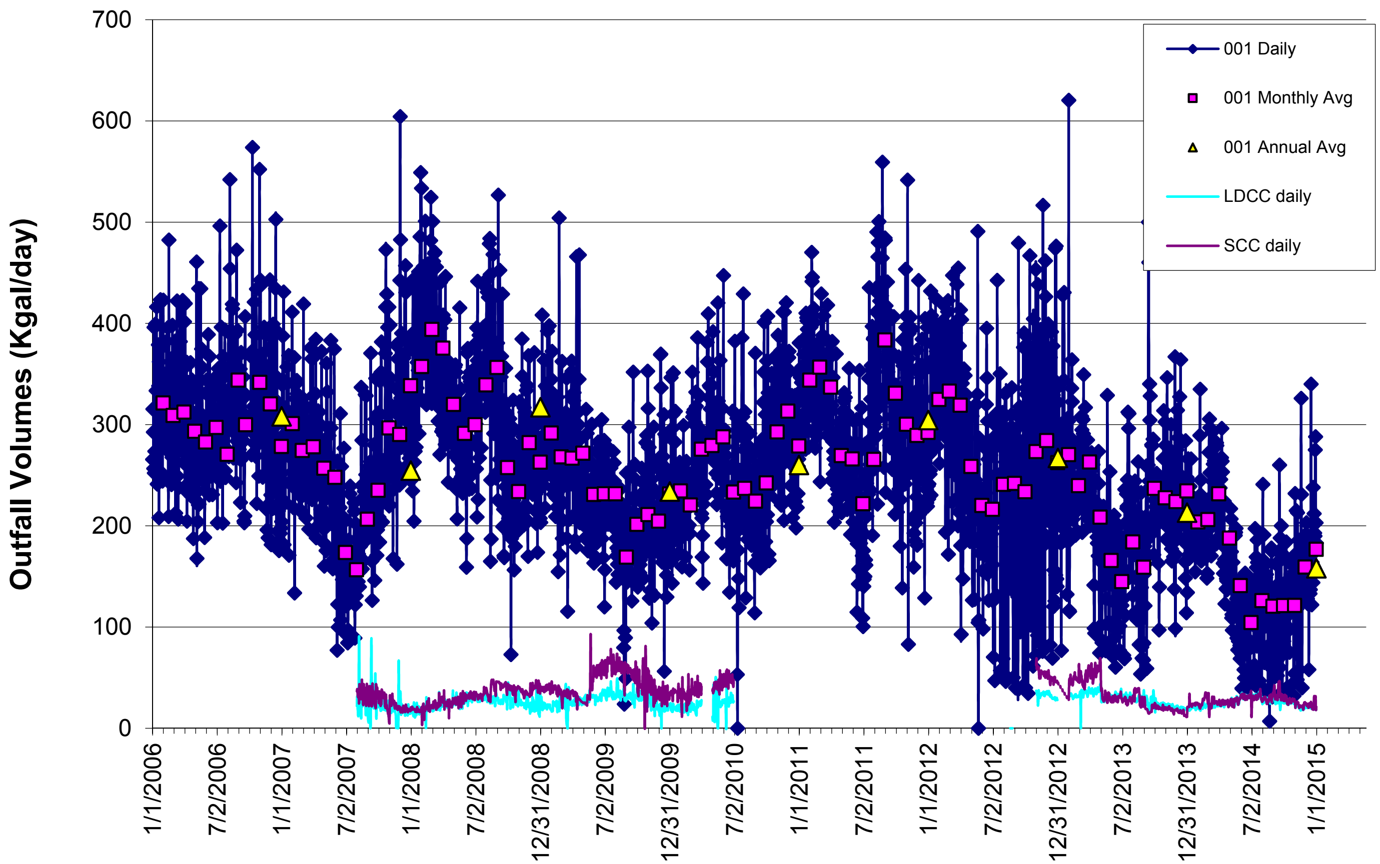

Figure 1.4-1 Daily, monthly average, and yearly average effluent release volumes (expressed as Kgal./day) for Outfall 001 from 2006 to December 2014, and daily effluent releases for Outfalls 03A027 (SCC) and 03A199 (LDCC) from August 2007 to January 2010 and from November 2012 to December 2014

Updated Process Schematic for the Power Plant, SWWS, and SERF Connections to Outfall 001

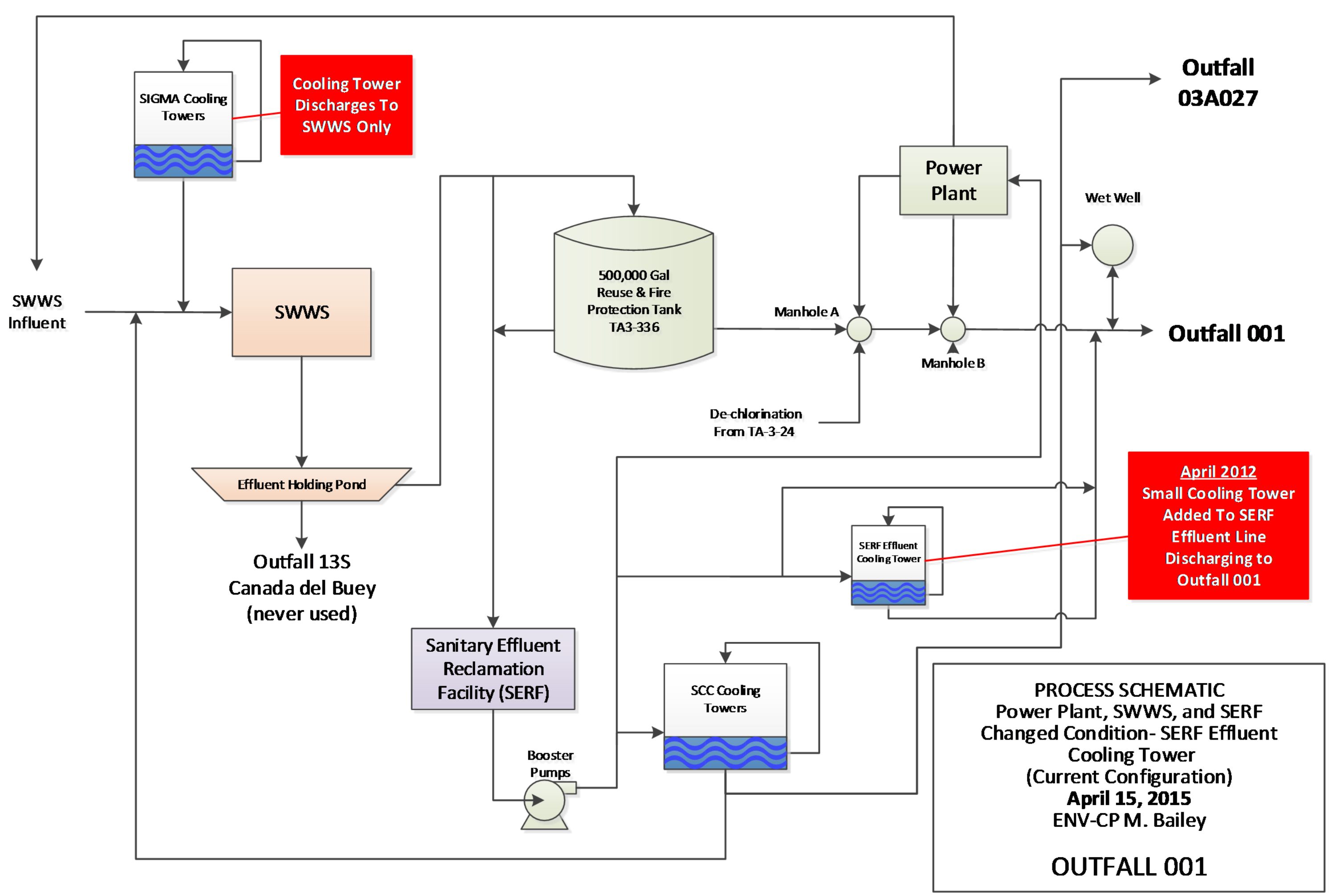

Figure 1.4-2 Updated process schematic for the power plant, SWWS, and SERF connections to Outfall 001 (current configuration)

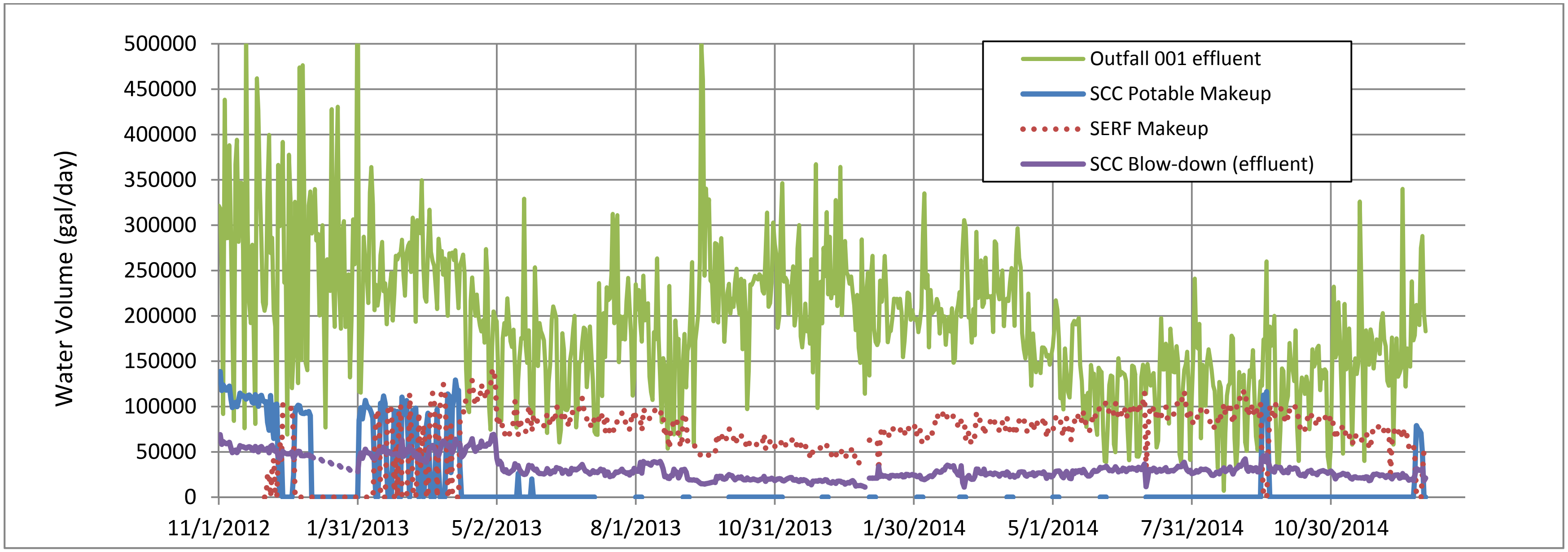

Figure 1.4-3 Daily water volumes (gal./day) from November 2012 to December 2014 for effluent released from Outfall 001, effluent from the SCC cooling towers, which release to Outfall 03A027, and makeup water sources (potable or SERF-blended water) used at the SCC cooling towers

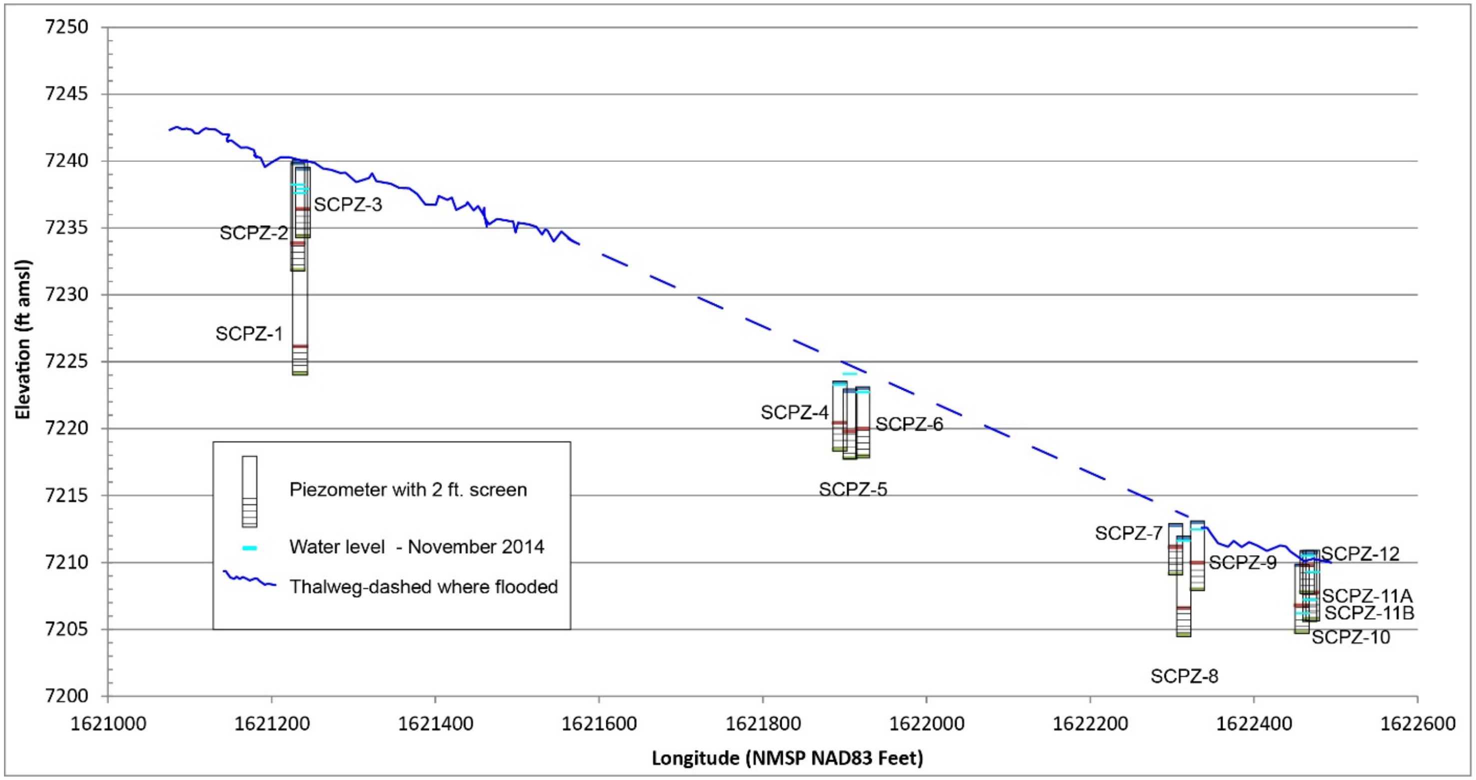

Figure 1.5-1 Schematic of piezometer transects and depths. The thalweg profile is a solid line, where present, and is dashed where the wetland is flooded but a distinct thalweg is not observed.

Table 1.5-1
Completion Data for Alluvial Piezometers

Parameter	Piezometer												
	SCPZ-1	SCPZ-2	SCPZ-3	SCPZ-4	SCPZ-5	SCPZ-6	SCPZ-7	SCPZ-8	SCPZ-9	SCPZ-10	SCPZ-11(A)	SCPZ-11(B)	SCPZ-12
Total length (ft)	20.5	11.4	8.3	8.3	8.3	8.3	8.3	11.4	8.3	8.3	8.3	8.3	8.3
Stick up (ft)	4.36	3.26	3.19	3.16	2.64	3.18	4.32	4.78	3.35	4.01	3.8	4.48	3.77
Top of screen (ft bgs)	13.8	6.0	3	3	3	3	1.6	5.3	3	3	3	1	3
Total depth (ft bgs)	16.2	8.3	5.4	5.4	5.4	5.4	4.0	7.6	5.4	5.4	5.4	5.4	5.4

Table 1.5-2
Alluvial Groundwater Sampling and Analysis Plan for Sandia Wetland Stabilization Monitoring

Suite	Frequency	Comment
EES Metals[a] (filtered)	Quarterly	Includes redox-sensitive metals Fe, Mn, Cr, As. Samples filtered using membrane size of 0.45 µm and 0.2 µm in March 2014, and 0.45 µm and 0.02 µm in July and November 2014.
EES Anions[b] (filtered)	Quarterly	Includes redox-sensitive anions sulfate and nitrate; nitrate is a wetland vegetation nutrient
Sulfide (unfiltered)	Quarterly	Redox indicator (reduction of sulfate)
Alkalinity/pH (unfiltered)	Quarterly	Organic matter degradation
Ammonia (unfiltered)	Quarterly	Indicator of organic matter degradation; wetland vegetation nutrient
DOC[c] (filtered)	Annually	Organic matter degradation
Cr(VI) (filtered)	Annually	Indicator of Cr(III) oxidizing to Cr(VI)
$\delta^{15}N$ ammonia (filtered)	Quarterly	Indicator of nitrogen sources and redox-related transformations
$\delta^{15}N/\delta^{18}O$ nitrate[d] (filtered)	Quarterly	Indicator of denitrification (redox process) and nitrogen
$\delta^{18}O/\delta D$ water (unfiltered)	Quarterly	Indicator of outfall discharge versus snowmelt and storm water runoff

[a] EES metals refers to metals analyses conducted at the Laboratory's Earth and Environmental Sciences (EES) analytical laboratory and consists of the following suite: Ag, Al, As, B, Ba, Be, Cd, Co, Cr, Cs, Cu, Fe, K, Li, Mg, Mn, Na, Ni, Pb, Rb, Se, Si, Sr, Ti, Tl, U, V, Zn, Hg, Mo, Sb, Sn, Th.

[b] EES anions refers to anion analyses conducted at the Laboratory's EES analytical laboratory and consists of the following suite: Br, F, Cl, NO_2, NO_3, PO_4, SO_4, $C_2O_4H_2$ (oxalic acid).

[c] DOC = Dissolved organic carbon.

[d] Collected only if nitrate concentrations become detectable.

Table 1.5-3
ISCO Bottle Configurations and Analytical Suites
Calendar Year 2014 Storm Water Sampling Plan

Bottle No.	Storm/Delay 0-1×4@1min/Delay 40-2×4@1min			Storm/Delay 0-6×1@5min/Delay 30-18×1@20min	
	Sample Collection Time (min)	Sandia E121, E122, E123		Sandia E121, E122, E123	
		Bottle Type	Analytical Suite	Sample Collection Time (min)	Analytical Suite 24 Bottle ISCO 1-L Poly Wedge
1	Max + 10	1-L Glass	PCB Congener (UF[a])	Trigger + 0	SSC
2	Max + 10	1-L Glass	PAH (UF)	Trigger + 5	SSC
3	Max + 10	1-L Glass	SVOC[b] (UF)	Trigger + 10	SSC, Particle Size
4	Max + 10	1-L Poly	TAL[c] metals (F[d]/UF)	Trigger + 15	Cl + SO4
5	Max + 50	1-L Glass	PCB Congener (UF)	Trigger + 20	SSC
6	Max + 50	1-L Glass	PAH (UF)	Trigger + 25	DOC
7	Max + 50	1-L Glass	SVOC (UF)	Trigger + 30	Alk+pH
8	Max + 50	1-L Poly	TAL metals (F/UF)	Trigger + 50	SSC, Particle Size
9	Max + 90	1-L Glass	PCB Congener (UF)	Trigger + 70	SSC
10	Max + 90	1-L Glass	PAH (UF)	Trigger + 90	SSC, Particle Size
11	Max + 90	1-L Glass	SVOC (UF)	Trigger + 110	SSC
12	Max + 90	1-L Poly	TAL metals (F/UF)	Trigger + 130	SSC
13	—[e]	—	—	Trigger + 150	SSC
14	—	—	—	Trigger + 170	SSC
15	—	—	—	Trigger + 190	SSC
16	—	—	—	Trigger + 210	SSC
17	—	—	—	Trigger + 230	SSC
18	—	—	—	Trigger + 250	SSC
19	—	—	—	Trigger + 270	SSC
20	—	—	—	Trigger + 290	SSC
21	—	—	—	Trigger + 310	SSC
22	—	—	—	Trigger + 330	SSC
23	—	—	—	Trigger + 350	SSC
24	—	—	—	Trigger + 370	SSC

Notes: E121 = Sandia right fork at Pwr Plant, E122 = Sandia left fork at Asph Plant, E123 = Sandia below Wetlands.

[a] UF = Unfiltered.

[b] SVOC = Semivolatile organic compound.

[c] TAL = Target analyte list.

[d] F = Filtered.

[e] — = None.

Table 2.0-1
Summary of Analytical Samples Collected during July and November 2014 Sampling Events

Location	July 2014	November 2014
SCPZ-1	Full suite collected	Full suite collected
SCPZ-2	Full suite collected	Full suite and field duplicate collected
SCPZ-3	Full suite collected	Full suite collected
SCPZ-4	Full suite collected	Full suite collected
SCPZ-5	Full suite collected	Full suite collected
SCPZ-6	Full suite collected	Full suite collected
SCPZ-7	Prioritized suite collected: Alk, NH3, sulfide, anions, metals, dissolved organic carbon (DOC), N15	Full suite collected
SCPZ-8	Full suite collected	Full suite collected
SCPZ-9	Prioritized suite collected: Alk, NH3, sulfide, anions, metals, DOC, N15	Well purged dry. Full suite collected after recharge
SCPZ-10	Full suite collected	Well purged dry. Full suite collected after recharge
SCPZ-11A	Prioritized suite collected: Alk, NH3, sulfide, anions, metals	Well purged dry. Prioritized suite collected: Alk, anions, metals (filtered at 0.02 µm)
SCPZ-11B	Full suite collected	Full suite collected
SCPZ-12	Full suite collected	Full suite collected
SCA-1DP	Full suite collected	Full suite collected
Sandia Right Fork at Power Plant (E121)	Full suite collected	Full suite and field duplicate collected
Sandia Left fork at Asphalt Plant South fork (E122)	Full suite collected	Full suite collected
Sandia below Wetlands (E123)	Full suite collected	Full suite collected

Table 2.0-2
Field Parameter Data for Piezometers and Surface Water Stations, July and November 2014 Sampling Events

Location Name	Date	Dissolved Oxygen (mg/L)	Oxidation-Reduction Potential (mV)	pH	Specific Conductance (µS/cm)	Temperature (°C)	Turbidity (NTU[a])	Discharge (gpm[b])
Surface Water Stations								
E121	7/30/2014	6.94	NR[c]	7.83	467	20.68	4.83	40.4
E121	11/4/2014	7.95	NR	7.84	519	14.3	1.44	193
E122	7/30/2014	6.91	NR	8.11	521	20.4	14	20.2
E122	11/4/2014	7.83	NR	8.12	476	12.29	2.84	13.5
E123	7/29/2014	8.6	NR	8.04	342	20.34	0.36	80.3
E123	11/4/2014	9.97	NR	8.19	474	10.1	13.7	204.7
Piezometers								
SCPZ-1	7/30/2014	1.17	-111.9	6.96	576	14.7	4.2	0.05
SCPZ-1	11/3/2014	0.52	-103.8	6.91	563	14.67	1.62	0.11
SCPZ-2	7/30/2014	1.04	-119.5	7.1	497	17.87	3.73	0.06
SCPZ-2	11/3/2014	0.6	-144	7.31	458	14.91	1.9	0.13
SCPZ-3	8/1/2014	1.01	-100.4	6.99	528	18.5	2.17	0.06
SCPZ-3	11/3/2014	1.17	-107.5	7.04	471	13.45	1.48	0.05
SCPZ-4	8/1/2014	1.69	-88.6	6.5	527	17.22	2.72	0.2
SCPZ-4	11/4/2014	1.73	-120.7	6.85	492	11.15	85.3	0.12
SCPZ-5	8/1/2014	0.96	-155.3	7	688	12.01	12.5	0.2
SCPZ-5	11/4/2014	1.69	-143.6	6.92	576	12.75	17.4	0.08
SCPZ-6	8/1/2014	2.55	-120.6	7	446	14.87	28.9	na[d]
SCPZ-7	8/4/2014	2.2	-124.3	6.75	621	18.19	249	0.05
SCPZ-7	11/3/2014	2.65	-35.8	6.1	714	9.77	105.7	0.16
SCPZ-8	8/4/2014	1.16	-105.6	6.72	527	11.16	14	0.05
SCPZ-8	11/3/2014	1.43	-51.8	6.32	585	9.83	4.5	0.25
SCPZ-9	8/4/2014	2.73	-100.2	6.83	420	14.5	147	0.05
SCPZ-9	11/3/2014	3.57	-58.6	6.9	638	12.41	28.5	0.05
SCPZ-10	7/31/2014	1.13	-33.3	6.36	760	17.35	999	na
SCPZ-10	11/3/2014	2.42	-50.5	6.62	858	11.09	609.7	na
SCPZ-11(A)	8/1/2014	1.04	-81.8	6.47	568	17.93	970	na
SCPZ-11(A)	11/4/2014	3.1	-35.3	6.76	607	15.76	268.7	na
SCPZ-11(B)	7/31/2014	1.02	-107.2	6.3	532	17.05	16.3	0.175
SCPZ-11(B)	11/3/2014	1.1	-73.2	6.58	513	9.9	10.8	0.05
SCPZ-12	7/31/2014	1.6	-121.5	6.44	475	12.33	15.8	0.05
SCPZ-12	11/4/2014	1.74	-68.4	6.61	470	9.16	83.4	0.07

[a] NTU = Nephelometric turbidity units.

[b] gpm = gallons per minute.

[c] NR = Not recorded.

[d] na= Not available. The well went dry and the sample was collected after recharge.

Table 2.0-3
Precipitation, Storm Water Peak Discharge, and Samples Collected at Gaging Stations E121, E122, and E123 for Each Sample-Triggering Storm Event in 2014

Storm Event Date	RG121.9 Total Precipitation (in.)	E121 Peak Discharge (cfs)	E122 Peak Discharge (cfs)	E123 Peak Discharge (cfs)
5/23/2014	0.36	13 NS[a]	5.8 NS	18 S[b]
7/7/2014	1.27	63 S	13 NS	80 S
7/8/2014	1.33	61 NS	10 S	76 S
7/14–7/15/2014	0.70	4.8S	3.6NS	12NS
7/15–7/16/2014	0.63	10S	3.7NS	20 S
7/19/2014	0.41	11 S	5.2 NS	18 S
7/27–7/28/2014	0.48	29 S	6.2S	26 NS
7/29/2014	1.24	36 NS	12 S	62 S
7/31/2014	1.34	66 S	19 S	109 S

[a] NS = Sample was not collected.

[b] S = Sample was collected.

Table 3.1-1
Travel Time of Flood Bore, Peak Discharge, Increase or Decrease in Peak Discharge, and Percent Change in Peak Discharge from Upgradient to Downgradient of the Wetland for Each Sample-Triggering Storm Event in 2014

Date	Travel Time from E121 to E123 (min)	Peak Discharge (cfs)		+/–[a]	%[a]	Travel Time from E122 to E123 (min)	Peak Discharge (cfs)		+/–	%
		E121	E123				E122	E123		
5/23	55	13	18	+	28	50	5.8	18	+	68
7/7	30	63	80	+	21	25	13	80	+	84
7/8	25	61	76	+	20	25	10	76	+	87
7/14–7/15	50	4.8	12	+	60	50	3.6	12	+	70
7/15–7/16	50	10	20	+	50	45	3.7	20	+	82
7/19	45	11	18	+	39	45	5.2	18	+	71
7/27–7/28	55	29	16	-	45	50	6.1	16	+	62
	45	14	26	+	46	45	6.2	26	+	76
7/29	30	36	62	+	42	30	12	62	+	81
7/31	10	66	109	+	40	15	19	109	+	83
Min	10	4.8	12	—[b]	20	15	3.6	12	—	62
Mean	39.5	30.8	43.8	—	39	38.0	8.4	43.8	—	76
Max	55	66	110	—	60	50	19	110	—	87

[a] + = Increase; – = decrease; % = percent change in peak discharge.

[b] — = Result is not applicable.

Table 3.1-2
Calculated Sediment Yield and Runoff Volume at
Gaging Stations E121, E122, and E123 for Each Sample-Triggering Storm Event in 2014

Station	Date	Sediment Yield (tons)	Sediment Volume (yd^3)	Runoff Volume (acre-feet)	Peak Discharge (cfs)
E121	7/7/2014	0.84	0.3	2.27	63
E121	7/14–7/15/2014	0.19	0.1	0.72	4.8
E121	7/15–7/16/2014	1.64	0.6	0.63	10
E121	7/19/2014	3.22	1.2	0.61	11
E121	7/27–7/28/2014	0.57	0.2	0.93	29
E121	7/31/2014	15.44	5.8	2.92	66
E122	7/8/2014	0.60	0.2	0.99	10
E122	7/27–7/28/2014	0.05	0.0	0.64	6.2
E122	7/29/2014	0.73	0.3	1.18	12
E122	7/31/2014	1.55	0.6	1.02	19
E123	5/23/2014	1.62	0.6	2.68	18
E123	7/7/2014	4.12	1.5	6.38	80
E123	7/8/2014	18.19	6.8	7.01	76
E123	7/15–7/16/2014	2.01	0.8	3.08	20
E123	7/19/2014	0.39	0.1	1.65	18
E123	7/29/2014	7.36	2.8	7.50	62
E123	7/31/2014	28.58	10.7	7.22	109

Table 4.6-1
Modified Sample Analytes and Preservation Requirements for Sandia Wetland

Suite	Frequency	Filtered?	Preservation	Field Storage	Holding Time	Ideal Volume	Minimum Volume	Comment
Metals	Quarterly	Y	Nitric acid	<4°C	6 mo	125 mL	50 mL	Filtered at 0.45 microns. Both filtered and unfiltered samples will be collected for base flow
Cr(VI)	Quarterly	N	$NH_4OH/(NH4)_2SO_4$ (liquid) buffer 1-mL to 100-mL of sample	4-6°C	14 days	100 mL	100 mL	EPA Method: 218.7
Anions	Quarterly	Y	None	<4°C	1 mo; NO_p 2 d	125 mL	100 mL	—[a]
Alkalinity/pH	Quarterly	N	None	<4°C	ASAP	125 mL	10 mL	—
Ammonium	Quarterly	Y	None	<4°C	1 mo	125 mL	125 mL	American Society for Testing and Materials method
Sulfide	Quarterly	N	Sulfide buffer pH 12	<4°C	24 h	15 mL	15 mL	—
Dissolved organic carbon	Annually	Y	Sulfuric acid	<4°C	1 mo	40 mL	40 mL	Collect during June sample event
PCB Congeners[b]	Quarterly	N	None	<4°C	40 days	1L	1L	Amber glass with Teflon lid (EPA Method 1668A); base flow only

Notes: If nitrate concentrations become elevated, $\delta^{15}N$ of nitrate will be added to this analyst list. All analyses will be performed in the LANL Geochemistry and Geomaterials Research Laboratory, with the following exceptions: (1) PCB congeners will be analyzed by an external laboratory, and (2) quarterly sample splits for filtered metals and anions from four piezometer locations will be sent to an external laboratory for verification purposes.

[a] — = None.

[b] PCB Congeners collected at gaging stations E121, E122, and E123 only (base flow).

Appendix A

Acronyms and Abbreviations,
Metric Conversion Table, and Data Qualifier Definitions

A-1.0 ACRONYMS AND ABBREVIATIONS

bgs	below ground surface
csf	cubic foot per second
DC	direct current
DGPS	differentially corrected global positioning system
DOC	dissolved organic carbon
EES	Earth and Environmental Sciences
EPA	Environmental Protection Agency (U.S.)
ESH	Environment, Safety, and Health
F	filtered
FAC	facultative plant
FACU	facultative upland plant
FACW	facultative wetland plant
GCS	grade-control structure
gpd	gallons per day
gpm	gallons per minute
GPS	global positioning system
IR	investigation report
LANL	Los Alamos National Laboratory
LDCC	Laboratory Data Communications Center
MY	monitoring year
NI	no indicator status
NMED	New Mexico Environment Department
NPDES	National Pollutant Discharge Elimination System
NTU	Nephelometric turbidity unit
OBL	obligate wetland plant
PAH	polycyclic aromatic hydrocarbon
PCB	polychlorinated biphenyl
RO	reverse osmosis
SCC	Strategic Computing Complex
SERF	Sanitary Effluent Reclamation Facility
SOM	solid organic matter
SSC	suspended sediment concentration

SVOC	semivolatile organic compound
SWWS	Sanitary Waste Water System
TA	technical area
TAL	target analyte list
TDS	total dissolved solids
TKN	total Kjeldahl nitrogen
TOC	total organic compound
TSS	total suspended sediments
UF	unfiltered
UPL	upland plant
VE	vertical exaggeration

A-2.0 METRIC CONVERSION TABLE

Multiply SI (Metric) Unit	by	To Obtain U.S. Customary Unit
kilometers (km)	0.622	miles (mi)
kilometers (km)	3281	feet (ft)
meters (m)	3.281	feet (ft)
meters (m)	39.37	inches (in.)
centimeters (cm)	0.03281	feet (ft)
centimeters (cm)	0.394	inches (in.)
millimeters (mm)	0.0394	inches (in.)
micrometers or microns (µm)	0.0000394	inches (in.)
square kilometers (km^2)	0.3861	square miles (mi^2)
hectares (ha)	2.5	acres
square meters (m^2)	10.764	square feet (ft^2)
cubic meters (m^3)	35.31	cubic feet (ft^3)
kilograms (kg)	2.2046	pounds (lb)
grams (g)	0.0353	ounces (oz)
grams per cubic centimeter (g/cm^3)	62.422	pounds per cubic foot (lb/ft^3)
milligrams per kilogram (mg/kg)	1	parts per million (ppm)
micrograms per gram (µg/g)	1	parts per million (ppm)
liters (L)	0.26	gallons (gal.)
milligrams per liter (mg/L)	1	parts per million (ppm)
degrees Celsius (°C)	9/5 + 32	degrees Fahrenheit (°F)

A-3.0 DATA QUALIFIER DEFINITIONS

Data Qualifier	Definition
U	The analyte was analyzed for but not detected.
J	The analyte was positively identified, and the associated numerical value is estimated to be more uncertain than would normally be expected for that analysis.
J+	The analyte was positively identified, and the result is likely to be biased high.
J-	The analyte was positively identified, and the result is likely to be biased low.
UJ	The analyte was not positively identified in the sample, and the associated value is an estimate of the sample-specific detection or quantitation limit.
R	The data are rejected as a result of major problems with quality assurance/quality control (QA/QC) parameters.

Appendix B

2014 Geomorphic Changes in Sandia Canyon Reach S-2

CONTENTS

Figures

Tables

Attachments

Attachment B-1 2014 Photographs of Geomorphic Conditions in Sandia Canyon Reach S-2

Attachment B-2 2014 Geomorphic Changes in Sandia Canyon Reach S2 Survey Data
(on CD included with this document)

B-1.0 INTRODUCTION

This report evaluates geomorphic changes that occurred in 2014 in Reach S-2, above the Sandia Canyon grade-control structure (GCS) within the Los Alamos National Laboratory (LANL or the Laboratory). Survey data from 16 cross-section transects above the GCS were reported previously (LANL 2011, 200902; LANL 2012, 218411; LANL 2014, 257590). This report compares the previous survey data with subsequent survey data obtained in fall 2014, following the summer 2014 monsoon season, as specified in the "Work Plan and Final Design for Stabilization of the Sandia Canyon Wetland" (LANL 2011, 207053) and in the modified version of this work plan approved by the New Mexico Environmental Department (NMED) on April 3, 2013 (Cobrain 2013, 256726). Additionally, baseline survey data are presented from 7 additional cross-section transects, 5 of which are located within and below the GCS. All 23 cross-section transect surveys will be resurveyed after the 2015 monsoon season, and the results will be presented in a report to NMED by April 30, 2016. Figures B-1.0-1 and B-1.0-2 show the locations of sites discussed in this report. Attachment B-1 presents photographs of areas of maximum erosion and deposition in Sandia Canyon Reach S-2.

B-2.0 HYDROLOGIC EVENTS DURING THE 2014 MONSOON SEASON

The largest of 10 recorded runoff events in 2014 at stream gages E121 and E122 (upstream of Reach S-2) and E123 (downstream of the wetland and GCS, Figures B-1.0-1 and B-1.0-2) occurred following heavy rains that fell on the Pajarito Plateau, Los Alamos townsite, and the Sierra de los Valles on July 29 and July 31 (see section 2.0 in the main body for additional detail). Twenty-four-hour rainfall totals measured by the E121.9 rain gage in Sandia Canyon on July 29 and July 31 were 1.24 in. and 1.34 in., respectively. The maximum measured discharge at these sites occurred on July 31 and was 66 cubic feet per second (cfs) at E121, 19 cfs at E122, and 109 cfs at E123 (Table B-2.0-1). These peak discharges are similar to the 2013 peak discharges of 68 cfs at E121, 18 at E122, and 108 cfs at E123 (LANL 2011, 200902; LANL 2012, 218411). Before 2013, peak discharge at E123 ranged from 23 cfs to 85 cfs over the period of record (since 1999, Table B-2.0-1); the 2013 and 2014 peak discharges at E123 were large. Peak discharge for 2013 and 2014 at E121 and E122 are more representative of the peak discharges during the period of record (Table B-2.0-1).

B-3.0 METHODS

A total of 23 cross-section transects were established at varying intervals across the approximate 2100 ft length of Sandia Canyon Reach S-2, from the outlet of the plunge pool to just downstream of the Sandia Canyon GCS (Figures B-1.0-1 and B-1.0-2). For monitoring year (MY) 2013, 16 of these cross-section transects were surveyed in February and March 2014 (LANL 2011, 200902; LANL 2012, 218411). For MY2014, these same 16 cross-section transects were resurveyed and baseline surveys at 7 additional cross-section transects were collected in November and December 2014. Cross-sections were renumbered in November 2014 and are labeled SGCS-1 through SGCS-23, from upstream to downstream (Table B-3.0-1).

The locations of all cross-section transects, gage stations and 13 piezometers are shown on an orthophotograph in Figure B-1.0-1. The cross-section transects, gage stations, piezometers, and boundaries of Sandia Canyon Reach S-2 are shown on the geomorphic map in Figure B-1.0-2 (geomorphic mapping from 2009; LANL 2009, 107453). In the following discussion, the cross-section transects are grouped geographically into six zones: the Plunge Pool Zone, the Wetland Transition Zone, the Alluvial Fan Deposition Zone, the Zone above Grade-Control Structure, the Grade-Control Structure Zone, and the Zone below Grade-Control Structure (Figures B-1.0-1 and B-1.0-2). The wetland extends from approximately SGCS-5 (in the Wetlands Transition Zone) to Sheet Pile 1 in the GCS (just downstream of SGCS-18).

B-3.1 Survey Techniques

Surveys were conducted using a combination of a differentially corrected global positioning system (GPS) and a total station tied to GPS control points, depending on clear sky view (e.g., minimal tree cover). Raw survey data (Northing and Easting coordinates using the New Mexico State Plane coordinate system and elevations of all survey points) for surveyed cross-sections are included electronically as Attachment B-2 (on CD included with this document). The locations of cross-section transect line endpoints are determined by rebar benchmarks, and the transect line is defined as the straight line connecting the rebar. A two-dimensional rotation was performed to transform the survey data (Northing and Easting coordinates) into the x-y coordinate system where the x-axis is along the cross-section transect line (x values are distance along the transect line) and the y-axis is perpendicular to the transect line (y values quantify deviation from the transect line). Distance along the transect line (x values) are also reported with the raw survey data in Attachment B-2. Distances between individual cross-sections were determined by measuring between the midpoints of adjacent cross-section transects. In addition to surveying along cross-sections, the perimeter of the plunge pool at the top of Reach S-2 was surveyed for both MY2013 and MY2014.

B-3.2 Calculation of Net Sediment Deposition along Cross-Sections

When repeat surveys along cross-sections are conducted, elevation changes are observed. Apparent elevation changes can occur as artifacts of the survey data collection (such as may result from different survey-point spacing or slight offest from the transect line). Actual elevation changes can occur from sediment erosion or deposition as well as other processes, including burrowing by animals, road blading or slope stabilization efforts, or differences in soil saturation or compaction between measurements.

Elevation changes occuring below 2014 high-water levels are expected to be dominated by sediment erosion or deposition. Elevation changes occurring above 2014 high water levels are expected to be from sediment erosion or deposition (e.g., alluvial fans, slope wash, aeolian transport, scour by small channels sourced by side drainages) as well as from other non-sediment transport processes (e.g., bioturbation, compaction). Elevation changes observed in the survey data that occurred above the 2014 high-water level were field checked and attributed to side drainage erosion/deposition processes in some cases, and other non-sediment transport processes in other cases.

In this report, for the purposes of calculating sediment deposition, all elevation changes are assumed to represent sediment erosion or deposition. Net sediment deposition along cross-section transects is reported over the entire length of each transect as well as over just the length of the obligate zone. The obligate zone delineations are the same as those from Appendix C, where the obligate zone is defined as the portion of the transect between the first and last occurrence of obligate wetland plants. Since the obligate zone is expected to occur within the flooding area (below high-water line), elevation changes in the obligate zone are expected to be dominated by sediment erosion or deposition rather than by other processes. In this report, the lateral extent of the wetland along a given transect is considered to be approximated by the obligate zone.

For each year, surveyed data points are linearly interpolated to generate a line approximating the ground surface along the transect. Subtraction of the integral of (or area under) the first year’s line from the integral of (or area under) the second year’s line yields net deposition. The net sediment deposition along a cross-section is an area because it is calculated in the plane of the cross-section (xz space). Negative values indicate erosion while positive values indicate deposition. For each cross-section, two net deposition values are reported: one for the entire length of the transect, and one calculated over just the obligate zone.

B-3.3 Estimation of Volume Changes within Zones

Within each zone with repeat cross-sections (Plunge Pool Zone, Wetlands Transition Zone, Alluvial Fan Deposition Zone, and Zone above Grade Control Structure), an estimated volume of net sediment deposition is calculated. The volume of net sediment deposition between two transects is calculated by multiplying the distance between the transects by the average net sediment deposition of the two transects (net sediment deposition over the entire transects). To obtain an estimated volume change for the zone, a weighted average of the volumes between individual transects is calculated, where the weighting is based on plan-view area between the transects. For instance, the sediment volume change between two short, closely spaced transects will have less influence on the weighed average than the sediment volume change between two long, widely spaced transects. To estimate the net volume of sediment deposition within the obligate zone between transects, the same calculation was performed as described above, using only the portion of the cross-sections within the obligate zone. The calculated volume of sediment deposition or erosion for each zone was then divided by the plan-view area of the zone to get an equivalent change in elevation, assuming deposition/erosion was spread equally over the entire zone.

B-3.4 Thalweg Survey and Characterization

A longitudinal channel thalweg profile was surveyed in three segments where the thalweg was a well-defined feature. The first segment was surveyed from the plunge pool outlet to the western edge of the wetland at SGCS-5, the second segment was surveyed in the eastern part of the wetland from SGCS-13 to immediately upstream of the GCS (just downstream of SGCS-19), and the third segment was surveyed between the two cross-sections (SGCS-22 and SGCS-23) located downstream of the GCS (Figures B-1.0-1 and B-1.0-2). The third segment was not previously surveyed and is thus a baseline measurement. Since the thalweg is not well-defined through the central and western portions of the wetland, it was not surveyed in these places. To estimate thalweg elevation change where the thalweg is not well-defined, the low point along each transect was used as a proxy for thalweg elevation. Distances along thalweg profiles used for the figures in this report were calculated using straight-line distance form the plunge and are also included in Attachment B-2

Thalweg sinuosity is calculated by dividing the length of the surveyed thalweg by the straightline distance between the endpoints. A thalweg sinuosity of 1 indicates that the thalweg is completely straight, while higher values indicate bends occur in the channel. Changes in thalweg elevation and sinuosity can indicate thalweg aggradation or incision as well as changes in the stream velocity or sediment transport capability.

B-3.5 Error Calculation

Vertical error was assigned to each cross-section based on instrument used. Points measured with GPS were assigned an error equal to the GPS vertical precision threshold for that cross-section. Points measured with total station were assigned an error equal to the vertical precision of the total station setup for that cross-section. Individual point errors were not used in this report but may be used in subsequent years. Horizontal error was small compared to the cross-section distances and was assumed to be zero for the purposes of calculating vertical change due to sediment deposition/erosion. No attempt was made to assign additional vertical error based on GPS and total station accuracy determination, human error while measuring, or other factors. Errors were propagated through the area and volume calculations by addition/subtraction (as the square root of the sum of the variances) or scaling, assuming that all measurements followed independent normal distributions. All errors are reported as 95% confidence intervals.

B-4.0 RESULTS

For each zone, a geomorphic map with transect locations is presented, followed by individual cross-section profiles. Cross-section figures include the MY2014 survey data and, for resurveyed cross-sections, the MY2013 baseline survey data. Surveyed cross-sections are shown in figures with a vertical exaggeration (VE) of 2.5 times. Channel thalweg figures include MY2013 and MY2014 survey data and are shown with a VE of 6.67 times. Tables summarize the elevation changes along each transect, interpolated sediment volume changes between transects, and changes to thalweg characteristics.

B-4.1 Plunge Pool Zone

Three cross-section transects were surveyed directly downstream of the plunge pool in the western end of reach S-2 (Figure B-4.1-1). The SGCS-1 transect spans the outlet at the eastern edge of the plunge pool and the SGCS-2 and SGCS-3 transects are downstream at 20-ft intervals. The perimeter of the plunge pool was also surveyed (Figure B-4.1-2). The cross-sections for SGCS-1, SGCS-2, and SGCS-3 were surveyed for MY2013 and MY2014, and the resulting profiles are shown in Figure B-4.1-3.

A comparison of the plunge pool perimeter in MY2013 and MY2014 indicates the plunge pool expanded during 2014. The expansion is mostly toward the southeast and east, with some expansion toward the north (Figure B-4.1-2).

Net sediment deposition likely occurred at one of the three plunge pool area cross-sections (SGCS-3). Net sediment erosion occurred at one cross-section (SGCS-1), and net sediment erosion likely occurred at the remaining cross-section (SGCS-2) during the summer 2014 monsoon season, as summarized in Table B-4.1-1. Maximum erosion along each cross-section ranged from about 1.4 ft to 2.9 ft, and maximum deposition ranged from about 0.4 ft to 1.4 ft. (Table B-4.1-1). For all three cross-sections, the majority of erosion is related to bank erosion, particularly on the north side of the channel, and the majority of deposition occurred within the channel (Figure B-4.1-3).

Normalized net sediment volume change for the Plunge Pool Zone was interpolated based on the net sediment deposition values for each cross-section. Net sediment erosion occurred in the Plunge Pool Zone (normalized net sediment deposition averaged −29 m^3/100 m ±31 m^3/100 m, Table B-4.1-2). This volume of sediment is equivalent to a −2.36 ± 0.65 cm change in elevation over the Plunge Pool Zone.

The obligate zone was not delineated for these transects, so net sediment deposition for individual transects and normalized net sediment deposition average for the Plunge Pool Zone are not reported.

B-4.2 Wetland Transition Zone

Five cross-section transects were surveyed in the Wetland Transition Zone, located in the western third of S-2 (Figure B-4.2-1). This zone starts about 400 ft downstream from the eastern extent of the Plunge Pool Zone, where the main stream channel begins to widen into the main wetland. Transects SGCS-5 through SGCS-8 are spaced sequentially at about 100-ft intervals starting about 100 ft downstream of SGCS-4. The cross-sections for SGCS-4 through SGCS-8 were surveyed for MY2013 and MY2014, and the resulting profiles are in Figure B-4.2-2. The five cross-sections document the uneven transition from channelized flow (upstream) to diffuse, nonchannelized flow in the wetland.

Net sediment deposition occurred at one of the five Wetland Transition Zone cross-sections (SGCS-8) and likely occurred at another (SGCS-5).Net sediment erosion occurred at one cross-section (SGCS-7) during the summer 2014 monsoon season, as summarized in Table B-4.2-1. Net sediment erosion or deposition may have occurred at the remaining two cross-sections, given the instrumental error, with net sediment deposition more likely than erosion at SGCS-4, and net sediment erosion more likely than deposition at SGCS-6 (Table B-4.2-1).

Within the obligate zone, net sediment deposition occurred at one of the five Wetland Transition Zone cross-sections (SGCS-4); net sediment deposition likely occurred at another (SGCS-5); net sediment erosion occurred at two cross-sections (SGCS-6 and SGCS-7); and net sediment erosion likely occurred at the remaining cross-section (SGCS-8) during the summer 2014 monsoon season (Table B-4.2-1).

Maximum erosion on each cross-section ranged from 0.4 ft to 1.4 ft, and maximum deposition on each cross-section ranged from 0.4 ft to 1.2 ft (Table B-4.2-1). Along SGCS-4, maximum aggradation (1.2 ft) occurred in the former main channel within the wetland, and maximum erosion (1.4 ft) occurred within a side channel outside of the wetland (Figure 4.2-2). Along SGCS-5, maximum erosion (0.4 ft) and maximum deposition (0.9 ft) occurred within the wetland, likely as a result of channel rearrangement (Figure 4.2-2). Along SGCS-6, minor erosion is distributed across a large portion of the transect with maximum erosion (0.7 ft) within the wetland; deposition is primarily sourced by an alluvial fan on the northeast side of the cross-section (Figure 4.2-2). Along SGCS-7, minor erosion is distributed across a large portion of the transect, with one moderate scour within the wetland, and the maximum erosion (1.3 ft) occuring within a small side channel to the north of the wetland (Figure 4.2-2). Along SGCS-8, minor erosion is distributed across a large portion of the transect, with maximum erosion (1.1 ft) occurring within a small side channel to the north of the wetland; deposition is primarily sourced by an alluvial fan on the north side of the cross-section (Figure 4.2-2).

Normalized net sediment volume change for the Wetland Transition Zone was interpolated based on the net sediment deposition values for each cross-section. Net sediment erosion likely occurred in the Wetland Transition Zone (normalized net sediment deposition averaged −34 m^3/100 m ±102 m^3/100 m, Table B-4.2-2). This volume of sediment is equivalent to a −0.48 ± 0.09 cm change in elevation over the Wetland Transition Zone.

Normalized net sediment volume change within the obligate zone of the Wetlands Transition Zone was interpolated based on net sediment deposition values for the part of each cross-section bounded by the obligate zone. Net sediment erosion possibly occurred within the obligate zone of the Wetlands Transition Zone; however, the magnitude of instrumental error is large compared with the net sediment volume change (normalized net sediment deposition averaged −13 m^3/100 m ±48 m^3/100 m, Table B-4.2-2). This volume of sediment is equivalent to a 0.09 ± 0.08 cm change in obligate zone elevation over the Wetland Transition Zone.

B-4.3 Alluvial Fan Deposition Zone

Four cross-section transects were surveyed in the Alluvial Fan Deposition Zone, approximately 300 ft downstream of the eastern extent of the Wetland Transitional Zone in the central part of S-2 (Figure B-4.3-1). Two cross-section transects (SGCS-10 and SGCS-11) were surveyed for MY2013 and resurveyed for MY2014; SGCS-10 and SGCS-11 share a northern endpoint. In November 2014, two additional transects (SGCS-9 and SGCS-12) were surveyed in this zone. The survey profiles from MY2013 and MY2014 for SGCS-10 and SGCS-11, and baseline profiles from MY2014 for SGCS-9 and SGCS-12 are shown in Figure B-4.3-2.

The purpose of monitoring the cross-sections in this zone is to record active sediment transport on a prograding alluvial fan that enters the wetland from a south tributary drainage. The southern end of SGCS-10 and SGCS-11 are on the tributary alluvial fan deposits, with the northern end of each section extending across the main wetland, providing representative sections in the central portion of the primary wetland (Figure B-4.3-1).

Over the entire transect, and within just the obligate zone, net sediment erosion likely occurred at cross-section SGCS-10 during the summer 2014 monsoon season. Net sediment erosion is more likely than net sediment deposition over the entire transect SGCS-11 and within the obligate zone of SGCS-11; however, the instrumental error is large enough relative to the net value that it is possible net deposition occurred instead (Table B-4.3-1).

Along both SGCS-10 and SGCS-11, maximum deposition (0.6 ft on SGCS-10, 0.7 ft on SGCS-11) occurred toward the northern side of the wetland, likely as a result of channel rearrangement (Figure B-4.3-2). Along both SGCS-10 and SGCS-11, maximum erosion (0.6 ft on SGCS-10, 0.7 ft on SGCS-11) is toward the southern side of the cross-sections and represents alluvial fan toe-cutting by the main longitudinal (Sandia) drainage.

Normalized net sediment volume change for the Alluvial Fan Deposition Zone was interpolated based on the net sediment deposition values for the two repeat cross-sections. Net sediment erosion may have occurred in the Alluvial Fan Deposition Zone; however, the magnitude of instrumental error is large compared with the net sediment volume change (normalized net sediment deposition averaged −115 m^3/100 m ±216 m^3/100 m, Table B-4.3-2). This volume of sediment is equivalent to a −1.72 ± 0.47 cm change in elevation over the Alluvial Fan Deposition Zone.

Normalized net sediment volume change within the obligate zone of the Alluvial Fan Deposition Zone was interpolated based on net sediment deposition values for the part of each cross-section bounded by the obligate zone. Net sediment erosion likely occurred within the obligate zone of the Alluvial Fan Deposition Zone (normalized net sediment deposition averaged −120 m^3/100 m ±140 m^3/100 m, Table B-4.3-2). This volume of sediment is equivalent to a −2.79 ± 0.38 cm change in obligate zone elevation over the Alluvial Fan Deposition Zone.

B-4.4 Zone above Grade-Control Structure

Six cross-section transects were surveyed in the Zone above Grade-Control Structure; the GCS consists of three subsurface sheet pile grade steps capped with concrete. SGCS-13, SGCS-14, SGCS-15, SGCS-16, SGCS-17, and SGCS-18 are 290 ft, 190 ft, 125 ft, 94 ft, 66 ft, and 42 ft upstream of Sheet Pile 1, respectively (Figure B-4.4-1). The purpose of the closely spaced cross-sections above the GCS is to provide detailed monitoring of the area immediately upstream of the GCS, including the area where a headcut was located before construction of the GCS (LANL 2013, 251743). Cross-section profiles for the Zone above Grade-Control Structure were surveyed for MY2013 and MY2014 (Figure B-4.4-2).

Over the entire transects, net sediment deposition occurred at three of the six Zone above Grade-Control Structure cross-sections (SGCS-14, SGCS-17, and SGCS-18), and net sediment erosion occurred at two cross-sections (SGCS-13 and SGCS-15) during the 2014 summer monsoon season, as summarized in Table B-4.4-1. The direction of net change (erosive or depositional) along SGCS-16 is difficult to distinguish given the instrumental error (Table B-4.4-1).

Within just the obligate zone, net sediment deposition occurred at two cross-sections: SGCS-14 and SGCS-18 (Table B-4.4-1). Net sediment erosion occurred at SGCS-13, SGCS-15, SGCS-16, and SGCS-17 (Table B-4.4-1).

Over the entire transects, maximum erosion ranged from 0.3 ft to 1.0 ft, and maximum deposition on each transect ranged from 0.4 ft to 0.8 ft (Table B-4.4-1). Along SGCS-13, maximum erosion (1.0 ft) occurred across the broad channel floor within the wetland, and maximum deposition (0.5 ft) occurred outside the wetland, likely related to side slope processes (Figure B-4.4-2). Along SGCS-14, maximum erosion (0.5 ft) and maximum deposition (0.8 ft) occurred within the wetland, likely as a result of channel rearrangement (Figure B-4.4-2). Along SGCS-15, maximum erosion (0.8 ft) and maximum deposition (0.4 ft) occurred within the wetland, with moderate scour outside the wetland toward the south of the transect (Figure B-4.4-2). Along SGCS-16 and SGCS-17, maximum deposition (0.5 ft on SGCS-16, 0.6 ft on SGCS-17) and maximum erosion (0.6 ft on both transects) occurred within the wetland, representing channel rearrangement processes (Figure B-4.4-2). Along SGCS-18, maximum erosion (0.3 ft) occurred within the wetland, and maximum deposition (0.5 ft) occurred just outside the wetland.

Normalized net sediment volume change for the Zone above Grade-Control Structure was interpolated based on the net sediment deposition values for each cross-section. Net sediment erosion occurred in the Zone above Grade-Control Structure (normalized net sediment deposition averaged −29m^3/100 m ±14 m^3/100 m, Table B-4.4-2). This volume of sediment is equivalent to a −0.70 ± 0.03 cm change in elevation over Zone above Grade-Control Structure.

Normalized net sediment volume change within the obligate zone of the Zone above GCS was interpolated based on net sediment deposition values for the part of each cross-section bounded by the obligate zone. Net sediment erosion occurred within the obligate zone of the Zone above Grade-Control Structure (normalized net sediment deposition averaged −26 m^3/100 m ±8 m^3/100 m, Table B-4.4-2). This volume of sediment is equivalent to a −1.04 ± 0.03 cm change in obligate zone elevation over the Zone above Grade-Control Structure.

B-4.5 Grade-Control Structure Zone and Zone below Grade-Control Structure

Three new baseline cross-sections were surveyed in the Grade-Control Structure Zone. SGCS-19 is located above Sheet Pile 1 and shares a southern end point with SGCS-18. SGCS-20 is located between Sheet Piles 1 and 2, and SGCS-21 is located between Sheet Piles 2 and 3. Cross-section locations are shown in Figure B-4.5-1. Baseline cross-section profiles for the Grade-Control Structure Zone are shown in Figure B-4.5-2.

Two new baseline cross-sections were surveyed in the Zone below Grade-Control Structure (Figure B-4.5-3). SGCS-22 is located approximately 125 ft below the GCS, and SGCS-23 is located approximately 225 ft below the GCS. Baseline cross-section profiles for the Zone below Grade-Control Structure are shown in Figure B-4.5-4.

B-4.6 Thalweg Characterization

A channel thalweg profile was surveyed from the eastern edge of the plunge pool downstream almost to transect SGCS-5 (Figures B-1.0-1, B-4.1-1, and B-4.2-1). Below line SGCS-5, the thalweg is poorly defined (diffuse) or absent as a mappable feature as a result of spreading of flow and channel branching within the active wetland. To approximate a thalweg gradient below SGCS-5, the lowest elevation along each transect was identified for cross-sections SGCS-6 though SGCS-8 in the Wetland Transition Zone and SGCS10 through SGCS-11 in the Alluvial Fan Deposition Zone (Tables B-4.2-1 and B-4.3-1). From just above SGCS-13 downstream to Sheet Pile 1 in the GCS, the thalweg is again well-defined and was surveyed (Figures B-1.0-1, B-4.4-1, and B-4.5-1). The thalweg was also surveyed from SGCS-22 to SGCS-23 below the GCS (Figures B-1.0-1 and B-4.5-3).

Thalweg elevation changes are reported for all transects surveyed in both MY2013 and MY2014 (Tables B-4.1-1, B-4.2-1, B-4.3-1, and B-4.4-1). The thalweg channel profile is presented in two figures: Figure B-4.6-1 shows the thalweg in the upper stretch of the reach (below the plunge pool to SGCS-5), and Figure B-4.6-2 shows the thalweg in the lower stretch of the reach (just above SGCS-13 to SGCS-23). In the channel thalweg figures, the distance along the survey can vary between the original survey and the resurvey because of changes in thalweg sinuosity, resulting in changes in thalweg gradient. Thalweg sinuousity values are presented in Table B-4.6-1.

On average, the channel thalweg in the Plunge Pool Zone aggraded by 0.4 ft in 2014 (Table B-4.6-2). While net erosion was calculated in the Plunge Pool Zone(Table B-4.1-2), there is no indication of headcut development as shown by thalweg aggredation in this area (Figure B-4.6-1).

B-5.0 DISCUSSION

B-5.1 Net Deposition along Surveyed Cross-Sections

Errors on measured values are reported for all applicable results in Table B-4.1-1 through Table B-4.6-2 and in Figures B-4.1-3, B-4.2-2, B-4.3-2, and B-4.4-2. The reported errors are derived from error measurements reported by GPS or total station instruments at the time of surveys. Horizontal errors are ignored in all calculations because they are insignificant compared with the distances involved. Specific pockets of erosion or deposition frequently have a greater magnitude of elevation change than the vertical error (e.g. maximum erosion on SGCS-4 is 1.4 ft +/−0.13 ft). These features can be confidently distinguished in the cross-section figures and were confirmed during field surveys. When net deposition along an entire transect is calculated, the net deposition is often similar in magnitude to the reported error.

It is expected that the accumulation (or removal) of sediment over several years will result in net sediment deposition values of greater magnitude than the associated error values. Thus, while the net erosion or deposition during a single year may be hard to distinguish, net erosion or deposition over several years is expected to be confidently distinguished.

During 2014 monsoonal flood events, net erosion occurred in each of the four areas with repeat survey data. However, some individual cross-sections recorded net deposition. During 2014, maximum aggradation of 1.4 ft within Reach S-2 occurred at SGCS-3 (Photo B1-1 in Attachment B-1; Figure B-4.1-3). During 2014, maximum erosion of 2.9 ft within Reach S-2 occurred at SGCS-2 (Photo B1-2 in Attachment B-1; Figure B-4.1-3).

Between MY2013 and MY2014, geomorphic changes in the Plunge Pool Zone consisted of bank erosion and channel deposition. Geomorphic changes in the Wetland Transition Zone and the Alluvial Fan Deposition zone consisted of channel rearrangement within the wetland, deposition by alluvial fans and slope wash from side drainages and slopes, and some scour of small channels outside the main wetland. Geomorphic changes in the Zone above Grade-Control Structure consisted largely of erosion and deposition within the wetland, with minor changes outside the wetland along most transects.

Alluvial fan deposits, originating from side drainages below the Los Alamos County Eco Station, were observed at the northern ends of cross-section lines SGCS-6 and SCGS-8 (Figures B-1.0-1 and B-4.2-1). Alluvial fan deposition in the vicinity of SGCS-6 extends for approximately 70 ft downstream (east) of SGCS-6 (Photo B1-3 in Attachment B-1), and alluvial fan deposition extends for approximately 30 ft upstream (west) and 100 ft downstream of SGCS-8 (Photo B1-4 in Attachment B-1). Sediment deposition from alluvial fans and slope wash from slopes to the north and south of Reach S-2 is included in calculations of net sediment deposition and erosion presented above but underestimates the contribution of these sources because the transects do not extend far enough to encompass the entirety of these features.

B-5.2 Estimates of Sediment Volume Changes in Reach S-2

The normalized net sediment deposition in all four zones with repeat surveys is negative, indicating erosion; however, in some zones the magnitude of instrumental error is large compared with the net sediment volume change. The values of normalized net sediment deposition are similar for three of the zones: the Plunge Pool Zone (−29 m^3/100m ±31 m^3/100 m, Table 4.1-2), the Wetlands Transition Zone (−34 m^3/100m ±102 m^3/100 m, Table 4.2-2), and the Zone above GCS (-29 m^3/100m ±14 m^3/100 m, Table 4.4-2). Normalized net sediment erosion in the Alluvial Fan Deposition Zone is greater than in the other three zones (normalized net sediment deposition is −115 m^3/100m ±216 m^3/100 m, Table 4.3-2). Because these volumes were calculated using net sediment deposition values over the entire length of each transect, the values represent a combination of longitudinal channel sediment transport processes, sediment transport processes from side slopes and drainages, and potentially some non-sediment transport processes.

The normalized net sediment deposition within the obligate zone is negative in all three zones with repeat surveys and defined obligate zones, indicating erosion; however, in some zones the magnitude of instrumental error is large compared to the net sediment volume change. The values of normalized net sediment deposition range from −6 to -120 m^3/100 m (Tables 4.2-1, 4.3-2, and 4.4-2). Since the obligate zone is within the part of the wetland that is flooded during monsoon events, it is likely these values represent changes dominated by longitudinal sediment transport (e.g., sediment erosion and deposition from channel rearrangement, scour or sediment deposition within the wetland). In the Wetlands Transition Zone and Zone above Grade-Control Structure, there is greater normalized net erosion over the entire transect than in the obligate zone. In the Alluvial Fan Deposition Zone, there is greater normalized net erosion within the obligate zone than over the entire transect.

While the four zones with repeat surveys had net erosion, only baseline surveys were conducted in some parts of Reach S-2 in MY2014, so no net sediment deposition could be estimated for these zones. The net sediment erosion in the zones with repeat measurements suggest that, overall, Reach S-2 was probably characterized by net erosion during 2014. As reported in 2009, an estimated 9940 m^3/100 m of post-1942 sediment existed in Reach S-2 (LANL 2004, 087390). If the normalized volume of sediment deposited from 1942–2008 (geomorphic mapping was completed in 2008) is interpreted as representing the accumulation of 66 yr of equal annual deposition, it represents approximately 151 m^3/100 m per year of sediment deposition. The 2014 net sediment deposition in each zone (ranging from −28 m^3/100m to −113 m^3/100 m; Tables 4.1-1, 4.2-1, 4.3-1, and 4.4-1) could be considered similar to the erosion of less than 1 yr of deposited sediment based on the average annual net sedimentation of 151 m^3/100 m derived above. Over the period of discharge record (since 1999, Table B-2.0-1), peak discharge at E123 (near the downstream boundary of Reach S-2, Figure B-1.0-2) was high in both 2013 and 2014 (Table B-2.0-1). The high discharge could be partially responsible for the net erosion observed in Reach S-2 in 2014.

B-5.3 Changes in the Thalweg

In the upper stretch of the reach (Plunge Pool Zone and Wetlands Transition Zone), there appears to be some aggradation of the thalweg, but the overall thalweg gradient in the western part of the reach appears to be stable since the previous survey. In the lower stretch of the reach (Zone above Grade-Control Structure), the thalweg appears to be incising.

There does appear to be a new nick point in the lower (eastern) stretch of the reach, just above SGCS-15. The nick point is located within a stretch where the thalweg is otherwise characterized by a shallow slope. Upstream of this stretch, the thalweg steepens, providing the potential for either the development of an additional nick point or the upstream migrate of the current one.

There is some evidence for a lengthening of the thalweg in the lower portion of the reach (the thalweg is well-defined over a larger stretch of the reach than in the previous survey), possibly indicating a tendency towards more channelized versus distributed flow. However, in both the upper and lower stretches of the reach where the thalweg is well defined, thalweg sinuosity has changed little since the previous survey.

B-6.0 CONCLUSIONS AND RECOMMENDATIONS

Erosion within the wetland proper is dominated by channel rearrangement (e.g., avulsion), and eroded areas are usually associated with nearby depositional pockets. In the upland/overbank zone, some areas of deposition occur from sediment input (e.g., alluvial fans, slope wash) from side slopes and drainages, and some localized scour within small side channels. Overall, erosion within the system seems to be associated with scouring in small side channels outside the wetland proper or channel rearrangement within the wetland.

A new channel associated with the nick point, located upgradient of Sheet Pile 1, is apparent. Local erosion below the new base level created by the GCS is also observed. Monitoring of these features in subsequent years will assess whether these features are transient adjustments to the new base level.

Seven new baseline cross-sections were surveyed in November 2014. All 7 baseline surveys, as well as the 16 original surveys, will be repeated following the 2015 monsoon season.

One recommendation for future monitoring, also presented in Appendix C, would be to establish and survey (if possible before the 2015 monsoon season) up to three additional transects between SCGS-3 and SCGS-4. Additionally, baseline mapping of the full extent of the alluvial fan deposits, originating from side drainages below the Los Alamos County Eco Station, should be established before the 2015 monsoon season and remapped annually to monitor the effects of the progradation of these deposits on the wetland system.

B-7.0 REFERENCES AND MAP DATA SOURCES

B-7.1 References

The following list includes all documents cited in this appendix. Parenthetical information following each reference provides the author(s), publication date, and ER ID or ESH ID. This information is also included in text citations. ER IDs were assigned by the Environmental Programs Directorate's Records Processing Facility (IDs through 599999), and ESH IDs are assigned by the Environment, Safety, and Health (ESH) Directorate (IDs 600000 and above). IDs are used to locate documents in the Laboratory's Electronic Document Management System and, where applicable, in the master reference set.

Copies of the master reference set are maintained at the NMED Hazardous Waste Bureau and the ESH Directorate. The set was developed to ensure that the administrative authority has all material needed to review this document, and it is updated with every document submitted to the administrative authority. Documents previously submitted to the administrative authority are not included.

Cobrain, D., April 3, 2013. FW: Sandia Wetland cross sections. E-mail message to D. Katzman (LANL) from D. Cobrain (NMED), Santa Fe, New Mexico. (Cobrain 2013, 256726)

LANL (Los Alamos National Laboratory), April 2004. "Los Alamos and Pueblo Canyons Investigation Report," Los Alamos National Laboratory document LA-UR-04-2714, Los Alamos, New Mexico. (LANL 2004, 087390)

LANL (Los Alamos National Laboratory), October 2009. "Investigation Report for Sandia Canyon," Los Alamos National Laboratory document LA-UR-09-6450, Los Alamos, New Mexico. (LANL 2009, 107453)

LANL (Los Alamos National Laboratory), February 2011. "Baseline Geomorphic Conditions at Sediment Transport Mitigation Sites in the Los Alamos and Pueblo Canyon Watersheds, Revision 1," Los Alamos National Laboratory document LA-UR-11-0936, Los Alamos, New Mexico. (LANL 2011, 200902)

LANL (Los Alamos National Laboratory), September 2011. "Work Plan and Final Design for Stabilization of the Sandia Canyon Wetland," Los Alamos National Laboratory document LA-UR-11-5337, Los Alamos, New Mexico. (LANL 2011, 207053)

LANL (Los Alamos National Laboratory), May 2012. "2011 Geomorphic Changes at Sediment Transport Mitigation Sites in the Los Alamos and Pueblo Canyon Watersheds," Los Alamos National Laboratory document LA-UR-12-21330, Los Alamos, New Mexico. (LANL 2012, 218411)

LANL (Los Alamos National Laboratory), December 2013. "Completion Report for Sandia Canyon Grade-Control Structure," Los Alamos National Laboratory document LA-UR-13-29285, Los Alamos, New Mexico. (LANL 2013, 251743)

LANL (Los Alamos National Laboratory), June 2014. "Sandia Wetland Performance Report, Baseline Conditions 2012–2014," Los Alamos National Laboratory document LA-UR-14-24271, Los Alamos, New Mexico. (LANL 2014, 257590)

B-7.2 Map Data Sources

The following list provides data sources for maps included in the main body of this report.

2000 LIDAR Hypsography; Los Alamos National Laboratory, Earth and Environmental Sciences GISLab; 1:1,200; Work in progress.

Drainage; Los Alamos National Laboratory, Environment and Remediation Support Services; 1:24,000; May 15, 2006.

Gaging stations; Los Alamos National Laboratory, Waste and Environmental Services Division; 1:2,500; March 19, 2011.

Grade control structures; Los Alamos National Laboratory, Environment and Remediation Support Services; Unknown; May 17, 2011.

LANL boundary; Los Alamos National Laboratory, KSL Site Support Services, Planning, Locating and Mapping Section; Unknown; August 16, 2010.

LANL area orthophoto; Los Alamos National Laboratory, Earth and Environmental Sciences GISLab; 1'=200'; April 22-30, 2011.

Location IDs; Los Alamos National Laboratory, ESH&Q Waste and Environmental Services Division; 1:2,500; May 19, 2011.

Other property boundary; Los Alamos National Laboratory, Earth and Environmental Sciences GISLab; Unknown; August 16, 2010.

Roads, surfaced; Los Alamos National Laboratory, KSL Site Support Services, Planning, Locating and Mapping Section; Unknown; November 30, 2010.

Technical area boundary; Los Alamos National Laboratory, Site Planning and Project Initiation Group, Infrastructure Planning Office; Unknown; August 16, 2010.

Watershed; Los Alamos National Laboratory, Environment and Remediation Support Services; 1:2,500; November 2, 2006.

Wells; Los Alamos National Laboratory, ESH&Q Waste and Environmental Services Division; 1:2,500; May 19, 2011.

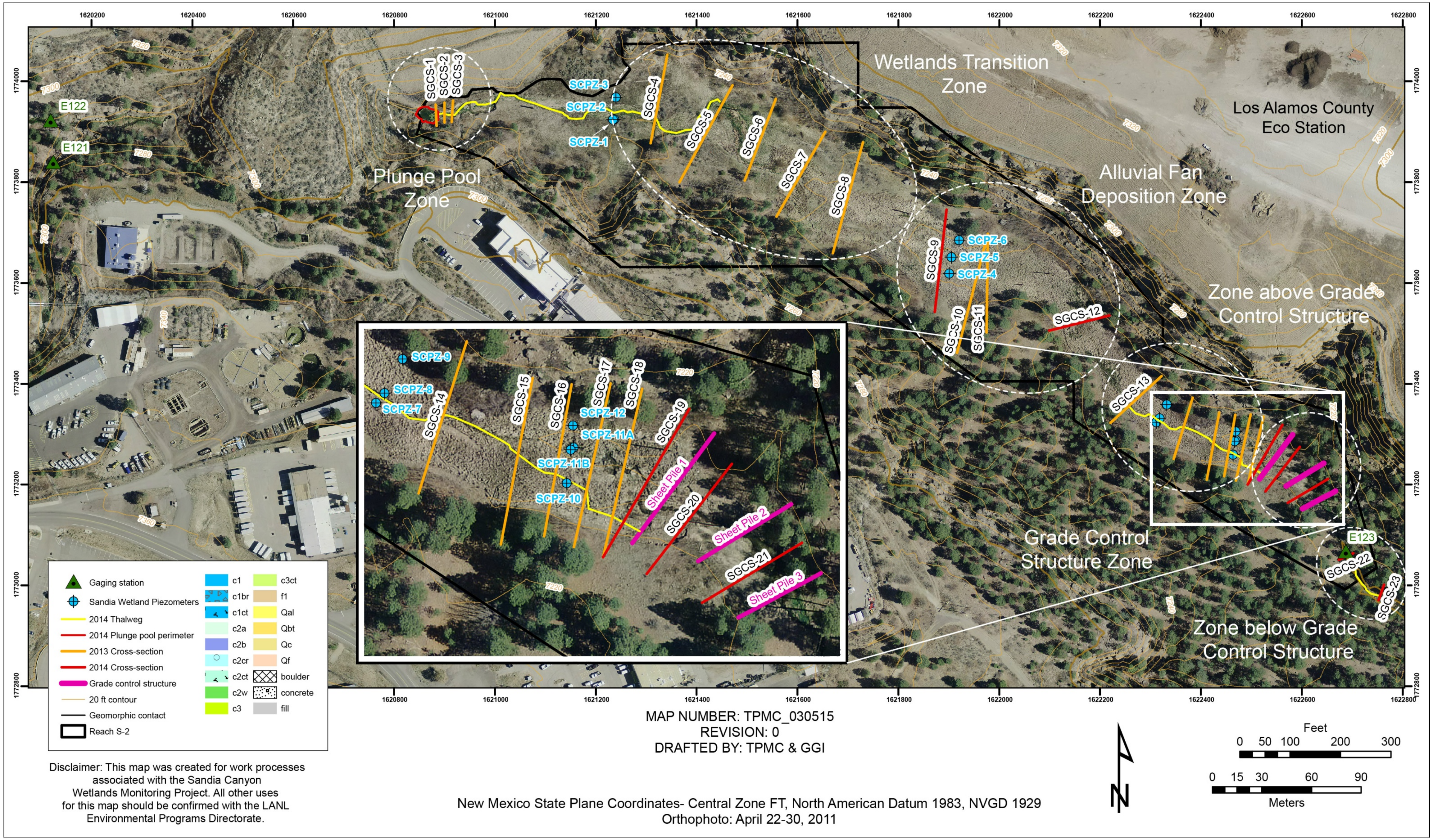

Figure B-1.0-1 Orthophoto with locations of cross-section transects, thalweg profiles, gage station E123, and piezometers in Sandia Canyon Reach S-2

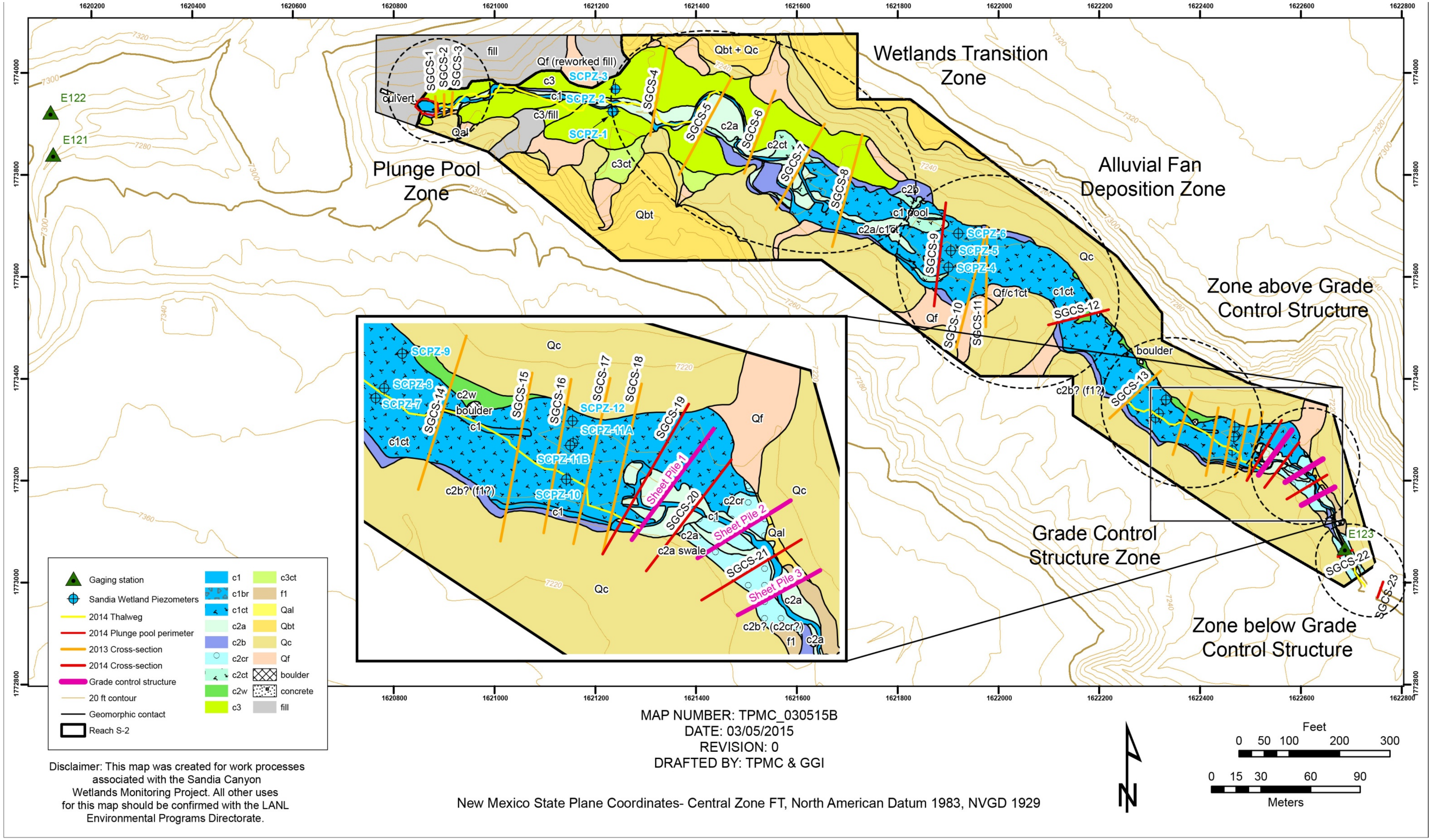

Figure B-1.0-2 Geomorphic map with boundaries of Reach S-2, and locations of cross-section transects, thalweg profiles, gage station E123, and piezometers in Sandia Canyon Reach S-2

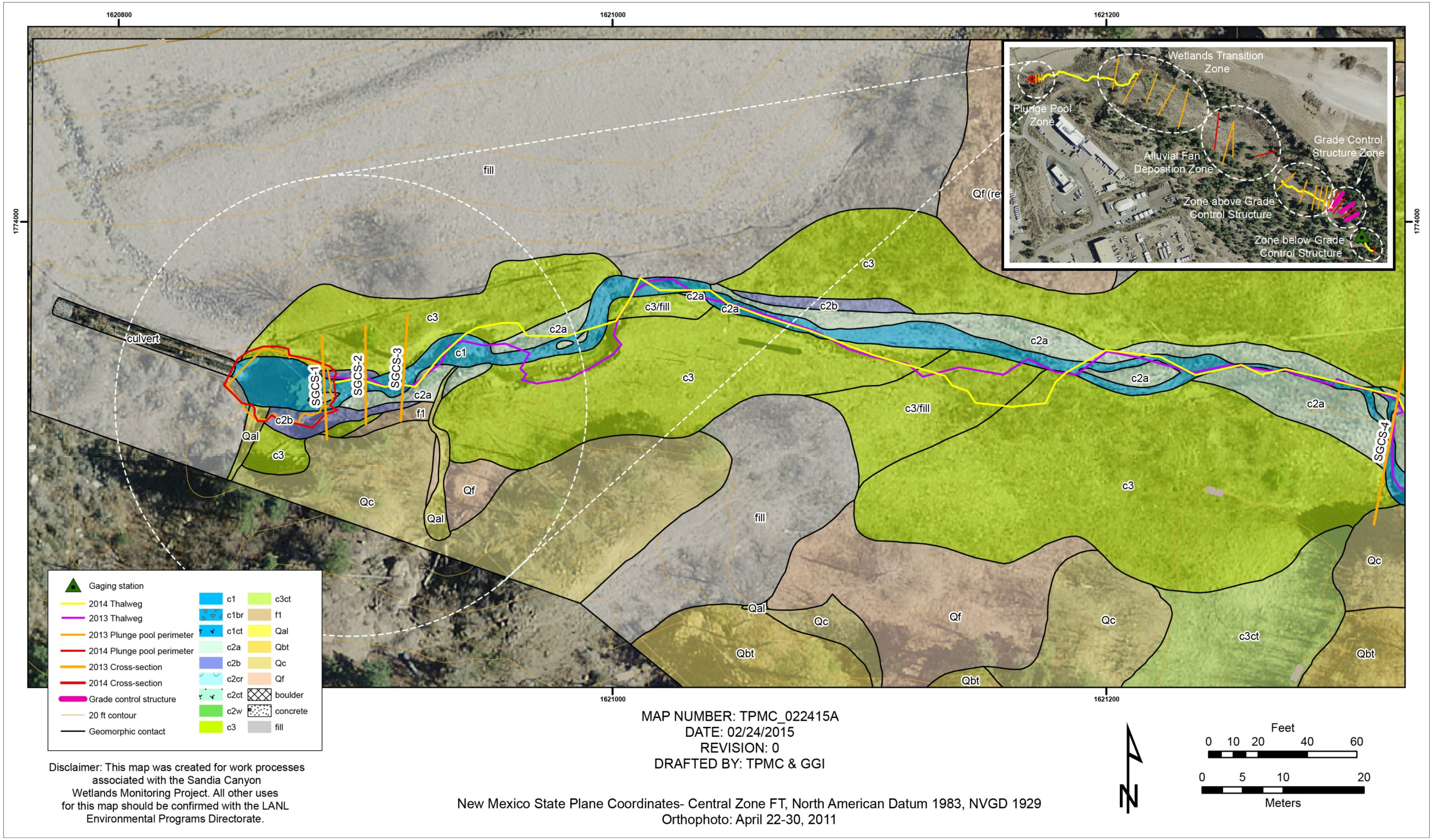

Figure B-4.1-1 **Geomorphic map overlain on an orthophoto showing the locations of cross-section transects and thalweg surveys at the Plunge Pool Zone in Sandia Canyon Reach S-2. The plunge pool perimeter as surveyed for MY2013 and MY2014 is shown in orange (MY2013) and red (MY2014).**

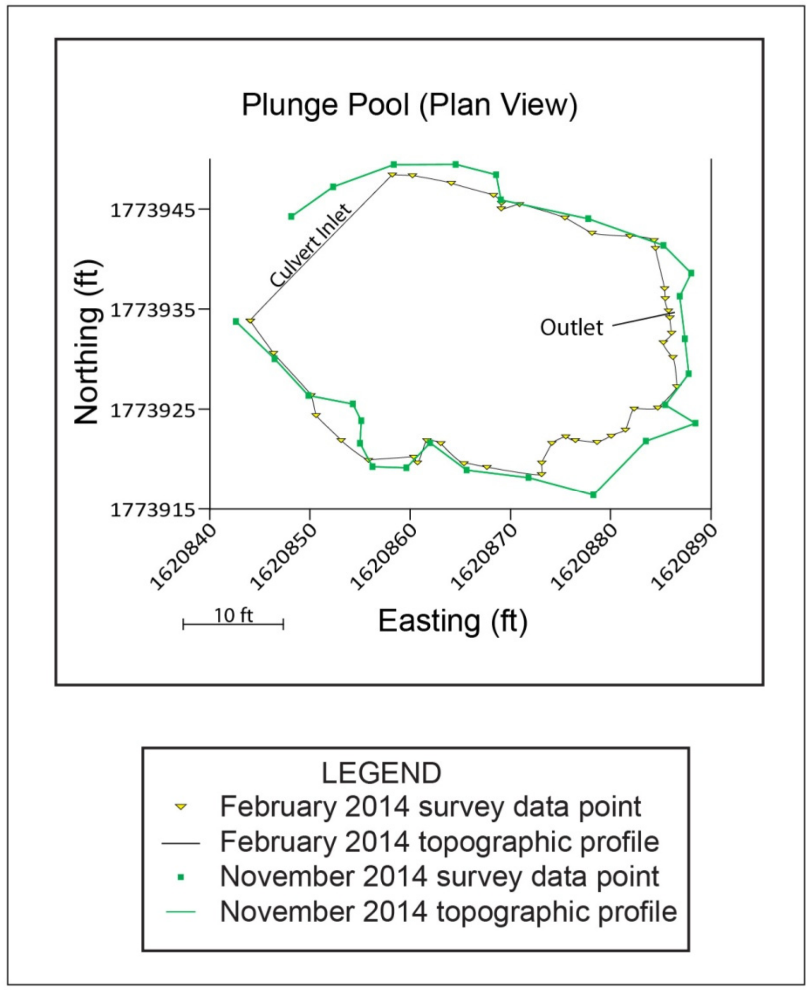

Figure B-4.1-2 Cross-section profiles in the Plunge Pool Zone in Sandia Canyon Reach S-2. Negative values of net sediment deposition indicate erosion. No obligate zone was defined in the Sandia Canyon Wetlands Plunge Pool Zone.

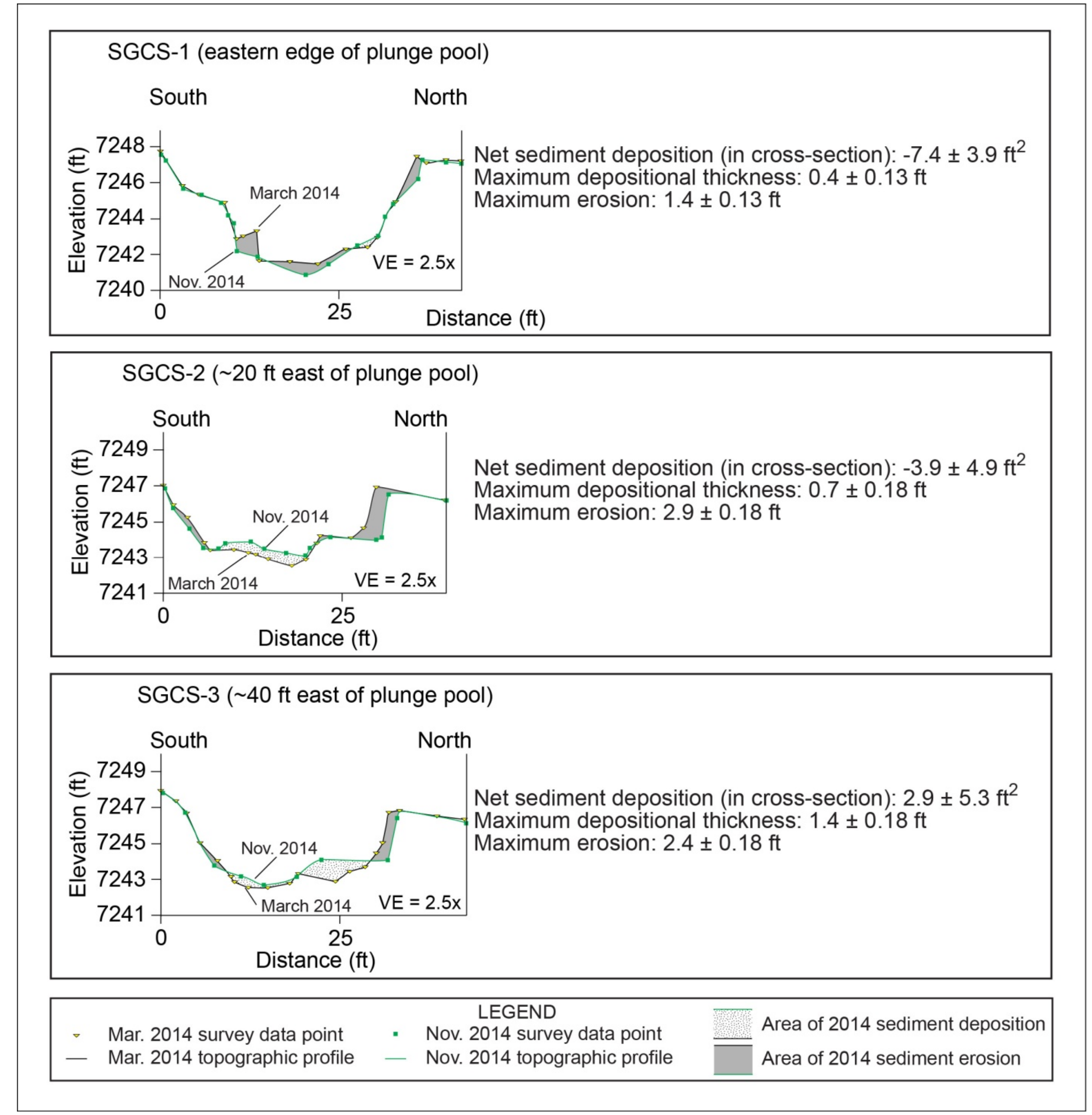

Figure B-4.1-3 Plan view of the Plunge Pool in Sandia Canyon Reach S-2

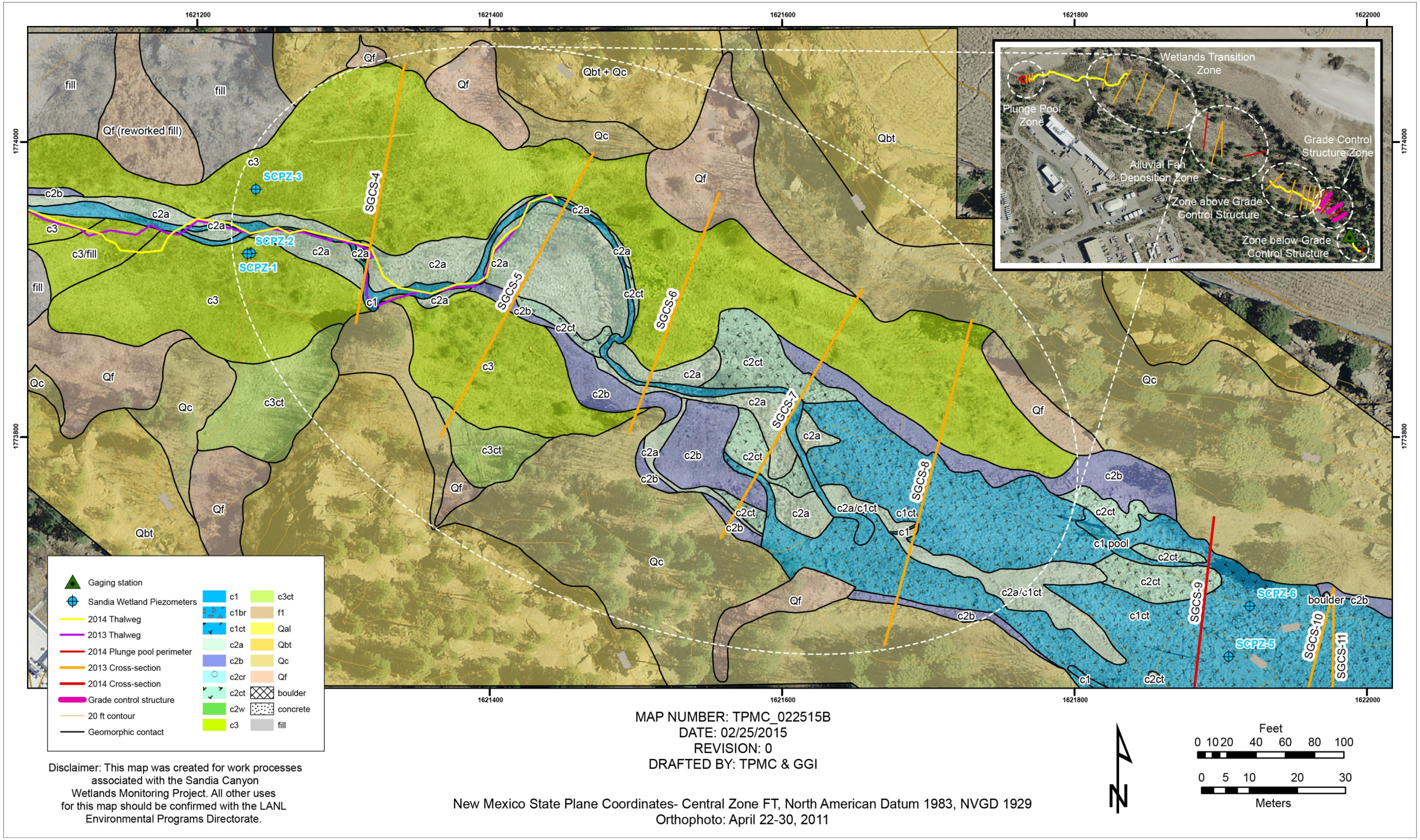

Figure B-4.2-1 Geomorphic map overlain on an orthophoto showing the locations of piezometers, cross-section transects, and thalweg surveys in the Wetland Transition Zone in Sandia Canyon Reach S-2

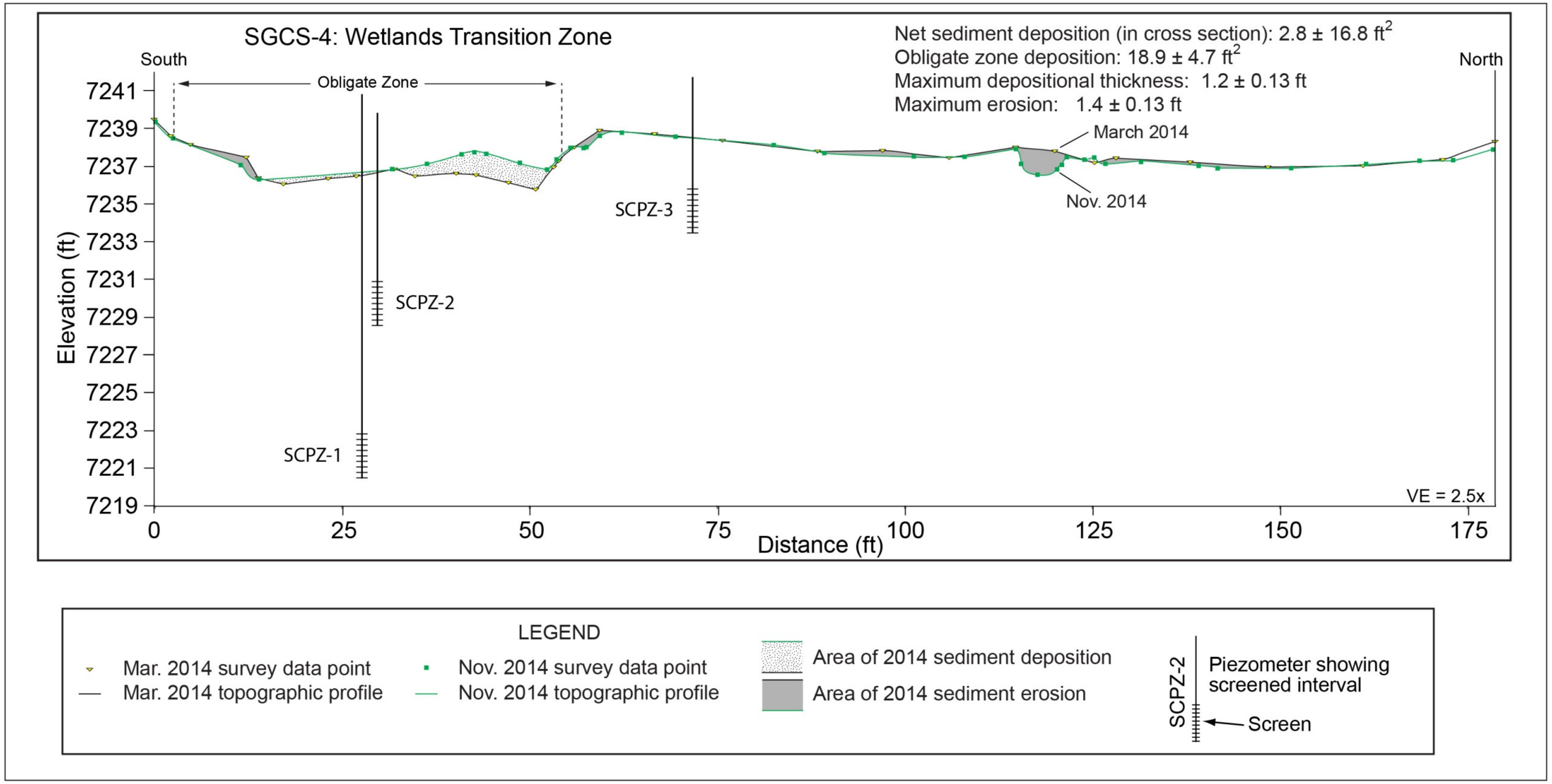

Figure B-4.2-2 Cross-section profile in the Wetland Transition Zone in Sandia Canyon. The obligate zones (see Appendix C) are defined using either the wetland vegetation perimeter mapping method, indicated here with an (*), or using the line intercept method.

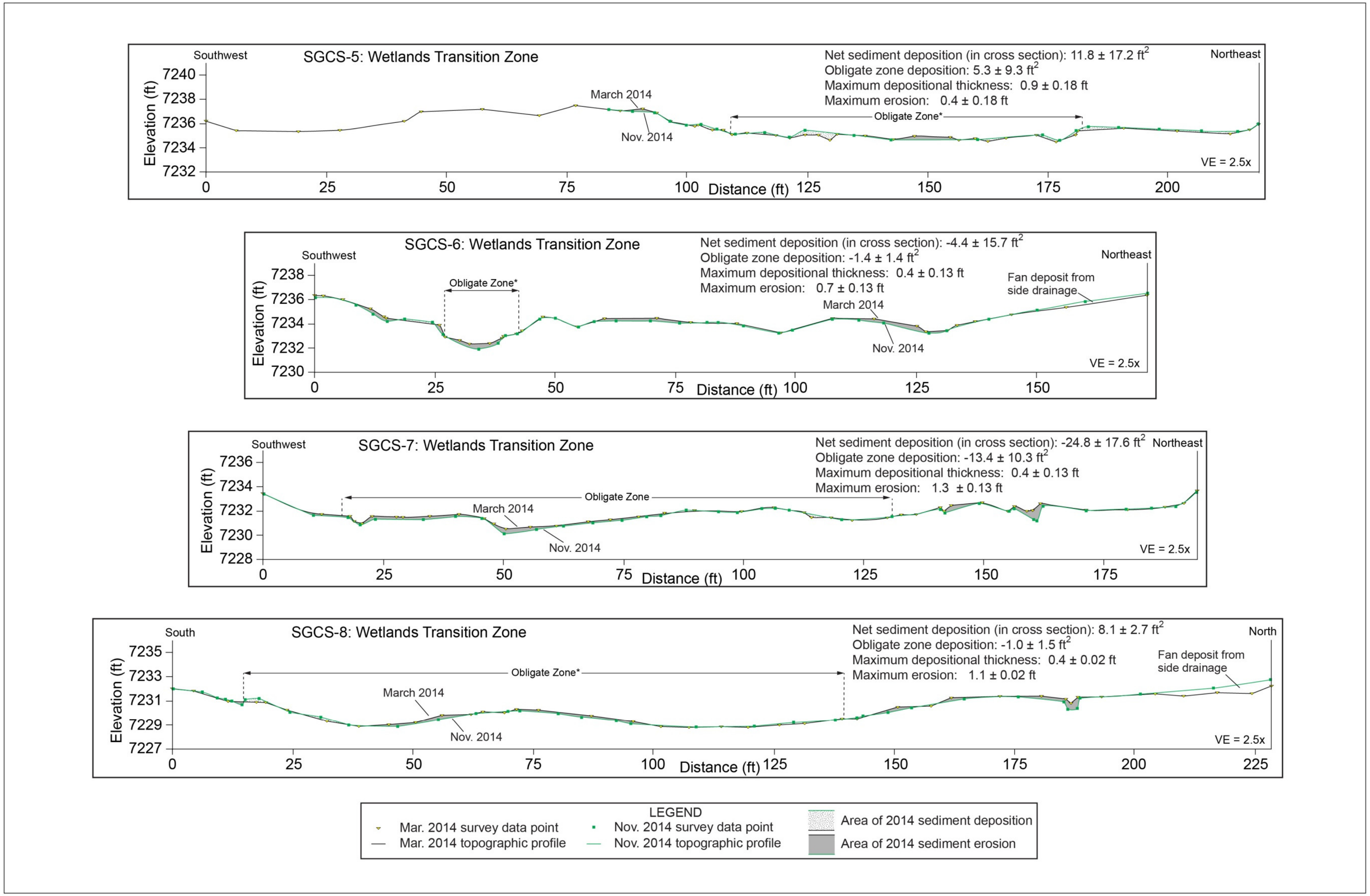

Figure B-4.2-2 (continued) **Cross-section profile in the Wetland Transition Zone in Sandia Canyon. Negative values of net sediment deposition indicate erosion. The obligate zones (see Appendix C) are defined using either the wetland vegetation perimeter mapping method, indicated here with an (*), or using the line intercept method.**

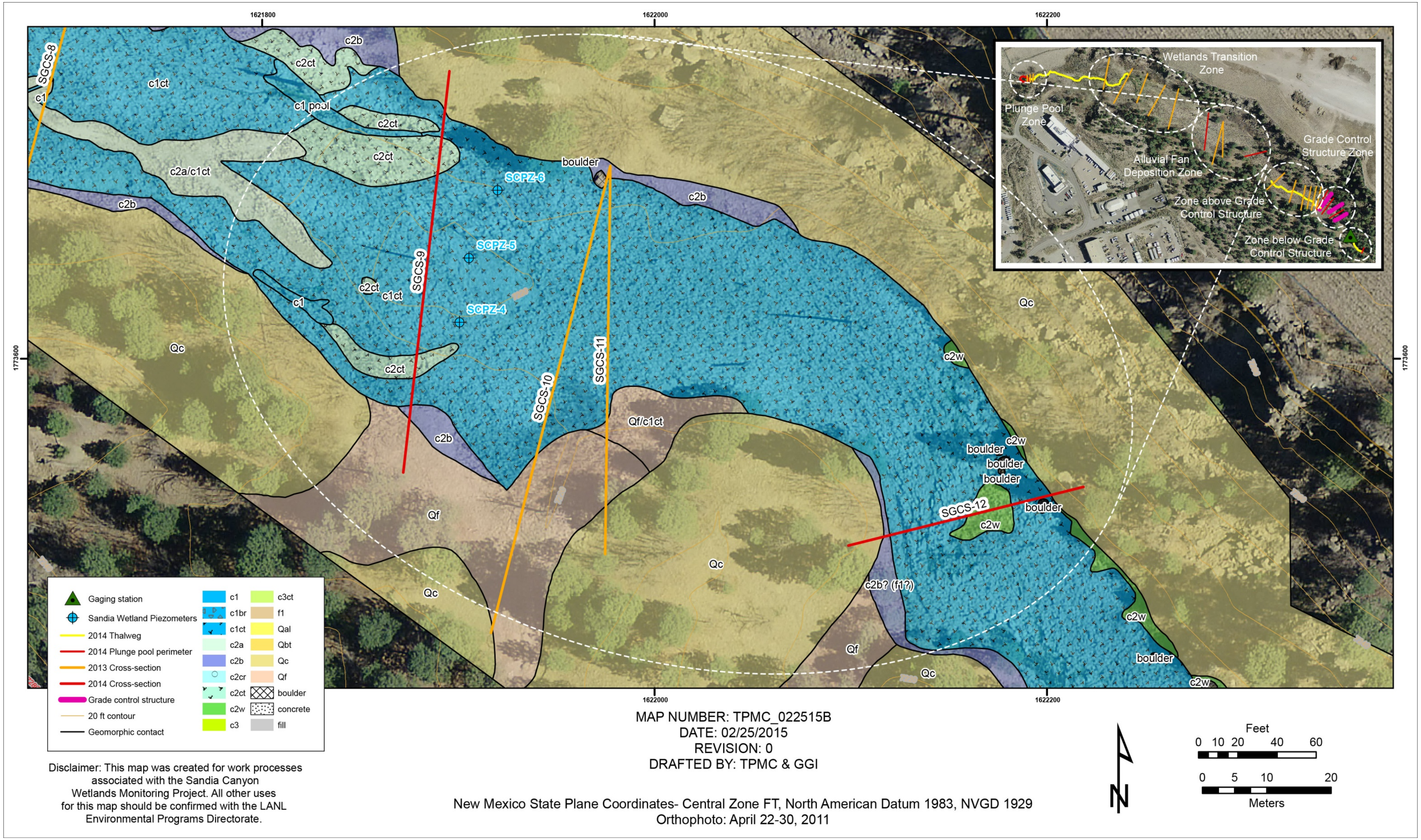

Figure B-4.3-1 **Geomorphic map overlain on an orthophoto showing the locations of piezometers, cross-section transects, and thalweg surveys at the Alluvial Fan Deposition Zone in Sandia Canyon Reach S-2**

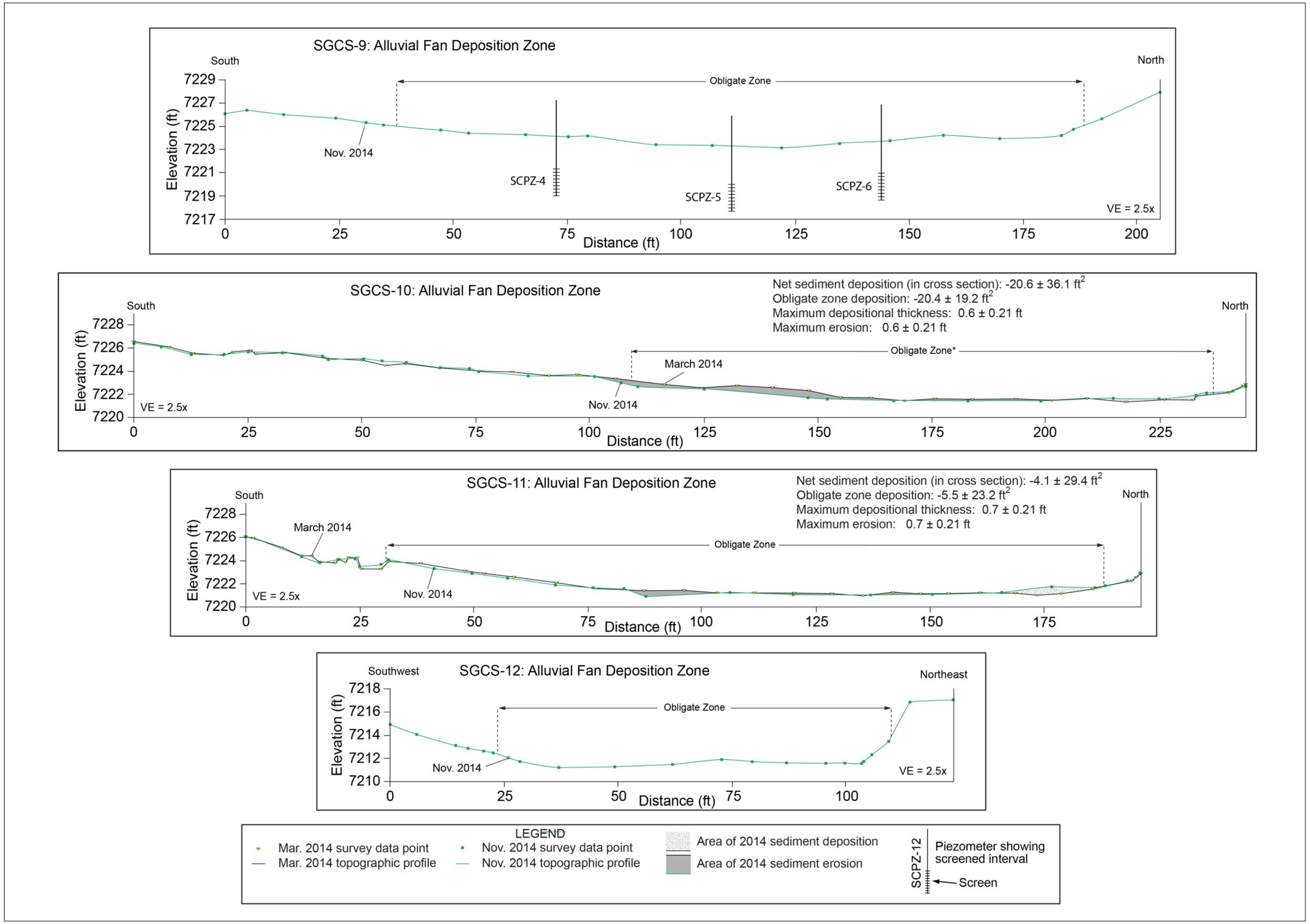

Figure B-4.3-2 **Cross-section profiles in the Alluvial Fan Deposition Zone in Sandia Canyon Reach S-2. Negative values of net sediment deposition indicate erosion. The obligate zones (see Appendix C) are defined using either the wetland vegetation perimeter mapping method, indicated here with an (*), or using the line intercept method.**

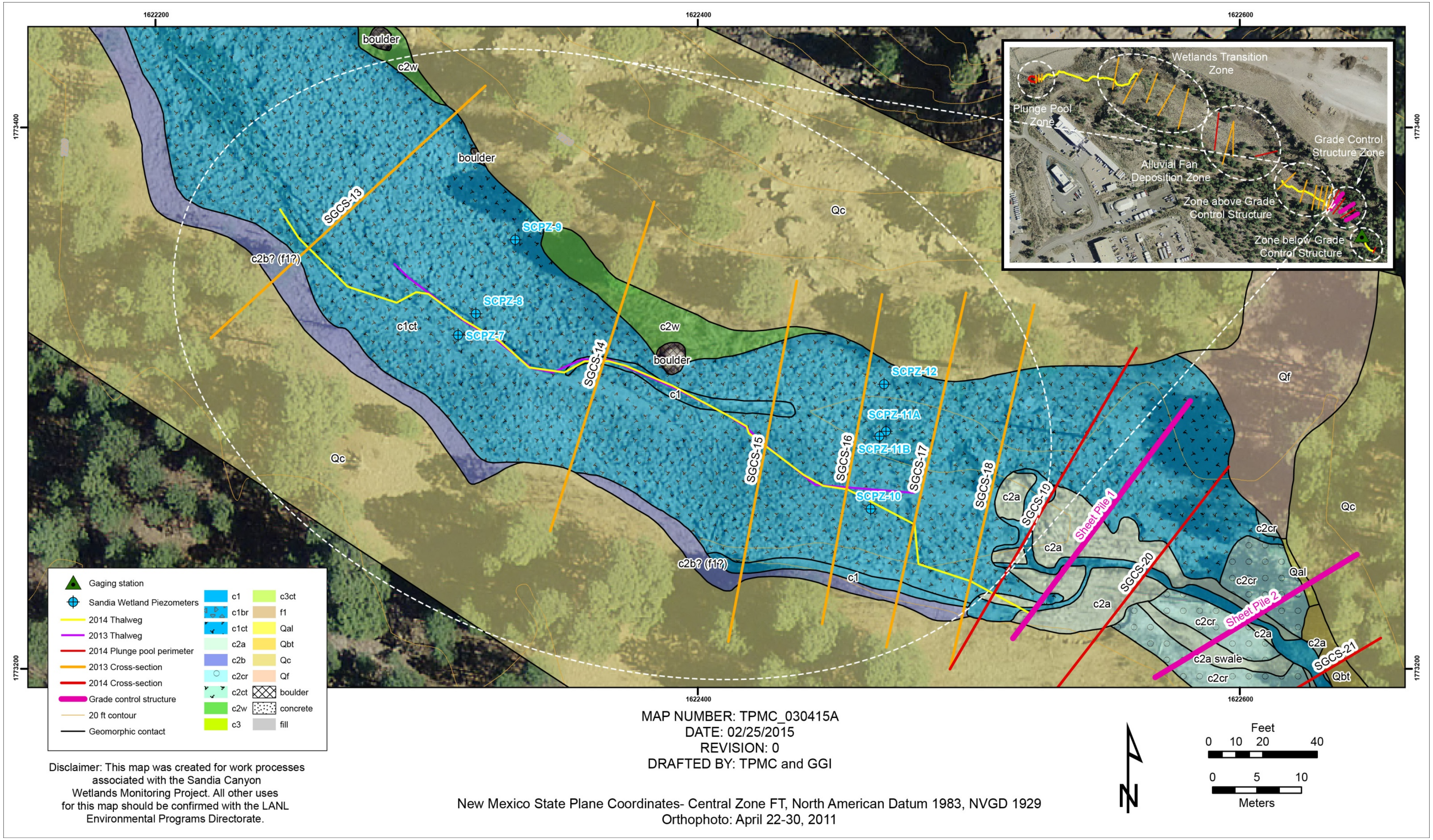

Figure B-4.4-1 Geomorphic map overlain on an orthophoto showing the locations of piezometers, cross-section transects, and thalweg surveys at the Zone above Grade-Control Structure in Sandia Canyon Reach S-2.

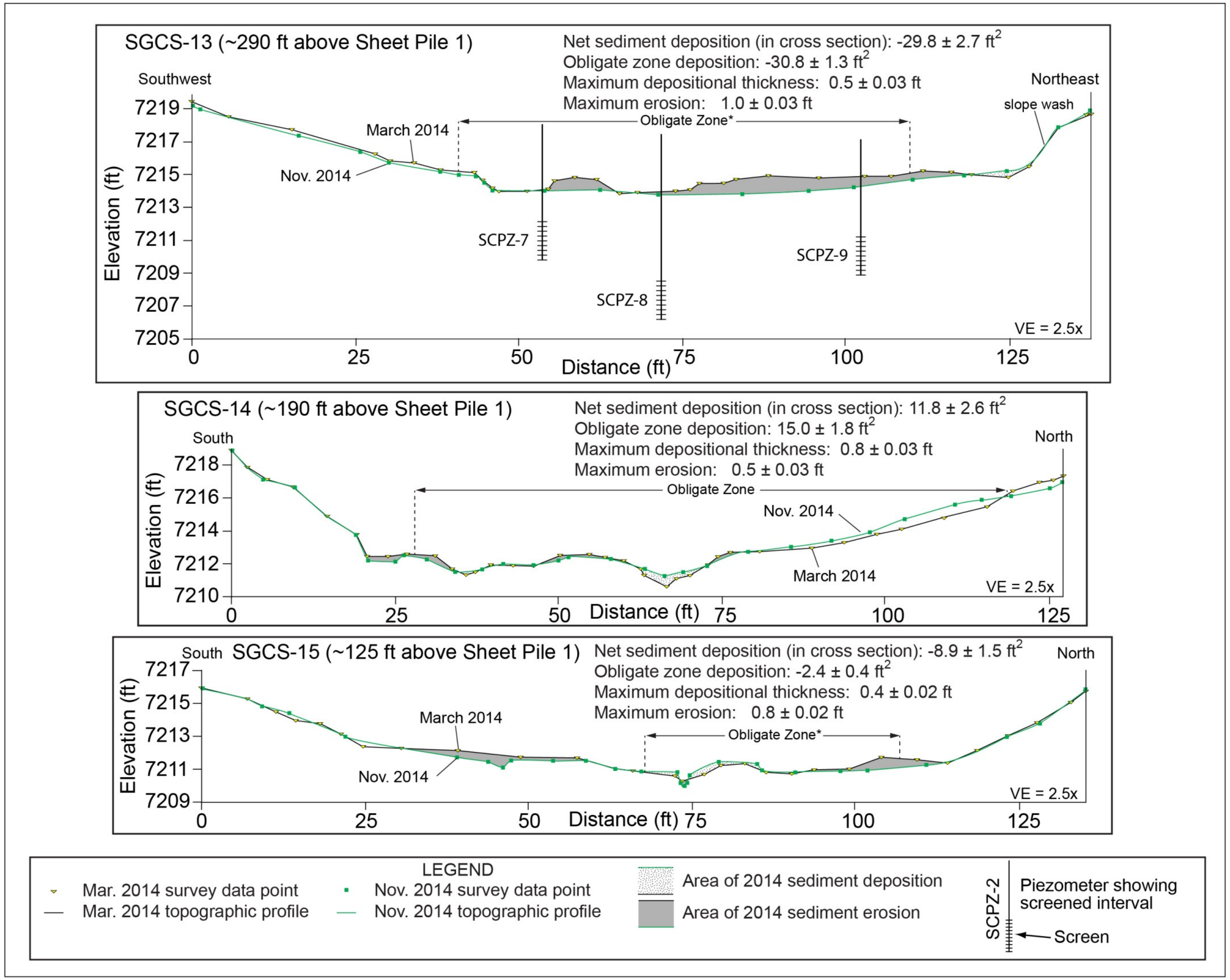

Figure B-4.4-2 Cross-section profiles in the Zone above Grade-Control Structure in Sandia Canyon Reach S-2. Negative values of net sediment deposition indicate erosion. The obligate zones (see Appendix C) are defined using either the wetland vegetation perimeter mapping method, indicated here with an (*), or using the line intercept method.

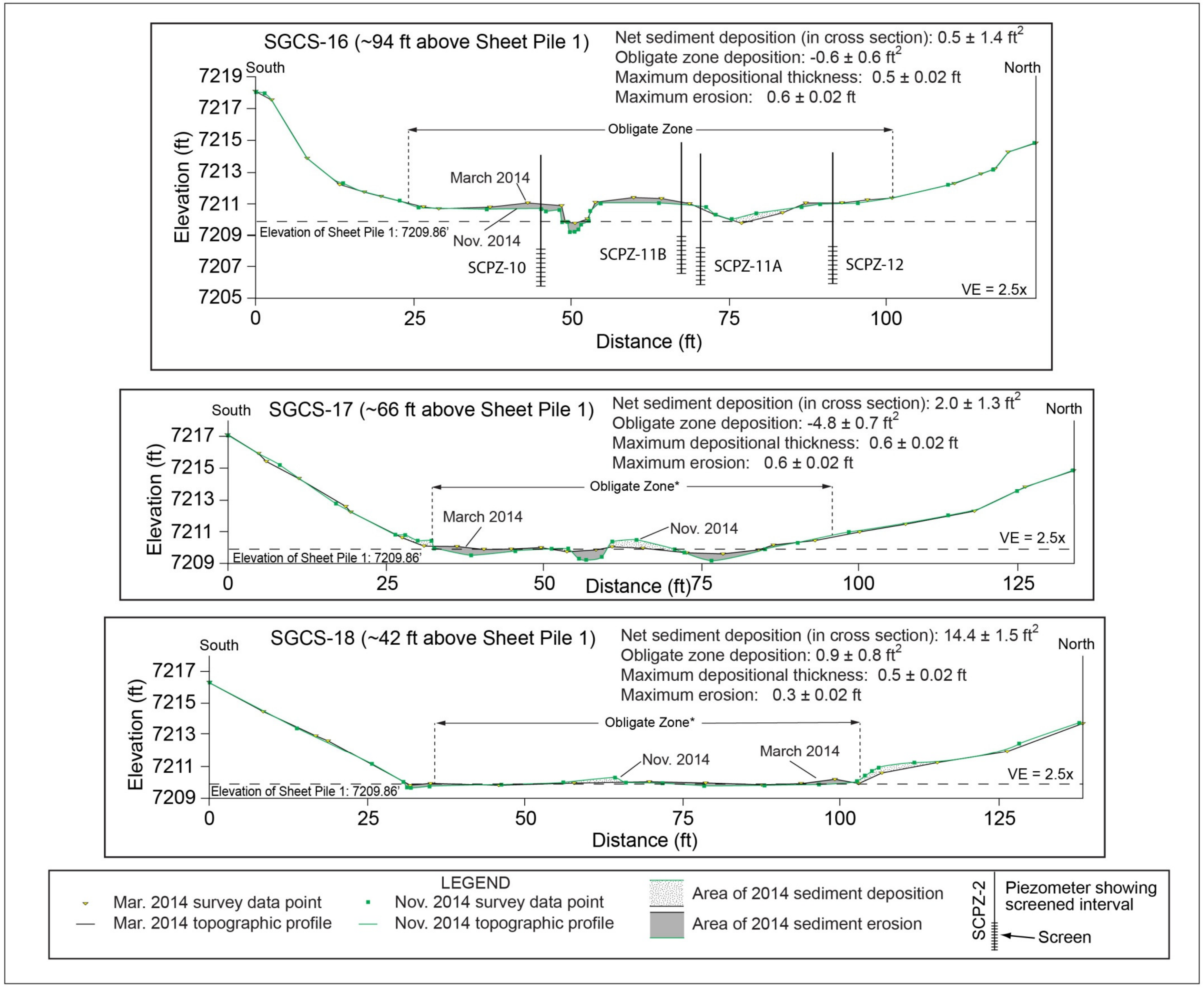

Figure B-4.4-2 (continued) **Cross-section profiles in the Zone above Grade-Control Structure in Sandia Canyon Reach S-2. Negative values of net sediment deposition indicate erosion. The obligate zones (see Appendix C) are defined using either the wetland vegetation perimeter mapping method, indicated here with an (*), or using the line intercept method.**

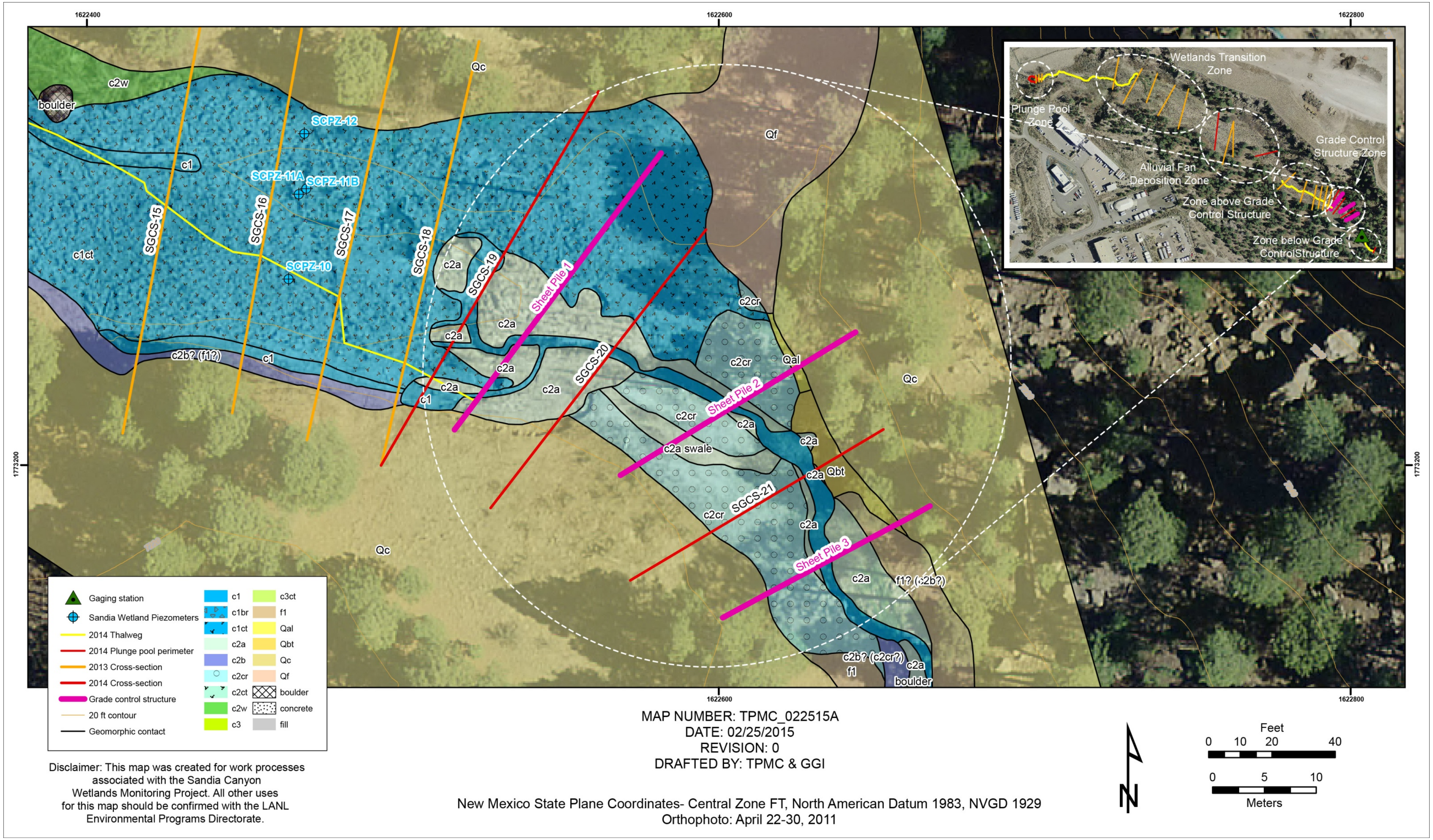

Figure B-4.5-1 Geomorphic map overlain on an orthophoto showing the locations of piezometers, cross-section transects, and thalweg surveys at the Grade-Control Structure Zone in Sandia Canyon Reach S-2

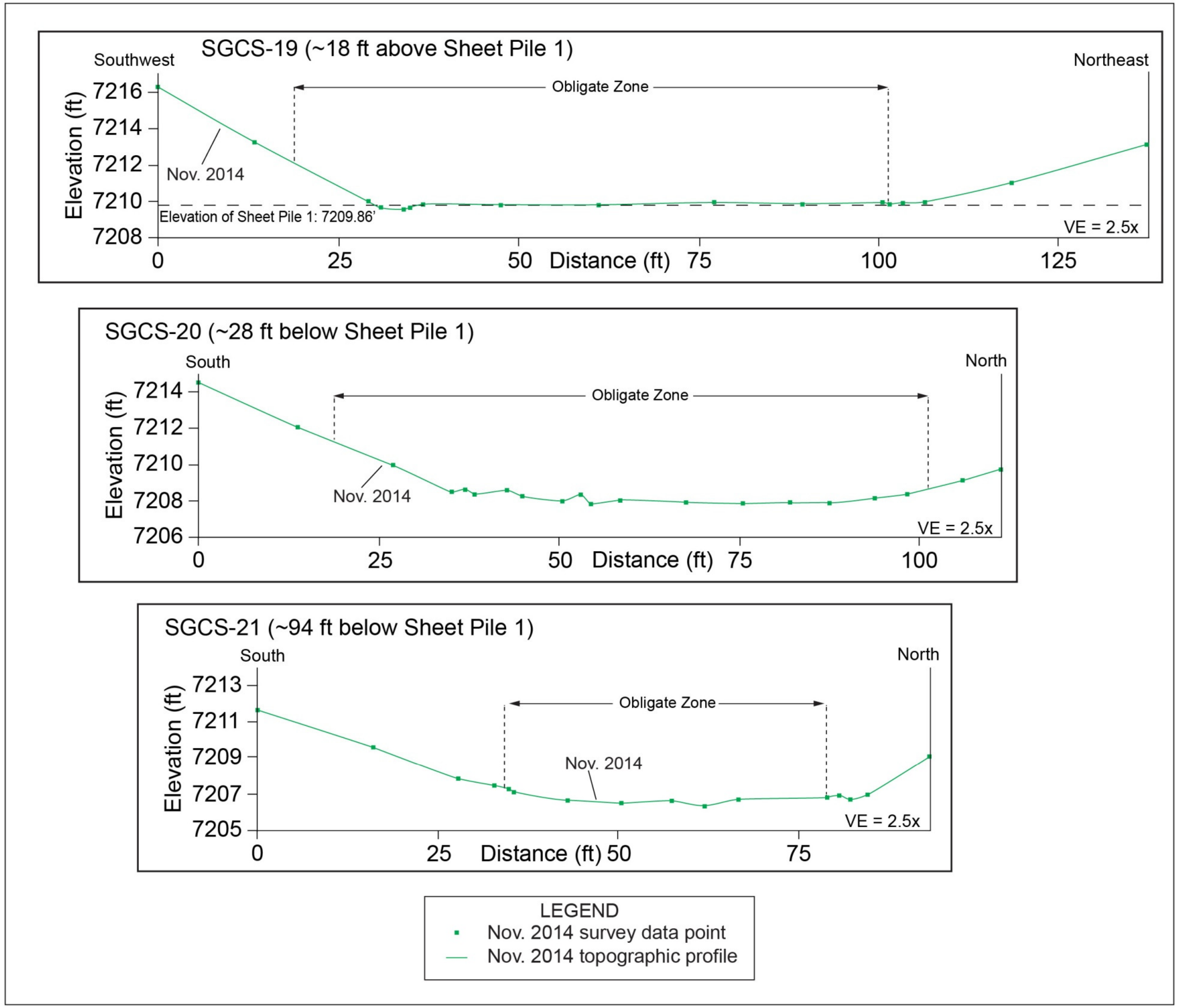

Figure B-4.5-2 Cross-section baseline profiles in the Grade-Control Structure Zone in Sandia Canyon Reach S-2. Obligate zones are the same as in Appendix C.

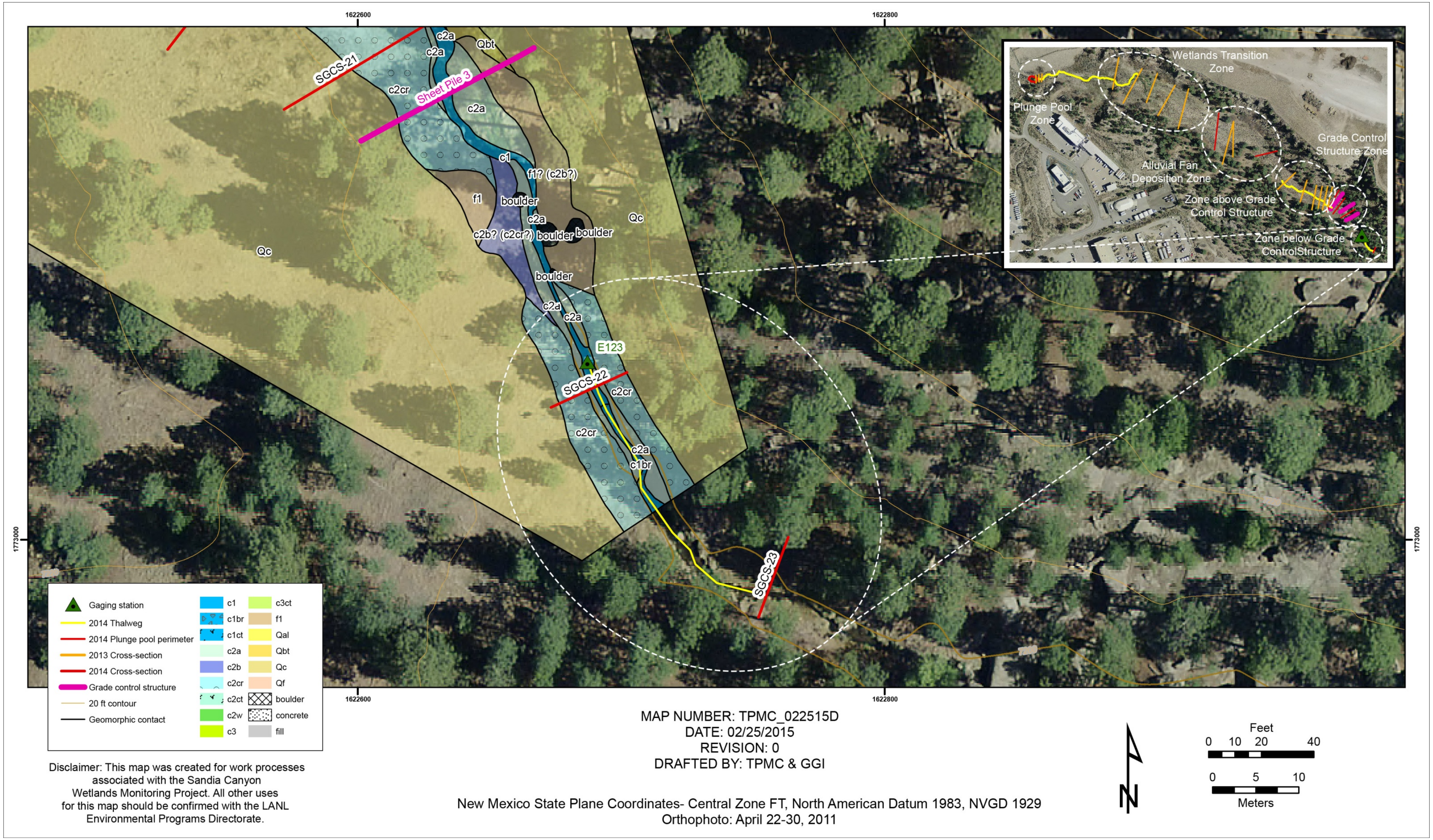

Figure B-4.5-3 Geomorphic map overlain on an orthophoto showing the locations of cross-section transects and thalweg surveys at the Zone below Grade-Control Structure in Sandia Canyon Reach S-2

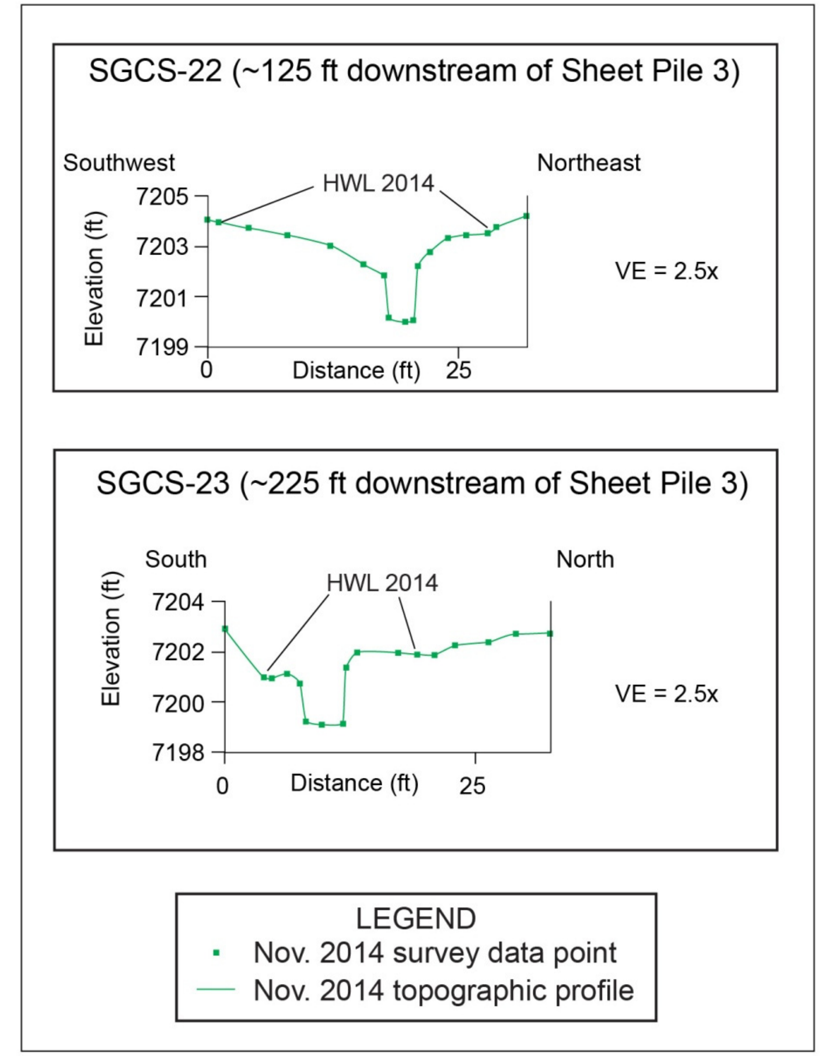

Figure B-4.5-4 Cross-section baseline profiles in the Zone below Grade-Control Structure in Sandia Canyon Reach S-2. No obligate zone was defined in the Sandia Canyon Wetlands Zone below the Grade Control Structure.

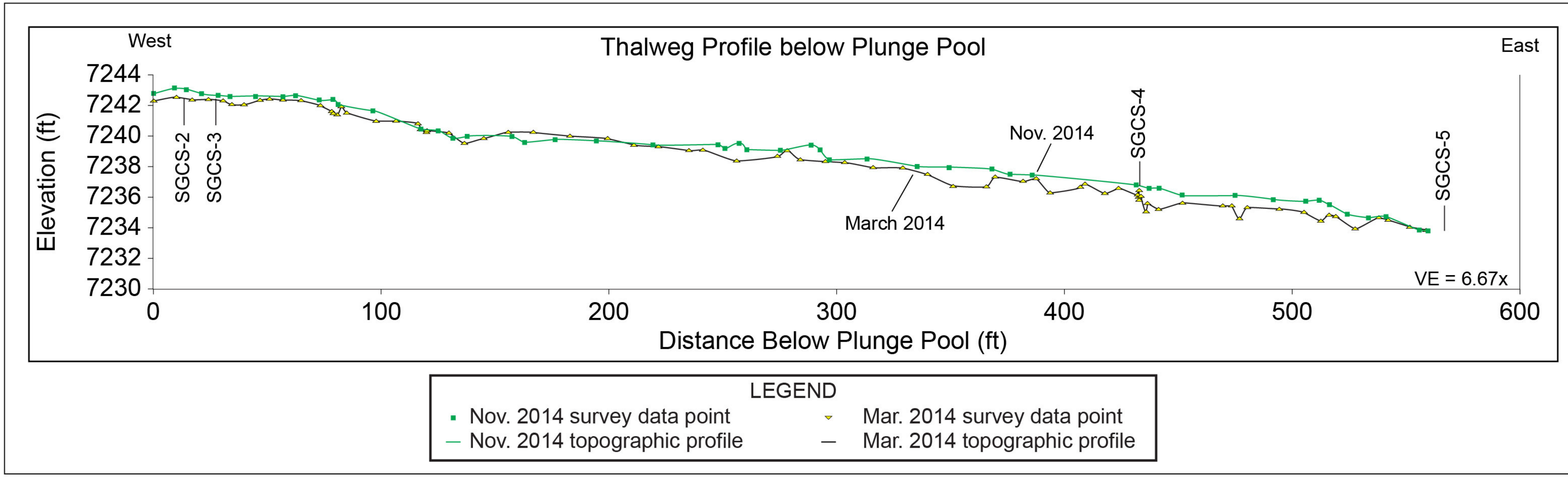

Figure B-4.6-1 **Thalweg profile in Plunge Pool Zone and Wetlands Transition Zone in Sandia Canyon Reach S-2**

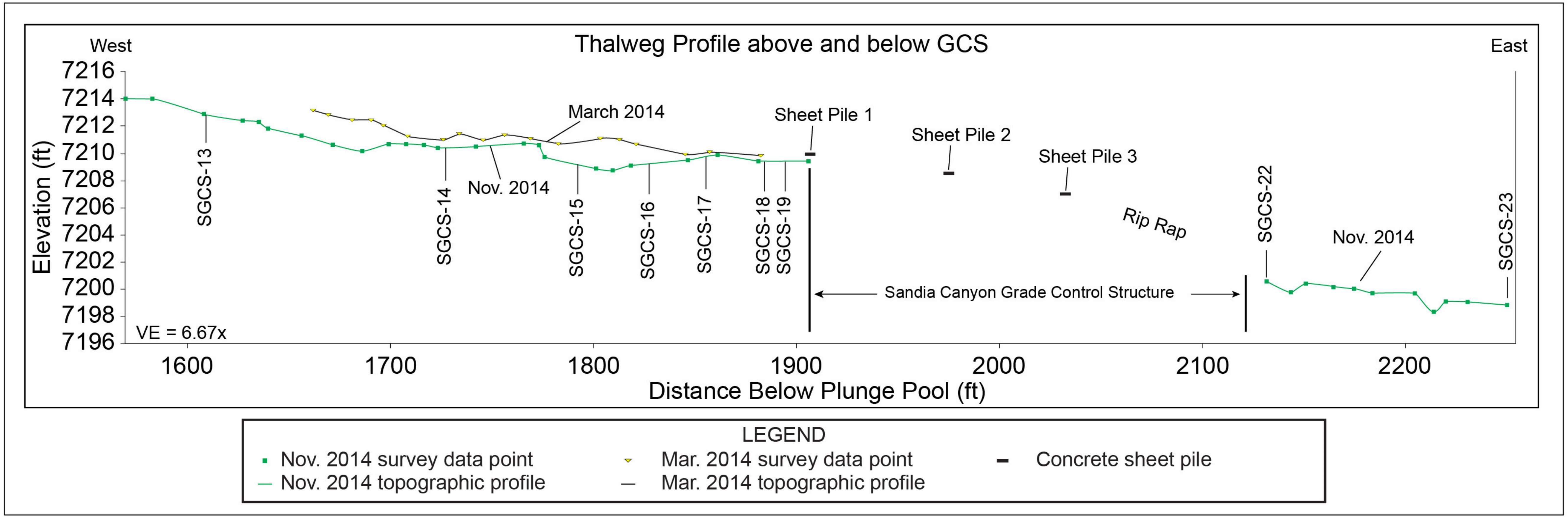

Figure B-4.6-2 Thalweg profiles at the Zone above Grade-Control Structure and the Zone below Grade-Control Structure in Sandia Canyon Reach S-2

Table B-2.0-1
Peak Annual Discharge at E121, E122, and E123

Year	Max Annual Discharge (cfs) Stream Gage E121	Max Annual Discharge (cfs) Stream Gage E122	Max Annual Discharge (cfs) Stream Gage E123
1998	—[a]	54.2	—
1999	—	0.3[b]	49.0
2000	—	—	23.0
2001	—	—	51.2
2002	100.2	—	23.0
2003	101.5	—	79.0
2004	98.1	—	34.5
2005	88.6	—	85.2
2006	85.6	8.5	72.8
2007	67.3	14.4	66.6
2008	70.0	16.4	81.0
2009	41.4	14.6	78.0
2010	22.2	9.8	74.2
2011	76.7	11.6	70.4
2012	27.7	19.1	34.1
2013	67.6	17.9	107.9
2014	65.5	19.0	109.5

[a] — = No data. Station not in operation.

[b] Data collected on 1/23/1999 and 1/24/1999.

Table B-3.0-1
Crosswalk of Nomenclature Changes of Sandia Canyon Wetlands Cross-Sections

2014 Name	2013 Name	Geomorphic Zone	Comments
SGCS-1	SGCS-16	Plunge Pool Zone	—*
SGCS-2	SGCS-15	Plunge Pool Zone	—
SGCS-3	SGCS-14	Plunge Pool Zone	—
SGCS-4	SGCS-13	Wetlands Transition Zone	Baseline Vegetation Survey in 2014
SGCS-5	SGCS-12	Wetlands Transition Zone	—
SGCS-6	SGCS-11	Wetlands Transition Zone	—
SGCS-7	SGCS-10	Wetlands Transition Zone	Baseline Vegetation Survey in 2014
SGCS-8	SGCS-9	Wetlands Transition Zone	—
SGCS-9	—	Alluvial Fan Deposition Zone	Baseline Geomorphic and Vegetation Surveys in 2014
SGCS-10	SGCS-8	Alluvial Fan Deposition Zone	—
SGCS-11	SGCS-7	Alluvial Fan Deposition Zone	Baseline Vegetation Survey in 2014
SGCS-12	—	Alluvial Fan Deposition Zone	Baseline Geomorphic and Vegetation Surveys in 2014
SGCS-13	SGCS-6	Zone above Grade-Control Structure	—
SGCS-14	SGCS-5	Zone above Grade-Control Structure	Baseline Vegetation Survey in 2014
SGCS-15	SGCS-4	Zone above Grade-Control Structure	—
SGCS-16	SGCS-3	Zone above Grade-Control Structure	Baseline Vegetation Survey in 2014
SGCS-17	SGCS-2	Zone above Grade-Control Structure	—
SGCS-18	SGCS-1	Zone above Grade-Control Structure	—
SGCS-19	—	Grade-Control Structure Zone	Baseline Geomorphic and Vegetation Surveys in 2014
SGCS-20	—	Grade-Control Structure Zone	Baseline Geomorphic and Vegetation Surveys in 2014
SGCS-21	—	Grade-Control Structure Zone	Baseline Geomorphic and Vegetation Surveys in 2014
SGCS-22	—	Zone below Grade-Control Structure	Baseline Geomorphic Survey in 2014
SGCS-23	—	Zone below Grade-Control Structure	Baseline Geomorphic Survey in 2014

* — = Not applicable.

Table B-4.1-1
Summary of 2014 Geomorphic Changes at the Sandia Canyon Wetlands Plunge Pool Zone

Transect Cross-Section Name	Transect Length (ft)	Obligate Zone Length[a] (ft)	Maximum New Sediment Thickness[b, c] (ft)	Maximum Erosion (ft)	Entire Transect Net Sediment Cross-Sectional Area[c] (ft^2)	Obligate Zone Net Sediment Cross-Sectional Area (ft^2)	Feb/Mar 2014 Thalweg Elevation[c] (ft)	Nov 2014 Thalweg Elevation[c] (ft)	2014 Thalweg Elevation[c] Change (ft)
SGCS-1	42.2	—[d]	0.4 (±0.13)	1.4(±0.13)	-7.4 (±3.9)	—	n/a[e]	n/a	n/a
SGCS-2	39.5	—	0.7 (±0.18)	2.9 (±0.18)	-3.9 (±4.9)	—	7242.50 (±0.12)	7243.10 (±0.13)	0.6 (±0.18)
SGCS-3	42.6	—	1.4 (±0.18)	2.4 (±0.18)	2.9 (±5.3)	—	7242.51 (±0.12)	7242.70 (±0.13)	0.2 (±0.18)

[a] Obligate zone defined in Appendix C.

[b] Positive number indicates aggradation, negative number indicates incision.

[c] All errors are reported as ±2 standard deviations. Individual point elevation error measurements were taken from the GPS or total station instruments at time of measurement. Reported error for one-dimensional measurements were calculated by summing the variances of the two neighboring measurement points, assuming the measurements were independent. Two- and three-dimensional errors were calculated by multiplying the one-dimensional error by the transect lengths and the distances between transects, respectively. Horizontal errors in transect length and distance between transects were insignificant compared with the distances involved and were ignored in all calculations.

[d] — = No obligate zone was defined in the Sandia Canyon Wetlands Plunge Pool Zone.

[e] n/a = Not applicable. No thalweg present, transect crosses plunge pool.

Table B-4.1-2
2014 Volume Changes at the Sandia Canyon Wetlands Plunge Pool Zone

Transect Bounding Zone	Distance between Transect Midpoints (m)	Normalized Net Sediment Deposition[a, b, c] (m^3/100 m)	Average Elevation Change between Transects (cm)
SGCS 1–2	5.3	-52 (±29)	-4.22 (±0.55)
SGCS 2–3	4.9	-5 (±34)	-0.37 (±0.75)
	Weighted Average[d]	-29 (±31)	-2.36 (±0.65)

[a] Positive number indicates aggradation, negative number indicates incision.

[b] Normalized net sediment deposition is total estimated volume per 100 ft divided by distance between surveyed cross-sections (to normalize to 100 m, 100 ft/0.305 m).

[c] All errors are reported as ±2 standard deviations. Individual point elevation error measurements were taken from the GPS or total station instruments at time of measurement. Reported error for one-dimensional measurements were calculated by summing the variances of the two neighboring measurement points, assuming the measurements were independent. Two- and three-dimensional errors were calculated by multiplying the one-dimensional error by the transect lengths and the distances between transects, respectively. Horizontal errors in transect length and distance between transects were insignificant compared with the distances involved and were ignored in all calculations.

[d] Weighted by average of transect lengths multiplied by the distance between them (i.e., relative proportion of bounding zone in plan view).

Table B-4.2-1
Summary of 2014 Geomorphic Changes at the Sandia Canyon Wetlands Transition Zone

Transect Cross-Section Name	Transect Length (ft)	Obligate Zone Length[a] (ft)	Maximum New Sediment Thickness[b, c] (ft)	Maximum Erosion[c] (ft)	Entire Transect Net Sediment Cross-Sectional Area[c] (ft^2)	Obligate Zone Net Sediment Cross-Sectional Area[c] (ft^2)	Feb/Mar 2014 Thalweg Elevation[c] (ft)	Nov 2014 Thalweg Elevation[c] (ft)	2014 Thalweg Elevation Change[c] (ft)
SGCS-4	178.2	50.2	1.2 (±0.13)	1.4 (±0.13)	2.8 (±16.8)	18.9 (±4.7)	7235.78 (±0.04)	7236.80 (±0.13)	1.0 (±0.13)
SGCS-5	134.9	73.2	0.9 (±0.18)	0.4 (±0.18)	11.8 (±17.2)	5.3 (±9.3)	7234.46 (±0.13)	7234.63 (±0.13)	0.2 (±0.18)
SGCS-6	173.1	15.5	0.4 (±0.13)	0.7 (±0.13)	-4.4 (±15.7)	-1.4 (±1.4)	7232.30[d] (±0.01)	7231.90[d] (±0.13)	-0.4 (±0.13)
SGCS-7	194.4	114	0.4 (±0.13)	1.3 (±0.13)	-24.8 (±17.6)	-13.4 (±10.3)	7230.52[d] (±0.01)	7230.10[d] (±0.13)	-0.4 (±0.13)
SGCS-8	228.2	124.6	0.4 (±0.02)	1.1 (±0.02)	8.1 (±2.7)	-1.0 (±1.5)	7228.76[d] (±0.01)	7229.09[d] (±0.01)	0.3 (±0.02)

[a] Obligate zone defined in Appendix C.

[b] Positive number indicates aggradation, negative number indicates incision.

[c] All errors are reported as ±2 standard deviations. Individual point elevation error measurements were taken from the GPS or total station instruments at time of measurement. Reported error for one-dimensional measurements were calculated by summing the variances of the two neighboring measurement points, assuming the measurements were independent. Two- and three-dimensional errors were calculated by multiplying the one-dimensional error by the transect lengths and the distances between transects, respectively. Horizontal errors in transect length and distance between transects were insignificant compared to the distances involved and were ignored in all calculations.

[d] No defined thalweg is present along transect. To approximate a thalweg gradient, the lowest elevation along each transect was used.

Table B-4.2-2
2014 Volume Changes at the Sandia Canyon Wetlands Transition Zone

Transect Bounding Zone	Distance between Transect Midpoint (m)	Normalized Net Sediment Deposition[a, b, c] (m^3/100 m)	Average Elevation Change between Transects (cm)	Obligate Zone Normalized Net Sediment Deposition[a, b, c] (m^3/100 m)	Average Elevation Change in the Obligate Zone between Transects (cm)
SGCS 4–5	35.9	68 (±112)	1.42 (±0.09)	112 (±49)	5.98 (±0.07)
SGCS 5–6	30.6	34 (±108)	0.73 (±0.11)	18 (±44)	1.34 (±0.21)
SGCS 6–7	32.1	-136 (±110)	-2.42 (±0.08)	-69 (±48)	-3.48 (±0.02)
SGCS 7–8	31.8	-78 (±83)	-1.20 (±0.08)	-67 (±48)	-1.84 (±0.08)
Weighted Average[d]		-34 (±102)	-0.48 (±0.09)	-2.36 (±0.65)	0.09 (±0.08)

[a] Positive number indicates aggradation, negative number indicates incision.

[b] Normalized net sediment deposition is total estimated volume per 100 ft divided by distance between surveyed cross-sections (to normalize to 100 m, 100 ft/0.305 m).

[c] All errors are reported as ±2 standard deviations. Individual point elevation error measurements were taken from the GPS or total station instruments at time of measurement. Reported error for one-dimensional measurements were calculated by summing the variances of the two neighboring measurement points, assuming the measurements were independent. Two- and three-dimensional errors were calculated by multiplying the one-dimensional error by the transect lengths and the distances between transects, respectively. Horizontal errors in transect length and distance between transects were insignificant compared with the distances involved and were ignored in all calculations.

[d] Weighted by average of transect lengths multiplied by the distance between them (i.e., relative proportion of bounding zone in plan view).

Table B-4.2-2

2014 Volume Changes at the Sandia Canyon Wetlands Transition Zone

Transect Bounding Zone	Distance between Transect Midpoint (m)	Normalized Net Sediment Deposition[a, b, c] (m^3/100 m)	Average Elevation Change between Transects (cm)	Obligate Zone Normalized Net Sediment Deposition[a, b, c] (m^3/100 m)	Average Elevation Change in the Obligate Zone between Transects (cm)
SGCS 4–5	35.9	68 (±112)	1.42 (±0.09)	112 (±49)	5.98 (±0.07)
SGCS 5–6	30.6	34 (±108)	0.73 (±0.11)	18 (±44)	1.34 (±0.21)
SGCS 6–7	32.1	-136 (±110)	-2.42 (±0.08)	-69 (±48)	-3.48 (±0.02)
SGCS 7–8	31.8	-78 (±83)	-1.20 (±0.08)	-67 (±48)	-1.84 (±0.08)
	Weighted Average[d]	-34 (±102)	-0.48 (±0.09)	-2.36 (±0.65)	0.09 (±0.08)

[a] Positive number indicates aggradation, negative number indicates incision.

[b] Normalized net sediment deposition is total estimated volume per 100 ft divided by distance between surveyed cross-sections (to normalize to 100 m, 100 ft/0.305 m).

[c] All errors are reported as ±2 standard deviations. Individual point elevation error measurements were taken from the GPS or total station instruments at time of measurement. Reported error for one-dimensional measurements were calculated by summing the variances of the two neighboring measurement points, assuming the measurements were independent. Two- and three-dimensional errors were calculated by multiplying the one-dimensional error by the transect lengths and the distances between transects, respectively. Horizontal errors in transect length and distance between transects were insignificant compared with the distances involved and were ignored in all calculations.

[d] Weighted by average of transect lengths multiplied by the distance between them (i.e., relative proportion of bounding zone in plan view).

Table B-4.3-1

Summary of 2014 Geomorphic Changes at the Sandia Canyon Wetlands Alluvial Fan Deposition Zone

Transect Cross-Section Name	Transect Length (ft)	Obligate Zone Length[a] (ft)	Maximum New Sediment Thickness[b, c] (ft)	Maximum Erosion[c] (ft)	Entire Transect Net Sediment Cross-Sectional Area[c] (ft^2)	Obligate Zone Net Sediment Cross-Sectional Area[c] (ft^2)	Feb/Mar 2014 Thalweg Elevation[c] (ft)	Nov 2014 Thalweg Elevation[c] (ft)	2014 Thalweg Elevation Change[c] (ft)
SGCS-10	240.9	127.8	0.6 (±0.21)	0.6 (±0.21)	-20.6 (±36.1)	-20.4 (±19.2)	7221.32d (±0.10)	7221.39 d (±0.19)	0.1 (±0.21)
SGCS-11	196.2	154.7	0.7 (±0.21)	0.7 (±0.21)	-4.1 (±29.4)	-5.5 (±23.2)	7220.98 d (±0.10)	7220.93 d (±0.19)	0.0 (±0.21)

[a] Obligate zone defined in Appendix C.

[b] Positive number indicates aggradation, negative number indicates incision.

[c] All errors are reported as ±2 standard deviations. Individual point elevation error measurements were taken from the GPS or total station instruments at time of measurement. Reported error for one-dimensional measurements were calculated by summing the variances of the two neighboring measurement points, assuming the measurements were independent. Two- and three-dimensional errors were calculated by multiplying the one-dimensional error by the transect lengths and the distances between transects, respectively. Horizontal errors in transect length and distance between transects were insignificant compared with the distances involved and were ignored in all calculations.

[d] No defined thalweg is present along transect. To approxiate a thalweg gradient, the lowest elevation along each transect was used.

Table B-4.3-2
2014 Volume Changes at the Sandia Canyon Wetlands Alluvial Fan Deposition Zone

Transect Bounding Zone	Distance between Transect Midpoint (m)	Normalized Net Sediment Deposition[a, b, c] (m^3/100 m)	Average Elevation Change between Transects (cm)	Obligate Zone Normalized Net Sediment Deposition[a, b, c] (m^3/100 m)	Average Elevation Change in the Obligate Zone between Transects (cm)
SGCS 10–11	10.8	-115 (±216)	-1.72 (±0.47)	-120 (±140)	-2.79 (±0.38)
Weighted Average[d]		-115 (±216)	-1.72 (±0.47)	-120 (±140)	-2.79 (±0.38)

[a] Positive number indicates aggradation, negative number indicates incision.

[b] Normalized net sediment deposition is total estimated volume per 100 ft divided by distance between surveyed cross-sections (to normalize to 100 m, 100 ft/0.305 m).

[c] All errors are reported as ±2 standard deviations. Individual point elevation error measurements were taken from the GPS or total station instruments at time of measurement. Reported error for one-dimensional measurements were calculated by summing the variances of the two neighboring measurement points, assuming the measurements were independent. Two- and three-dimensional errors were calculated by multiplying the one-dimensional error by the transect lengths and the distances between transects, respectively. Horizontal errors in transect length and distance between transects were insignificant compared with the distances involved and were ignored in all calculations.

[d] Weighted by average of transect lengths multiplied by the distance between them (i.e., relative proportion of bounding zone in plan view).

Table B-4.4-1
Summary of 2014 Geomorphic Changes at the Sandia Canyon Wetlands Zone above Grade-Control Structure

Transect Cross-Section Name	Transect Length (ft)	Obligate Zone Length[a] (ft)	Maximum New Sediment Thickness[b, c] (ft)	Maximum Erosion[c] (ft)	Entire Transect Net Sediment Cross-Sectional Area[c] (ft^2)	Obligate Zone Net Sediment Cross-Sectional Area[c] (ft^2)	Feb/Mar 2014 Thalweg Elevation[c] (ft)	Nov 2014 Thalweg Elevation[c] (ft)	2014 Thalweg Elevation Change[c] (ft)
SGCS-13	137.5	69.1	0.5 (±0.03)	1.0 (±0.03)	-29.8 (±2.7)	-30.8 (±1.3)	7213.81 (±0.00)	7214.00 (±0.03)	0.2 (±0.03)
SGCS-14	126.8	88.3	0.8 (±0.03)	0.5 (±0.03)	11.8 (±2.6)	15 (±1.8)	7210.57 (±0.01)	7211.24 (±0.03)	0.7 (±0.03)
SGCS-15	135.3	39	0.4 (±0.02)	0.8 (±0.02)	-8.9 (±1.5)	-2.4 (±0.4)	7210.31 (±0.01)	7209.98 (±0.01)	-0.3 (±0.02)
SGCS-16	123.4	57.6	0.5 (±0.02)	0.6 (±0.02)	0.5 (±1.4)	-0.6 (±0.6)	7209.78 (±0.01)	7209.23 (±0.01)	-0.5 (±0.02)
SGCS-17	113.9	63.6	0.6 (±0.02)	0.6 (±0.02)	2.0 (±1.3)	-4.8 (±0.7)	7209.73 (±0.01)	7209.23 (±0.01)	-0.5 (±0.02)
SGCS-18	137.8	67.3	0.5 (±0.02)	0.3 (±0.02)	14.4 (±1.5)	0.9 (±0.8)	7209.79 (±0.01)	7209.68 (±0.01)	-0.1 (±0.02)

[a] Obligate zone defined in Appendix C.

[b] Positive number indicates aggradation, negative number indicates incision.

[c] All errors are reported as ±2 standard deviations. Individual point elevation error measurements were taken from the GPS or total station instruments at time of measurement. Reported error for one-dimensional measurements were calculated by summing the variances of the two neighboring measurement points, assuming the measurements were independent. Two- and three-dimensional errors were calculated by multiplying the one-dimensional error by the transect lengths and the distances between transects, respectively. Horizontal errors in transect length and distance between transects were insignificant compared with the distances involved and were ignored in all calculations.

Table B-4.4-2
2014 Volume Changes at the
Sandia Canyon Wetlands Zone above Grade-Control Structure

Transect Bounding Zone	Distance between Transect Midpoint (m)	Normalized Net Sediment Deposition [a,b,c] (m^3/100 m)	Average Elevation Change between Transects (cm)	Obligate Zone Normalized Net Sediment Deposition [a, b, c] (m^3/100 m)	Average Elevation Change in the Obligate Zone between Transects (cm)
SGCS 13-14	33.5	-84 (±17)	-2.08 (±0.02)	-73 (±10)	-3.06 (±0.02)
SGCS 14-15	20.9	13 (±14)	0.34 (±0.03)	59 (±9)	3.02 (±0.04)
SGCS 15-16	10.0	-39 (±10)	-0.99 (±0.04)	-14 (±4)	-0.95 (±0.03)
SGCS 16-17	8.4	12 (±9)	0.32 (±0.04)	-25 (±4)	-1.36 (±0.04)
SGCS 17-18	7.7	76 (±9)	1.98 (±0.04)	-18 (±5)	-0.91 (±0.04)
Weighted Average [d]		-29 (±14)	-0.70 (±0.03)	-26(±8)	-1.04 (±0.03)

[a] Positive number indicates aggradation, negative number indicates incision.

[b] Normalized net sediment deposition is total estimated volume per 100 ft divided by distance between surveyed cross-sections (to normalize to 100 m, 100 ft/0.305 m).

[c] All errors are reported as ±2 standard deviations. Individual point elevation error measurements were taken from the GPS or total station instruments at time of measurement. Reported error for one-dimensional measurements were calculated by summing the variances of the two neighboring measurement points, assuming the measurements were independent. Two- and three-dimensional errors were calculated by multiplying the one-dimensional error by the transect lengths and the distances between transects, respectively. Horizontal errors in transect length and distance between transects were insignificant compared with the distances involved and were ignored in all calculations.

[d] Weighted by average of transect lengths multiplied by the distance between them (i.e., relative proportion of bounding zone in plan view).

Table B-4.6-1
Thalweg Sinuosity at the Sandia Canyon Wetlands

Year	Length (ft)	Straight Line Distance (ft)	Sinuosity
Upper Thalweg			
2013	705.2	558.8	1.26
2014	663.0	559.7	1.18
Lower Thalweg			
2013	220.5	210.2	1.05
2014	335.9	314	1.07

Table B-4.6-2
Summary of 2014 Thalweg Elevation Changes by Zone

Zone	2014 Average Thalweg Elevation Change (ft) [a, b]
Plunge Pool	0.4 (±0.18)
Wetland Transition	0.1 (±0.12)
Alluvial Fan Deposition	0.0 (±0.21)
Above GCS	-0.1 (±0.02)

[a] Positive number indicates aggradation, negative number indicates incision.

[b] All errors are reported as ±2 standard deviations. Individual point elevation error measurements were taken from the GPS or total station instruments at time of measurement. Reported error for one-dimensional measurements were calculated by summing the variances of the two neighboring measurement points, assuming the measurements were independent. Two- and three-dimensional errors were calculated by multiplying the one-dimensional error by the transect lengths and the distances between transects, respectively. Horizontal errors in transect length and distance between transects were insignificant compared with the distances involved and were ignored in all calculations.

Attachment B-1

2014 Photographs of Geomorphic Conditions in Sandia Canyon Reach S-2

Photo B1-1 SGCS-3 looking north. Survey rod indicates location of maximum (1.4 ft) sediment deposition.

Photo B1-2 SGCS-2 looking north. Survey rod indicates location of maximum (2.9 ft) sediment erosion.

Photo B1-3 Alluvial fan deposition extending to the east from SGCS-6. Looking upstream (west) toward SGCS-6.

Photo B1-4 Alluvial fan deposition in the area of SGCS-8, looking north. Person is at approximate location of north endpoint of SGCS-8.

Attachment B-2

2014 Geomorphic Changes in
Sandia Canyon Reach S2 Survey Data
(on CD included with this document)

Appendix C

2014 Wetlands Vegetation Monitoring
in Sandia Canyon Reach S-2

CONTENTS

Figures

Tables

Attachments

C-1.0 INTRODUCTION

This report presents vegetation survey data collected in 2014 in Sandia Canyon Reach S-2 within Los Alamos National Laboratory (LANL or the Laboratory). The survey data document baseline vegetation conditions in Reach S-2 for the purpose of annual vegetation monitoring. This monitoring is specified in the “Work Plan and Final Design for Stabilization of the Sandia Canyon Wetland” (LANL 2011, 207053), the modified version of the work plan approved by the New Mexico Environmental Department (NMED) on April 3, 2013 (Cobrain 2013, 256726), and in the “2014 Annual Monitoring Report for Sandia Canyon Wetland Grade-Control Structure (SPA-2012-00050-ABQ)” (LANL 2014, 600083). These surveys will be repeated at maximum vegetation growth (late summer) in 2015, and the results will be presented in the 2015 Sandia Wetland Performance Report. The 2015 report will include estimates of temporal and spatial changes in vegetation cover and composition occurring since the previous survey and will evaluate if any unintended vegetation changes have occurred, such as loss of wetland species or areal extent. Figure C-1.0-1 shows the locations of sites discussed in this report. Attachment C-1 presents photographs of the baseline vegetation conditions in Sandia Canyon Reach S-2. Attachment C-2 presents baseline vegetation survey data collected in 2014.

C-2.0 VEGETATION MONITORING METHODS

Two vegetation survey methods were used in 2014 at Reach S-2: line intercept (Coulloudon et al. 1999, 600337) and vegetation perimeter mapping. The line intercept method data set provides a comprehensive species list, quantifies vegetative canopy cover and species composition along transects, and allows delineation and characterization of the wetland area. The vegetation perimeter mapping documents the spatial distribution and areal extent of targeted wetland species. Vegetation surveys employing both methods were completed in late September 2014 to capture vegetation at maximum growth.

A total of 10 transects were surveyed in September 2014 in Sandia Canyon Reach S-2 (Figure C-1.0-1). These 10 vegetation transects are a subset of 23 transects established in February–March 2014 and November–December 2014 for the purpose of evaluating geomorphic changes in Sandia Canyon Reach S-2 (see LANL 2014, 257590, and Appendix B of the report for a description of the methods). The vegetation survey transect locations were selected to capture representative sections of the Sandia wetland and the engineered grade-control structure (GCS). Transects SGCS-4 and SGCS-7 are located in the western part of Reach S-2, while transects SGCS-9, SGCS-11, and SGCS-12 are centrally located (Figure C-1.0-1). Transects SGCS-9 and SGCS-12 were established in November–December 2014 to monitor encroachment of willows and sediment to the Central Cattail Zones. The five transects in the eastern region of Reach S-2 focus on the GCS. Two transects, SGCS-14 and SGCS-16, are located above the GCS. SGCS-19, SGCS-20, and SGCS-21 are located upstream of Sheet Piles 1, 2, and 3, respectively, and these three transects are used to monitor the planted wetland species from the GCS installation (LANL 2014, 600083).

C-2.1 Line Intercept Method

Vegetation canopy cover and species composition data were collected using the line intercept method (Coulloudon et al. 1999, 600337). A species intercept occurs when a species crosses the vertical plane containing the tape measure (Photos C1-1 and C1-2 in Attachment C-1). The intercepted tape distances of all plant species along the established transect are recorded, as well as the occurrence of non-living categories such as logs, rocks, bare ground, and open water (channels). Non-living objects are only recorded if the intercepted area along the transect is devoid of vegetation. For example, bare ground or logs are not recorded if vegetation canopy is also present. Canopy cover from different and overlapping species is accounted for by recording the tape intercept distances for both species. Species overlap, areas along the line that are occupied by more than one species, is common and any interception with the tape distance must be recorded (Photo C1-2 in Attachment C-1). Species not identified in the field are sampled for later identification using taxonomic keys. Raw survey species identification and tape distance data are included electronically as Attachment C-2 (on CD included with this document).

C-2.1-1 Plant Species Indicators

Plant species indicator status was used to delineate wetland zones from zones outside the wetland. The indicator status provides the probability that a species occurs in a wetlands versus outside a wetlands. Table C-2.1-1 lists the indicator definitions of the wetland plant species. The relevant indicator types for this report are obligate wetland plants (OBL), facultative wetland plants (FACW), facultative plants (FAC), facultative upland plants (FACU), obligate upland plants (UPL), and plants that do not have an indicator status for wetland systems (NI). The NI species are usually species that are never or very rarely found in wetland systems and therefore not given any status. Throughout this report, "obligate," when used alone, refers to obligate wetland plants but not to obligate upland plants.

Each species found in the study area was assigned an indicator status according to Reed (1988, 600338). For instance, a cattail (*Typha latifolia*) is an obligate wetland species expected to occur almost always (estimated probability of >99%) in wetlands and rarely (estimated probability of <1%) in non-wetlands.

C-2.1-2 Vegetative Canopy Cover and Species Composition

For an individual species, canopy cover percentage is calculated by summing all intercept lengths, distance between intercepts where the species is present, and expressing this total as a proportion of tape length (Coulloudon et al. 1999, 600337).The vegetative canopy cover is the sum of individual species canopy cover percentages for all living categories. Vegetative canopy cover can be more than 100% because of overlap of different plant species. For example, consider a 100 ft long transect containing only 2 species. Species A covers 50 ft and species B covers 70 ft (with a 20 ft overlap). Species A has 50% canopy cover [(50 ft/100 ft)*100], species B has 70% canopy cover [(70 ft/100 ft)*100], and the vegetative canopy cover for the transect is 120% (50% + 70%). A vegetative canopy cover greater than 100% is common where low vegetation occurs under a higher-overstory canopy.

Species composition is determined by dividing the species intercept length by the total intercept length of all species as well as non-living categories (Coulloudon et al. 1999, 600337). This ratio is reported as a percentage. The sum of all individual species composition and non-living composition percentages will always be 100%. In the above example, the species composition of species A is 42% [(50 ft/120 ft) *100] and the species composition of species B is 58% [(70 ft/120 ft)* 100].

C-2.1-3 Obligate Zone Delineation and Characterization

For the reporting purpose of this appendix, the obligate wetland plants (OBL) were used to define the wetland zone or the obligate zone. The differentiation between the obligate and non-obligate zones allows analysis of vegetation as related to the occurrence in wetlands. The obligate zone for this purpose is defined as the area bound by obligate species occurrence. Using line intercept transect data, the obligate zone is defined as the section of the transect between the first identified obligate species and the last identified obligate species. The non-obligate zone is the area bordering the obligate zone and is usually topographically higher than the wetland zone. While both zones can contain non-obligate (FACW, FAC, FACU, UPL, and NI) species, only the obligate zone can contain OBL species.

In this report, three metrics are reported to characterize the obligate zone. The first metric is the percentage of transect in the obligate zone. This is calculated by dividing the length of the obligate zone by the total transect length and converting to a percentage. The second metric is the percentage of obligate zone with obligate occurrence, which is the vertical projection of obligate presence within the obligate zone expressed as a percentage. This is calculated by first determining the sections of the line within the obligate zone that are covered by any OBL species. This metric is based on the presence or absence of a species, so a section of transect is considered to be covered by OBL whether it contains one or many OBL species. The combined length of sections covered by OBL is divided by the obligate zone length and converted to a percentage. The third metric is the vegetative canopy cover in the obligate zone. This is calculated by summing the intercept lengths of all living categories (OBL and non-OBL), dividing by the length of the obligate zone, and converting to a percentage.

For example, consider an obligate zone that extends from 20 ft to 70 ft on a 100-ft transect. OBL species A covers 20 ft to 50 ft, OBL species B covers 30 ft to 50 ft, FACW species C (a non-OBL species) covers 50 ft to 60 ft, and OBL species D covers 60 ft to 70 ft. The percent of transect in the obligate zone is 50% [(70 ft - 20 ft)/100 ft)*100]. The percent of the obligate zone with obligate occurrence is 80% [([(50 ft – 20 ft) + (70 ft – 60 ft)]/50 ft)*100]. The vegetation canopy cover in the obligate zone is 140% [([30 ft + 20 ft + 10 ft + 10 ft]/50ft)*100].

C-2.2 Wetland Vegetation Perimeter Mapping

The vegetation perimeter mapping documents the spatial distribution and areal extent of targeted (cattail and willow) wetland species. Surveys were conducted using a combination of a differentially corrected global positioning system (DGPS) and a total station tied to GPS control points, depending on tree cover. Raw survey data (x and y coordinates using the New Mexico State Plane coordinate system and elevations of all survey points) for surveyed perimeters are included electronically as Attachment C-2 (on CD included with this document).

C-3.0 MONITORING RESULTS

Baseline data collected during the first year yielded quantifiable data for comparison to future surveys. Initial results show high overall species diversity and high abundance of wetlands species. A comprehensive species list, vegetative canopy cover and species composition, obligate zone delineation and characterization, and wetland vegetation perimeters are reported in the following sections and associated tables and figures. Figure C-3.0-1 shows the locations of the vegetation cross-sections and wetland vegetation mapping results. A representative photo of each transect is presented in Attachment C-1, Photos C1-3 through C1-12.

C-3.1 Comprehensive Species List

A comprehensive species list was compiled from transect data collected with the line intercept method. Table C-3.1-1 catalogs species symbol, scientific name, common name, indicator category, life form, and obligate/non-obligate classification for each of the 57 species identified along the 10 transects during the 2014 baseline survey (LANL 2014, 257590). The species list contains only those species identified along transects and therefore is not necessarily an exhaustive list of all species present in Sandia Canyon Reach S-2.

Graminoid and forb life forms each represent about 40% of the 57 observed species (Table C-3.1-2). The remaining species consist of shrubs (~11%) and trees (~9%). Of the 57 observed species, 13 species (~23%) are OBL indicator species (Table C-3.1-3). The 13 obligate species are dominated by graminoids (8 species or ~61%) with some forbs (4 species or~ 31%) and only one shrub species (~8%, see Table C-3.1-2). The 44 non-obligate species are mostly forbs (~41%) and graminoids (~36%) but have greater diversity of shrubs and trees (~11% each, Table C-3.1-2) than the obligate species. Of the 57 identified species, 23% are OBL indicators, 18% are FACW indicators, 10% are FAC indicators, 12% are FACU indicators, 5% are UPL indicators, and 32% have NI status (Table C-3.1-3).

C-3.2 Vegetative Canopy Cover and Species Composition

Canopy cover and species composition were calculated for each species from data collected using the line intercept method. These metrics were also calculated for non-living categories (e.g., logs, bare ground, open water) using the same methods as for living categories. Tables C3-1 through C3-10 in Attachment C-3 presents, for each transect, percent canopy cover and composition for individual species or non-living categories identified along the transect, and organized by rank order of abundance. Total vegetative canopy cover and composition as well as total non-living cover and composition are also presented at the bottom of each table.

In general, the farthest upstream transect (SGCS-4) and farthest downstream transects (SGCS-16, SGCS-19, SGCS-20, and SGCS-21) have less vegetative canopy cover than the centrally located transects (Table C-3.2-1). The remaining transects (SGCS-7, SGCS-9, SGCS-11, SGCS-12, and SGCS-14) have vegetative canopy cover greater than 100% (Table C-3.2-1). This difference is attributed to smaller forb species occurring within dense cattail stands in the central portions of transects and canopy cover overlap from willows and/or trees growing above grasses or forbs at the edges of transects.

Table C-3.2-2 lists the most abundant (greatest composition) species within each transect, omitting non-vegetative categories (algae, water, bare ground, litter, logs). In 9 of the 10 transects, an obligate indicator species has the greatest composition. In 4 of those 9 transects, the species with second greatest composition is also an obligate indicator (Table C-3.2-2). The only transect with a non-obligate indicator with greatest species composition is SGCS-4 (Table C-3.2-2), the farthest upstream transect for which vegetation data were collected in 2014.

C-3.3 Obligate Zone Delineation and Characterization

For each transect, the obligate zone was defined between the first and last occurrence of OBL species along the line. The percent obligate occurrence within the obligate zone and the vegetative cover within the obligate zone were calculated. Vegetation and non-living presence were calculated in the same manner as the percent obligate occurrence, where each section of the line is classified as either containing any vegetation or only non-living categories. Table C-3.3-1 presents the transect length, obligate zone length, and percent of the transect in the obligate zone. Table C-3.3-2 presents the vegetative canopy cover, vegetation presence, and non-vegetative presence, expressed as percentages, for the obligate and non-obligate zones as well as the obligate occurrence within the obligate zone.

Figures C-3.3-1 through C-3.3-4 show topographic profiles, obligate zone boundaries, distribution of obligate species (all OBL indicators binned) within the obligate zone, and the distribution of two individual obligate species (broad-leafed cattail and coyote willow) for each transect.

In subsequent years, changes in the percent of transect in the obligate zone can be compared with monitor expansion or contraction of the wetland area (since the total transect length will remain constant year to year). The percent obligate occurrence within the obligate zone can be used to describe how much of the obligate zone actually contains obligates rather than other species or non-living categories. The obligate zone in one transect, SGCS-12, is completely covered by obligate indicator species (Table C-3.3-2 and Figure C-3.3-2). In four transects (SGCS-9, SGCS-14, SGCS-16, and SGCS-21), more than 90% of the obligate zone contains obligate indicators (Table C-3.3-2 and Figures C-3.3-2, C-3.3-3 and C-3.3-4). Two transects (SGCS-19 and SGCS-20) have relatively sparse obligate occurrence within the obligate zone (59.5% and 55.5%, respectively, Figure C-3.3-4 and Table C-3.3-1).

In a similar fashion, the vegetation presence and non-living presence percentages help to describe how much of the obligate zone contains any vegetation. The vegetative canopy cover percentage allows comparison of abundance of vegetation within the obligate zones of different transects (or from year to year for the same transect) but does not provide information if some of the obligate zone is, for instance, occupied by bare ground or an open channel. For example, despite a 92.2% vegetative canopy cover within the obligate zone, almost 20% of the obligate zone of SGCS-4 is occupied by non-living categories (Table C-3.3-2). This finding indicates that several species grow in the same areas (overlap) within the obligate zone. Two transects (SGCS-12 and SGCS-21) have 100% vegetative presence within the obligate zone and similar vegetative canopy cover (128.2% and 131.2%, respectively [Table C-3.3-2]). A third transect (SGCS-9) has 100% vegetative presence within the obligate zone, but lower canopy over (115.6% [Table C-3.3-2]). SGCS-11 and SGCS-14 have similar vegetative presence within the obligate zone (99.5% and 99.8%, respectively [Table C-3.3-2]). However, SGCS-14 has a much higher vegetative canopy cover (131.6%) than SGCS-11 (109.3%), indicating a greater density (more overlapping species) of vegetation in the obligate zone.

C-3.4 Wetland Vegetation Area

The perimeter of wetland vegetation was surveyed using a combination of a DGPS and a total station tied to global positioning system (GPS) control points, depending on tree cover. Four distinct zones were mapped and are shown on Figure C-3.0-1: (1) West Cattail; (2) West Willow/Cattail; (3) Central Cattail; and (4) GCS Vegetation. The area encompassed by each zone is listed in Table C-3.4-1. The West Cattail Zone is a narrow strip of cattails that parallels the open channel at the head of the study area and encompassed an area of 3770 ft^2. The West Willow/Cattail Zone encompassed 10,301 ft^2 and was primarily dominated by coyote willows with several narrowleaf cottonwood trees as well as stands of cattails. Narrowleaf cottonwood was observed while mapping but was never encountered on any transects and was not included in the comprehensive species list. The Central Cattail Zone encompassed 104,708 ft^2 and is the dominant vegetation feature of the study area. The planted wetland area surrounding the GCS (GCS Vegetation Zone) encompassed 11,378 ft^2. The four zones provide wetland extent and can be compared in future surveys to determine if the wetland area is expanding or contracting.

C-4.0 CONCLUSIONS AND RECOMMENDATIONS

This appendix presents the annual vegetation monitoring baseline of Sandia Canyon Reach S-2. Vegetation data were collected along 10 transects to support calculations, including species composition and vegetative canopy cover percentages, obligate zone delineation and characterization, and wetland vegetation area extent. In general, the farthest upstream transects and farthest downstream transects have less vegetative canopy cover than the centrally located transects. In the majority of transects, obligate species dominate the composition. In subsequent years, a comparison of metrics characterizing the obligate zone is expected to quantify wetland zone expansion or contraction at the transect locations, as well as provide information about the occurrence of obligates and overall vegetative cover within the obligate zone. The extent of the wetland system in the upstream areas begins as a narrow zone strictly adjacent to a defined channel and gradually expands across a much wider area before eventually returning to a narrow channel system above the GCS.

One recommendation for future monitoring would be to establish up to three additional transects between SCGS-3 and SCGS-4. This area has a narrow band of cattails that were mapped, but the adjacent upland species were not documented. Additionally, vegetation should be recorded along geomorphic transects SCGS-5 and SCGS-6. These transects encompass cattail stand boundaries that could change in extent over time.

C-5.0 REFERENCES AND MAP DATA SOURCES

C-5.1 References

The following list includes all documents cited in this appendix. Parenthetical information following each reference provides the author(s), publication date, and ER ID or ESH ID. This information is also included in text citations. ER IDs were assigned by the Environmental Programs Directorate's Records Processing Facility (IDs through 599999), and ESH IDs are assigned by the Environment, Safety, and Health (ESH) Directorate (IDs 600000 and above). IDs are used to locate documents in the Laboratory's Electronic Document Management System and, where applicable, in the master reference set.

Copies of the master reference set are maintained at the NMED Hazardous Waste Bureau and the ESH Directorate. The set was developed to ensure that the administrative authority has all material needed to review this document, and it is updated with every document submitted to the administrative authority. Documents previously submitted to the administrative authority are not included.

LANL (Los Alamos National Laboratory), October 2009. "Investigation Report for Sandia Canyon", Los Alamos National Laboratory document LA-UR-09-6450, Los Alamos, New Mexico. (LANL 2009, 107453)

Cobrain, D., April 3, 2013. FW: Sandia Wetland cross sections. E-mail message to D. Katzman (LANL) from D. Cobrain (NMED), Santa Fe, New Mexico. (Cobrain 2013, 256726)

Coulloudon, B., K. Eshelman, J. Gianola, N. Habich, L. Hughes, C. Johnson, M. Pellant, P. Podborny, A. Rasmussen, B. Robles, P. Shaver, J. Spehar, and J. Willoughby, 1999. "Sampling Vegetation Attributes," Interagency Technical Reference 1734-4, Cooperative Extension Service, U.S. Department of Agriculture Forest Service (National Resource Conservation Service), and U.S. Department of the Interior Bureau of Land Management, Denver, Colorado. (Coulloudon et al. 1999, 600337)

LANL (Los Alamos National Laboratory), September 2011. "Work Plan and Final Design for Stabilization of the Sandia Canyon Wetland," Los Alamos National Laboratory document LA-UR-11-5337, Los Alamos, New Mexico. (LANL 2011, 207053)

LANL (Los Alamos National Laboratory), June 2014. "Sandia Wetland Performance Report, Baseline Conditions 2012–2014," Los Alamos National Laboratory document LA-UR-14-24271, Los Alamos, New Mexico. (LANL 2014, 257590)

LANL (Los Alamos National Laboratory), December 15, 2014. "2014 Annual Monitoring Report for Sandia Canyon Wetland Grade-Control Structure (SPA-2012-00050-ABQ)," Los Alamos National Laboratory letter and attachments (ENV-DO-14-0378) to K.E. Allen (USACE) from A.R. Grieggs (LANL), Los Alamos, New Mexico. (LANL 2014, 600083)

Reed, P.B.J., September 1988. "National List of Plant Species That Occur in Wetlands: 1988 National Summary," Biological Report 88(24), U.S. Department of the Interior, Fish and Wildlife Service, Washington D.C. (Reed 1988, 600338)

C-5.2 Map Data Sources

The following list provides data sources for maps included in the main body of this appendix.

2000 LIDAR Hypsography; Los Alamos National Laboratory, Earth and Environmental Sciences GIS Lab; 1:1,200; Work in progress.

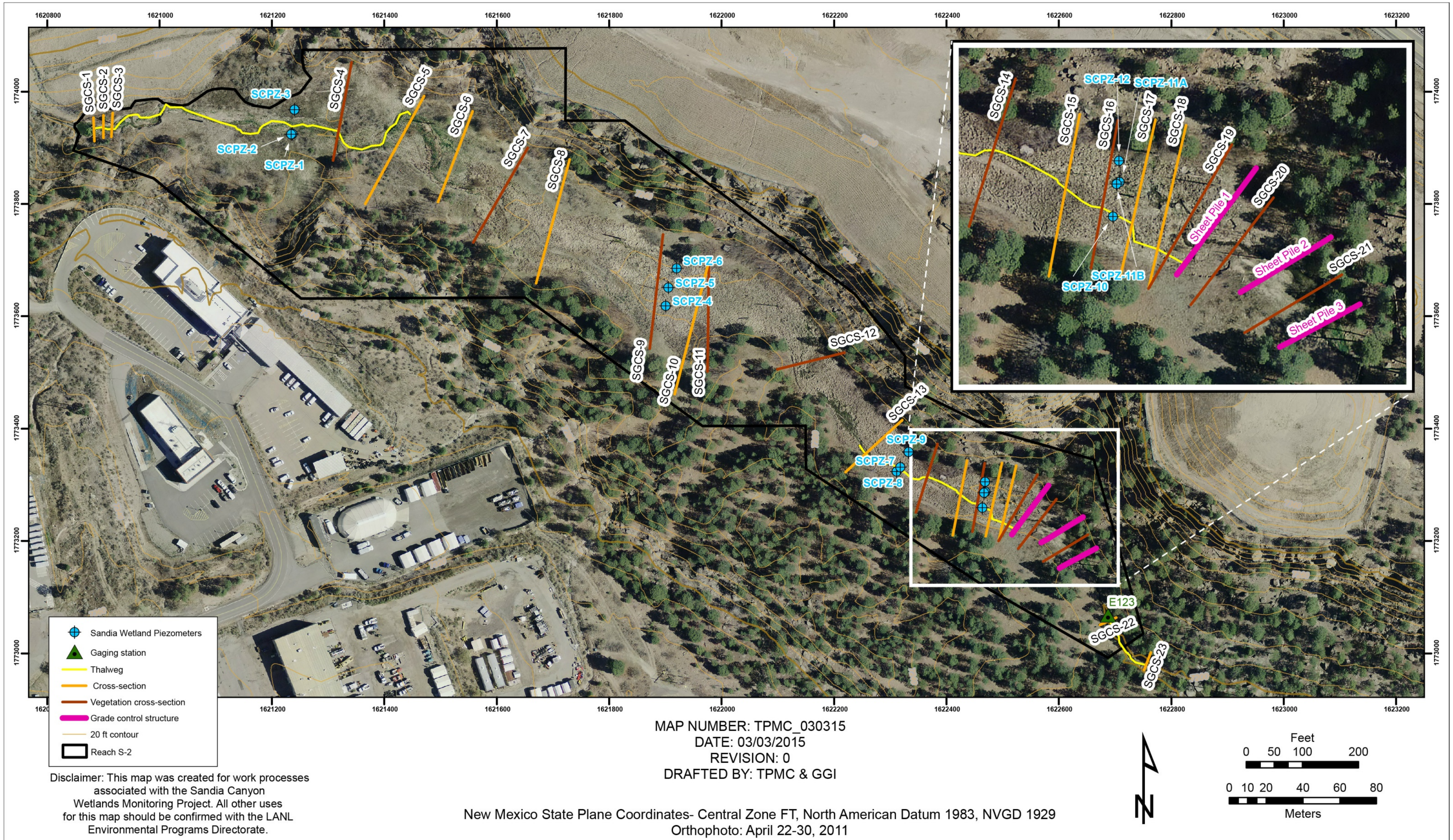

Figure C-1.0-1 Locations of cross-sections, piezometers, sheet piles, and thalweg profiles in Sandia Canyon Reach S-2

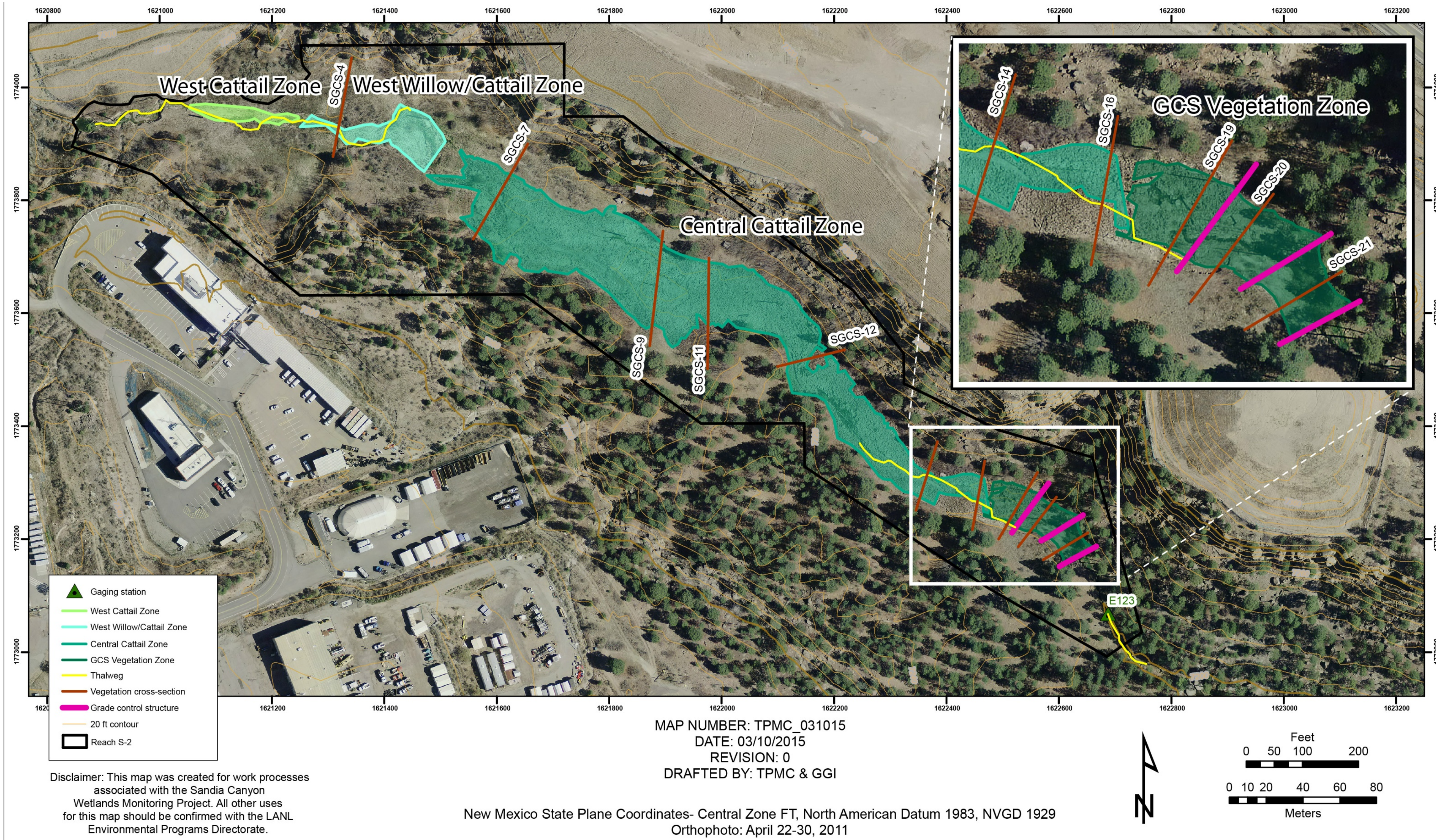

Figure C-3.0-1 2014 vegetation perimeter mapping results at Sandia Canyon Reach S-2

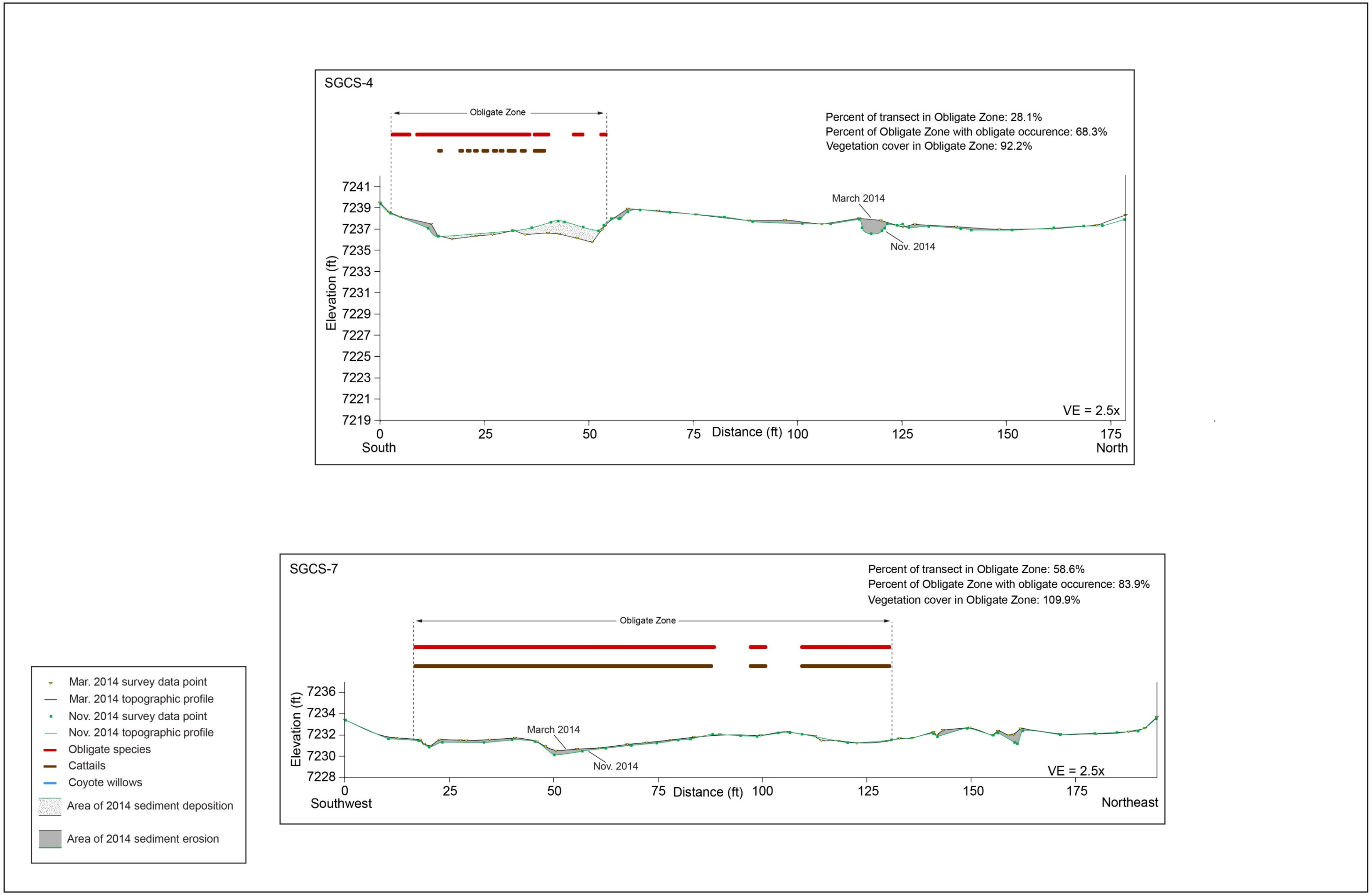

Figure C-3.3-1 Spatial distribution of obligate species on transects SGCS 4 and SGCS-7 in Sandia Canyon Reach S-2. Geomorphic cross-sections from Appendix B in this report.

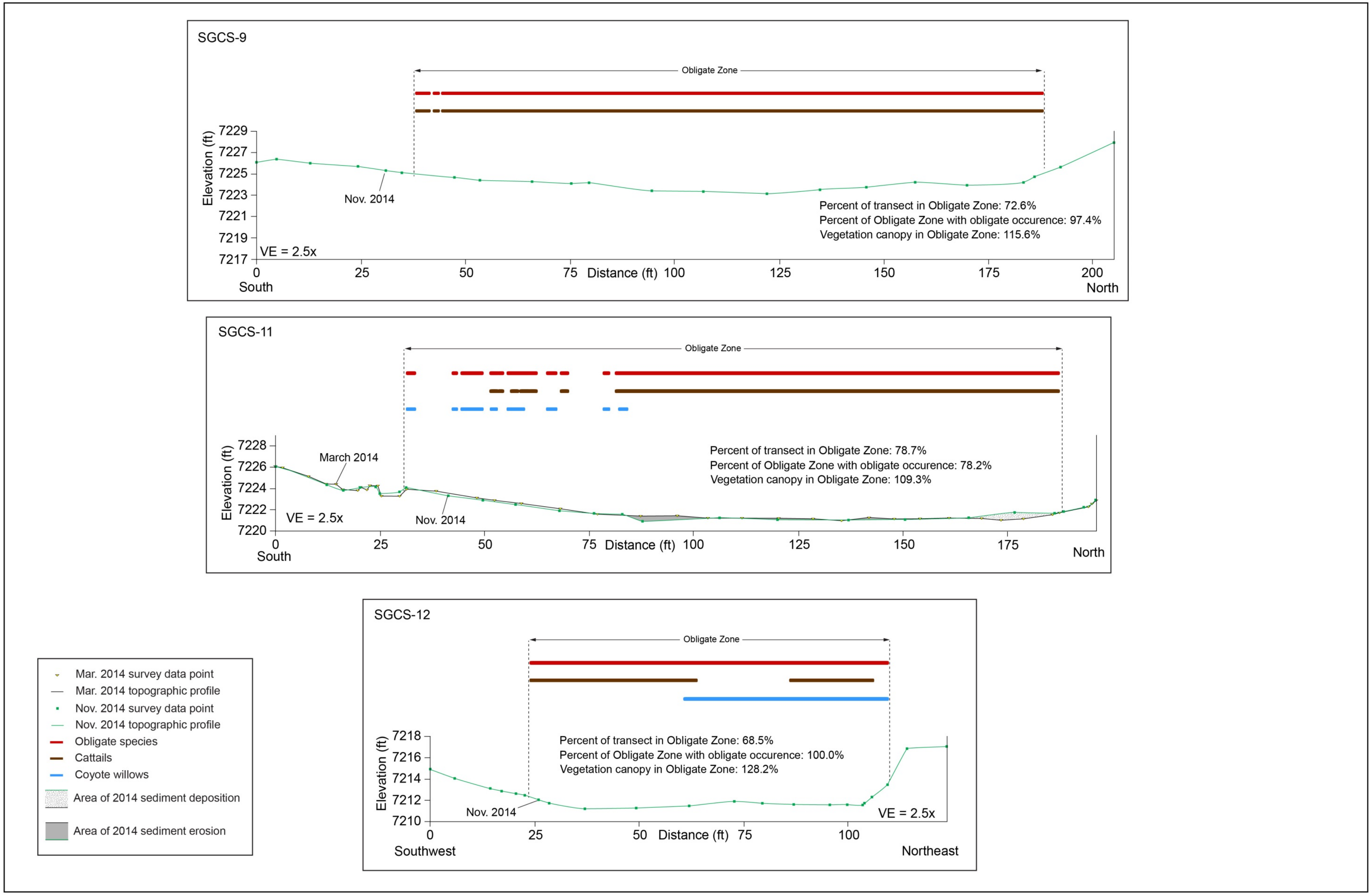

Figure C-3.3-2 Spatial distribution of obligate species on transects SGCS-9, SGCS-11, and SGCS-12 in Sandia Canyon Reach S-2. Geomorphic cross-sections from Appendix B in this report.

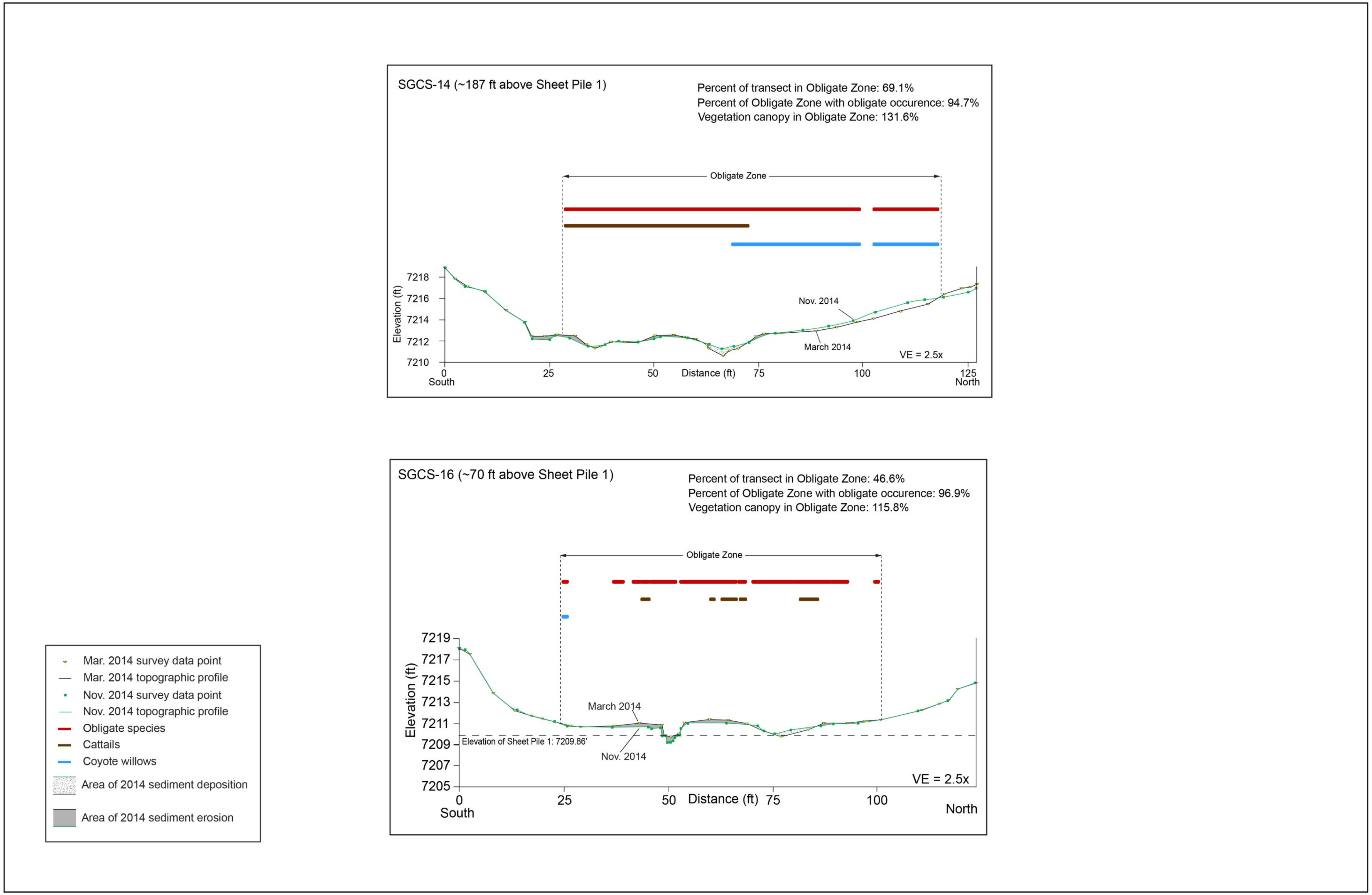

Figure C-3.3-3 Spatial distribution of obligate species on transects SGCS-14 and SGCS-16 in Sandia Canyon Reach S-2. Geomorphic cross-sections from Appendix B in this report.

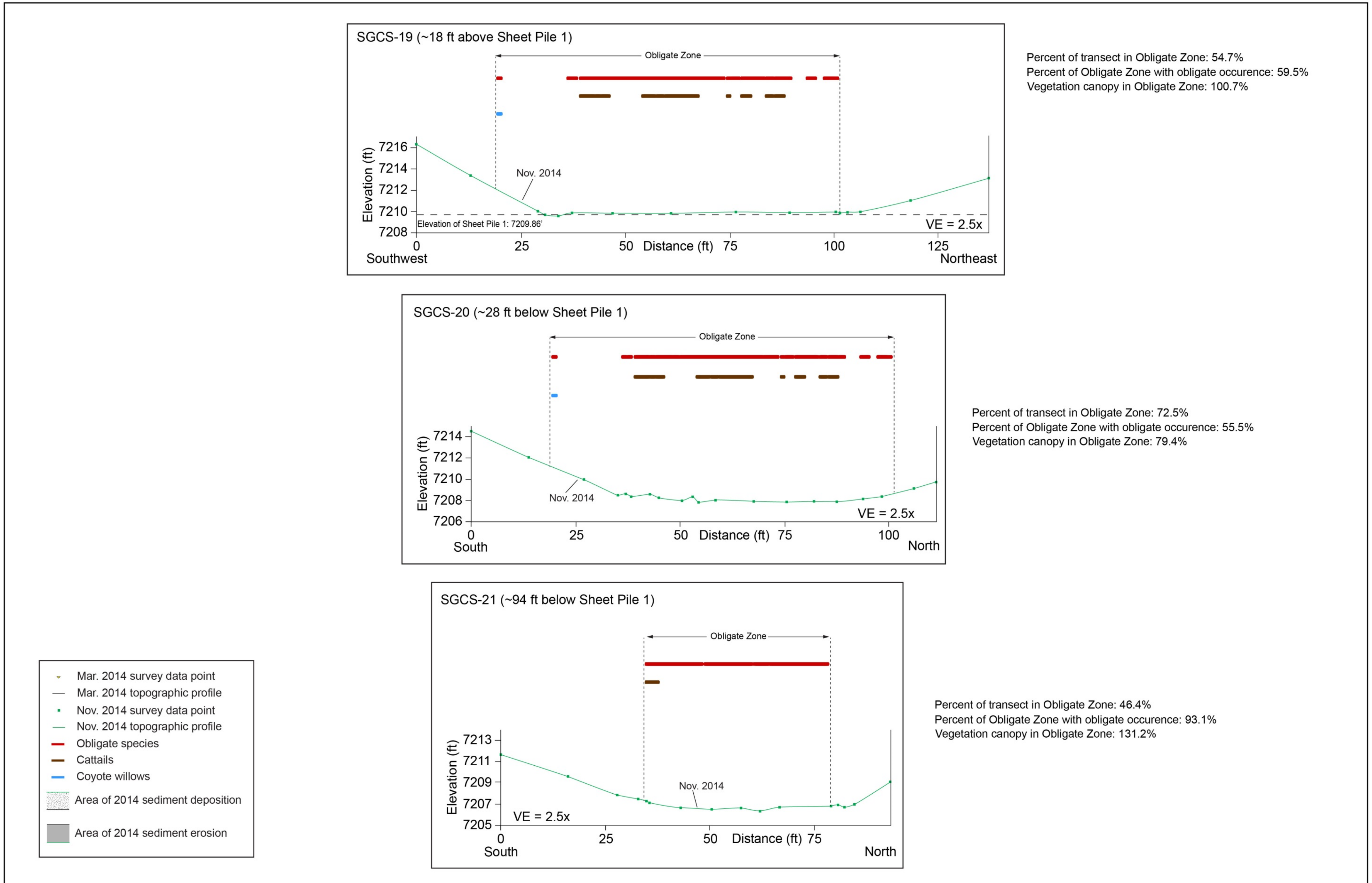

Figure C-3.3-4 Spatial distribution of obligate species on transects SGCS-19, SGCS-20, and SGCS-21 in Sandia Canyon Reach S-2. Geomorphic cross-sections from Appendix B in this report.

Table C-2.1-1
Wetland Plant Species Indicator Definitions

Indicator Acronym	Full Title	Definition*
OBL	Obligate Wetland Plants	Occur almost always (estimated probability of >99%) in wetlands but occasionally are found in non-wetlands (estimated probability of <1%).
FACW	Facultative Wetland Plants	Usually occur in wetlands (estimated probability of 67 to 99%) but occasionally are found in non-wetlands (estimated probability 1 to 33%).
FAC	Facultative Plants	Share an equal likelihood (estimated probability 33 to 67% of occurring in either wetlands or non-wetlands.
FACU	Facultative Upland Plants	Usually occur in non-wetlands (estimated probability 67 to 99%) but occasionally are found in wetlands (estimated probability 1 to 33%).
UPL	Obligate Upland Plants	Occur almost always (estimated probability >99%) in non-wetlands.
NI	No Indicator Status	Unable to determine indicator status.

* Source: Reed (1988, 600338).

Table C-3.1-1
2014 Comprehensive Species List

Symbol	Scientific Name	Common Name	Indicator Category*	Lifeform	Classification
ACNE	Acer negundo	Boxelder	FACW	Tree	Non-Obligate
AGGI	Agrostis gigantea	Giant redtop	FACW	Graminoid	Non-Obligate
ANGE	Andropogon gerardii	Big bluestem	FACU	Graminoid	Non-Obligate
ARDR	Artemisia dracunculus	Dragon sagewort	NI	Shrub	Non-Obligate
ASSP	Asteraceae Spp.	Thistle	FACW	Forb	Non-Obligate
BEFE	Berberis fendleri	Colorado barberry	NI	Forb	Non-Obligate
BOGR	Bouteloua gracilis	Blue grama	NI	Graminoid	Non-Obligate
BRAN	Bromus anomalus	Nodding brome	NI	Graminoid	Non-Obligate
BRTE	Bromus tectorum	Cheatgrass	NI	Graminoid	Non-Obligate
CAAQ	Carex Aquatilis	Water sedge	OBL	Graminoid	Obligate
CASP	Unidentified Carex Species	Carex (sedge)	OBL	Graminoid	Obligate
CEIN	Cenchrus incertus	Sand burr	NI	Graminoid	Non-Obligate
CHNA	Chrysothamnus nauseosus	Rubber rabbitbrush	NI	Shrub	Non-Obligate
CHVI	Chloris virgata	Showy windmill	NI	Graminoid	Non-Obligate
CIIN	Chichorium intybus	Chicory	NI	Forb	Non-Obligate
ELAN	Eleagnus angustifolia	Russian olive	FACW	Tree	Non-Obligate
ELEL	Elymus elymoides	Squirreltail	UPL	Graminoid	Non-Obligate
ELPA	Eleocharis palustris	Common spikerush	OBL	Graminoid	Obligate
EPCI	Epilobium ciliatum	Fringed willowherb	FACW	Forb	Non-Obligate
ERCI	Erodium cicutarium	Redstem stork’s bill	NI	Forb	Non-Obligate

Table C-3.1-1 continued

Symbol	Scientific Name	Common Name	Indicator Category*	Lifeform	Classification
GLBO	Glyceria Borealis	Small floating mannagrass	OBL	Graminoid	Obligate
HEAN	Helianthus annuus	Common sunflower	FAC	Forb	Non-Obligate
JUBA	Juncus balticus	Baltic rush	OBL	Graminoid	Obligate
JULO	Juncus longistylus	Longstyle rush	FACW	Graminoid	Non-Obligate
JUSC	Juniperus scopularum	Rocky Mountain juniper	NI	Tree	Non-Obligate
JUTE	Juncus tenuis	Poverty rush	FACW	Graminoid	Non-Obligate
JUTO	Juncus Torreyi	Torrey rush	FACW	Graminoid	Non-Obligate
KOMY	Kobresia mysuroides	Ballardi bog sedge	FACU	Graminoid	Non-Obligate
KOSC	Kochia scoparia	Mock cypress	FAC	Forb	Non-Obligate
LEMI	Lemna minor	Common duckweed	OBL	Forb	Obligate
LILE	Linum lewisii	Lewis flax	NI	Forb	Non-Obligate
LUAR	Lupinus argenteus	Silvery lupine	UPL	Forb	Non-Obligate
MEOF	Melilotus officinalis	Yellow sweetclover	FACU	Forb	Non-Obligate
MIGL	Mimulus glabratus	Roundleaf monkeyflower	OBL	Forb	Obligate
MIGU	Mimulus guttatus	Seep monkeyflower	OBL	Forb	Obligate
MUMO	Muhlenbergia montana	Mountain muhly	UPL	Graminoid	Non-Obligate
PASM	Pascopyrum smithii	Western wheatgrass	FAC	Graminoid	Non-Obligate
PIPO	Pinus ponderosa	Ponderosa pine	FACU	Tree	Non-Obligate
POHI	Potentilla hippiana	Wooly cinquefoil	NI	Forb	Non-Obligate
POPR	Poa pratensis	Kentucky bluegrass	FACU	Graminoid	Non-Obligate
QUGA	Quercus gambelii	Gambel oak	NI	Tree	Non-Obligate
RICE	Ribes cereum	Wax currant	FAC	Shrub	Non-Obligate
ROWO	Rosa woodsii	Wood's rose	FACU	Shrub	Non-Obligate
RUCR	Rumex crispus	Curly dock	FACW	Forb	Non-Obligate
RUID	Rubus idaeus	American red raspberry	FAC	Forb	Non-Obligate
SAEX	Salix exigua	Narrowleaf (coyote) willow	OBL	Shrub	Obligate
SAIR	Salix irrorata	Bluestem willow	FACW	Shrub	Non-Obligate
SCAC	Scirpus Acutus	Hardstem bullrush	OBL	Graminoid	Obligate
SCPU	Schoenoplectus pungens	Common threesquare	OBL	Graminoid	Obligate
SCTA	Scirpus Tabernaemontani	Softstem bulrush	OBL	Graminoid	Obligate
SEVA	Securigera varia	Purple crownvetch	NI	Forb	Non-Obligate
SPCO-A	Sphaeralcea coccinea	Scarlet globemallow	NI	Forb	Non-Obligate
SPCO-B	Sporobolus contractus	Spike dropseed	NI	Graminoid	Non-Obligate
TAOF	Taraxacum officinale	Common dandelion	FACU	Forb	Non-Obligate
TYLA	Typha latifolia	Broad-leafed cattail	OBL	Forb	Obligate
VEHA	Verbena hastata	Swamp verbena	FAC	Forb	Non-Obligate
VETH	Verbascum thapsus	Common mullein	NI	Forb	Non-Obligate

* Source: Reed (1988, 600338).

Table C-3.1-2
2014 Species Composition Percentage by Life Form

Species Count	Tree	Shrub	Graminoid	Forb
Overall				
57	8.8%	10.5%	40.4%	40.4%
Obligate Species				
13	0%	7.7%	61.5%	30.8%
Non-Obligate Species				
44	11.4%	11.4%	36.4%	40.9%

Table C-3.1-3
2014 Species Composition Percentage by Indicator Status

Obligate Wetland Plants (OBL)	Facultative Wetland Plants (FACW)	Facultative Plants (FAC)	Facultative Upland Plants (FACU)	Obligate Upland Plants (UPL)	No Indicator Status (NI)
22.8%	17.5%	10.5%	12.3%	5.3%	31.6%

Note: n = 57 species.

Table C-3.2-1
Percent Canopy Cover and Percent Species Composition for Each Transect (Entire Length)

Transect	Percent Canopy Cover		Percent Species Composition	
	Vegetative	Non-Vegetative*	Vegetative	Non-Vegetative*
SGCS-4	87.6%	18.2%	82.8%	17.2%
SCGS-7	100.2%	11.9%	89.4%	10.6%
SGCS-9	123.7%	1.6%	98.8%	1.2%
SGCS-11	100.3%	9.7%	91.2%	8.8%
SGCS-12	104.9%	17.8%	85.5%	14.5%
SGCS-14	131.0%	0.9%	99.3%	0.7%
SGCS-16	98.5%	17.7%	84.8%	15.2%
SGCS-19	78.7%	32.8%	70.6%	29.4%
SGCS-20	67.1%	44.1%	60.4%	39.6%
SGCS-21	84.8%	31.6%	72.9%	27.1%

* Non-vegetative categories: algae, logs, litter, bare ground, water.

Table C-3.2-2
Summary of 2014 Ranked Order of Species Composition

Transect	Species Rank 1			Species Rank 2			Species Rank 3		
	Species	Indicator Status	Composition	Species	Indicator Status	Composition	Species	Indicator Status	Composition
SGCS-4	Western wheatgrass	FAC	27.9%	Common threesquare	OBL	15.9%	Giant redtop	FACW	10.6%
SGCS-7	Broad-leafed cattail	OBL	43.5%	Giant redtop	FACW	15.5%	Western wheatgrass	FAC	7.4%
SGCS-9	Broad-leafed cattail	OBL	56.5%	Russian olive	FACW	9.2%	Thistle	FACW	8.3%
SGCS-11	Broad-leafed cattail	OBL	51.4%	Giant redtop	FACW	12.7%	Ballardi bog sedge	FACU	11.0%
SGCS-12	Broad-leafed cattail	OBL	38.3%	Narrowleaf (coyote) willow	OBL	31.6%	Gambel oak	NI	3.9%
SGCS-14	Narrowleaf (coyote) willow	OBL	26.4%	Broad-leafed cattail	OBL	25.1%	Ponderosa pine	FACU	21.3%
SGCS-16	Broad-leafed cattail	OBL	27.3%	Ponderosa pine	FACU	13.9%	Narrowleaf willow (coyote willow)	OBL	11.6%
SGCS-19	Small floating mannagrass	OBL	12.0%	Swamp verbena	FAC	11.2%	Blue grama	NI	9.2%
SGCS-20	Broad-leafed cattail	OBL	16.6%	Small floating mannagrass	OBL	6.7%	Softstem bulrush	OBL	6.2%
SGCS-21	Softstem bulrush	OBL	12.1%	Common threesquare	OBL	10.7%	Baltic rush	OBL	9.0%

Note: Omitting non-vegetative categories: algae, logs, litter, bare ground, water.

Table C-3.3-1
Vegetation Survey Transect Length and Percentage of Obligate Zone

Transect	Total Transect Length (ft)	Obligate Zone Length (ft)	Percent of Transect in the Obligate Zone
SGCS-4	178.8	50.2	28.1%
SCGS-7	194.7	114.0	58.6%
SGCS-9	205.0	148.9	72.6%
SGCS-11	196.6	154.7	78.7%
SGCS-12	123.1	84.3	68.5%
SGCS-14	127.7	88.3	69.1%
SGCS-16	123.7	57.6	46.6%
SGCS-19	137.3	75.1	54.7%
SGCS-20	111.6	80.9	72.5%
SGCS-21	93.4	43.3	46.4%

Table C-3.3-2
Comparison of Canopy Cover to the Vegetative and Non-Living Presence along Transects in Obligate and Non-Obligate Zones

Transect	Obligate Zone				Non-Obligate Zone		
	Vegetative Canopy Cover	Obligate Occurrence	Vegetative Presence	Non-Vegetative Presence*	Vegetative Canopy Cover	Vegetative Presence	Non-Vegetative Presence*
SGCS-4	92.2%	68.3%	80.5%	19.5%	85.8%	82.6%	17.4%
SCGS-7	109.9%	83.9%	93.8%	6.2%	86.5%	80.0%	20.0%
SGCS-9	115.6%	97.4%	100.0%	0.0%	145.1%	94.3%	5.7%
SGCS-11	109.3%	78.2%	99.5%	0.5%	66.8%	56.3%	43.7%
SGCS-12	128.2%	100.0%	100.0%	0.0%	54.1%	43.6%	56.4%
SGCS-14	131.6%	94.7%	99.8%	0.2%	129.7%	97.5%	2.5%
SGCS-16	115.8%	96.9%	98.1%	1.9%	83.5%	68.5%	31.5%
SGCS-19	100.7%	59.5%	86.8%	13.2%	52.3%	52.3%	47.7%
SGCS-20	79.4%	55.5%	69.6%	30.4%	34.9%	34.9%	65.1%
SGCS-21	131.2%	93.1%	100%	0.0%	44.7%	42.9%	57.1%

* Non-vegetative categories: algae, logs, litter, bare ground, water.

Table C-3.4-1
Wetland Vegetation Area Totals

Zone Name	Zone Description	Area Total (ft^2)	Area Total (m^2)
West Cattail	Cattail stand west of SGCS-4	3,770	350
West Willow/Cattail	Willow dominated stand at SGCS-4	10,301	957
Central Cattail	Cattail stand inclusive of SGCS-7 to SGCS-16.	104,708	9,728
GCS Vegetation	Wetland vegetation directly in and around the GCS (replanted)	11,378	1,057
	Total	**130,157**	**12,092**

Attachment C-1

Photographs of Sandia Wetlands Vegetation Monitoring

Photo C1-1 September 2014 photograph of the middle of transect SGCS-4.This photo demonstrates the line intercept method in which all vegetation that intersects the plane perpendicular to the ground surface and extending through the tape line is surveyed.

Photo C1-2 September 2014 photograph of the north end of transect SGCS-14, looking south. This photo shows overlapping vegetation, as well as vegetation intersecting the survey plane above the tape line.

Photo C1-3 September 2014 photograph of the south end of transect SGCS-4, looking north

Photo C1-4 September 2014 photograph of the south end of transect SGCS-7, looking north

Photo C1-5 September 2014 photograph of cross-section SGCS-9 at the southern edge of thick Typha latifolia (broad-leafed cattail), looking north

Photo C1-6 September 2014 photograph of the south end of transect SGCS-11, looking north

Photo C1-7 September 2014 photograph of the south end of transect SGCS-12, looking north

Photo C1-8 September 2014 photograph of the south end of transect SGCS-14, looking north

Photo C1-9 September 2014 photograph of the south end of transect SGCS-16, looking north

Photo C1-10 October 2014 photograph of the north end of transect SGCS-19, upstream of Sheet Pile 1, looking south

Photo C1-11 October 2014 photograph of the north end of transect SGCS-20, upstream of Sheet Pile 2, looking south

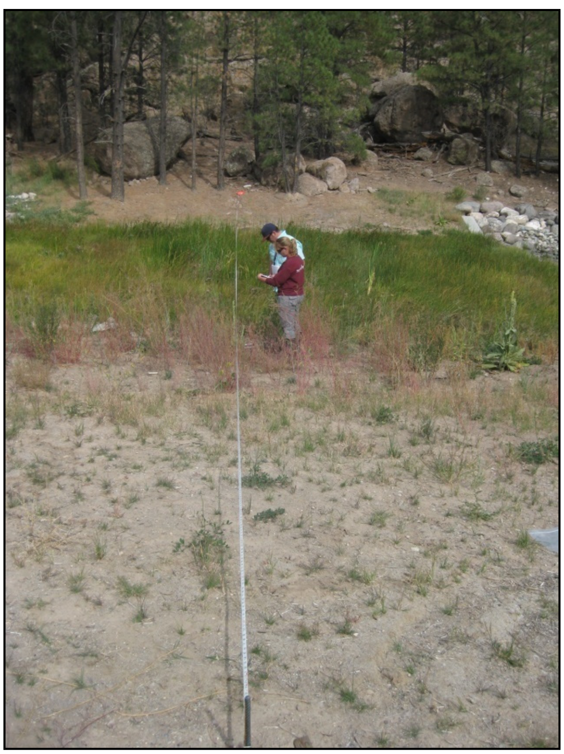

Photo C1-12 October 2014 photograph of the south end of transect SGCS-21, upstream of Sheet Pile 3, looking north

Attachment C-2

2014 Baseline Vegetation Survey Data
(on CD included with this document)

Attachment C-3

Rank Order of Percent Canopy Cover and Individual Species Composition Summary Tables

Table C3-1
2014 Ranked Order of Species Abundance on Transect SGCS-4 (Entire Length)

Species Rank	Species Name	Common Name	Life Form	Indicator Status	Percent Canopy Cover	Percent Composition
1	Pascopyrum smithii	Western wheatgrass	Graminoid	FAC	29.6%	27.9%
2	Schoenoplectus pungens	Common threesquare	Graminoid	OBL	16.8%	15.9%
3	—*	Bare ground	Non-living	—	15.7%	14.8%
4	Agrostis gigantea	Giant redtop	Graminoid	FACW	11.2%	10.6%
5	Artemisia dracunculus	Dragon sagewort	Shrub	NI	9.3%	8.8%
6	Quercus gambelii	Gambel oak	Tree	NI	5.1%	4.8%
7	Bromus tectorum	Cheatgrass	Graminoid	NI	4.6%	4.3%
8	Juniperus scopularum	Rocky Mountain juniper	Tree	NI	2.7%	2.5%
9	Typha latifolia	Broad-leafed cattail	Forb	OBL	2.3%	2.2%
10	—	Water	Non-living	—	2.2%	2.1%
11	Rumex crispus	Curly dock	Forb	FACW	1.6%	1.5%
12	Securigera varia	Purple crownvetch	Forb	NI	1.0%	1.0%
13	Chrysothamnus nauseosus	Rubber rabbitbrush	Shrub	NI	0.8%	0.8%
14	Chichorium intybus	Chicory	Forb	NI	0.7%	0.6%
15	Bromus anomalus	Nodding brome	Graminoid	NI	0.6%	0.5%
16	Cenchrus incertus	Sand burr	Graminoid	NI	0.4%	0.4%
17	Elymus elymoides	Squirreltail	Graminoid	UPL	0.4%	0.4%
18	—	Log	Non-living	—	0.3%	0.3%
19	Taraxacum officinale	Common dandelion	Forb	FACU	0.2%	0.2%
20	Asteraceae Spp.	Thistle	Forb	FACW	0.1%	0.1%
21	Rosa woodsii	Wood's rose	Shrub	FACU	0.1%	0.1%
				Vegetative	**87.6%**	**82.8%**
				Non-Vegetative	**18.2%**	**17.2%**
				Total	**105.9%**	**100.0%**

Notes: FAC = facultative plant; OBL = obligate wetland plant; FACW = facultative wetland plant; NI = no indicator status; UPL = upland plant; FACU = facultative upland plant.

*— = Not applicable.

Table C3-2
2014 Ranked Order of Species Abundance on Transect SGCS-7 (Entire Length)

Species Rank	Species Name	Common Name	Life Form	Indicator Status	Percent Canopy Cover	Percent Composition
1	Typha latifolia	Broad-leafed cattail	Forb	OBL	48.7%	43.5%
2	Agrostis gigantea	Giant redtop	Graminoid	FACW	17.4%	15.5%
3	—*	Bare ground	Non-living	—	11.9%	10.6%
4	Pascopyrum smithii	Western wheatgrass	Graminoid	FAC	8.3%	7.4%
5	Rumex crispus	Curly dock	Forb	FACW	5.5%	4.9%
6	Elymus elymoides	Squirreltail	Graminoid	UPL	4.1%	3.7%
7	Artemisia dracunculus	Dragon sagewort	Shrub	NI	3.7%	3.3%
8	Schoenoplectus pungens	Common threesquare	Graminoid	OBL	2.8%	2.5%
9	Quercus gambelii	Gambel oak	Tree	NI	2.7%	2.4%
10	Asteraceae Spp.	Thistle	Forb	FACW	1.7%	1.6%
11	Bromus anomalus	Nodding brome	Graminoid	NI	1.4%	1.3%
12	Chrysothamnus nauseosus	Rubber rabbitbrush	Shrub	NI	1.2%	1.1%
13	Berberis fendleri	Colorado barberry	Forb	NI	1.1%	1.0%
14	Sphaeralcea coccinea	Scarlet globemallow	Forb	NI	0.6%	0.5%
15	Epilobium ciliatum	Fringed willowherb	Forb	FACW	0.4%	0.4%
16	Bouteloua gracilis	Blue grama	Graminoid	NI	0.3%	0.2%
17	Linum lewisii	Lewis flax	Forb	NI	0.2%	0.1%
				Vegetative	**100.2%**	**89.4%**
				Non-Vegetative	**11.9%**	**10.6%**
				Total	**112.1%**	**100.0%**

Notes: Notes: FAC = facultative plant; OBL = obligate wetland plant; FACW = facultative wetland plant; NI = no indicator status; UPL = upland plant; FACU = facultative upland plant.

*— = Not applicable.

Table C3-3
2014 Ranked Order of Species Abundance on Transect SGCS-9 (Entire Length)

Species Rank	Species Name	Common Name	Life Form	Indicator Status	Percent Canopy Cover	Percent Composition
1	Typha latifolia	Broad-leafed cattail	Forb	OBL	70.8%	56.5%
2	Eleagnus angustifolia	Russian olive	Tree	FACW	11.5%	9.2%
3	Asteraceae Spp.	Thistle	Forb	FACW	10.3%	8.3%
4	Agrostis gigantea	Giant redtop	Graminoid	FACW	5.8%	4.6%
5	Pinus Ponderosa	Ponderosa pine	Tree	FACU	4.9%	3.9%
6	Rumex crispus	Curly dock	Forb	FACW	3.8%	3.0%
7	Rubus idaeus	American red raspberry	Forb	FAC	3.1%	2.5%
8	Pascopyrum smithii	Western wheatgrass	Graminoid	FAC	2.7%	2.2%
9	Andropogon gerardii	Big bluestem	Graminoid	FACU	2.1%	1.7%
10	Epilobium ciliatum	Fringed willowherb	Forb	FACW	1.9%	1.5%
11	Juncus tenuis	Poverty rush	Graminoid	FACW	1.8%	1.4%
12	—*	Bare ground	Non-living	—	1.6%	1.2%
13	Bouteloua gracilis	Blue grama	Graminoid	NI	1.3%	1.0%
14	Quercus gambelii	Gambel oak	Tree	NI	1.1%	0.9%
15	Artemisia dracunculus	Dragon sagewort	Shrub	NI	1.0%	0.8%
16	Erodium cicutarium	Redstem stork's bill	Forb	NI	0.6%	0.5%
17	Rosa woodsii	Wood's rose	Shrub	FACU	0.5%	0.4%
18	Elymus elymoides	Squirreltail	Graminoid	UPL	0.4%	0.3%
19	Muhlenbergia montana	Mountain muhly	Graminoid	UPL	0.2%	0.2%
				Vegetative	**123.7%**	**98.8%**
				Non-Vegetative	**1.6%**	**1.2%**
				Total	**125.2%**	**100.0%**

Notes: FAC = facultative plant; OBL = obligate wetland plant; FACW = facultative wetland plant; NI = no indicator status; UPL = upland plant; FACU = facultative upland plant.

*— = Not applicable.

Table C3-4
2014 Ranked Order of Species Abundance on Transect SGCS-11 (Entire Length)

Species Rank	Species Name	Common Name	Life Form	Indicator Status	Percent Canopy Cover	Percent Composition
1	Typha latifolia	Broad-leafed cattail	Forb	OBL	56.5%	51.4%
2	Agrostis gigantea	Giant redtop	Graminoid	FACW	13.9%	12.7%
3	Kobresia mysuroides	Ballardi bog sedge	Graminoid	FACU	12.1%	11.0%
4	—*	Bare ground	Non-living	—	8.8%	8.0%
5	Salix exigua	Narrowleaf (coyote) willow	Shrub	OBL	6.6%	6.0%
6	Quercus gambelii	Gambel oak	Tree	NI	2.6%	2.4%
7	Rosa woodsii	Wood's rose	Shrub	FACU	2.2%	2.0%
8	Bouteloua gracilis	Blue grama	Graminoid	NI	1.6%	1.4%
9	Asteraceae Spp.	Thistle	Forb	FACW	1.5%	1.4%
10	Juncus tenuis	Poverty rush	Graminoid	FACW	1.5%	1.4%
11	Andropogon gerardii	Big bluestem	Graminoid	FACU	1.0%	0.9%
12	—	Log	Non-living	—	0.5%	0.5%
13	—	Litter	Non-living	—	0.4%	0.4%
14	Mimulus glabratus	Roundleaf monkeyflower	Forb	OBL	0.4%	0.3%
15	Verbena hastata	Swamp verbena	Forb	FAC	0.3%	0.2%
				Vegetative	**100.3%**	**91.2%**
				Non-Vegetative	**9.7%**	**8.8%**
				Total	**110.0%**	**100.0%**

Notes: FAC = facultative plant; OBL = obligate wetland plant; FACW = facultative wetland plant; NI = no indicator status; UPL = upland plant; FACU = facultative upland plant.

*— = Not applicable.

Table C3-5
2014 Ranked Order of Species Abundance on Transect SGCS-12 (Entire Length)

Species Rank	Species Name	Common Name	Life Form	Indicator Status	Percent Canopy Cover	Percent Composition
1	Typha latifolia	Broad-leafed cattail	Forb	OBL	46.9%	38.3%
2	Salix exigua	Narrowleaf (coyote) willow	Shrub	OBL	38.7%	31.6%
3	—*	Litter	Non-living	—	13.7%	11.2%
4	Quercus gambelii	Gambel oak	Tree	NI	4.8%	3.9%
5	Andropogon gerardii	Big bluestem	Graminoid	FACU	4.3%	3.5%
6	—	Bare ground	Non-living	—	4.1%	3.3%
7	Agrostis gigantea	Giant redtop	Graminoid	FACW	3.2%	2.6%
8	Ribes cereum	Wax currant	Shrub	FAC	1.7%	1.4%
9	Mimulus glabratus	Roundleaf monkeyflower	Forb	OBL	1.1%	0.9%
10	Berberis fendleri	Colorado Barberry	Forb	NI	1.0%	0.8%
11	Bouteloua gracilis	Blue grama	Graminoid	NI	0.9%	0.7%
12	Potentilla hippiana	Wooly cinquefoil	Forb	NI	0.9%	0.7%
13	Lupinus argenteus	Silvery lupine	Forb	UPL	0.6%	0.5%
14	Rosa woodsii	Wood's rose	Shrub	FACU	0.4%	0.3%
15	Elymus elymoides	Squirreltail	Graminoid	UPL	0.2%	0.2%
				Vegetative	**104.9%**	**85.5%**
				Non-Vegetative	**17.8%**	**14.5%**
				Total	**122.7%**	**100.0%**

Notes: FAC = facultative plant; OBL = obligate wetland plant; FACW = facultative wetland plant; NI = no indicator status; UPL = upland plant; FACU = facultative upland plant.

*— = Not applicable.

Table C3-6
2014 Ranked Order of Species Abundance on Transect SGCS-14 (Entire Length)

Species Rank	Species Name	Common Name	Life Form	Indicator Status	Percent Canopy Cover	Percent Composition
1	Salix exigua	Narrowleaf (coyote) willow	Shrub	OBL	34.8%	26.4%
2	Typha latifolia	Broad-leafed cattail	Forb	OBL	33.1%	25.1%
3	Pinus Ponderosa	Ponderosa pine	Tree	FACU	28.1%	21.3%
4	Quercus gambelii	Gambel oak	Tree	NI	22.4%	17.0%
5	Agrostis gigantea	Giant redtop	Graminoid	FACW	6.5%	4.9%
6	Rosa woodsii	Wood's rose	Shrub	FACU	1.6%	1.2%
7	Verbena hastata	Swamp verbena	Forb	FAC	1.4%	1.1%
8	Pascopyrum smithii	Western wheatgrass	Graminoid	FAC	1.1%	0.8%
9	Asteraceae Spp.	Thistle	Forb	FACW	0.8%	0.6%
10	*—	Log	Non-living	—	0.8%	0.6%
11	Bromus anomalus	Nodding brome	Graminoid	NI	0.5%	0.4%
12	Epilobium ciliatum	Fringed willowherb	Forb	FACW	0.5%	0.4%
13	Elymus elymoides	Squirreltail	Graminoid	UPL	0.2%	0.1%
14	—	Bare ground	Non-living	—	0.2%	0.1%
Vegetative					**131.0%**	**99.3%**
Non-Vegetative					**0.9%**	**0.7%**
Total					**131.9%**	**100.0%**

Notes: FAC = facultative plant; OBL = obligate wetland plant; FACW = facultative wetland plant; NI = no indicator status; UPL = upland plant; FACU = facultative upland plant.

*— = Not applicable.

Table C3-7
2014 Ranked Order of Species Abundance on Transect SGCS-16 (Entire Length)

Species Rank	Species Name	Common Name	Life Form	Indicator Status	Percent Canopy Cover	Percent Composition
1	Typha latifolia	Broad-leafed cattail	Forb	OBL	31.8%	27.3%
2	Pinus Ponderosa	Ponderosa pine	Tree	FACU	16.2%	13.9%
3	*—	Bare ground	Non-living	—	13.8%	11.9%
4	Salix exigua	Narrowleaf willow (coyote willow)	Shrub	OBL	13.5%	11.6%
5	Eleagnus angustifolia	Russian olive	Tree	FACW	6.9%	5.9%
6	Epilobium ciliatum	Fringed willowherb	Forb	FACW	6.5%	5.6%
7	Poa pratensis	Kentucky bluegrass	Graminoid	FACU	6.5%	5.6%
8	—	Water	Non-living	—	3.9%	3.3%
9	Mimulus glabratus	Roundleaf monkeyflower	Forb	OBL	3.7%	3.2%
10	Melilotus officinalis	Yellow sweetclover	Forb	FACU	3.6%	3.1%
11	Bouteloua gracilis	Blue grama	Graminoid	NI	3.5%	3.0%
12	Kochia scoparia	Mock cypress	Forb	FAC	3.4%	2.9%
13	Salix irrorata	Bluestem willow	Shrub	FACW	1.2%	1.0%
14	Asteraceae Spp.	Thistle	Forb	FACW	0.7%	0.6%
15	Verbena hastata	Swamp verbena	Forb	FAC	0.4%	0.3%
16	Helianthus annuus	Common sunflower	Forb	FAC	0.3%	0.3%
17	Sporobolus contractus	Spike dropseed	Graminoid	NI	0.2%	0.2%
				Vegetative	**98.5%**	**84.8%**
				Non-Vegetative	**17.7%**	**15.2%**
				Total	**116.2%**	**100.0%**

*— = Not applicable.

Table C3-8
2014 Ranked Order of Species Abundance on Transect SGCS-19 (Entire Length)

Species Rank	Species Name	Common Name	Life Form	Indicator Status	Percent Canopy Cover	Percent Composition
1	— [a]	Bare ground	Non-living	—	24.4%	21.9%
2	Glyceria Borealis	Small floating mannagrass	Graminoid	OBL	13.4%	12.0%
3	Verbena hastata	Swamp verbena	Forb	FAC	12.5%	11.2%
4	Bouteloua gracilis	Blue grama	Graminoid	NI	10.3%	9.2%
5	Melilotus officinalis	Yellow sweetclover	Forb	FACU	9.7%	8.7%
6	—	Water	Non-living	—	8.4%	7.6%
7	Scirpus Tabernaemontani	Softstem bulrush	Graminoid	OBL	6.1%	5.5%
8	Schoenoplectus pungens	Common threesquare	Graminoid	OBL	5.8%	5.2%
9	Typha latifolia	Broad-leafed cattail	Forb	OBL	5.5%	5.0%
10	Juncus Torreyi	Torrey rush	Graminoid	FACW	4.2%	3.7%
11	Scirpus Acutus	Hardstem bullrush	Graminoid	OBL	2.8%	2.5%
12	Kochia scoparia	Mock cypress	Forb	FAC	1.7%	1.6%
13	Epilobium ciliatum	Fringed willowherb	Forb	FACW	1.7%	1.5%
14	Unidentified Carex Species	Carex (sedge)	Graminoid	OBL	1.2%	1.0%
15	Chrysothamnus nauseosus	Rubber rabbitbrush	Shrub	NI	0.9%	0.8%
16	Poa pratensis	Kentucky bluegrass	Graminoid	FACU	0.9%	0.8%
17	Juncus longistylus	Longstyle rush	Graminoid	FACW	0.8%	0.7%
18	Eleocharis palustris	Common spikerush	Graminoid	OBL	0.4%	0.4%
19	Salix exigua	Narrowleaf (Coyote) willow	Shrub	OBL	0.4%	0.3%
20	Juncus balticus	Baltic rush	Graminoid	OBL	0.3%	0.3%
21	Chloris virgata	Showy windmill	Graminoid	NI	0.1%	0.0% [b]
				Vegetative	**78.7%**	**70.6%**
				Non-Vegetative	**32.8%**	**29.4%**
				Total	**111.6%**	**100.0%**

[a] — = Not applicable.

[b] Chloris virgata is present for 0.1 ft of transect SGCS-19 and makes up less than 0.1% composition of the line.

Table C3-9
2014 Ranked Order of Species Abundance on Transect SGCS-20 (Entire Length)

Species Rank	Species Name	Common Name	Life Form	Indicator Status	Percent Canopy Cover	Percent Composition
1	—*	Bare ground	Non-living	—	34.2%	30.8%
2	Typha latifolia	Broad-leafed cattail	Forb	OBL	18.5%	16.6%
3	Glyceria Borealis	Small floating mannagrass	Graminoid	OBL	7.4%	6.7%
4	—	Algae	Algae	—	7.1%	6.4%
5	Scirpus Tabernaemontani	Softstem bulrush	Graminoid	OBL	6.9%	6.2%
6	Melilotus officinalis	Yellow sweetclover	Forb	FACU	6.2%	5.6%
7	Juncus Torreyi	Torrey rush	Graminoid	FACW	6.0%	5.4%
8	Unidentified Carex Species	Carex (sedge)	Graminoid	OBL	4.5%	4.0%
9	Bouteloua gracilis	Blue grama	Graminoid	NI	4.4%	3.9%
10	Verbena hastata	Swamp verbena	Forb	FAC	3.5%	3.1%
11	—	Water	Non-living	—	2.8%	2.5%
12	Scirpus Acutus	Hardstem bullrush	Graminoid	OBL	2.7%	2.4%
13	Lemna minor	Common duckweed	Forb	OBL	2.5%	2.3%
14	Poa pratensis	Kentucky bluegrass	Graminoid	FACU	2.3%	2.1%
15	Schoenoplectus pungens	Common threesquare	Graminoid	OBL	1.3%	1.2%
16	Salix irrorata	Bluestem willow	Shrub	FACW	0.4%	0.4%
17	Salix exigua	Narrowleaf (coyote) willow	Shrub	OBL	0.3%	0.2%
18	Kochia scoparia	Mock cypress	Forb	FAC	0.2%	0.2%
				Vegetative	**67.1%**	**60.4%**
				Non-Vegetative	**44.1%**	**39.6%**
				Total	**111.2%**	**100.0%**

*— = Not applicable.

Table C3-10
2014 Ranked Order of Species Abundance on Transect SGCS-21 (Entire Length)

Species Rank	Species Name	Common Name	Life Form	Indicator Status	Percent Canopy Cover	Percent Composition
1	—*	Bare ground	Non-living	—	23.9%	20.5%
2	Scirpus Tabernaemontani	Softstem bulrush	Graminoid	OBL	14.0%	12.1%
3	Schoenoplectus pungens	Common threesquare	Graminoid	OBL	12.4%	10.7%
4	Juncus balticus	Baltic rush	Graminoid	OBL	10.5%	9.0%
5	Bouteloua gracilis	Blue grama	Graminoid	NI	8.2%	7.1%
6	Kochia scoparia	Mock cypress	Forb	FAC	7.9%	6.8%
7	Unidentified Carex Species	Carex (sedge)	Graminoid	OBL	4.9%	4.2%
8	Carex Aquatilis	Water sedge	Graminoid	OBL	4.8%	4.1%
9	—	Water	Non-living	—	4.4%	3.8%
10	Juncus Torreyi	Torrey rush	Graminoid	FACW	4.1%	3.5%
11	—	Algae	Algae	—	3.3%	2.9%
12	Verbena hastata	Swamp verbena	Forb	FAC	3.3%	2.9%
13	Melilotus officinalis	Yellow sweetclover	Forb	FACU	2.9%	2.5%
14	Mimulus guttatus	Seep monkeyflower	Forb	OBL	2.9%	2.5%
15	Eleocharis palustris	Common spikerush	Graminoid	OBL	2.8%	2.4%
16	Typha latifolia	Broad-leafed cattail	Forb	OBL	2.6%	2.2%
17	Poa pratensis	Kentucky bluegrass	Graminoid	FACU	2.1%	1.8%
18	Verbascum thapsus	Common mullein	Forb	NI	0.6%	0.6%
19	Salix irrorata	Bluestem willow	Shrub	FACW	0.5%	0.5%
20	Acer negundo	Boxelder	Tree	FACW	0.1%	0.1%
				Vegetative	**84.8%**	**72.9%**
				Non-Vegetative	**31.6%**	**27.1%**
				Total	**116.4%**	**100.0%**

*— = Not applicable.

Appendix D

Geochemical and Hydrologic Trends

This appendix presents geochemical and hydrologic trends based on recent monitoring in and around the Sandia Wetland. Interpretation of the data is discussed in the main body of this report.

Appendix D is organized in four sections. Section D-1.0 shows hydrographs and concentration data associated with base flow and storm water. Section D-2.0 shows analytical results from the alluvial system. Section D-3.0 shows water level and other physical parameters from the alluvial system. Section D-4.0 shows figures relevant to overall geochemical patterns in the wetland.

D-1.0 STORM WATER AND BASE FLOW: ANALYTICAL RESULTS AND HYDROGRAPHS

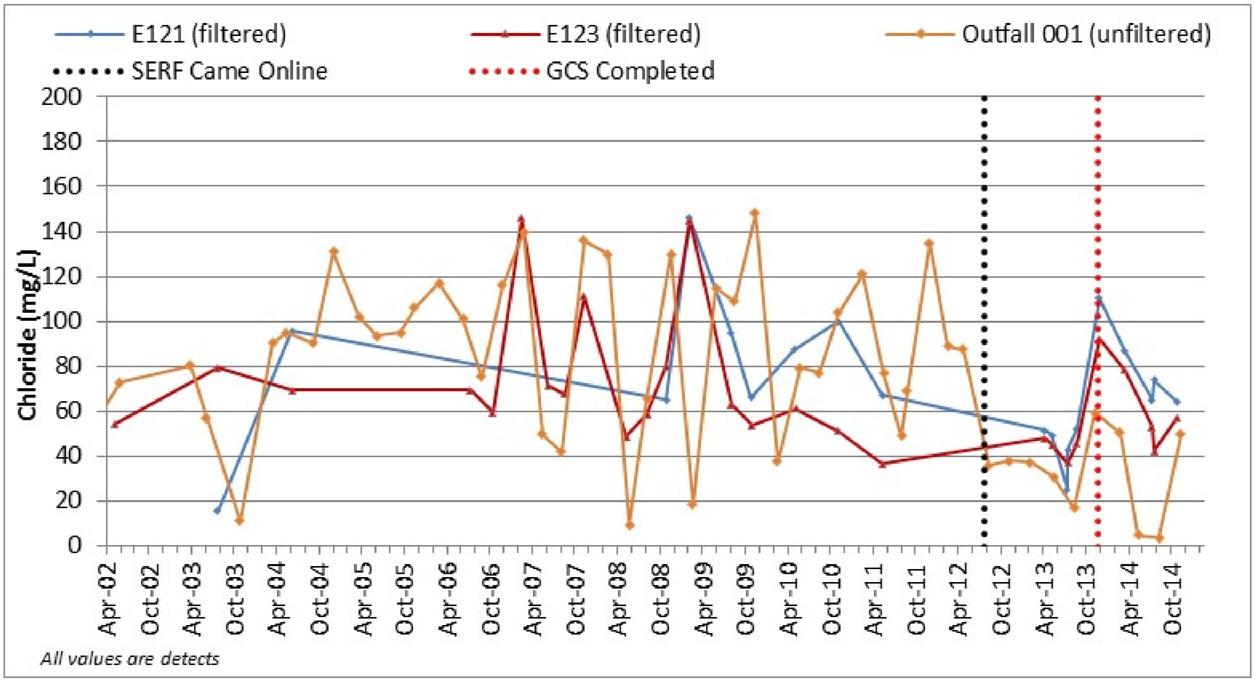

Figure D-1.0-1 Time-series plot showing chloride concentrations at gaging stations E121, E123 and National Pollutant Discharge Elimination System– (NPDES-) permitted Outfall 001

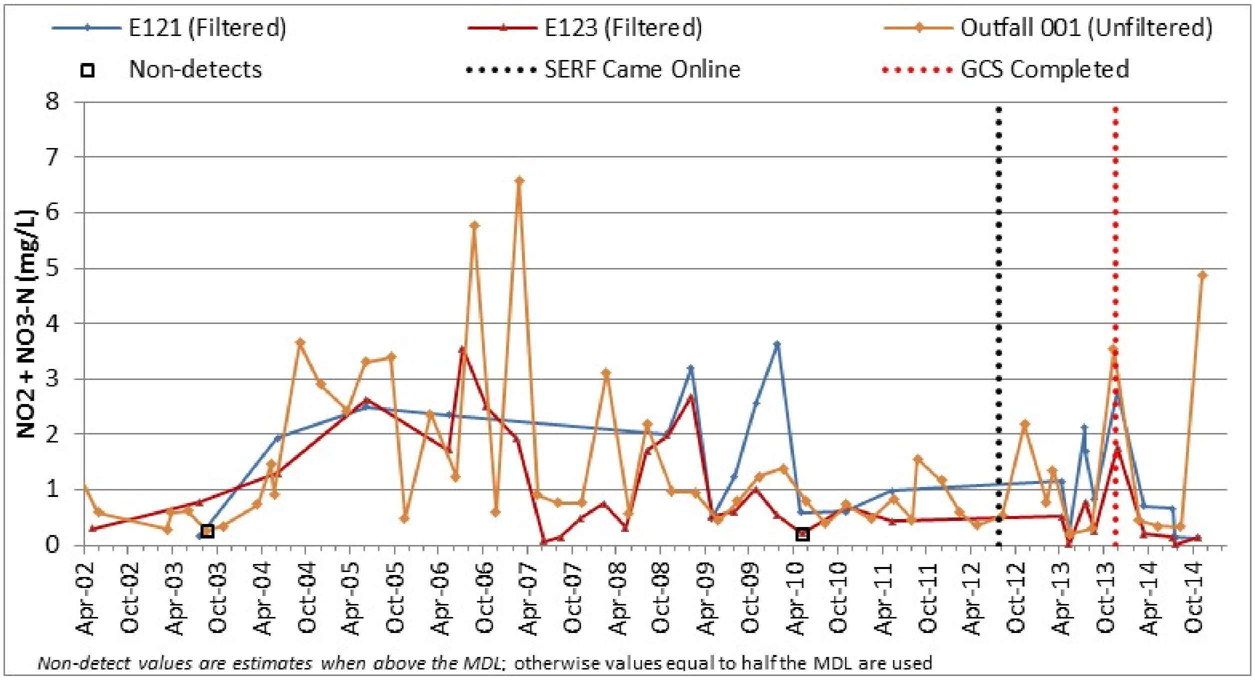

Figure D-1.0-2 Time-series plot showing nitrate plus nitrite as nitrogen concentrations at gaging stations E121, E123, and NPDES Outfall 001

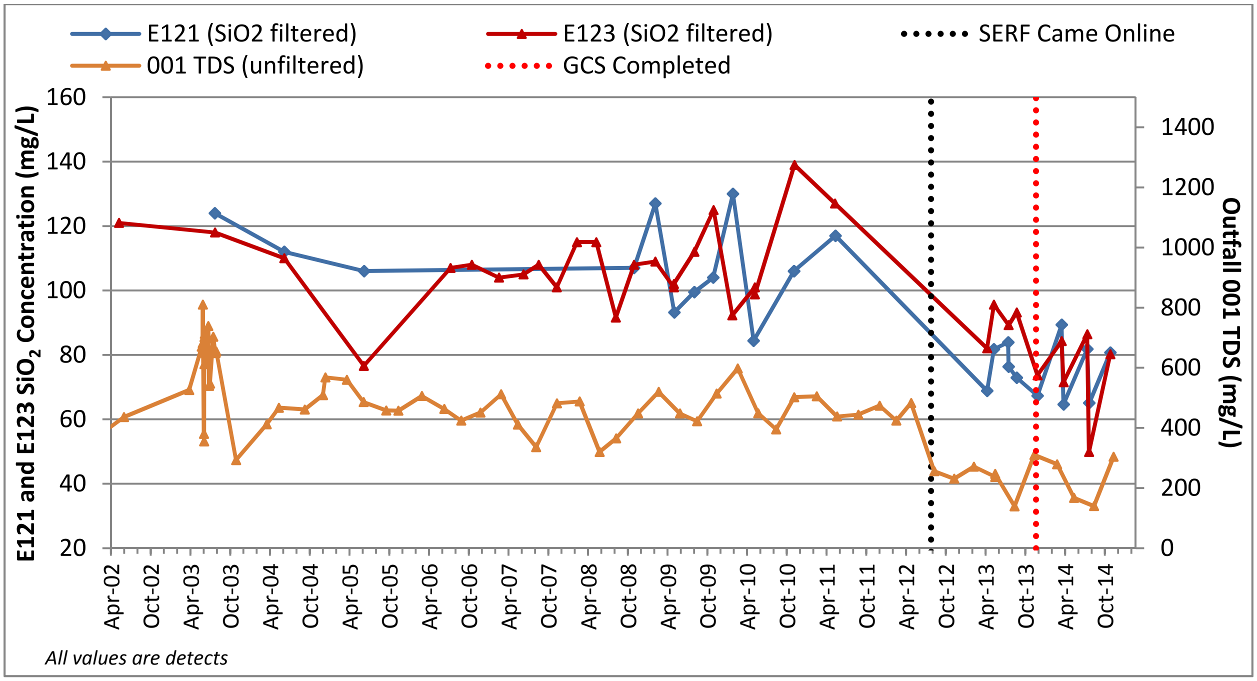

Figure D-1.0-3 Time-series plot showing silicon dioxide concentrations and total dissolved solids (TDS) at gaging stations E121, E123, and NPDES Outfall 001

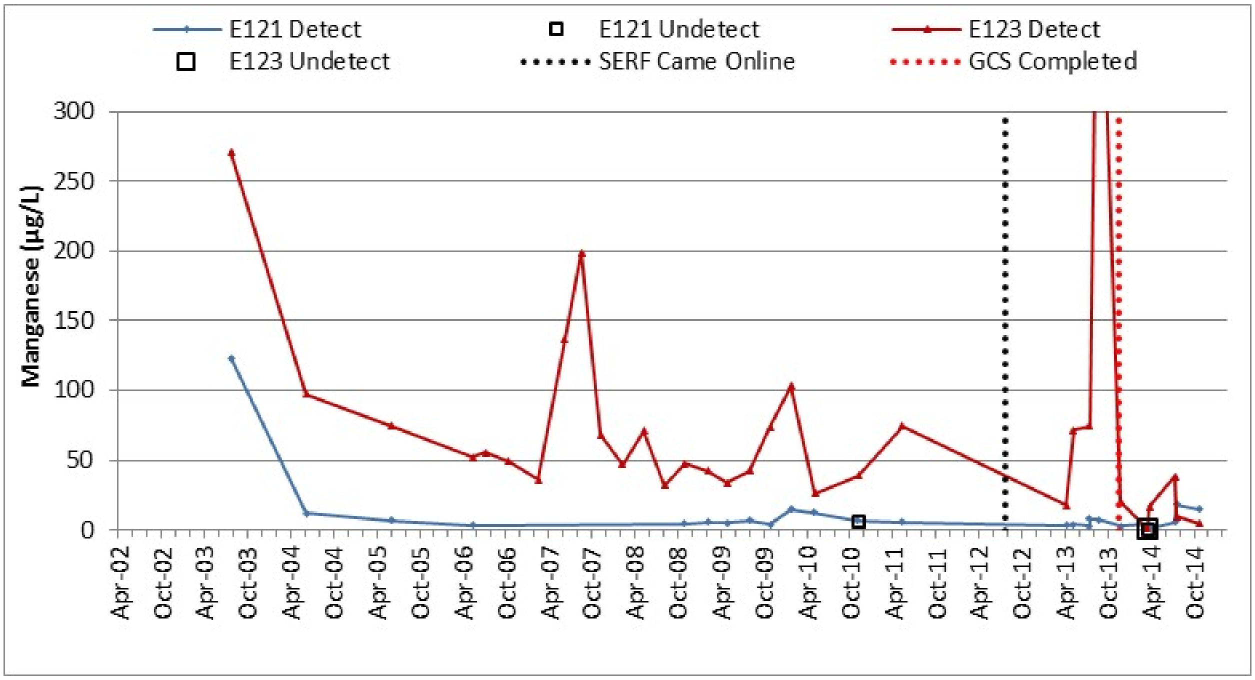

Figure D-1.0-4 Time-series plot showing manganese concentrations (filtered) at gaging stations E121 and E123. The highest concentration of manganese plots off the scale of the chart and was 495.5 µg/L on August 30, 2013.

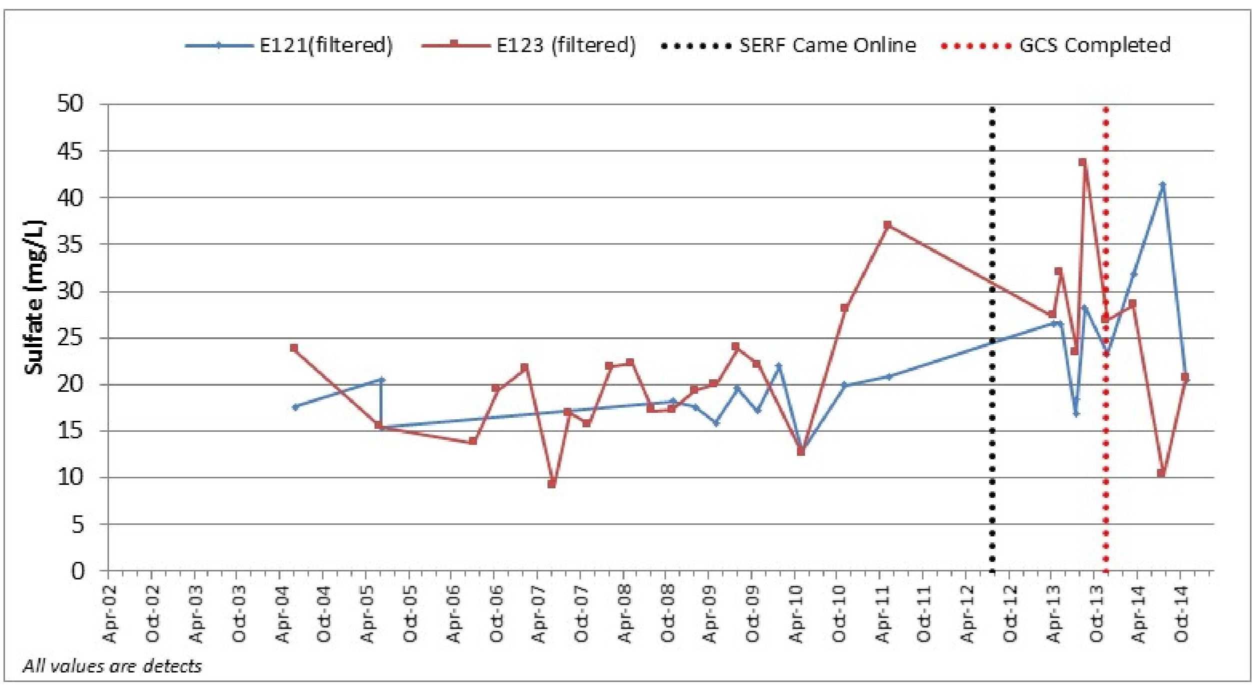

Figure D-1.0-5 Time-series plot showing sulfate concentrations at gaging stations E121 and E123

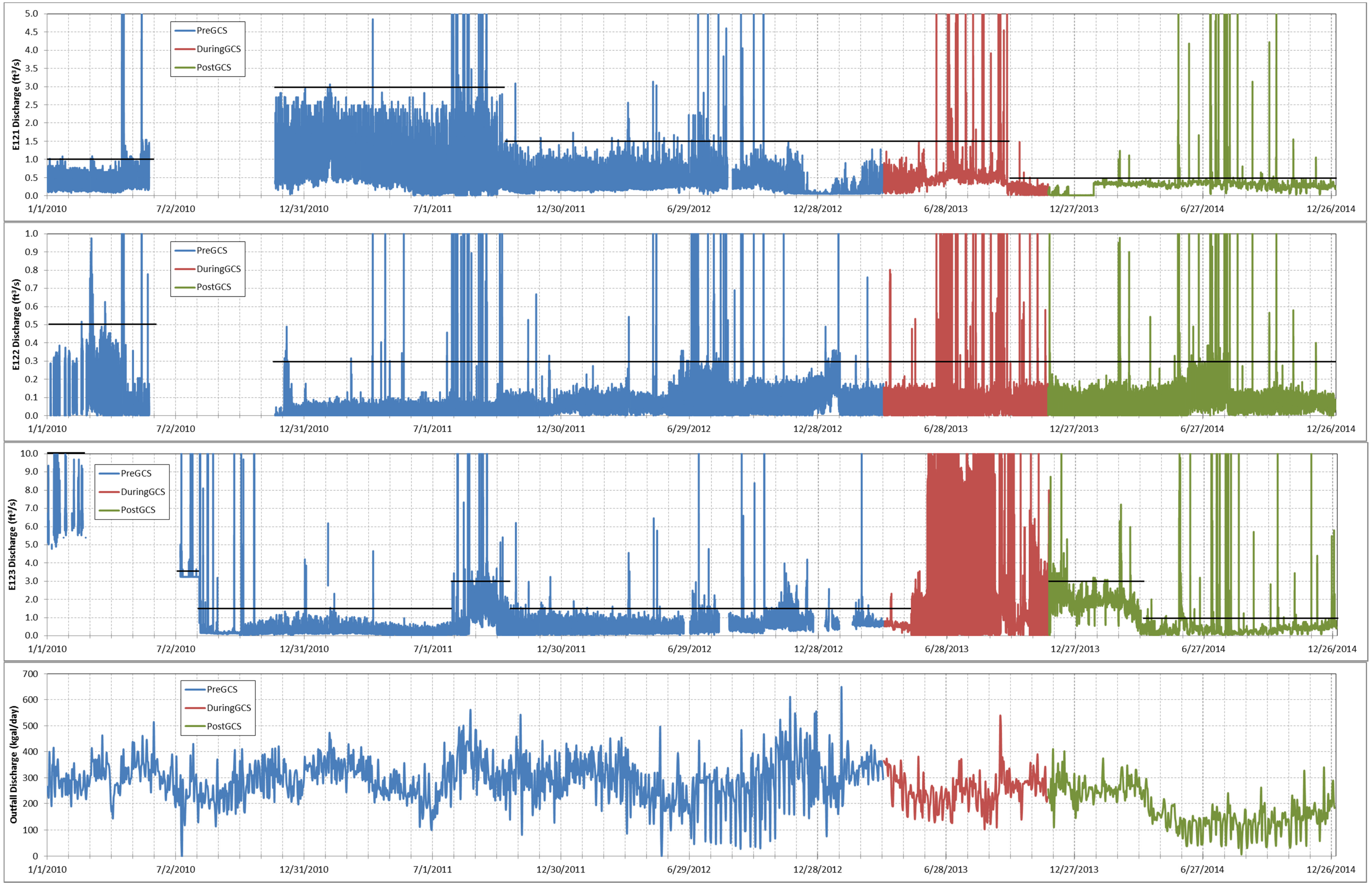

Figure D-1.0-6 Time-series plots from 2010 to 2014 showing discharge at E121, E122, E123, and total discharge from Outfalls 001, 03A027, and 03A199; solid black horizontal lines indicate approximate base flow discharge at the surface water gaging stations, which vary throughout the 5-yr period.

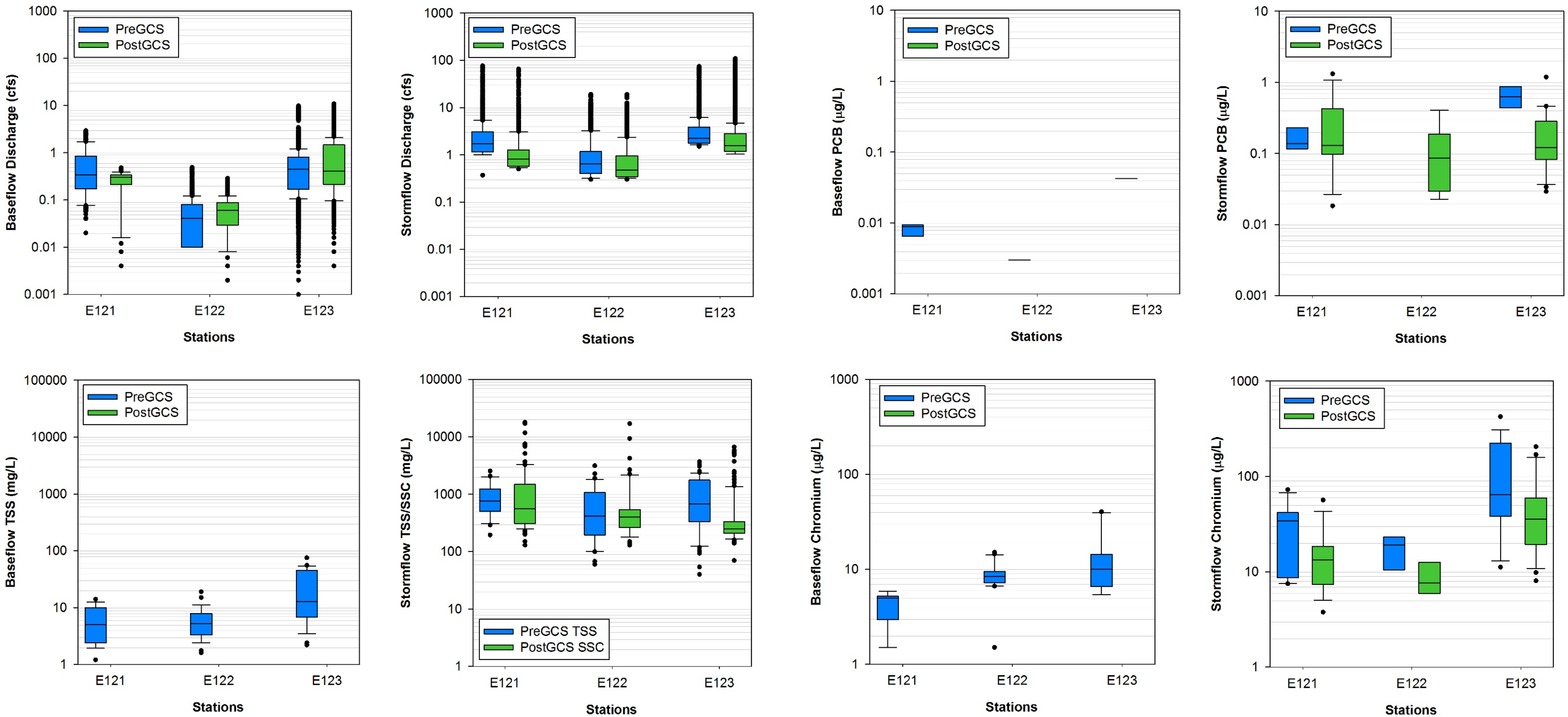

Figure D-1.0-7 Box and whisker plots of discharge, total suspended sediments (TSS)/suspended sediment concentration (SSC), polychlorinated biphenyls (PCBs), and unfiltered chromium for base flow and storm flow at gaging stations E121, E122, and E123, pre- and post-construction of the grade-control structure (pre-GCS and post-GCS, respectively)

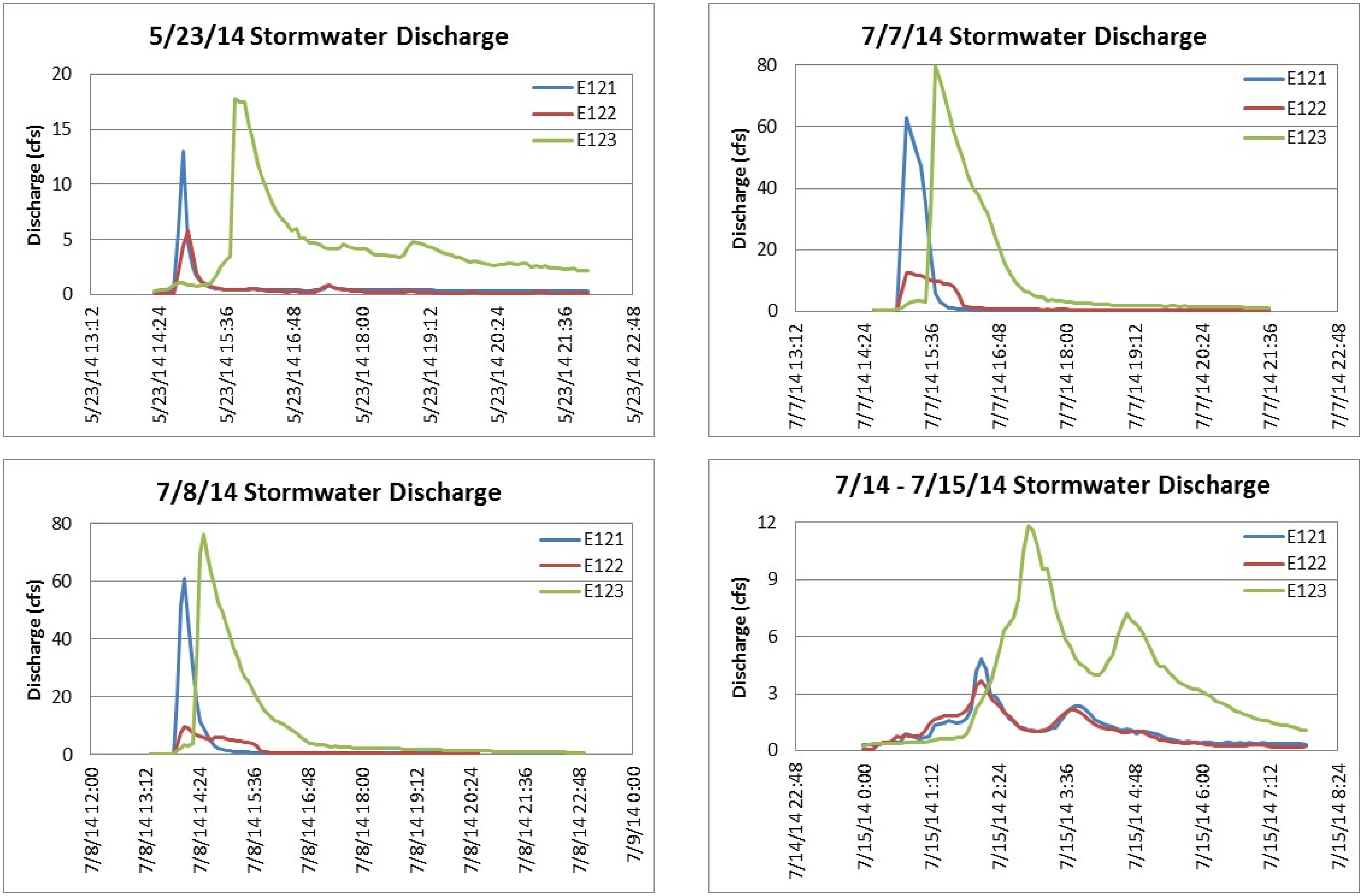

Figure D-1.0-8 Hydrographs of storm water discharge at E121, E122, and E123 during each sample-triggering storm event in 2014

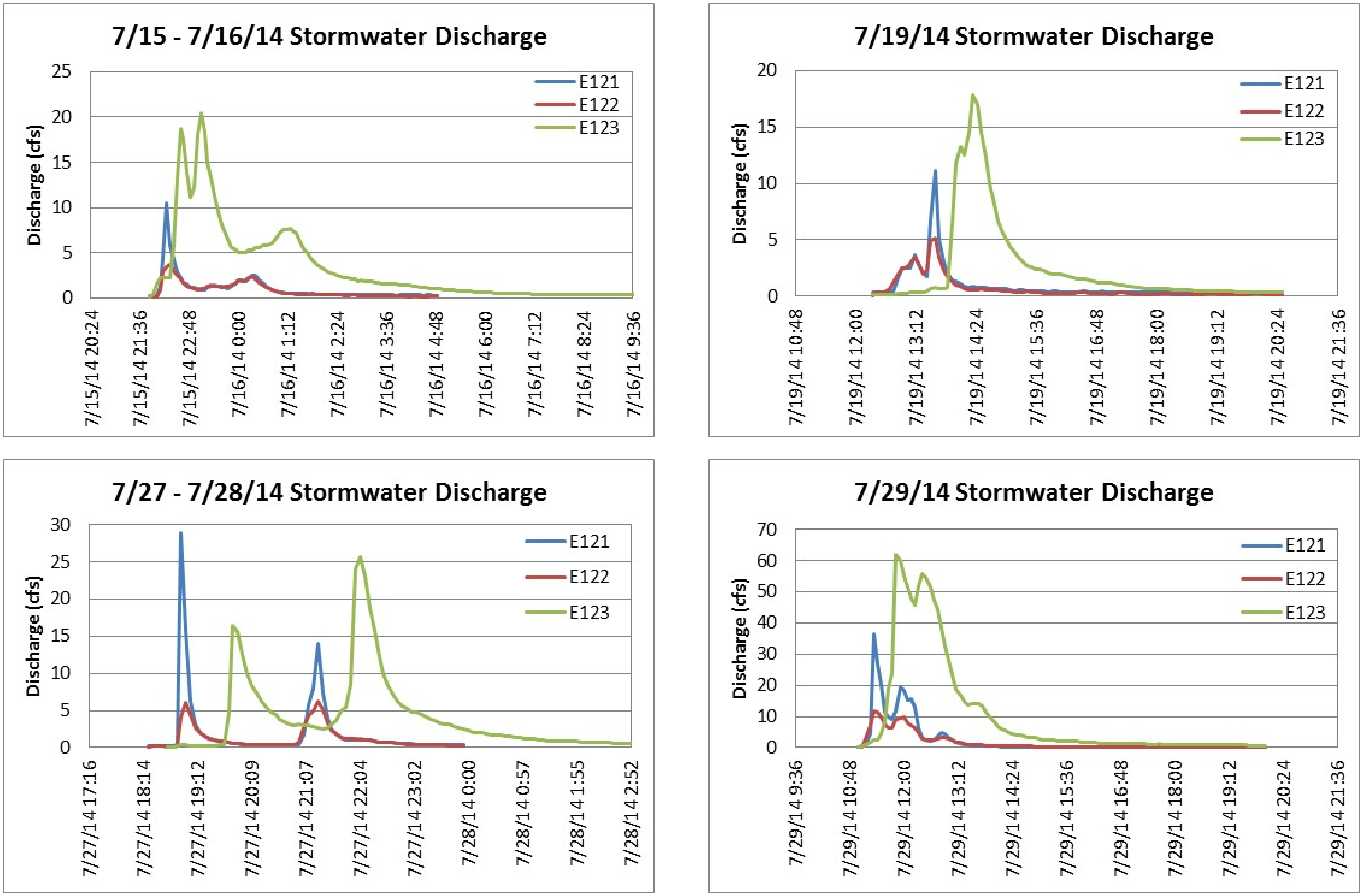

Figure D-1.0-8 (continued) **Hydrographs of storm water discharge at E121, E122, and E123 during each sample-triggering storm event in 2014**

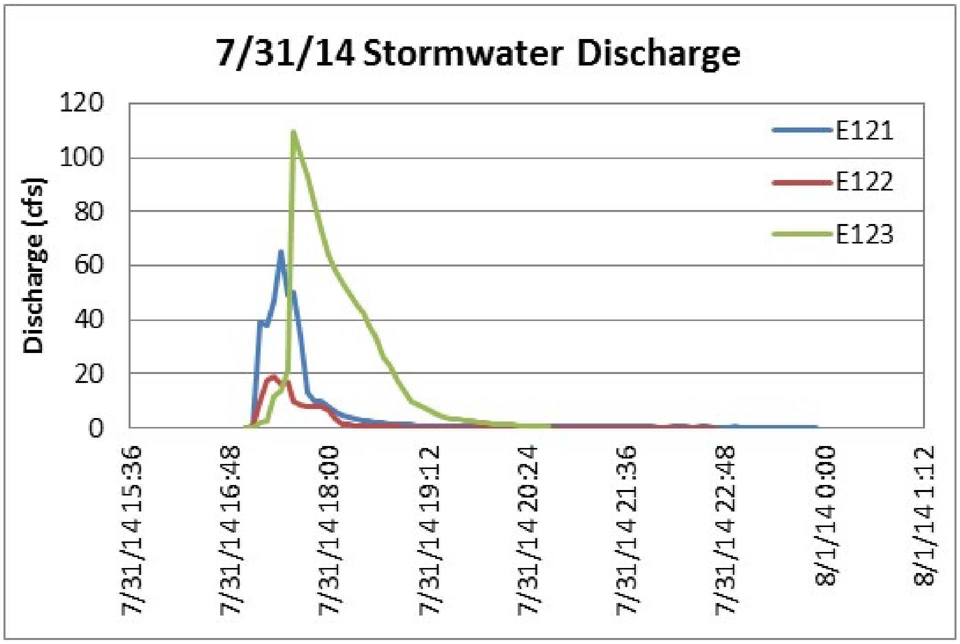

Figure D-1.0-8 (continued) **Hydrographs of storm water discharge at E121, E122, and E123 during each sample-triggering storm event in 2014**

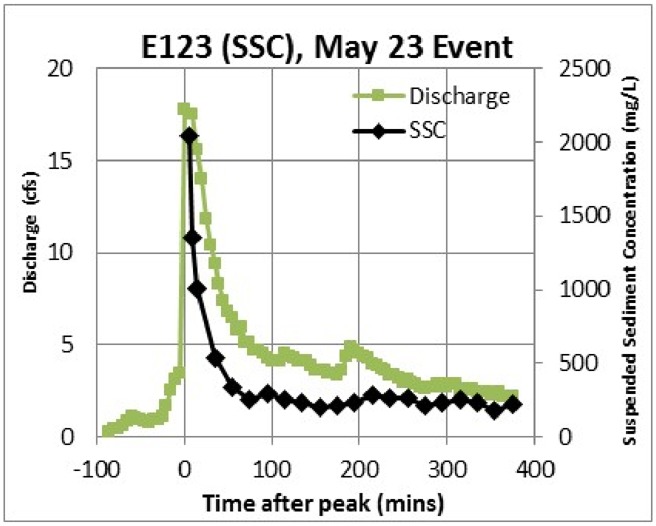

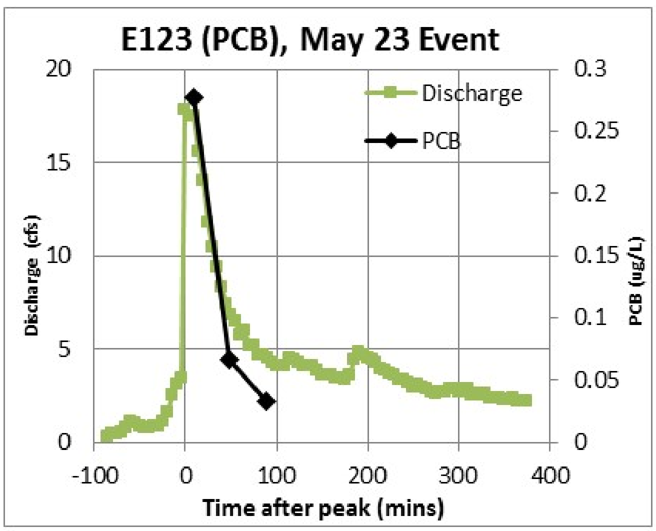

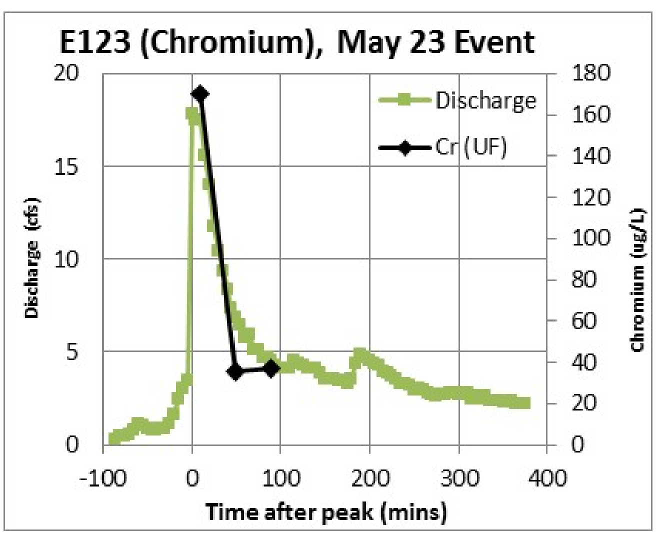

Figure D-1.0-9 Discharge, SSC, PCBs, and chromium (unfiltered) when available at E121, E122, and E123 during each sample-triggering storm event in 2014

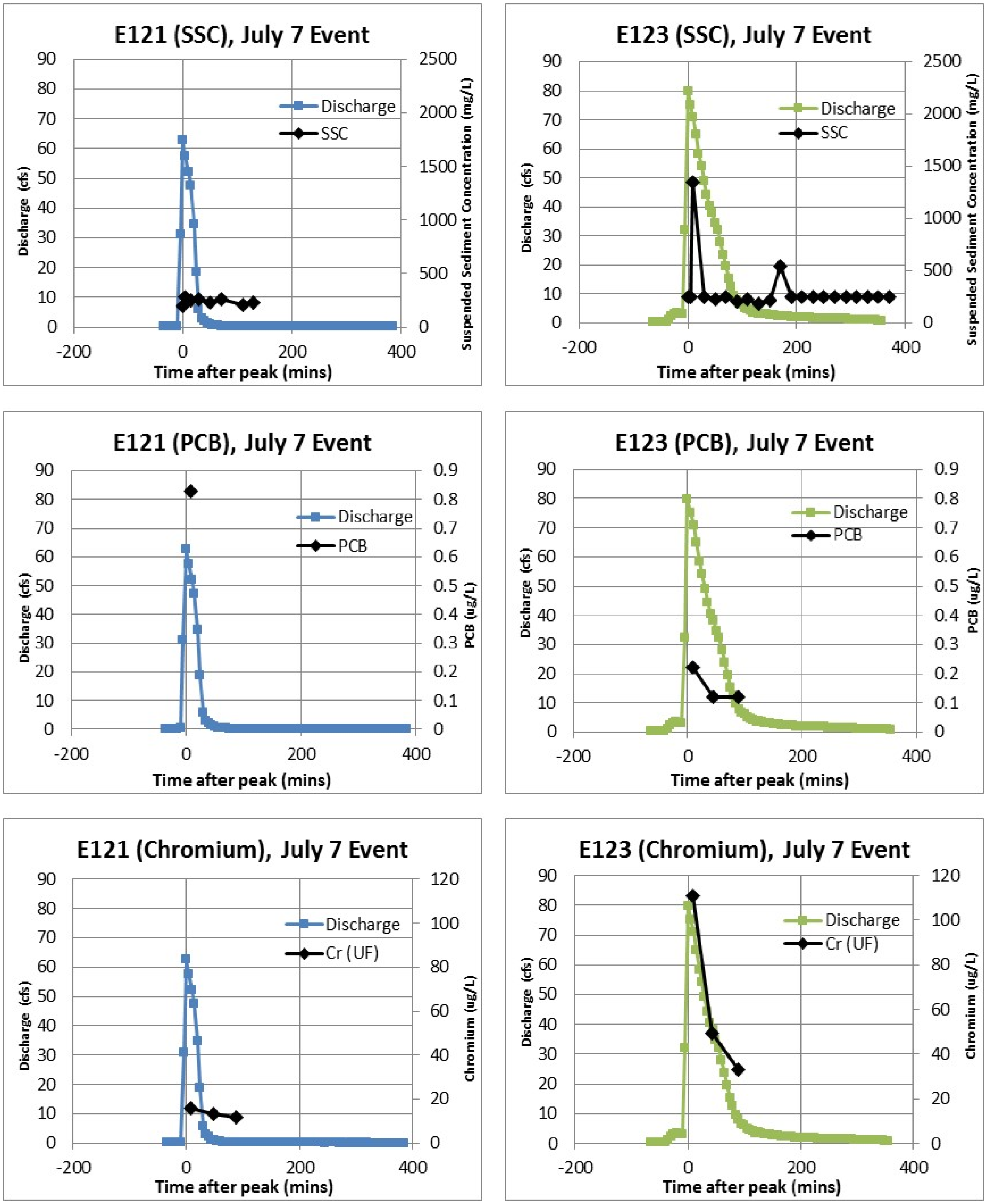

Figure D-1.0-9 (continued) **Discharge, SSC, PCBs, and chromium (unfiltered) when available at E121, E122, and E123 during each sample-triggering storm event in 2014**

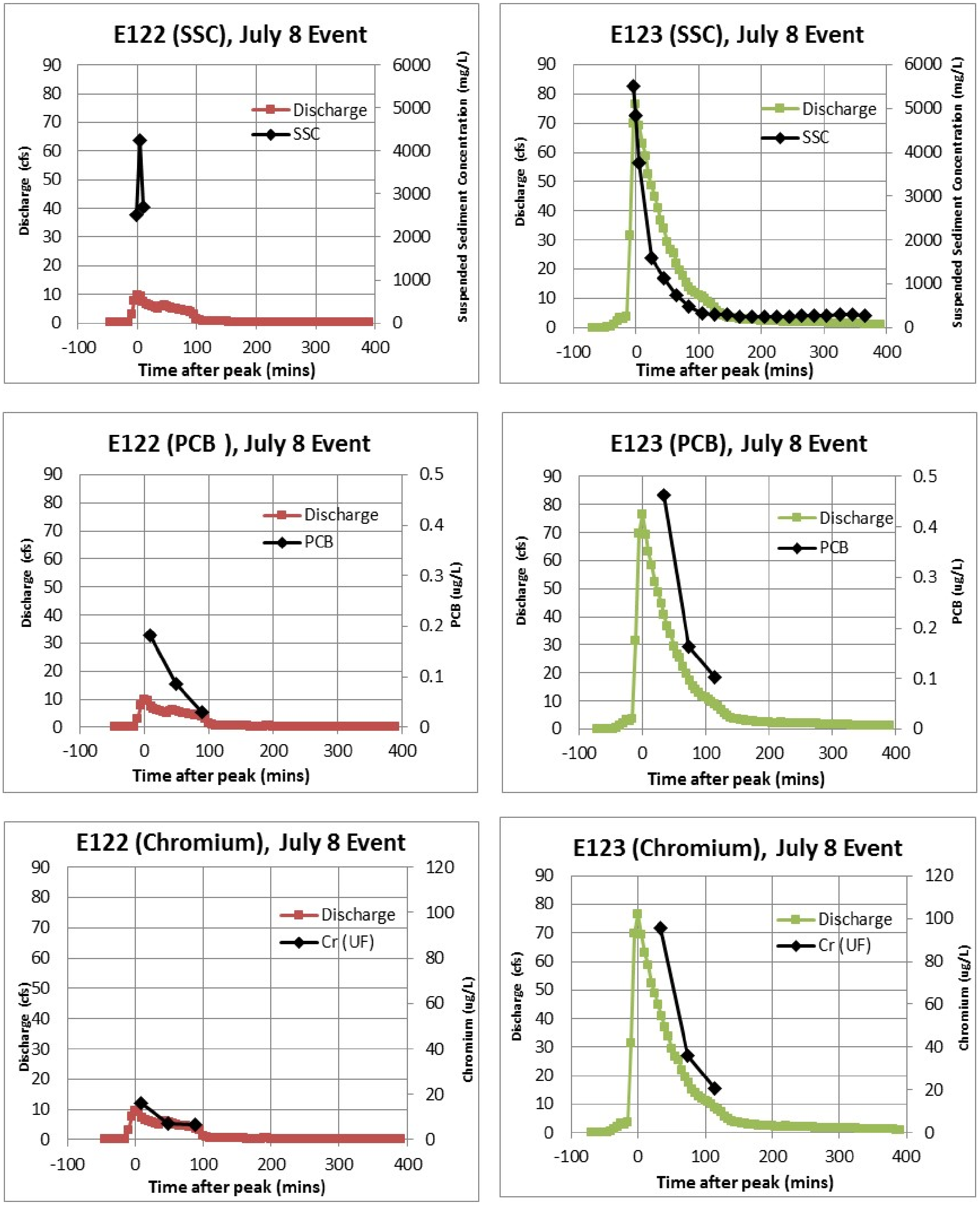

Figure D-1.0-9 (continued) **Discharge, SSC, PCBs, and chromium (unfiltered) when available at E121, E122, and E123 during each sample-triggering storm event in 2014**

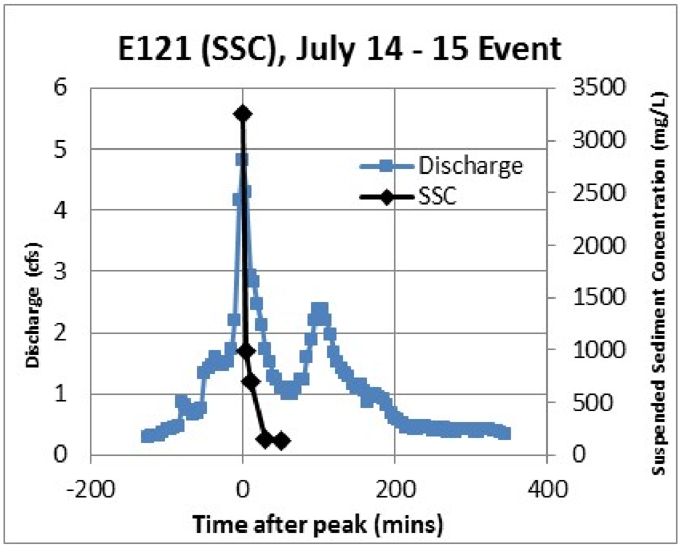

Figure D-1.0-9 (continued) **Discharge, SSC, PCBs, and chromium (unfiltered) when available at E121, E122, and E123 during each sample-triggering storm event in 2014**

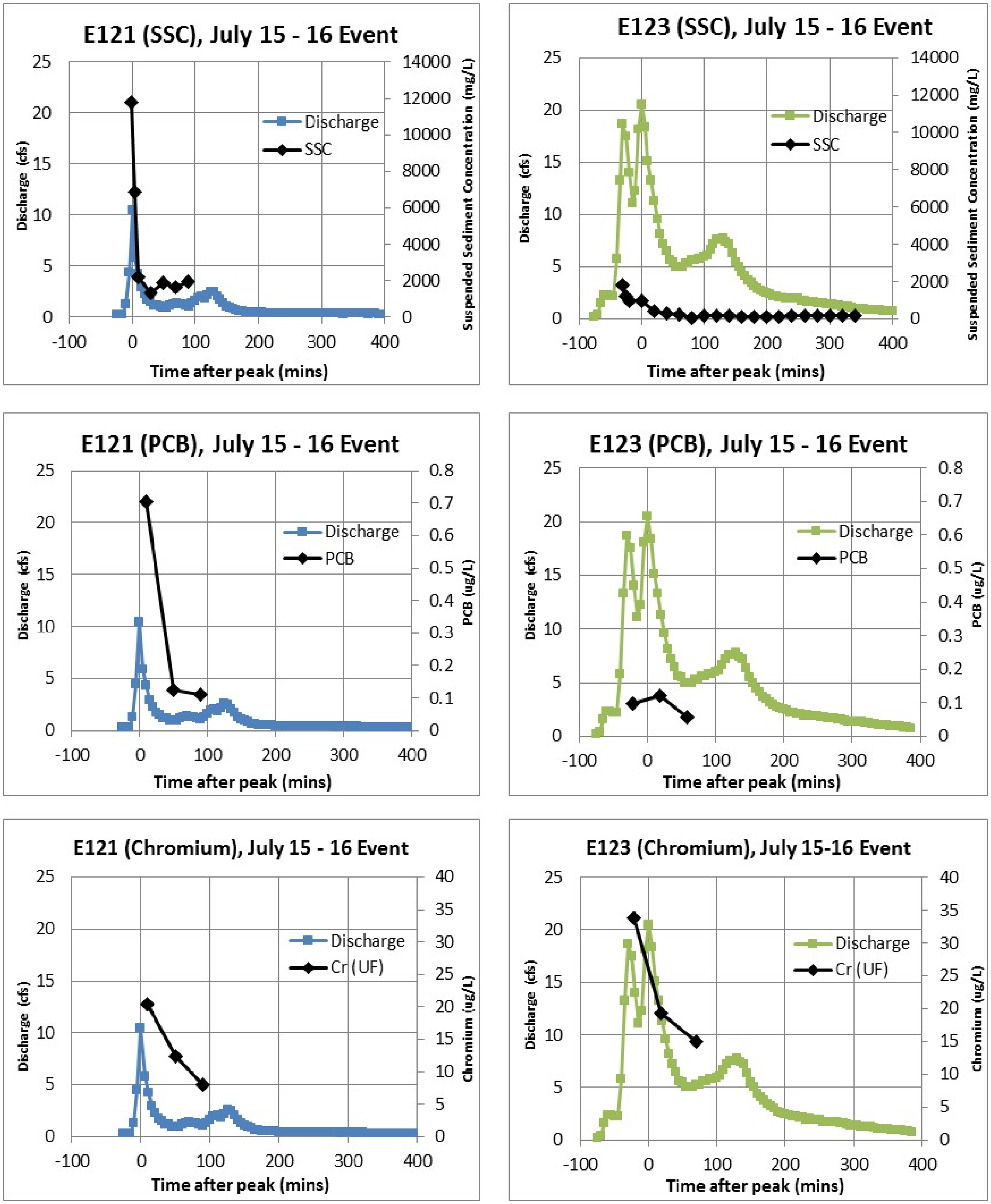

Figure D-1.0-9 (continued) **Discharge, SSC, PCBs, and chromium (unfiltered) when available at E121, E122, and E123 during each sample-triggering storm event in 2014**

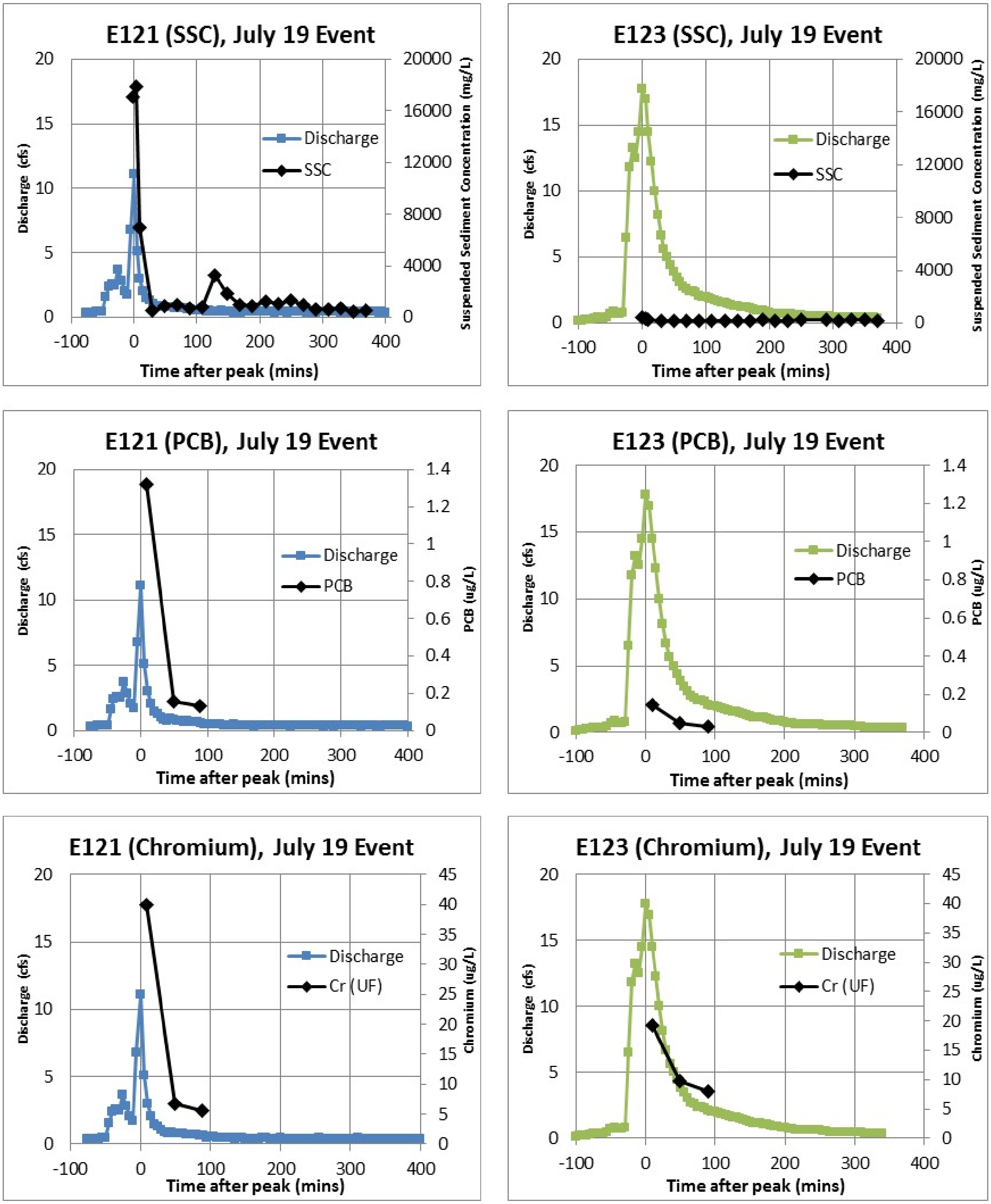

Figure D-1.0-9 (continued) **Discharge, SSC, PCBs, and chromium (unfiltered) when available at E121, E122, and E123 during each sample-triggering storm event in 2014**

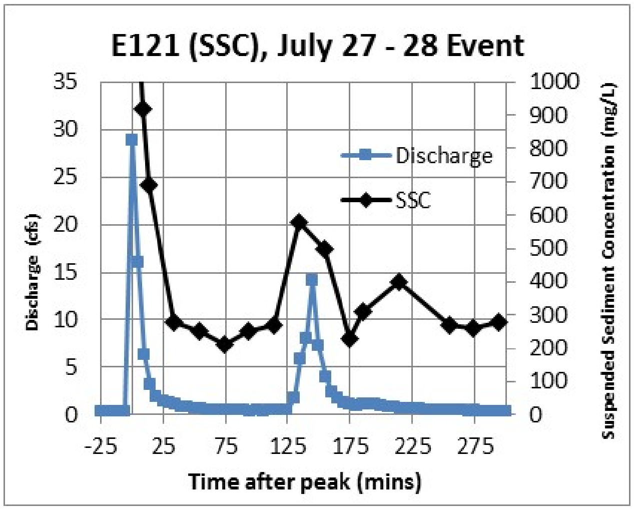

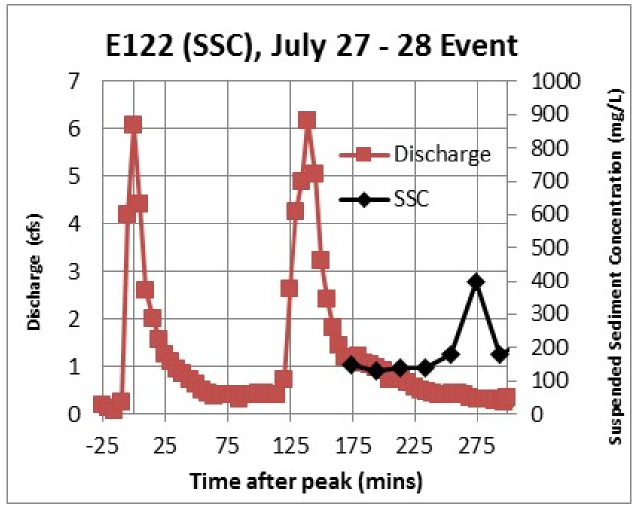

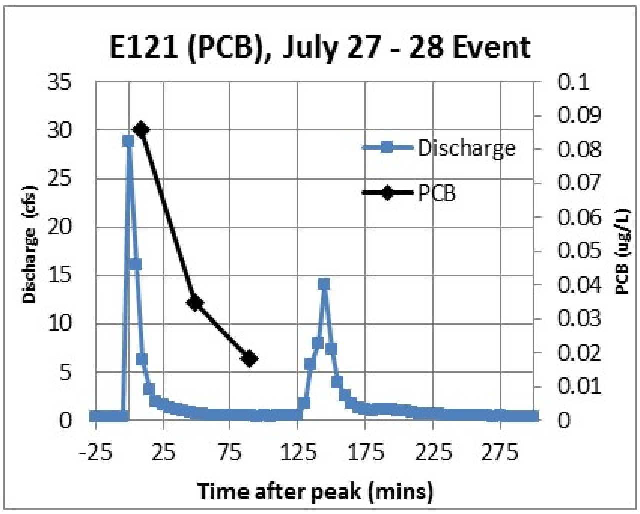

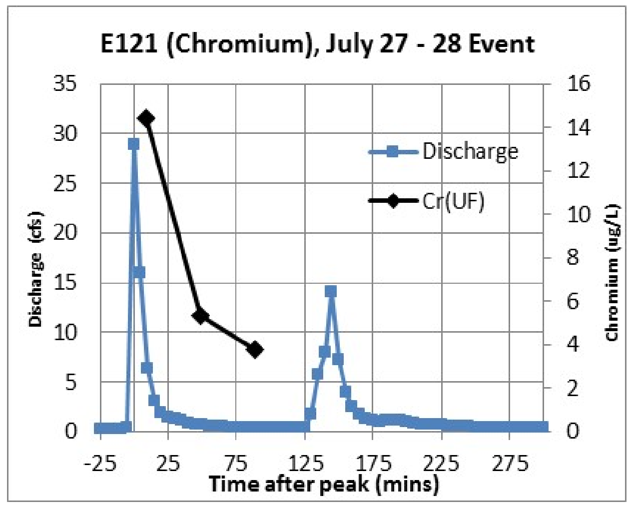

Figure D-1.0-9 (continued) **Discharge, SSC, PCBs, and chromium (unfiltered) when available at E121, E122, and E123 during each sample-triggering storm event in 2014**

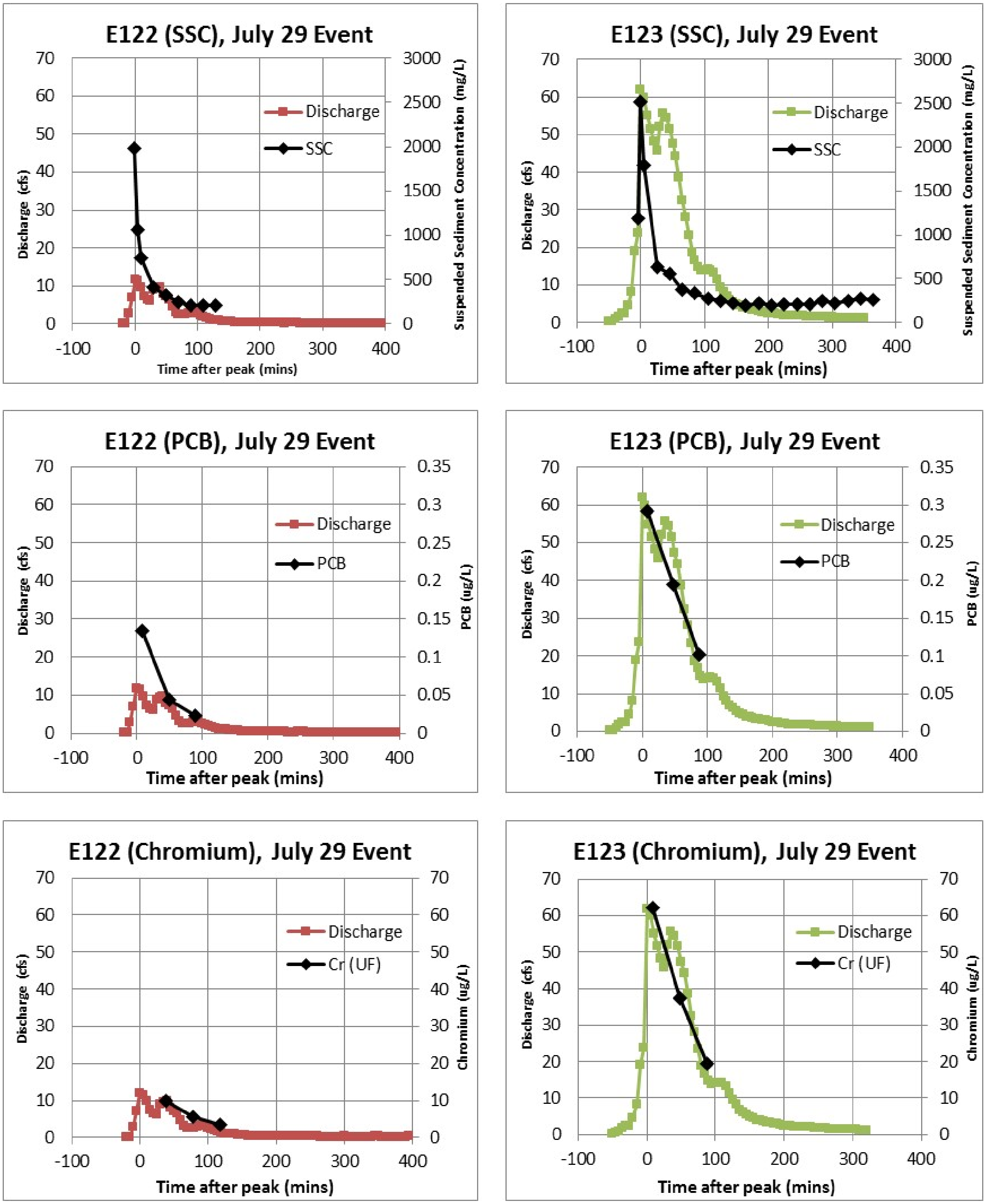

Figure D-1.0-9 (continued) **Discharge, SSC, PCBs, and chromium (unfiltered) when available at E121, E122, and E123 during each sample-triggering storm event in 2014**

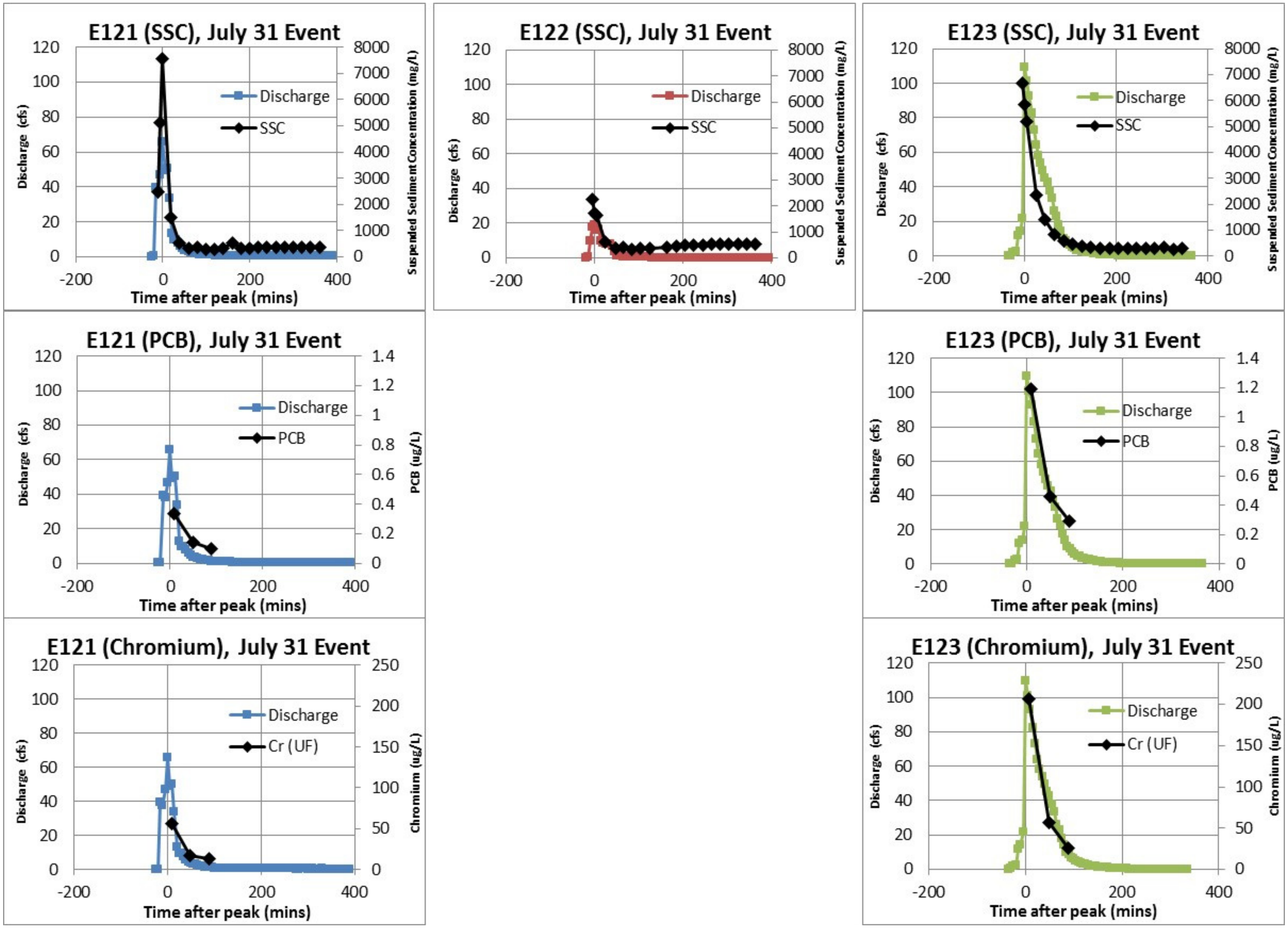

Figure D-1.0-9 (continued) **Discharge, SSC, PCBs, and chromium (unfiltered) when available at E121, E122, and E123 during each sample-triggering storm event in 2014**

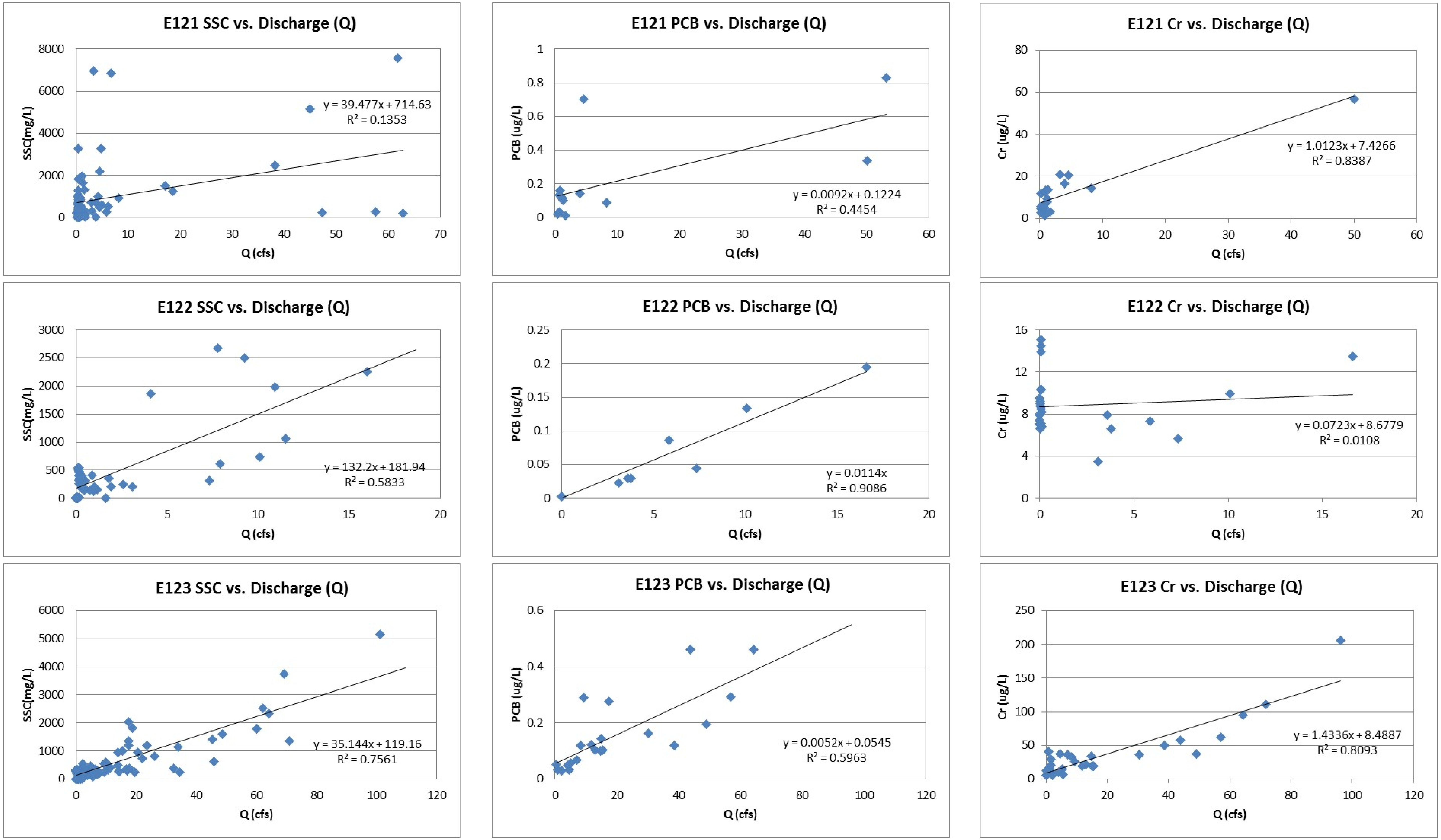

Figure D-1.0-10 Storm and base flow discharge (Q) correlations with SSC, PCBs, and chromium (unfiltered) at E121, E122, and E123 with standardized residual outliers removed; the y-intercept of the PCB-discharge relationship at E122 was set to 0 because a negative y-intercept leads to errors when calculating mass flux.

D-2.0 ALLUVIAL SYSTEM: ANALYTICAL RESULTS

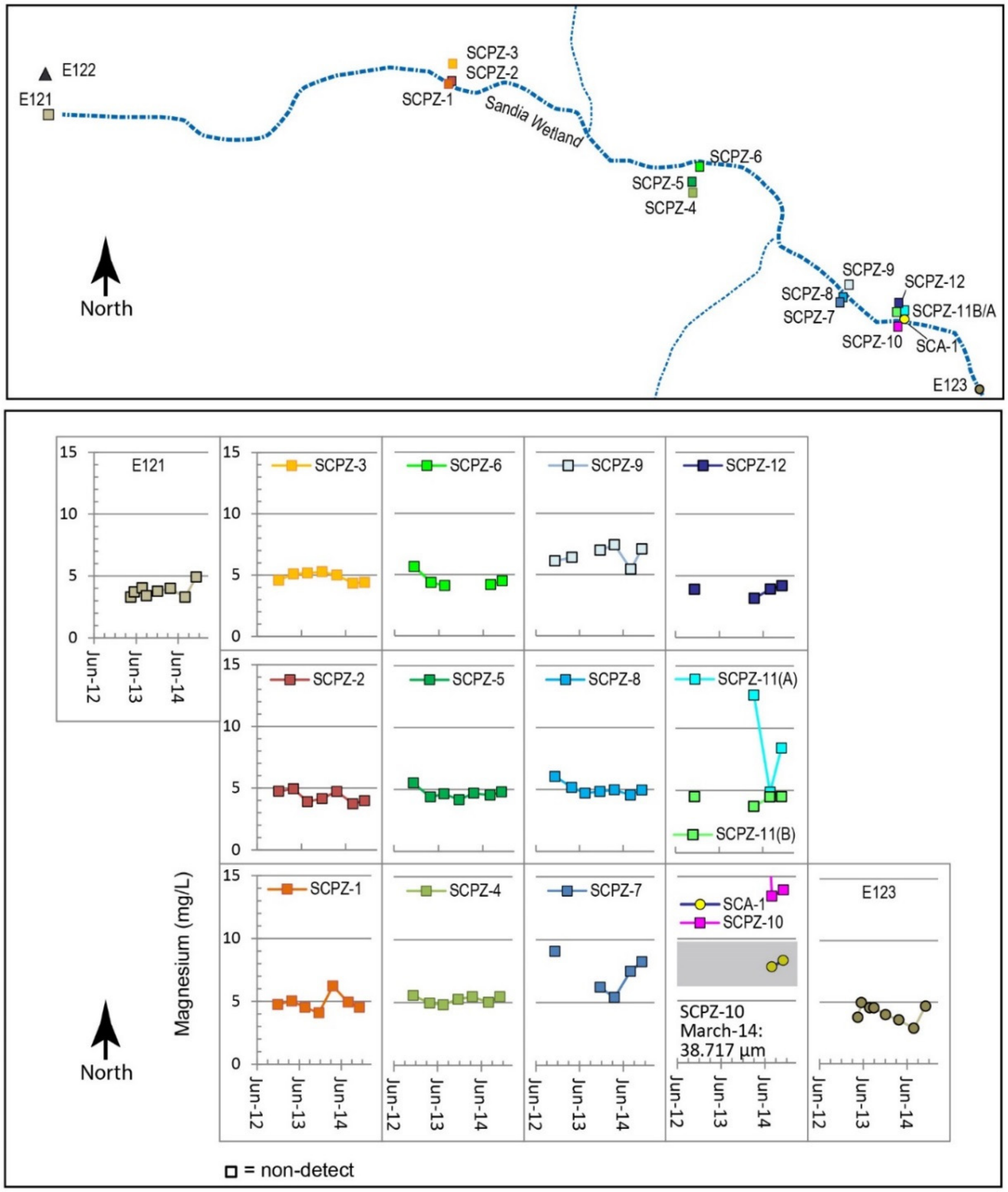

Figure D-2.0-1 **Magnesium concentrations in Sandia wetland surface water and piezometers. Surface water stations include E121, E122, and E123. Piezometers are labeled with the prefix SCPZ and are arranged in four transects from west to east. Alluvial well SCA-1 is located at the east end of the wetland. Data are plotted for the full period of wetland monitoring. The historical data range for SCA-1 is shaded in gray on the plot for SCPZ-10/SCA-1.**

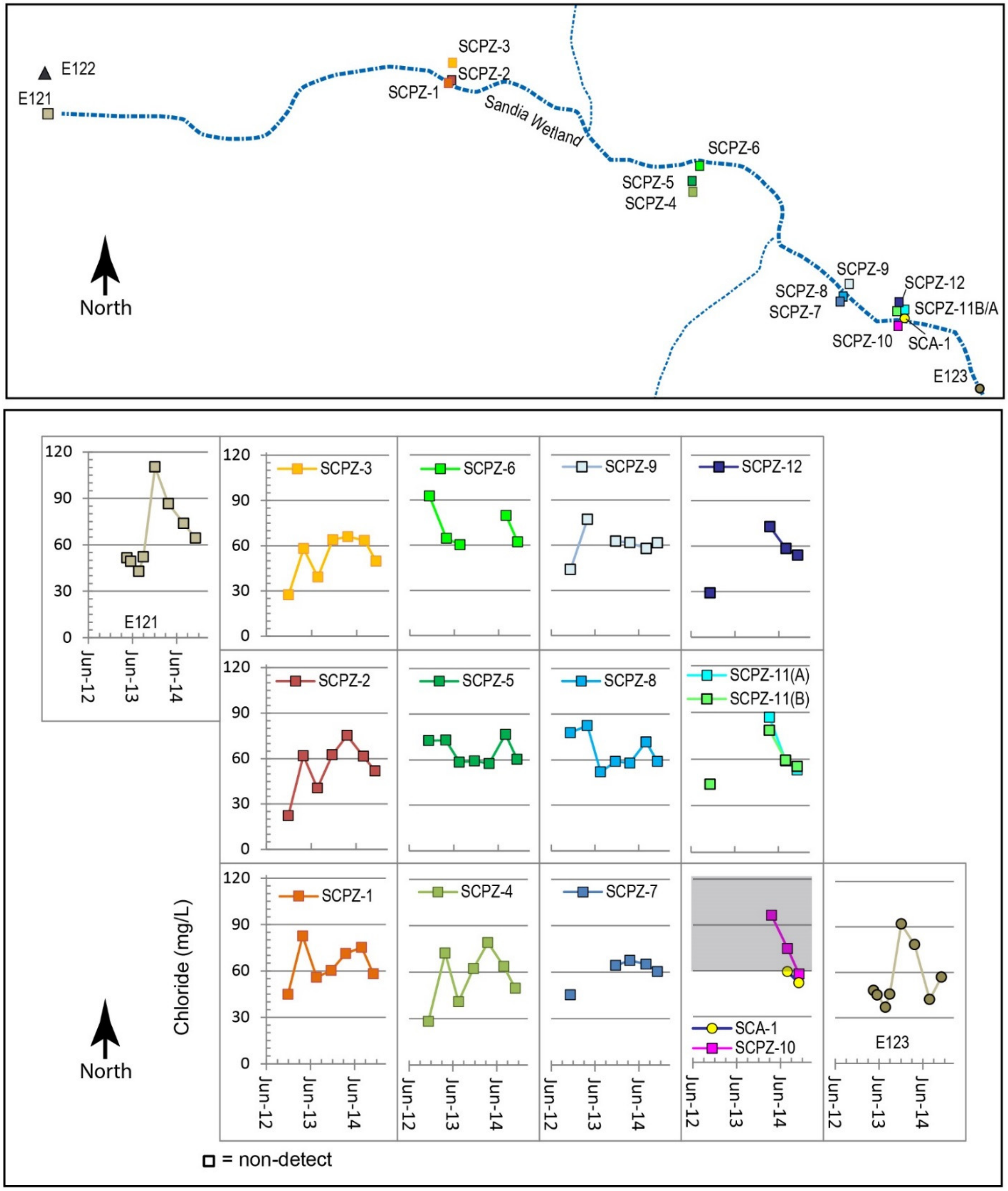

Figure D-2.0-2 **Chloride concentrations in Sandia wetland surface water and piezometers. Surface water stations include E121, E122, and E123. Piezometers are labeled with the prefix SCPZ and are arranged in four transects from west to east. Alluvial well SCA-1 is located at the east end of the wetland. Data are plotted for the full period of wetland monitoring. The historical data range for SCA-1 is shaded in gray on the plot for SCPZ-10/SCA-1.**

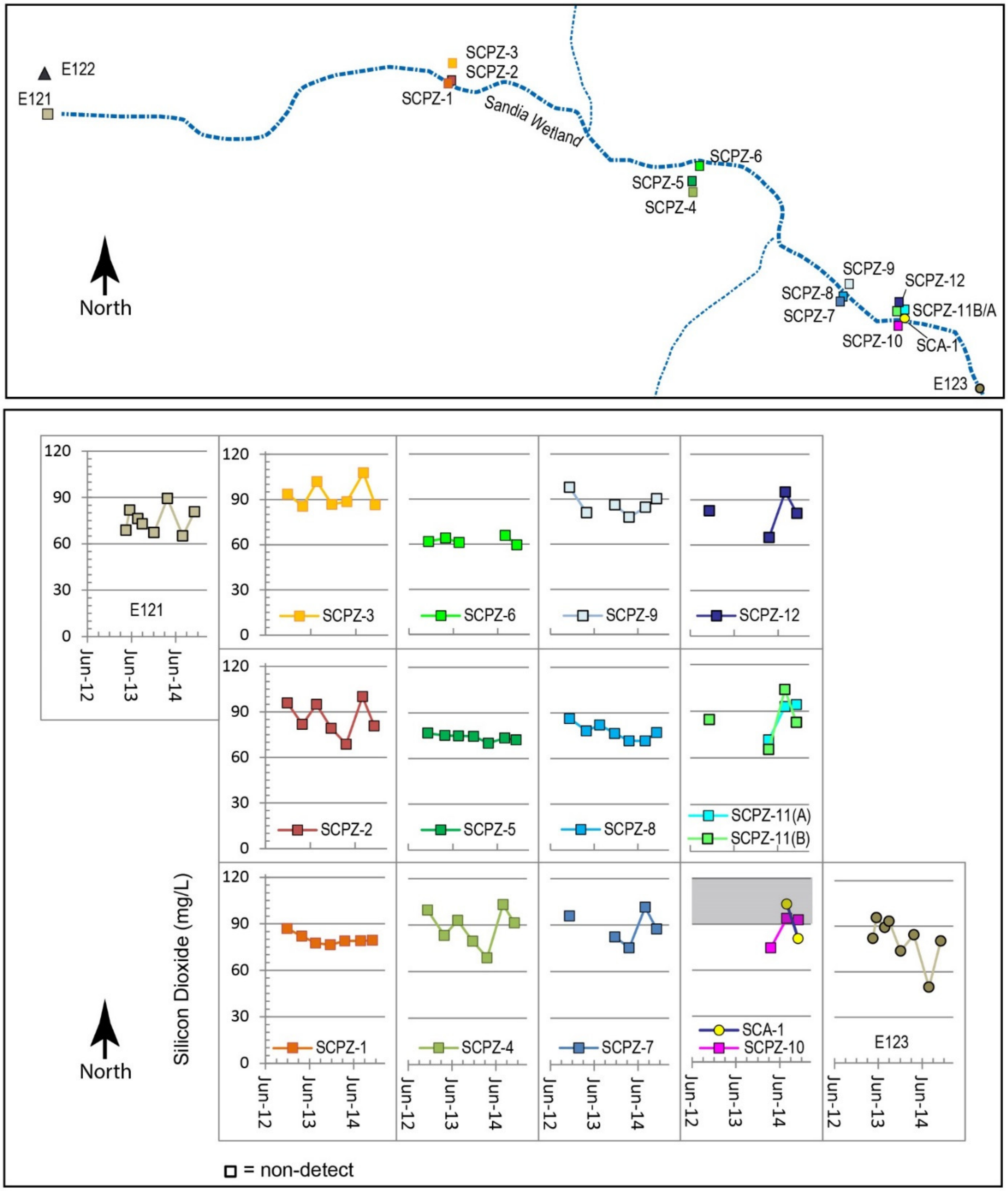

Figure D-2.0-3 Silicon dioxide concentrations in Sandia wetland surface water and piezometers. Surface water stations include E121, E122, and E123. Piezometers are labeled with the prefix SCPZ and are arranged in four transects from west to east. Alluvial well SCA-1 is located at the east end of the wetland. Data are plotted for the full period of wetland monitoring. The historical data range for SCA-1 is shaded in gray on the plot for SCPZ-10/SCA-1.

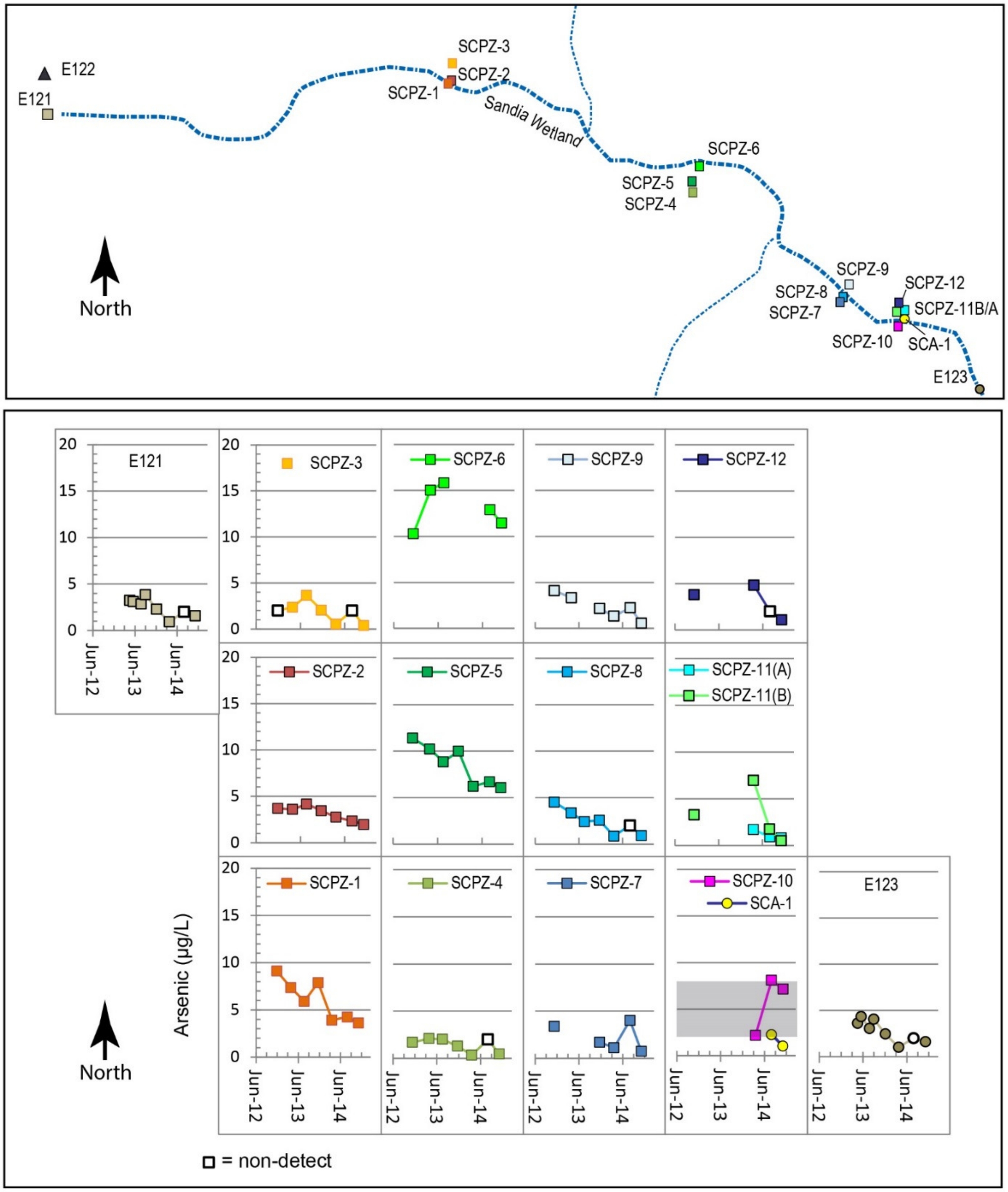

Figure D-2.0-4 Arsenic concentrations in Sandia wetland surface water and piezometers. Surface water stations include E121, E122, and E123. Piezometers are labeled with the prefix SCPZ and are arranged in four transects from west to east. Alluvial well SCA-1 is located at the east end of the wetland. Data are plotted for the full period of wetland monitoring. The historical data range for SCA-1 is shaded in gray on the plot for SCPZ-10/SCA-1.

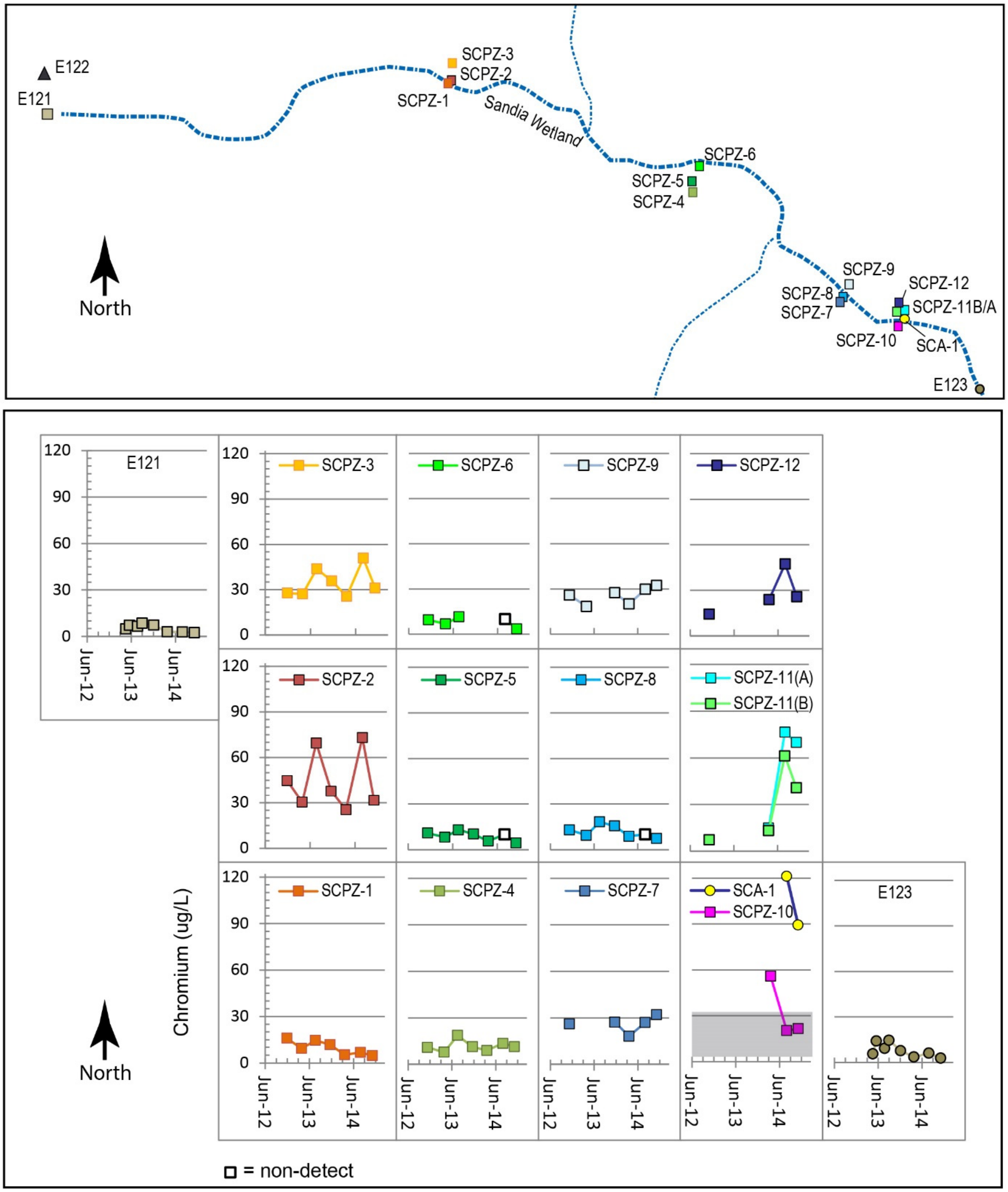

Figure D-2.0-5 Chromium concentrations in Sandia wetland surface water and piezometers. Surface water stations include E121, E122, and E123. Piezometers are labeled with the prefix SCPZ and are arranged in four transects from west to east. Alluvial well SCA-1 is located at the east end of the wetland. Data are plotted for the full period of wetland monitoring. The historical data range for SCA-1 is shaded in gray on the plot for SCPZ-10/SCA-1.

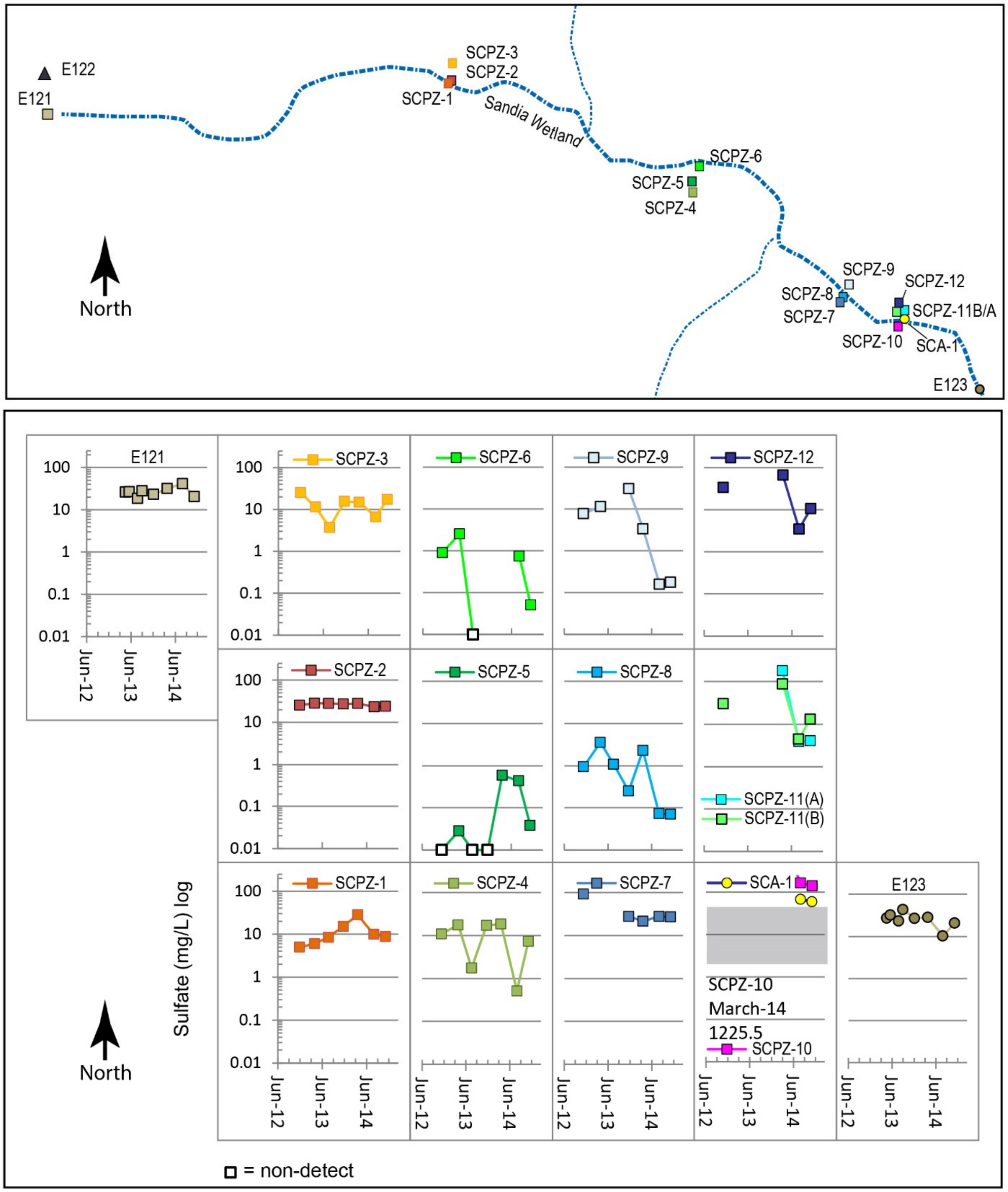

Figure D-2.0-6 Sulfate concentrations in Sandia wetland surface water and piezometers. Surface water stations include E121, E122, and E123. Piezometers are labeled with the prefix SCPZ and are arranged in four transects from west to east. Alluvial well SCA-1 is located at the east end of the wetland. Data are plotted for the full period of wetland monitoring. The historical data range for SCA-1 is shaded in gray on the plot for SCPZ-10/SCA-1.

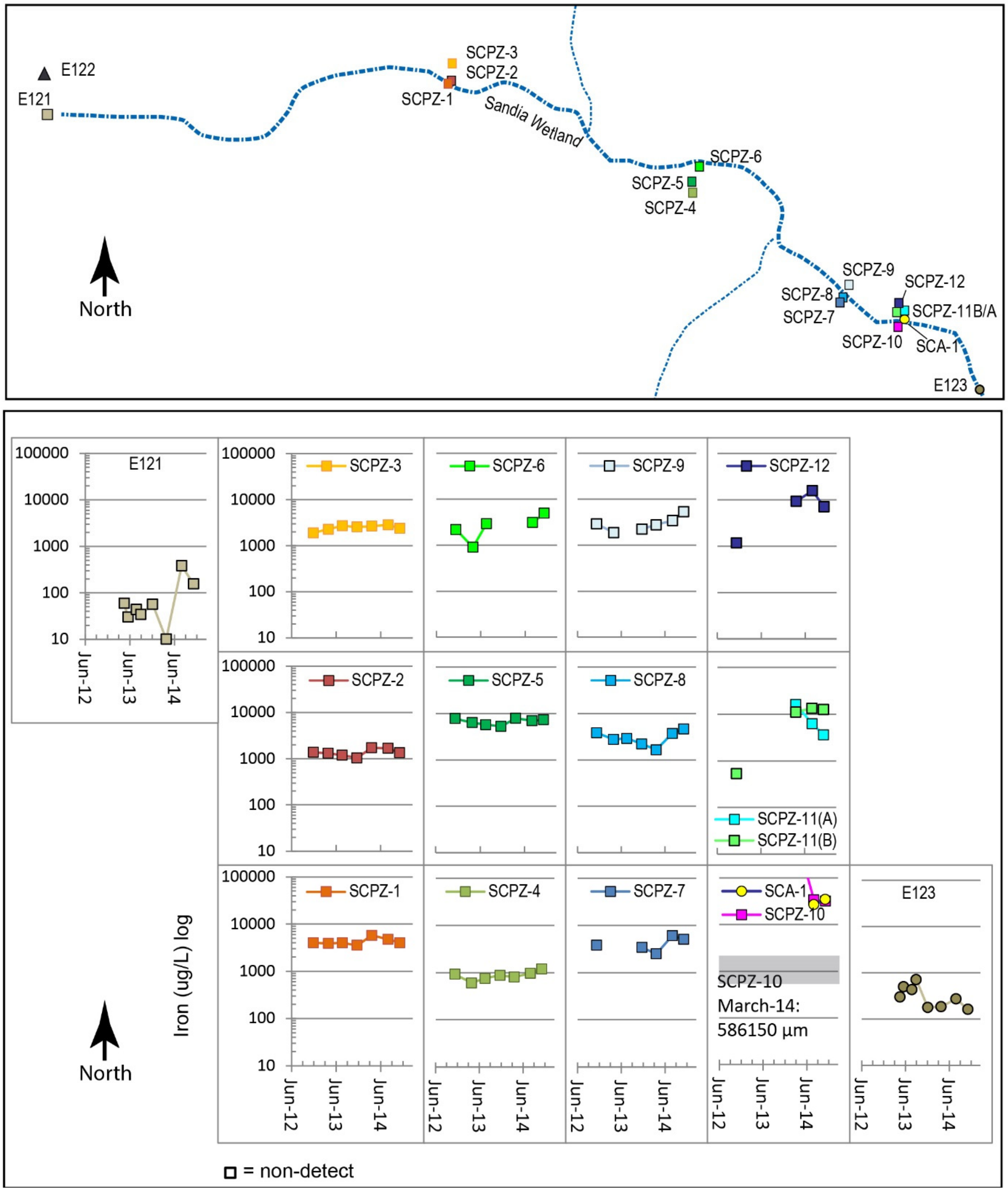

Figure D-2.0-7 Iron concentrations in Sandia wetland surface water and piezometers. Surface water stations include E121, E122, and E123. Piezometers are labeled with the prefix SCPZ and are arranged in four transects from west to east. Alluvial well SCA-1 is located at the east end of the wetland. Data are plotted for the full period of wetland monitoring. The historical data range for SCA-1 is shaded in gray on the plot for SCPZ-10/SCA-1.

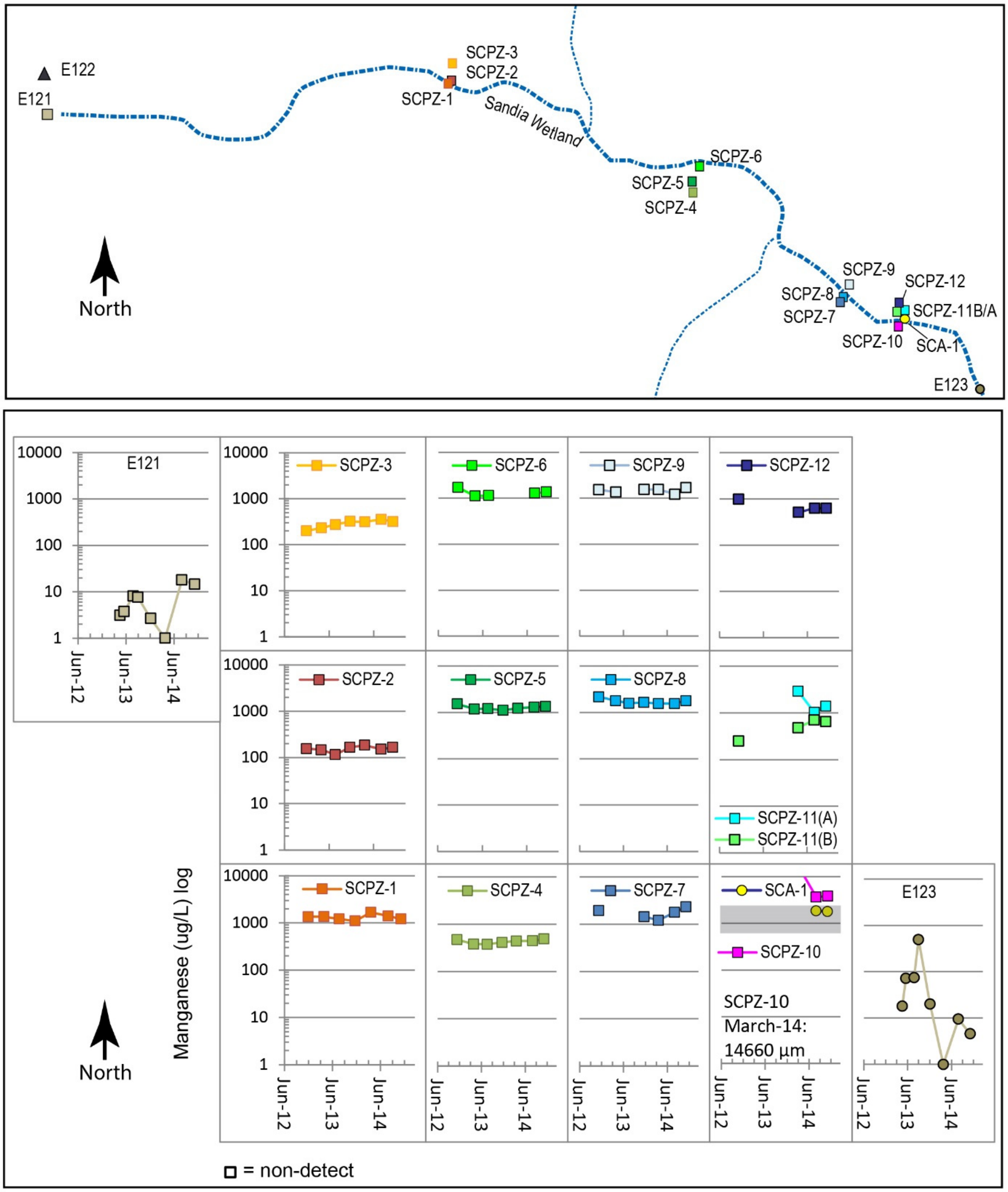

Figure D-2.0-8 **Manganese concentrations in Sandia wetland surface water and piezometers. Surface water stations include E121, E122, and E123. Piezometers are labeled with the prefix SCPZ and are arranged in four transects from west to east. Alluvial well SCA-1 is located at the east end of the wetland. Data are plotted for the full period of wetland monitoring. The historical data range for SCA-1 is shaded in gray on the plot for SCPZ-10/SCA-1.**

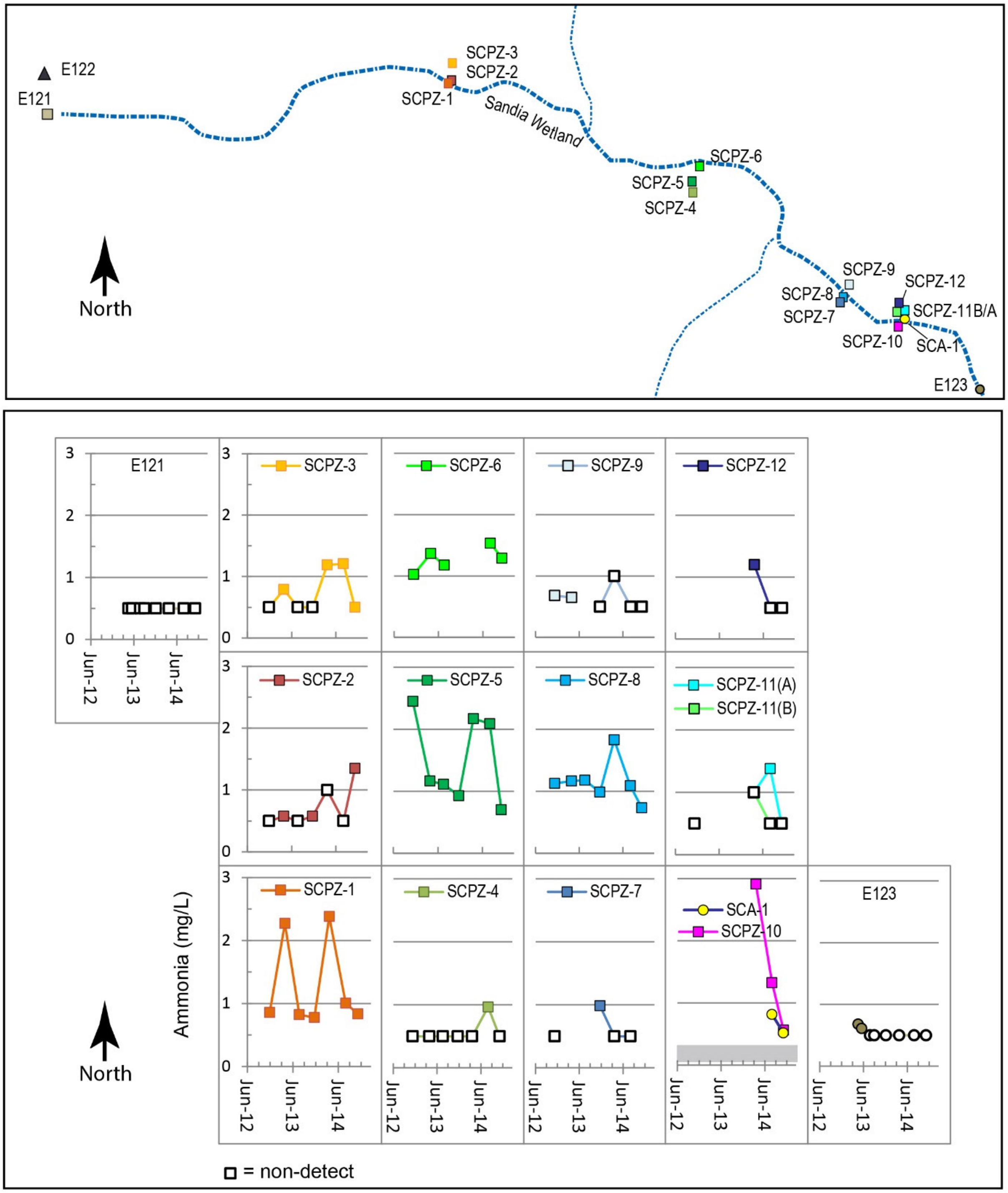

Figure D-2.0-9 Ammonium concentrations in Sandia wetland surface water and piezometers. Surface water stations include E121, E122, and E123. Piezometers are labeled with the prefix SCPZ and are arranged in four transects from west to east. Alluvial well SCA-1 is located at the east end of the wetland. Data are plotted for the full period of wetland monitoring. The historical data range for SCA-1 is shaded in gray on the plot for SCPZ-10/SCA-1.

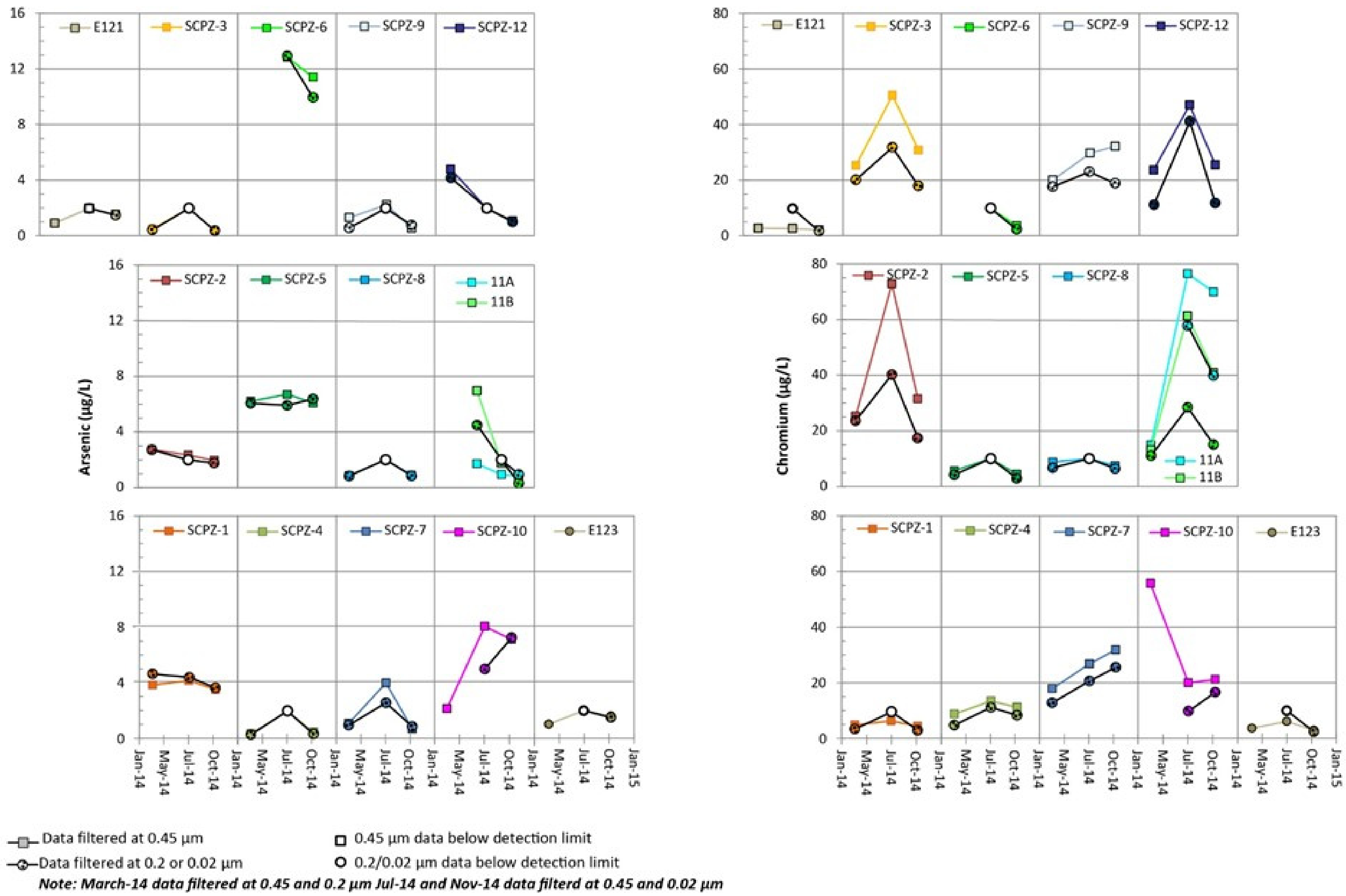

Figure D-2.0-10 Comparison of filtered versus microfiltered concentrations of arsenic and chromium at piezometer (SCPZ locations) and gaging stations (E121, E123) for March, July, and November 2014 sampling events. Where microfiltered samples are not shown, they were not collected.

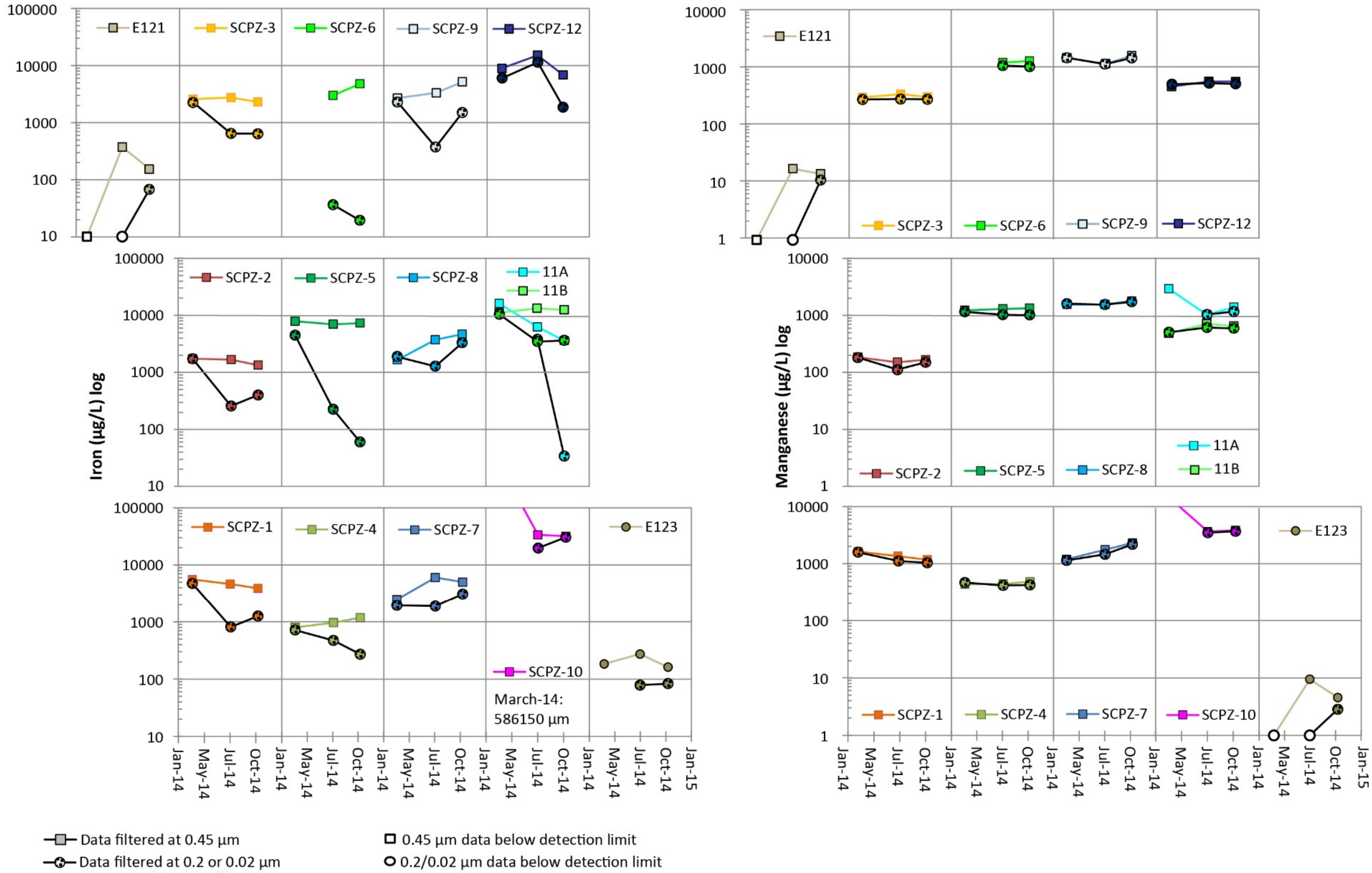

Note: March-14 data filtered at 0.45 and 0.2 µm Jul-14 and Nov-14 data filterd at 0.45 and 0.02 µm

Figure D-2.0-11 Comparison of filtered versus microfiltered concentrations of iron and manganese at piezometer (SCPZ locations) and gaging stations (E121, E123) for March, July, and November 2014 sampling events. Samples collected in March at SCPZ-10 were filtered at 0.45 µm only and were 586,150 µg/L for iron and 14,660 µg/L for manganese.

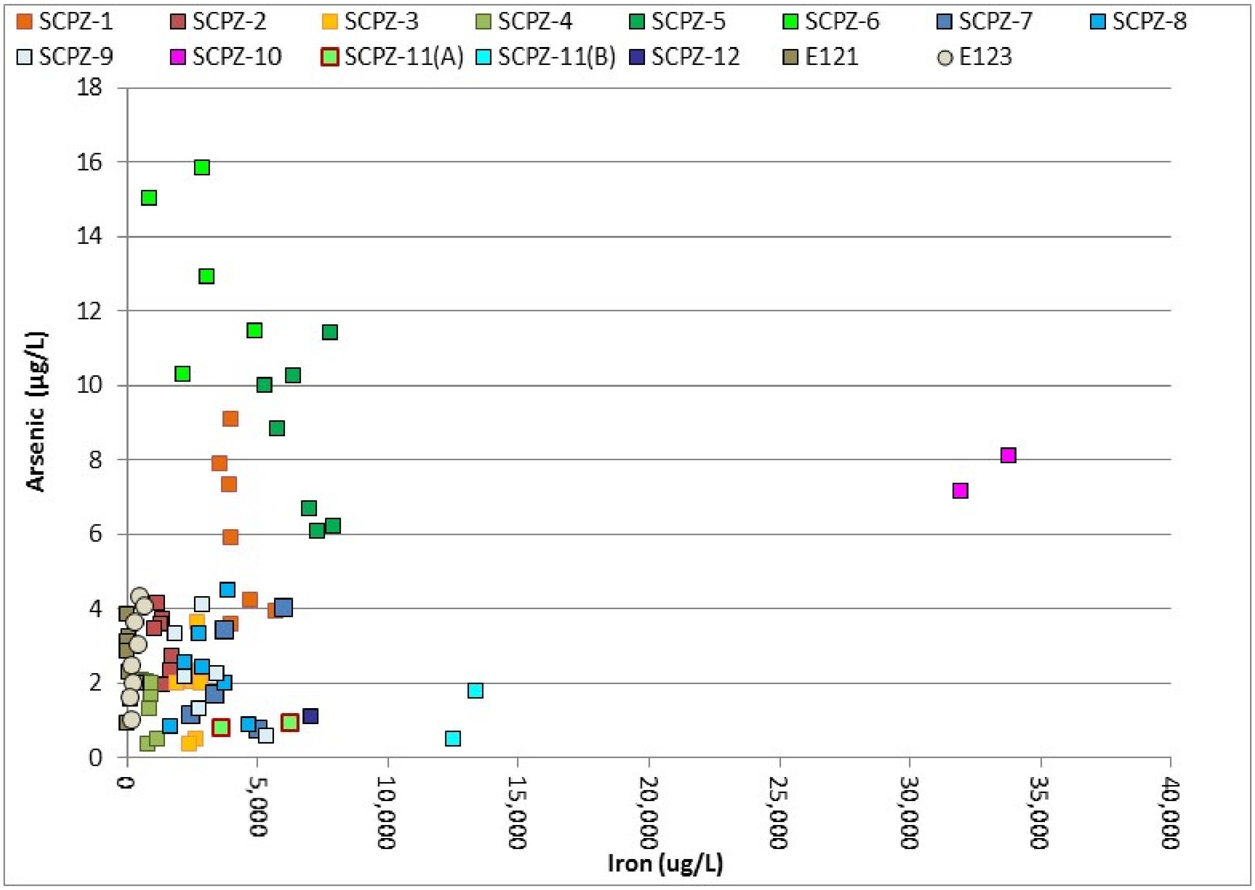

Figure D-2.0-12 Cross-plot of arsenic versus iron for piezometers and surface water gages E121 and E123

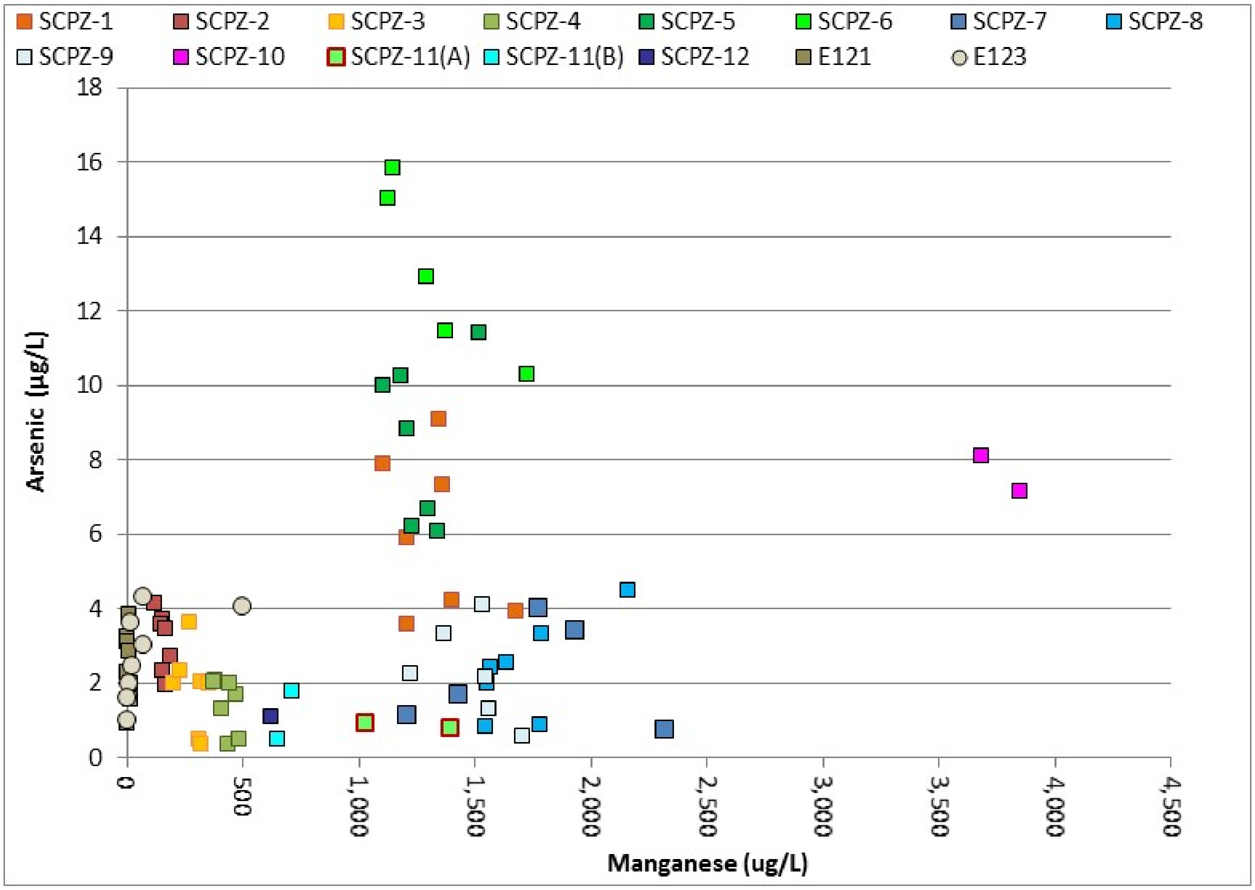

Figure D-2.0-13 Cross-plot of arsenic versus manganese for piezometers and surface water gages E121 and E123

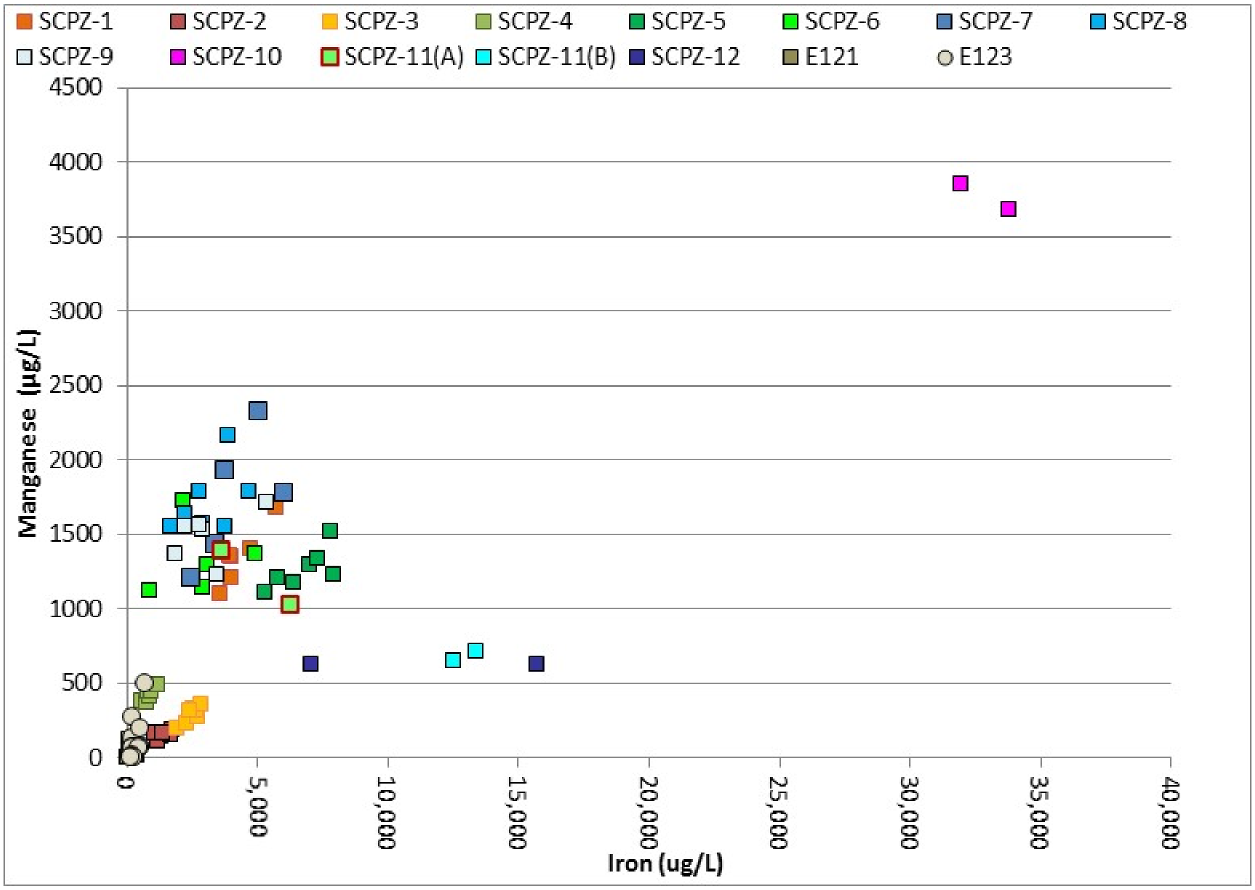

Figure D-2.0-14 Cross-plot of manganese versus iron for piezometers and surface water gages E121 and E123

D-3.0 ALLUVIAL SYSTEM: PHYSICAL FIELD PARAMETERS

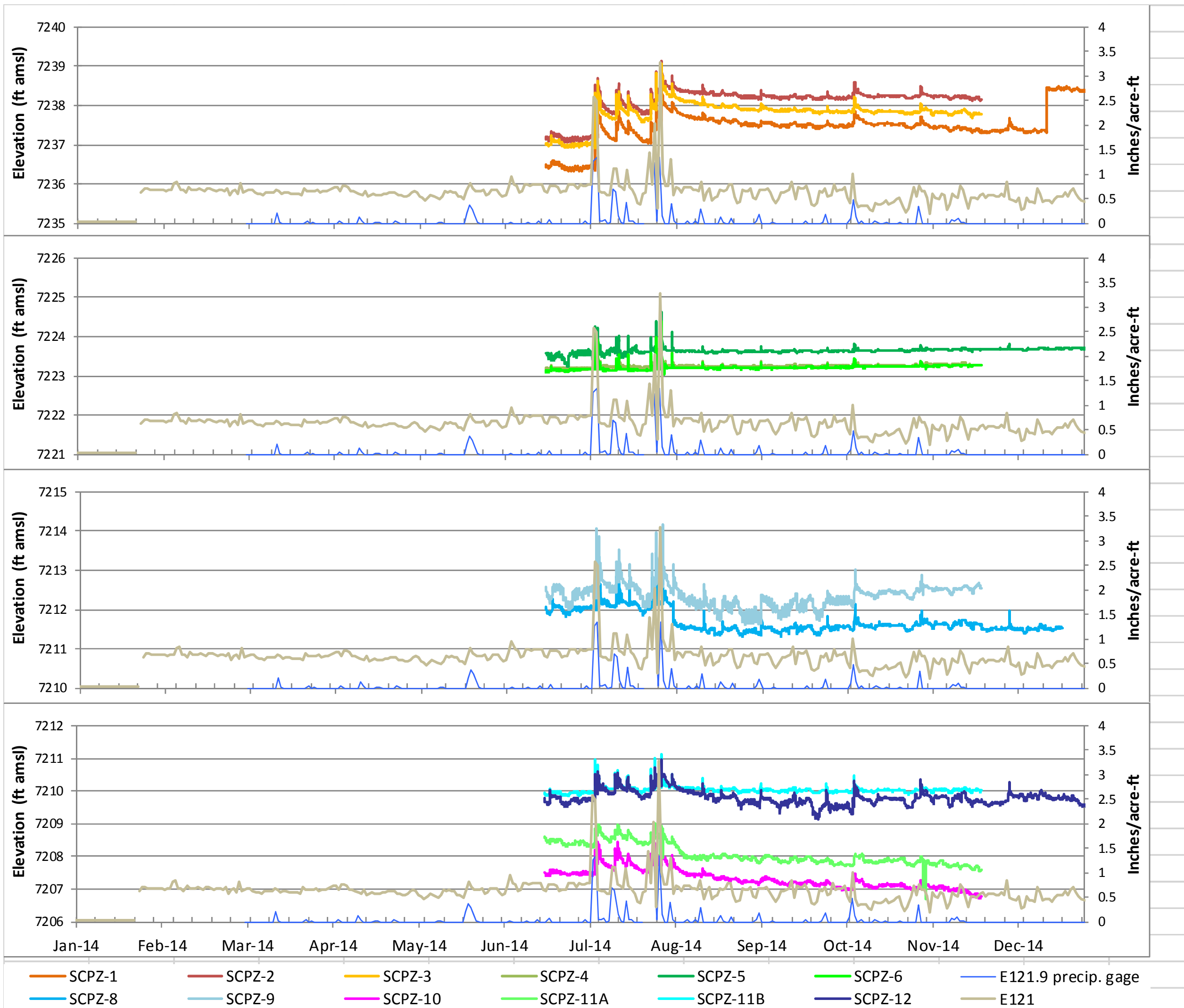

Figure D-3.0-1 Water levels recorded in sondes located in piezometers and precipitation data from precipitation gage E121.9 and surface water gage E121 during 2014

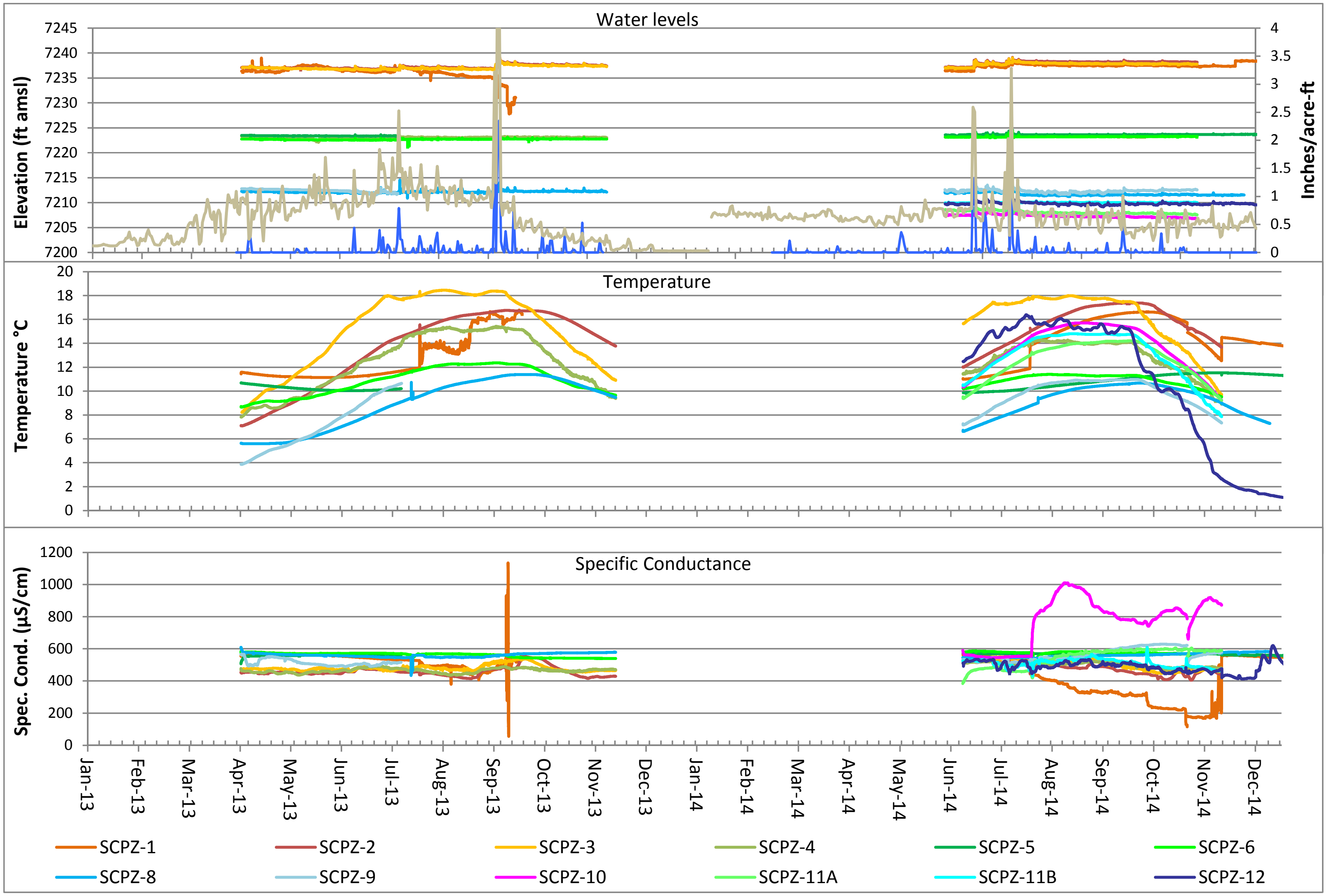

Figure D-3.0-2 Time series of water level, temperature, and specific conductance at piezometers from 2013–2014. Daily precipitation totals for the E121.9 precipitation gage and E121 surface water gage are also shown on the water level plot. The sonde in SCPZ-1 malfunctioned in 2013 and has errors from reinstallation at various depths during 2014.

D-4.0 ALLUVIAL SYSTEM: GEOCHEMICAL PATTERNS

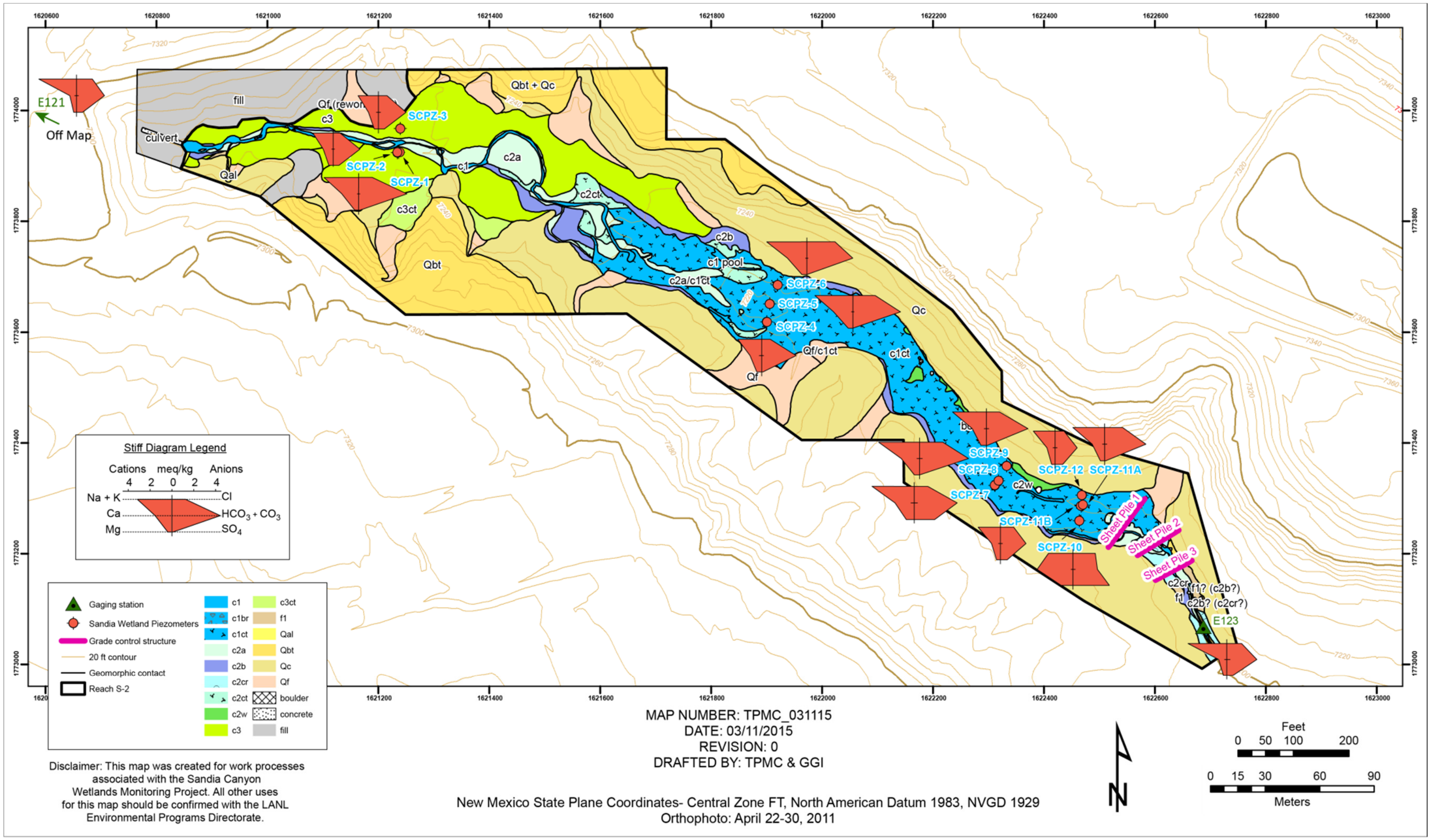

Figure D-4.0-1 Map showing stiff diagrams for piezometer waters within the wetland

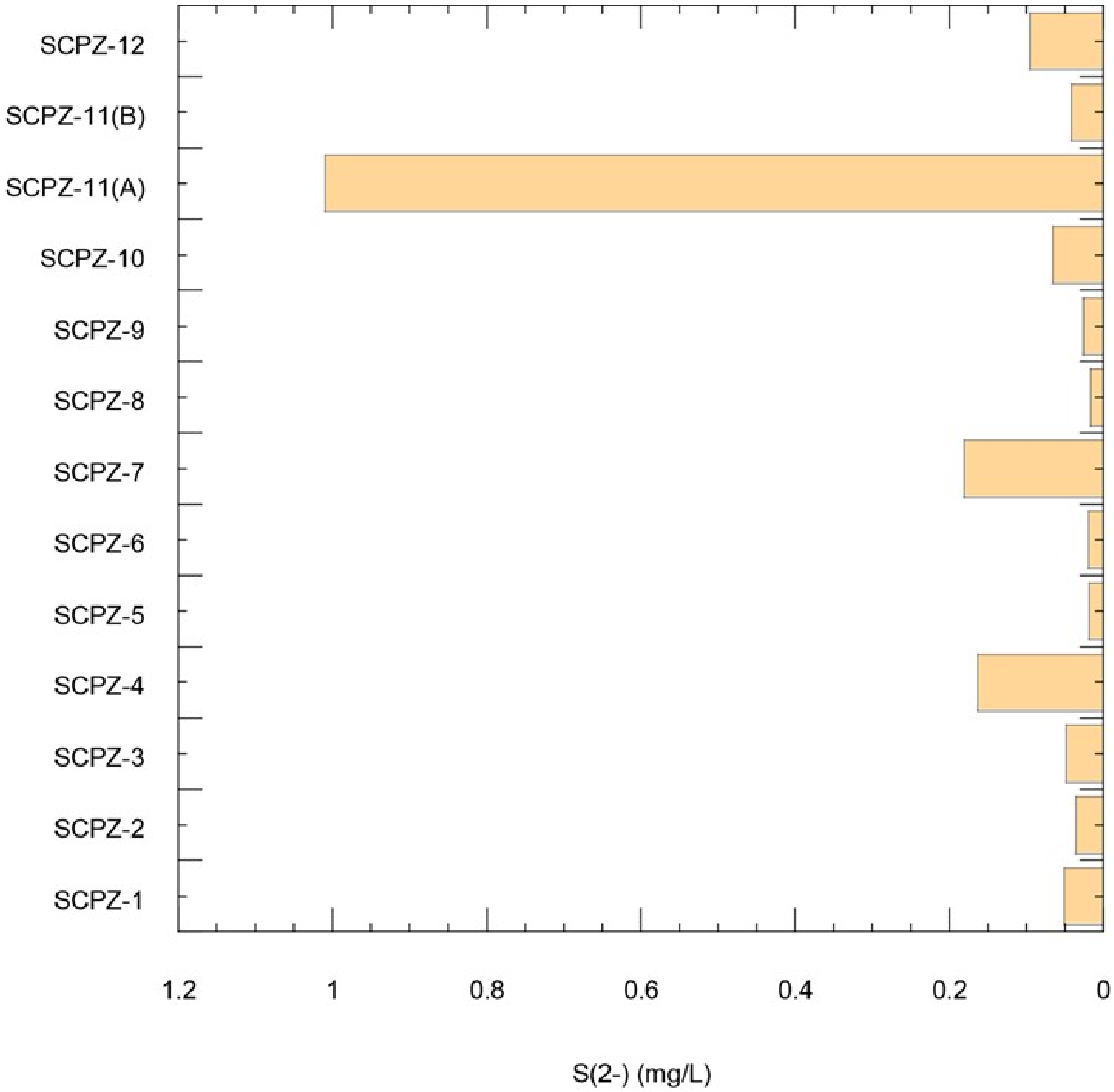

Figure D-4.0-2 Average concentrations of sulfide measured in piezometers from November 2012–November 2014

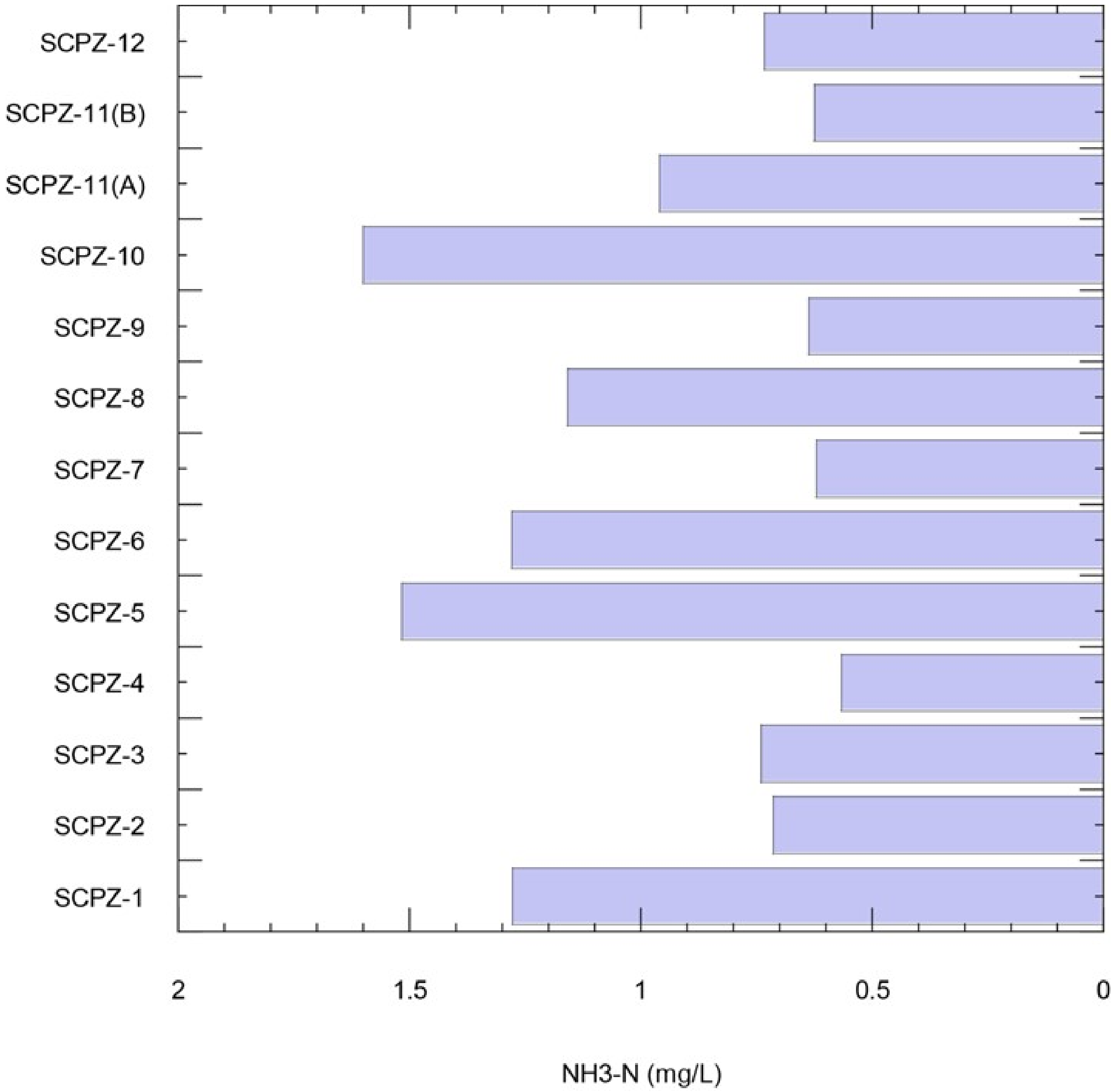

Figure D-4.0-3 Average concentrations of ammonia as nitrogen measured in piezometers from November 2012–November 2014

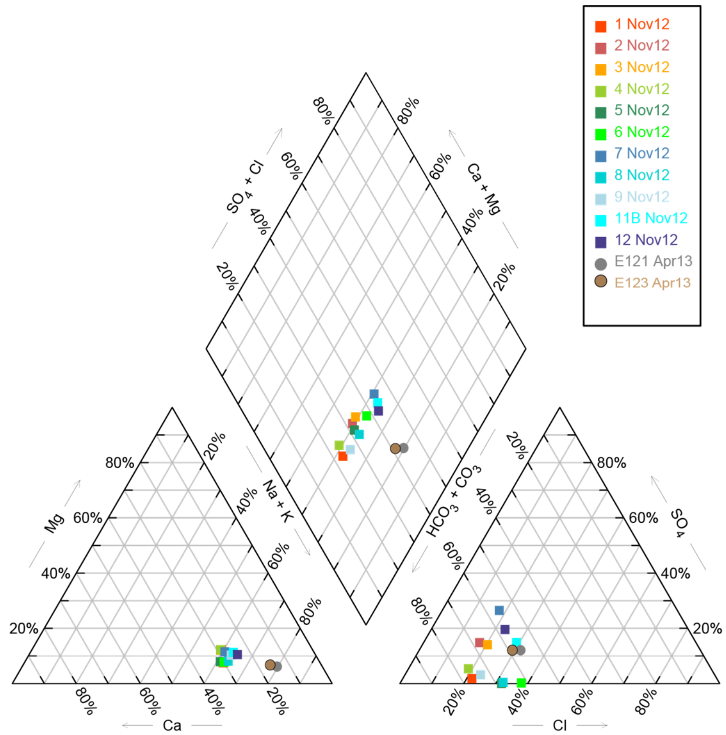

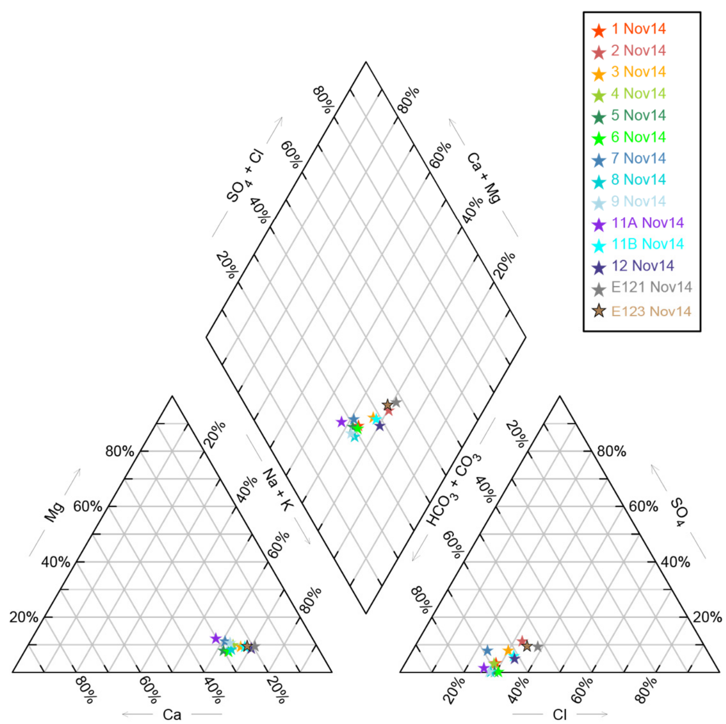

Figure D-4.0-4 Trilinear plot of Sandia wetland piezometers comparing major ion chemistry from November 2012 with that from November 2014. Some piezometer locations are only shown in the 2014 plot because samples were not collected at these locations in 2012. Also shown are data from gaging stations E121 (above wetland) and E123 (below wetland) from April 2013 (no 2012 data were available) and November 2014.

Appendix E

Analytical Data and Frequency of Detects Tables
(on CD included with this document)